



**University of  
Reading**

**Combining instrumental data rescue techniques  
with meteorological metrology to develop  
applied historical climatological analyses**

**Thesis**

*Submitted to the University of Reading for the degree of*

**Doctor of Philosophy**

**Stephen David Burt**

**April 2021**

*v1.1 June 2021*

University of Reading, Department of Meteorology

*Supervisor: Professor Ed Hawkins*

*This page intentionally blank*



## Contents

Abstract .....	5
<i>Declaration</i>	
<i>Acknowledgements</i>	
<i>List of Figures</i>	
<i>List of Tables</i>	
<i>Word count</i>	
<b>Chapter 1: Introduction and context.....</b>	<b>11</b>
<b>Chapter 2: Contextual summary of selected published works .....</b>	<b>13</b>
2.1 Section 1: Meteorological metrology .....	13
2.2 Section 2: Data rescue: work on long instrumental meteorological series	22
2.3 Section 3: Applied historical climatology .....	34
<b>Chapter 3: Summary .....</b>	<b>44</b>
3.1 Summary and conclusions.....	44
3.2 The broader context – why does it matter? .....	45
3.3 Future research directions .....	47
3.4 Publication metrics.....	49
3.5 References.....	52
3.6 Author bibliography.....	57
<b>Appendix: Selected published works.....</b>	<b>61</b>
Copies of published works included within this thesis .....	63 ff

### *A note on references*

References are cited in standard Harvard academic format thus: (Smith, Jones et al, 2021).  
Additionally, references to the author’s work are shown together with the item sequence number for ease of reference in the author’s bibliography which follows: thus (Burt 2021 – bibl. #15).

*This page intentionally blank*

## Abstract

The linking theme within this thesis is meteorological data rescue, whereby records of past weather and climate in handwritten manuscript or published form are digitised and made available to the wider research community, thereby adding to our knowledge of past weather and climate.

Specifically, the hourly observational record from the Ben Nevis Summit Observatory (1883-1904) and the daily climatological series from the Radcliffe Observatory in Oxford (since 1772) and Durham University Observatory (since 1841) are examined in detail – the records from Oxford and Durham comprising respectively the longest and second-longest single-site temperature and rainfall series in England. Both records have been affected to a minor extent by urban growth, and one paper explains ‘picking apart’ the signal of Oxford’s urban heat island from observed background climate warming during the last 150 years. Oxford’s non-instrumental records have also been used to publish a unique near-200 year record of thunderstorm occurrence in the city, while the recently-published twice-daily barometric pressure series from Durham (1843-1960) — by far the longest such record in northern England — fills a large spatial and temporal gap in reanalysis source data, and will lead to improvements in atmospheric circulation analyses. The validity of the dataset was investigated using a reanalysis dataset as a novel underpinning benchmark to identify errors in the digitised series. Throughout the published works included within this thesis, the importance of both instrumental and non-instrumental metrology and metadata in assembling, analysing and publishing the data series are emphasised; specific research relating to the performance of air temperature sensors and the calibration of meteorological instruments is described. Finally, data rescue and modern synoptic analyses are combined to prepare original case studies of significant climatological events, with particular emphasis on extremes of atmospheric pressure over the North Atlantic and the British and Irish Isles within the last 200 years. Examples of the latter are presented, from a body of work now spanning almost 40 years.

Individually and in total, published works included in this thesis contribute to society’s collective body of knowledge on, and thus improved understanding of, past and present weather and climate within the British and Irish Isles and north-west Europe.

*NOTE*

*The vast majority of the work included herein was researched and written up in the author’s own time, without external sources of funding.*

*This page intentionally blank*

## **Declaration**

I confirm that this is my own work and the use of all material from other sources has been properly and fully acknowledged.

Stephen David Burt

## **Acknowledgements**

I am delighted to be able to thank and acknowledge my supervisor, Ed Hawkins, for his inspiration on the numerous data rescue projects we have worked on together, and for his invaluable advice and support while preparing this thesis. My profound thanks also go to the joint Heads of the Department of Meteorology at Reading, Andrew Charlton-Perez and Bob Plant, for their enthusiastic encouragement for me to undertake this project, and to my joint author on the Oxford and Durham books, Tim Burt (no relation), for his wise advice and assistance throughout.

Finally, thanks to my wife of almost 40 years, Helen, for putting up with a lifetime's passion for meteorology, and for her love and support throughout – thank you, as ever.

## List of Figures

**Figure 1.** The Ben Nevis Observatory from a contemporary photograph. Source: Royal Meteorological Society collection, held as part of the Met Office archive at National Records of Scotland, courtesy Royal Meteorological Society

**Figure 2.** Three-hourly humidity (%; red line) at the Ben Nevis Summit Observatory for the period 1-14 December 1902, compared with the 850 hPa humidity field from an enhanced 20CRv3 reanalysis for the same period (mean of the 80 member ensemble in green; 5% and 95% percentiles in grey, and ensemble minimum in faint grey). The 36 hour period of anticyclonic subsidence commencing 0600 GMT 7 December is captured well in the reanalysis, within the uncertainty of relatively coarse model resolution: the summit observatory humidity fell to zero at 0300 GMT 8 December.

**Figure 3.** Individual response times (seconds) versus ventilation speed for the various temperature sensors examined; Figure 3 in Burt & de Podesta, 2020. Plots are colour-coded by sensor size as shown in the legend on right.

**Figure 4** Ice-skating on Whiteknights Lake, Reading, 13 February 1929, during 'The Great Frost'. From One Hundred Years of Reading Weather by Roger Brugge and Stephen Burt, 2015. Photograph courtesy of Reading Central Library, image 1394 315

**Figure 5.** Annual mean temperatures (°C) at Oxford (since 1814), Durham (since 1844) and at Reading University (since 1908), together amounting to some 363,000 digitised daily values, in work undertaken by the author and co-authors since 2015. It is perhaps instructive to consider that to generate this apparently simple plot required the digitisation, careful quality control and dataset assembly of 497 station-years of record, comprising in all some 363,000 records of daily maximum and minimum temperatures, very little of which was previously available in readily-accessible digital format.

**Figure 6.** The morning observation being taken at the Radcliffe Meteorological Station, Oxford. Photograph by the author

**Figure 7.** Ten-year running means of thunderstorm frequency (plotted at year ending) for Oxford (dark red line) 1828-2019, alongside similar averages for sites in west London – Kew Observatory (1877-1980, green line), Heathrow Airport (LHR, 1949-2005, dark blue line) and Northolt (1984-2019, light blue line). Figure 8 from Burt (2021)

**Figure 8.** The first page of surviving manuscript meteorological records from Durham Observatory, showing twice-daily observations for 23-29 July 1843. (Durham University Library)

**Figure 9.** Location of pressure observations within the International Surface Pressure Database for (9a) 1850 and (9b) 1925. Twice-daily records from Durham Observatory are available from July 1843 and will significantly increase the density of observations in and around the British and Irish Isles, particularly prior to 1925. Plots obtained from NOAA PSL at <https://psl.noaa.gov/cgi-bin/data/ISPD/stationplot.pl>

**Figure 10.** Comparison between annual mean MSL pressure (hPa) at Durham Observatory and the 20th Century Reanalysis version 3 (20CRv3) for 1850 to 1960: the blue line shows the average arithmetic difference post-QC and the orange line the average root mean square error post-QC: the faint grey line shows the average RMS error pre-QC. Digitisation and careful quality control of the Durham record revealed a previously unknown bias in the 20CRv3 reanalysis dataset between 1914 and 1919, which is the subject of current investigation and rectification. The large pre-QC bias from 1949 resulted from incorrect barometer temperature observations together with a change in the barometer scale.

**Figure 11.** Approximate distribution of rainfall for the rainfall day of 16 August 2004 in north Cornwall – the Boscastle Storm. Units are millimetres: isohyets are at 5, 20, 50, 100 and 200 mm. Figure 3 from Burt 2005 – bibl. #39.

**Figure 12.** British Isles surface chart for midnight GMT 20 December 1982, showing cloud, wind, present and past weather and temperature (°C). The isobars are drawn every 4 mbar. Figure 3 from Burt 1983 – bibl. #57.

**Figure 13.** The world's first published barograph chart – Luke Howard's 'clockbarometer' (mercury barograph) record from Tottenham, north London, for December 1821, showing the extreme depth of the depression of 25 December. The values are not corrected to MSL (add about 4 hPa) and the original scale is in inches of mercury (inHg) – millibar equivalents are given on the right. From Howard (1822), Plate XIII, reproduced as Figure 3 in Burt 2007a – bibl. #34.

**Figure 14.** The highest MSL barometric pressures observed anywhere in the British and Irish Isles for November to April since about 1800, plotted against the date on which they occurred. The March 2020 event lies well outside the 'envelope' of all previous events within the last 200 years or more. The January 2020 event is also highlighted. Expanded version of Figure 11 in Burt 2020b – bibl. #3 – showing the pronounced midwinter 'bump' which (until March 2020) clearly delimited all previous occasions on which 1048 hPa was attained or surpassed.

## List of Tables

**Table 1.** Publication metrics from Clarivate Web of Science, Scopus, ResearchGate and Google Scholar, updated to 23 June 2021. Papers included in this thesis subset are highlighted in bold.

## Word count

The total word count for this thesis, including chapter and section headings, tables and figure captions but excluding reference lists, tables and bibliography, is approximately as follows:

Abstract	320	words
Chapter 1	535	
Chapter 2	12 310	
Chapter 3	2 640	
Included papers	49 685	
<b>Total word count</b>	<b>65 490</b>	

*This page intentionally blank*



# Chapter 1

## Introduction and context

This document sets out a subset of the author’s published papers for consideration of the award of **Doctor of Philosophy through Published Works** with the intention of answering the following question:

*How does the systematic recovery of old meteorological observations (‘data rescue’), together with better awareness of past and present instrumental metrology and metadata, improve our knowledge of past and present weather events and climate trends?*

This section outlines the context and relevance to the main thesis question of nine publications by the author, together comprising a coherent and substantial body of original work and in doing so providing fresh insights into the past and present climatology of the North Atlantic and British and Irish Isles. Three core concepts are common to the work presented — **meteorological metrology**, **data rescue** and **applied climatology**. As the science of measurement, **metrology** plays an essential (if sometimes overlooked) role within meteorology: understanding the physical basis for meteorological measurements, past and present, is vital in understanding both use and limitations. **Data rescue** covers the creation of a digital dataset from original hardcopy records — whether hardcopy manuscript or printed — and often involves a variety of methods, from digitisation by individuals through web-based citizen science to advanced optical character recognition techniques. Careful consideration of data rescue and metrology aspects helps compile invaluable historical weather and climate datasets, forming the basis for methodical **applied climatology** studies and analyses. All three concepts combine to contribute to an **improved societal understanding of past and present weather and climate, climate change** and the range of climatological extremes.

Chapter 2 sets out the importance and relevance of meteorological metrology and observing methodologies. Three example publications consider how the three core concepts are applied to data rescue and extreme-value climatological analysis, in quantifying the performance of commercial air temperature sensors, and in guidance for meteorological observers in establishing best-practice instrument calibration procedures.

Chapter 2 then summarises data rescue projects involving two of the longest instrumental meteorological records in the United Kingdom, namely Oxford’s Radcliffe Observatory (where records began in 1772) and Durham University Observatory (since 1841), referencing two book chapters and an open-access journal paper. Almost all of the records from Oxford and Durham, including site and instrumental metadata, were previously available only in manuscript within restricted-access university archives. As a result of the author’s work, together with his joint contributor, these long records have now been digitised and published.

Chapter 2 continues with the methodical synthesis of historical and current observations to provide original insights into climatological extremes, particularly extremes of barometric pressure over the North Atlantic and British and Irish Isles. Three published papers sit within the context of an extensive and substantial body of contributions on the topic, now extending over almost 40 years.

Chapter 3 concludes with a closing summary, an analysis of the author's broader impact, and identifies related future research directions. Publication metrics and a complete bibliography of the author's relevant publications in meteorology and climatology since 1975, amounting to over 60 items in total, complete this chapter. The nine referenced papers (six papers and three book chapters) then follow in the same sequence to which they are referred in Chapter 2.

# Chapter 2

## Contextual summary of selected published works

### 2.1: Meteorological metrology

**Metrology** is the science of measurement, and plays an essential role within meteorological measurements. Collaboration between metrologists and meteorologists has been ongoing over several decades, through combined working groups on (for example) WMO’s CIMO guide (Commission for Instruments and Methods of Observation: WMO 1973, WMO 2018), and the GRUAN project (Global Climate Observing System (GCOS) Reference Upper-air Network: <https://www.gruan.org>). Collaboration has if anything strengthened within the last decade, including for example the establishment of the MeteoMet project (Merlone et al, 2015) and ongoing ‘first-principles’ reviews of specifically temperature-related metrology (Merlone, 2021). Due consideration of meteorological metrology and relevant instrumental data (metadata) are as essential for assessing the quality and accuracy of datasets derived from the digitisation of ‘rescued’ manuscript or printed climatological weather and climate records as for contemporary instrumentation (see, for example, Cerveny et al, 2007; Cerveny, 2018; Skansi et al, 2017; Weidner et al, 2020), and examples of both are provided in this section.

#### **Paper 1: The enigma of extremely low humidities observed on Britain’s highest mountain – one of the wettest spots in Europe**

**Near-zero humidities on Ben Nevis, Scotland, revealed by pioneering nineteenth century observers and modern volunteers**, by Stephen Burt and Ed Hawkins. *International Journal of Climatology*, 2019, **39**, pp. 4451-4466.

*Bibliography # 15. Word count 6115, excluding references.*

*Authorship statement:* SB contribution 80% (paper structure and content, definition and selection of events, database preparation, calculations and analysis, case studies, comparison with modern records, submission): EH 20% (main database preparation, reanalysis contributions, critical review)

---

A meteorological observatory was established at the summit of Ben Nevis, at 1345 m above mean sea level (MSL) the highest mountain in the British Isles, by the Scottish Meteorological Society in November 1883 (**Figure 1**); thereafter, high-quality manual instrumental and ‘eye’ observations were made hourly until its closure in October 1904. There are numerous contemporary and more recent accounts of the history of the observatory and the life of the observers at this most inhospitable location (Anon, 1893; Kilgour, 1905; Duncan and Weston, 1983; Roy, 2004).



**Figure 1.** *The Ben Nevis Observatory from a contemporary photograph. Source: Royal Meteorological Society collection, held as part of the Met Office archive at National Records of Scotland, courtesy Royal Meteorological Society*

Simultaneous observations were made at a low-level site in Fort William, at the foot of the mountain less than 10 km distant. The observations from both sites were themselves published in full, in four large volumes, by the Royal Society of Edinburgh (Buchan, 1890; Buchan and Omond, 1902; Buchan and Omond, 1905; Omond, 1910). These data arguably represent the most detailed set of weather observations for this period anywhere in the UK, and certainly in a montane environment. The published volumes lay largely unused in libraries until a very successful Zooniverse citizen science project managed by the authors commencing in September 2017 attracted more than 3000 volunteers, who succeeded in transcribing almost the entirety of the published records into a digital dataset in just a few weeks; the process and the dataset is described more fully in Hawkins, Burt, Brohan et al, 2019 – bibl. #16.

Owing to descent of air warmed by subsidence within anticyclones, hilltop and mountain summits in the British and Irish Isles and north-west Europe occasionally experience instances of very low relative humidity, the incidence generally increasing with altitude. Variations in atmospheric water content at elevated levels in mid-latitudes are much greater than at lowland sites, alternating long periods of saturation with relatively frequent spells when the humidity falls to 20 per cent or less. The phenomenon has been remarked upon previously for Ben Nevis and the Cairngorms by Green (1953, 1965, 1966, 1967) and for Great Dun Fell in Cumbria by Burt (2011). Using the newly-accessible digital database, the paper examined in detail numerous instances of such conditions on the Ben Nevis Observatory record. Although relative humidity was calculated by the observers at the time, psychrometric theory was in its infancy in the late 19th century and the contemporary humidity tables used by the observers were subsequently found to be seriously in error in the low pressure environment of the observatory (the mean station-level pressure at the summit of Ben Nevis is close to 850 hPa), particularly in conditions of very dry air. Fortunately, the original published records included both dry- and wet-bulb thermometer readings, rather than dry-bulb together with humidity derived from contemporary tables, and from these a more reliable relative humidity value could be calculated using modern psychrometric algorithms. However, the latter are critically dependent upon two variables – the state of the wet-bulb (or ice-bulb, at temperatures

below 0 °C), and the ventilation of the wet-bulb thermometer itself. Careful consideration of both metrological and metadata aspects of the newly ‘rescued’ dataset was required in order to assess the reliability (or otherwise) of the Ben Nevis Observatory humidity records, and from there assess the climatological frequency of near-zero relative humidity at the site and thereby compare with more recent measurements from modern automatic weather stations on other Scottish mountains.

Detailed examination of observer comments from the observatory logbooks provided clear evidence of specific efforts made by the observers to maintain a wet ‘wet-bulb’ during occasions of very dry air. Because the wet-bulb muslin dries out very rapidly in low humidity conditions, particularly at anything other than very light wind speeds, a drying wet-bulb would be likely to decrease the depression of the wet-bulb below the dry-bulb temperature, and thus result in an incorrect, higher, derived humidity value (the detailed metrological reasoning being set out in the paper). A second metrological assessment related to the ventilation of the wet-bulb within the Stevenson screen in use. Work by Harrison and Wood (2012) showed that the key psychrometer coefficient in the humidity calculation varied with ventilation, particularly below 1 m s<sup>-1</sup>. To take this into account, estimates of wet-bulb ventilation within the screen were based upon wind force estimated by the observers, reduced by a factor to allow for diminution by the screen structure itself, and an appropriate value of the psychrometer coefficient from Harrison and Wood’s paper was then selected for use in the calculation. Further, derivations of a range of ‘real-world’ values of the psychrometric coefficient were derived by reversing the psychrometric equation, using the observed temperature and assumed in-screen wet-bulb ventilation rate. Working backwards from the reasonable assumption that the humidity *was* close to zero, and by substitution of two nominal humidity values (0% and 5%) into the psychrometric equation, the value of the psychrometric coefficient required to satisfy either of the two nominal humidity values was easily obtained. The bounded range of values thus derived provided highly satisfactory and independent confirmation of laboratory-derived coefficients.

Comparisons were also made with modern-day humidity records from two high-level automated mountain sites run by the Met Office in the Scottish mountains, including Aonach Mòr (1130 m AMSL), only 3.5 km north-east of the site of the Ben Nevis Observatory. The frequency distribution of observed relative humidity for the Ben Nevis Observatory matched the other mountain sites remarkably closely, providing a convincing demonstration of the validity of the ‘rescued’ temperature and humidity dataset — despite observations being made a century apart, and with entirely different instrument technologies — and quantitatively demonstrated that humidity profiles at high-altitude sites are strikingly different from those at lower altitudes. Further, three case studies were compared with reanalysis data using the 20th Century Reanalysis (Compo *et al*, 2011), and showed remarkable agreement with model 850 hPa humidity. This is particularly worthy of note when it is considered that the reanalysis is based almost entirely on assimilation of station level pressures and sea surface temperatures only, and that the nearest assimilated pressure observations were from Aberdeen Observatory, almost 200 km to the east of Ben Nevis. This is also the subject of continuing work, see below.

The original aspects of this publication can be summarised as follows:

- (i) The systematic identification, from a 20-year hourly record, of all occasions when very dry air was observed at the summit of Ben Nevis. Prior to the availability of the digital database and rapid data-processing facilities, previous researchers were able to select only isolated instances identified in the observatory logbook (not all were so logged). It would be impossibly time-consuming and tedious to identify all such instances ‘by eye’ from the published tabulated records of dry- and wet-bulb temperatures (in all, over 180,000 observations), particularly as humidity calculations require individual reworking for the observed station-level pressure in each case;
- (ii) The generation of frequency distributions for mountain humidity profiles, comparing both historical and contemporary datasets;
- (iii) The ‘reverse engineering’ of the psychrometric equation to derive ‘real world’ values of the psychrometric coefficient at extremely low values of atmospheric moisture, which found excellent agreement with laboratory evaluations by Harrison and Wood (2012);
- (iv) Comparison of historical mountain data with reanalysis 850 hPa humidity fields from the 20th century reanalysis dataset, not previously attempted.

**Media interest** This work attracted considerable media interest upon publication, including an article by the BBC’s Science Correspondent Jonathan Amos on the BBC News website front page (‘Soggy Ben Nevis can be remarkably dry’, 18 March 2019, <https://www.bbc.co.uk/news/science-environment-47615716>).

**Continuing work** Further, more detailed comparisons between (observed) Ben Nevis Observatory humidity and (reanalysis) 850 hPa humidity fields are ongoing. **Figure 2** compares the hourly humidity at the Ben Nevis Observatory for the period 1-14 December 1902 against the 850 hPa humidity field (mean and 90% confidence interval, from 80 ensemble members, from the nearest gridpoint to the mountain; gridpoint spacing is about 50 km at this latitude) from an enhanced 20th Century reanalysis database (20CRv3; Slivinski et al, 2019, 2020).

This more detailed reanalysis (version 462) assimilates the much denser network of pressure observations (only) from the British and Irish Isles and north-west Europe generated from the previous Ben Nevis (Hawkins et al, 2019) and *Daily Weather Report* (Craig and Hawkins, 2020) data rescue projects (the Fort William and Ben Nevis pressure observations are station level records, whereas the published *Daily Weather Report* sites reported MSL pressures). This example illustrates how successive data rescue projects can build upon preceding work, building datasets whose total is greater than the sum of its parts. This study, which has not yet been published, demonstrates the facility and reliability with which reanalysis models can successfully reproduce distinctive and realistic upper-air features such as subsidence-induced compression warming and drying at 850 hPa, even though model-assimilated data consists only of surface pressure observations.

Of course, the relationship between model and ‘rescued’ historical observations shown in Figure 2 is not exact: indeed, at a horizontal gridpoint spacing of tens of kilometres, a 3 hour timestep and

limited vertical resolution (64 levels; Slivinski et al, 2020), it is unrealistic to expect it to be. Vertical gradients of both temperature and humidity near anticyclonic subsidence inversions can be extremely sharp (Burt, 2011), and a relatively coarse vertical model resolution will act to ‘smear out’ inversion features. Nonetheless, the reanalysis at 850 hPa – despite its limited or ‘sparse’ assimilation dataset – reproduces the broad features of the period concerned as confirmed by the hourly humidity record from the summit observatory.

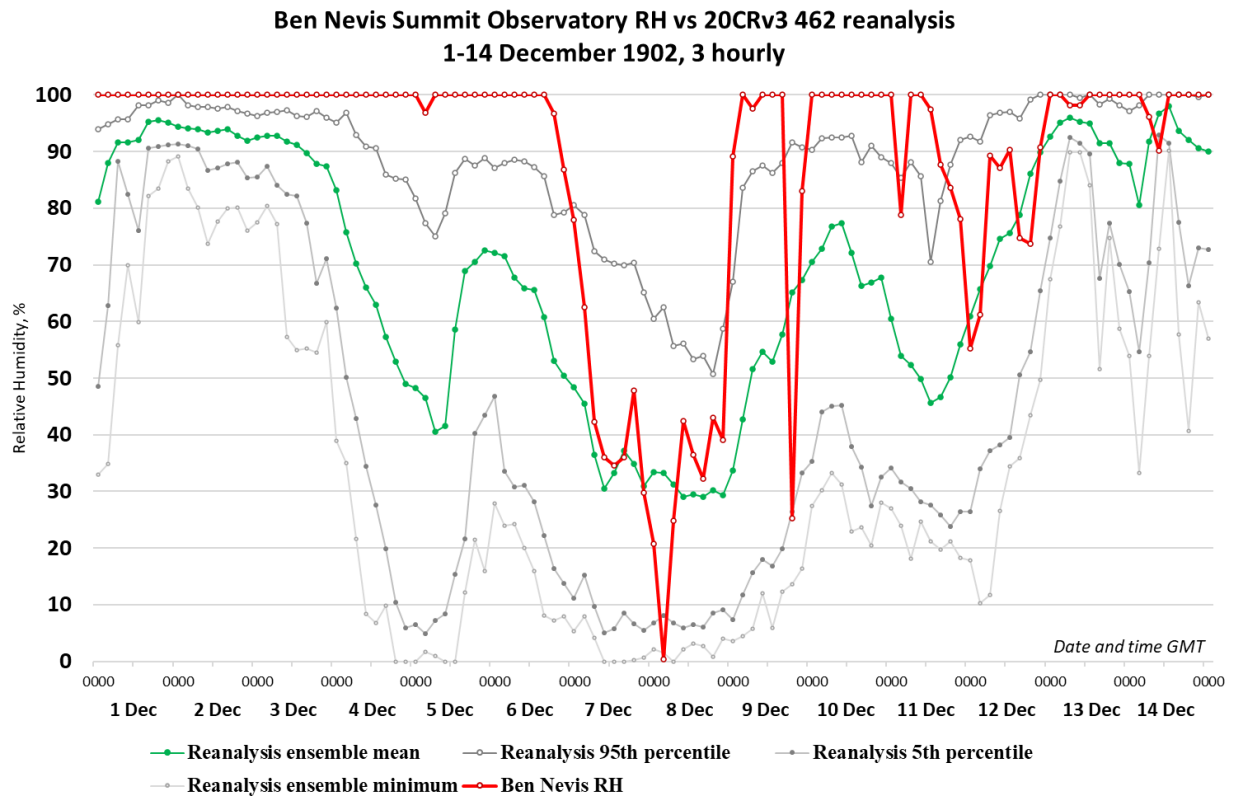


**Figure 2.** Three-hourly humidity (% , red line) at the Ben Nevis Summit Observatory for the period 1-14 December 1902, compared with the 850 hPa humidity field from an enhanced 20CRv3 reanalysis for the same period (mean of the 80 member ensemble in green; 5% and 95% percentiles in grey, and ensemble minimum in faint grey). The 36 hour period of anticyclonic subsidence commencing 0600 GMT 7 December is captured well in the reanalysis, within the uncertainty of relatively coarse model resolution: the summit observatory humidity fell to zero at 0300 GMT 8 December.

## **Paper 2: Determining response profiles of contemporary air temperature sensors**

**Response times of meteorological air temperature sensors**, by Stephen Burt and Michael de Podesta (National Physical Laboratory, Teddington). *Quarterly Journal of the Royal Meteorological Society*, 2020, 146, pp. 2789-2800.

*Bibliography # 5. Word count 5510, excluding references.*

*Authorship statement: SB contribution 50% (topic/paper proposal, literature review, laboratory work, database preparation and results analysis, paper assembly and submission): MdeP 50% (theory review, development of cooling models, critical review)*

---

This paper originated from the first author's discussions with the Met Office, several meteorological equipment manufacturers and the National Physical Laboratory regarding the content of the World Meteorological Organization's Commission for Instruments and Methods of Observation (CIMO) guide recommendations on thermometer response time (WMO 2014, WMO 2018), together with British and International Standard ISO 17714, *Meteorology — Air temperature measurements — Test methods for comparing the performance of thermometer shields/screens and defining important characteristics* (ISO 2007).

The WMO CIMO guide recommendation (section 2.1.3.3) is that the 63 % response time  $\tau$  for an air temperature sensor be 20 seconds, although — as airflow speed influences response time — the minimum airflow speed at which this applies should also be specified in the document. A 63 % response time  $\tau_{63} = 20$  s implies that 95 % of a step change be registered within  $3\tau_{63}$  or 60 s, the WMO recommended averaging interval for air temperature: rapid air temperature changes on this timescale are not uncommon, often associated with convective squalls, frontal systems or sea breeze circulations.

A series of pilot tests were carried out in the laboratories of the University of Reading's Department of Meteorology to measure the response time of a sample of commercial platinum resistance thermometers (PRTs) from various sources. The results showed that wide variations existed within the sample; for some sensors,  $\tau_{63}$  at  $1 \text{ m s}^{-1}$  airflow exceeded 100 s, five times the WMO CIMO recommendation (**Figure 3**). In fact, none of the sensors tested met WMO specifications, although all were and are being used in operational meteorological equipment for numerous National Meteorological Services. Despite the rapid advance of automation within meteorological air temperature measurements in recent decades, it was a major surprise to discover that extensive literature searches revealed almost nothing had been published on sensor time responses within the last 50 years. In contrast, the critical importance of short (sub-minute) sensor response times in deriving accurate and consistent maximum and minimum air temperatures in meteorological measurements has been restated and emphasised in numerous recent papers (for example, Lin et al 2005; Lin and Hubbard 2008; Harrison and Burt 2020 – bibl. #9), particularly within the context of the current rapid transition of 'thermometers' from traditional liquid-in-glass



to electrical resistance sensors within National Meteorological Services around the world (see, for example, Clark et al, 2014, Strangeways, 2019 and Venema, 2020).

An expanded range of more detailed response time laboratory experiments were carried out in 2018/19 on a wider range of PRTs from various manufacturers, and preliminary results presented at the World Meteorological Organization’s TECO (Technical Conference on meteorological and environmental instruments and methods of observation) conference in Amsterdam, the Netherlands, in October 2018.

The research presented clearly demonstrated that *none* of the wider range of sensors tested met the WMO CIMO guide specification; indeed some would take several minutes to respond to a change in air temperature in light wind conditions.

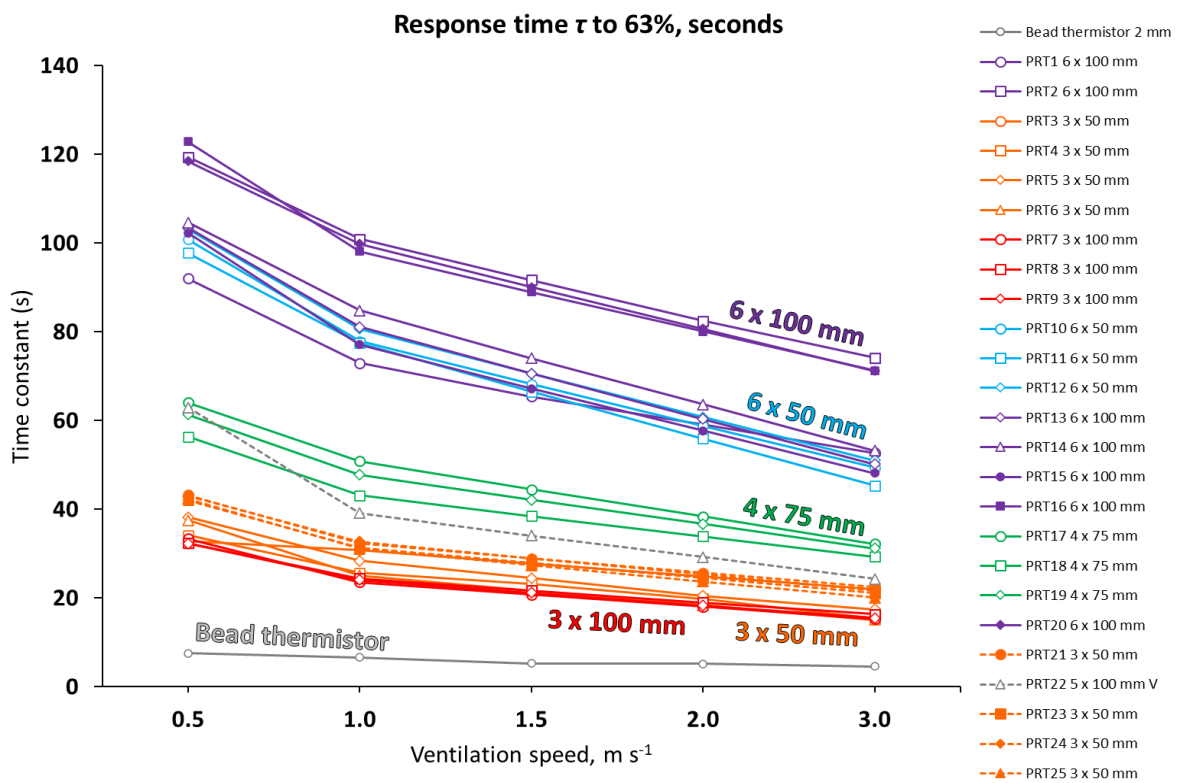


**Figure 3.** Individual response times (seconds) versus ventilation speed for the various temperature sensors examined; Figure 3 in Burt & de Podesta, 2020. Plots are colour-coded by sensor size as shown in the legend on right.

Following the presentation, there was considerable interest and reaction from both manufacturers and instrument suppliers as well as several National Meteorological Services, and the work was written up for publication. At that time, Michael de Podesta from the UK’s National Physical Laboratory suggested a joint ‘metrology-meteorology’ approach, specifically a joint paper combining both laboratory results and practical theoretical numerical cooling models. Michael is a member of the MeteoMet project committee (Merlone et al, 2015), established to build closer links between the meteorological and metrological communities, and his group has published material on errors in air temperature sensors (de Podesta et al, 2018). Combining both laboratory work with

theoretical studies presented an opportunity to update a field lacking in modern quantitative and theoretical studies with original contributions, and influence both instrument specification/performance and procurement tenders to meet WMO's performance criteria.

The resulting paper is necessarily more strongly focused on 'metrology' than the other concepts outlined in the introduction. If, as expected, its findings and recommendations on sensor performance are incorporated into the next version of the current CIMO guide (expected to become a subset document within the WMO Integrated Global Observing System, or WIGOS, manual and guide – WMO, 2019), it will influence climatological air temperature measurements at both national and international levels for the next generation of meteorological instrumentation — indeed, some manufacturers have already indicated that this work will dictate their choice of temperature sensor in response to future procurement tenders. This in turn will result in more reliable, more accurate and more consistent measurements of air temperature — increasingly important as climate change (and its accurate determination) continues to be a major influence on both science and government policies around the world.

However, it is clear that the introduction of improved technologies and observing systems within existing meteorological networks will require particularly careful change management, including parallel running of both systems at certain key sites, to avoid the inadvertent introduction of damaging break-points into the climate record. Long-period sites are particularly vulnerable in this regard, especially where a manual observation routine is replaced by an automatic system; examples abound of the deterioration in record quality following such changes (Burt 2012, Chapter 5). An instructive lesson in how *not* to implement a change in sensor technology can be found in the transition within the US from Cotton Region Shelters (similar to Stevenson screens) combined with liquid-in-glass temperature sensors, to an electronic sensor in a small multiplate radiation screen, the Maximum-Minimum Temperature Sensor or MMTS. Analysis of the CRS-MMTS changeover in the mid-1980s showed a clear breakpoint in the records from almost every site affected by the transition (Quayle et al, 1991; Doesken 2005). The ideal of establishing 'greenfield' Climate Reference Networks consisting of long-term, representative sites to provide reliable climate information using regularly updated metrology-traceable sensors and exposures, as already implemented in the US Climate Reference Network for example (USCRN; Diamond et al, 2013; also Thorne et al, 2018; Merlone, 2021) has obvious and long-lasting merits; but the establishment of such 'reference' sites has to be considered as *an addition to*, rather than a replacement for, existing national and regional networks of long-period sites.

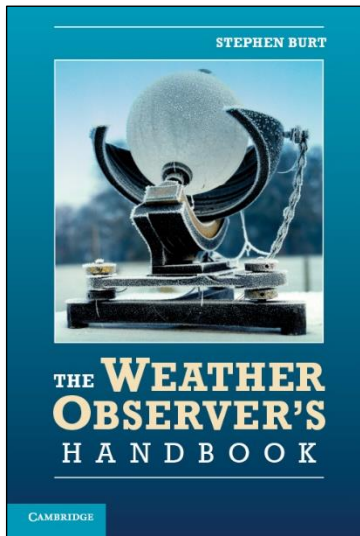
### **Publication 3: Practical calibration methods for amateur and professional meteorological observers**

**Calibration.** Chapter 15 in *The Weather Observer's Handbook*, by Stephen Burt. Cambridge University Press, New York and London, 2012, 444 pp.

*Bibliography #28. Word count 8115 excluding references.*

*Authorship statement: Sole authorship.*

---



*The Weather Observer's Handbook* was written in response to a demand from both amateur and professional users for a comprehensive and up-to-date book on the use and exposure of weather stations, and builds upon the author's long experience with meteorological instruments and observing practices. It is intended as a practical observing manual, and builds upon the World Meteorological Organization's best practice observing guideline, at that time the CIMO manual (WMO 2014, WMO 2018), part of the WIGOS manual (WMO 2019). The CIMO guide is necessarily intended for a narrow technical professional audience within National Meteorological and Hydrological Services organisations.

*The Weather Observer's Handbook* covers all aspects of the main meteorological sensors (temperature, precipitation, atmospheric pressure, humidity, wind speed and direction, grass and earth temperatures, sunshine and solar radiation) as well as site and exposure guidelines, dataloggers, time standards and metadata, together with chapters on collecting, storing and making best use of data captured. *The Weather Observer's Handbook* received very warm reviews, from the *Bulletin of the American Meteorological Society* to *The Sky at Night*. To date, it has sold over 2000 copies and is regularly cited, including within the current WMO CIMO guide itself. Cambridge University Press are proposing a second edition for 2023.

The particular chapter included here (Publication 3) is on the topic of instrument calibration, a metrology-focus subject covered by very few other publications outside of professional disciplines. Professional users, such as national meteorological services, turn to their own technician organisations or calibration partners for regular or bespoke calibration requirements, but most users outside professional meteorology have no such recourse. As the success of online sites such as the Met Office Weather Observations Website (WOW, [wow.metoffice.gov.uk](http://www.metoffice.gov.uk)) or WeatherObs (<https://www.weatherobs.com>) show, 'amateur' or 'citizen science' sites hugely outnumber 'professional' synoptic stations. Data from such 'citizen science' networks are increasingly being seen as a cost-effective means to improve both spatial and temporal density of meteorological observational data input, for example in high-resolution forecasting models and for high-density

studies of urban heat islands (applications in Barnard et al, 2016; Chapman et al, 2017; Kirk et al, 2021).

However, few if any low-cost weather stations include sensors with any traceable calibrations (often, without *any* calibrations). This chapter was written specifically to pass on low-cost, *in situ* practical and tested calibration methods for temperature, precipitation, humidity and pressure sensors, whether directly or by comparison with sensors of known accuracy where available (such as how to calibrate barometers from the synoptic network). Readers are shown that it is not difficult to calibrate the full sensor suite from new weather stations to near-professional standards, and to check for sensor drift by regular recalibration. Although little of the material is truly original, its merit lies in collating relevant information about instrument calibration, often from highly technical or obscure sources, and making the information easily understandable and available to a large audience. In doing so, it has improved the quality and accuracy of meteorological observations appearing on the various online data portals. *The Weather Observer's Handbook* is still in print and on sale, and continues to provide valuable support to the perception and quality of citizen science meteorological observations.

## 2.2: Data rescue: work on four long instrumental meteorological series

Aspects of data rescue, metadata, error detection/correction and publication of important, long-period historical climatological records figure prominently in the author's bibliography, starting with two early papers which examined the long series of temperature and rainfall records made at **Rugby School** in Warwickshire, commencing in 1855 (Burt 1975, 1976 – bibl. 63, 64). Not surprisingly, the temperature records from Rugby, in the heart of the English Midlands, provided an excellent single-site proxy to Manley's Central England Temperature series, and the examination of single-site trends and extremes provided a good indication of the expected range of climatic elements at a typical 'Central England' location. The entire daily rainfall series 1871 to 1993 (along with monthly temperature means from 1871 to 1993) was digitised and is available in the Met Office archive.

A project with Roger Brugge, a colleague from the Department of Meteorology at the **University of Reading**, in 2014-15 led to the digitisation, data rescue, dataset creation and publication in book and online form of the history, metadata and entire meteorological records made by the University of Reading since 1901 in our book *One Hundred Years of Reading Weather* (Brugge and Burt 2015 – bibl. #24). Reading Library and Museum Services became involved at an early stage and contributed much useful photographic material from their archives (**Figure 4**). Publication costs were part-subsidised by the Department of Meteorology to commemorate the 50th anniversary of the Department (1965-2015).

This project and the resulting publication has led to greatly increased awareness and usage of the university's climatological records within the Department, elsewhere within the university, and

within the wider local public. In particular, a Public Lecture by the two authors in February 2016 was the university's best-attended Public Lecture on record, and presentations on *One Hundred Years of Reading Weather* — based on the public lecture — and outreach tours of the university's Atmospheric Observatory have proved popular with local groups every year since.



**Figure 4** Ice-skating on Whiteknights Lake, Reading, 13 February 1929, during 'The Great Frost'. From *One Hundred Years of Reading Weather* by Roger Brugge and Stephen Burt, 2015. Photograph courtesy of Reading Central Library, image 1394 315

Three papers in this section refer to more recent, and continuing work, on the two longest continuous climatological series in England – that from the **Radcliffe Observatory in Oxford** (where records began in 1772) and from the **Durham University Observatory** (from 1841). Both records remained largely inaccessible and in manuscript form within the respective universities until gradually opened up through the work of the author and his co-author (emeritus Professor of Geography at the University of Durham, Tim Burt – no relation). A book by us on the long Oxford record, *Oxford Weather and Climate since 1767*, was published by Oxford University Press in 2019, and a similar volume for Durham, *Durham Weather and Climate since 1841*, will be published by OUP in spring 2022. The daily Oxford temperature, rainfall and sunshine records have now been digitised and made freely available online; the Durham record (daily temperature, barometric pressure and rainfall from 1843 or 1850 to date, sunshine 1880-1999) will follow during 2021.

**Figure 5** shows the mean annual temperature at each of the three sites (Oxford, since 1814; Durham, since 1844 and Reading University, since 1908). The consistent interannual variation and quality of agreement between the three sites is visually evident. The two sites in southern England, Oxford and Reading (40 km apart), are in very close accord, while being clearly set apart from the more northern (and thus cooler) record from Durham, some 365 km north-north-west of Reading. The change of site at Reading in 1968, from the urban town-centre site at London Road to the better exposure within the parkland campus site at Whiteknights 2 km distant, can be distinguished even on this small scale of plot.

There is great scientific value in being able to compare and contrast such long-series, amongst other reasons to assess breakpoints in the series, compare regional trends and (in temperature records such as these) to distinguish site-specific urbanisation effects from climate change.

The Oxford records form the basis of two publications in this section, and Durham the third.

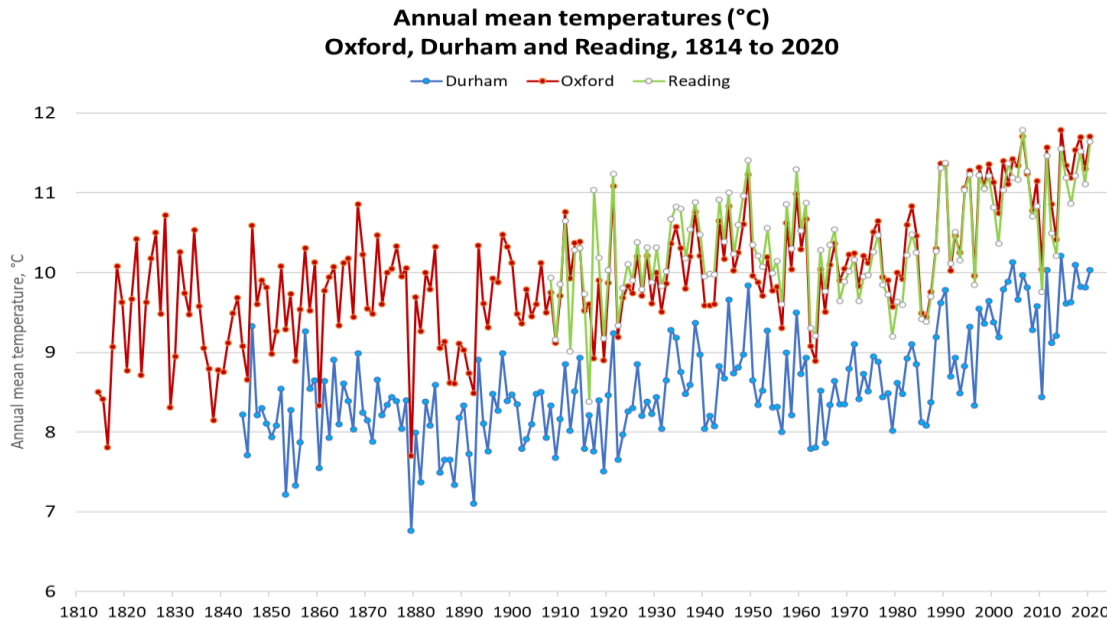


**Figure 5.** Annual mean temperatures (°C) at Oxford (since 1814), Durham (since 1844) and at Reading University (since 1908), together amounting to some 363,000 digitised daily values, in work undertaken by the author and co-authors since 2015. It is perhaps instructive to consider that to generate this apparently simple plot required the digitisation, careful quality control and dataset assembly of 497 station-years of record, comprising in all some 363,000 records of daily maximum and minimum temperatures, very little of which was previously available in readily-accessible digital format.

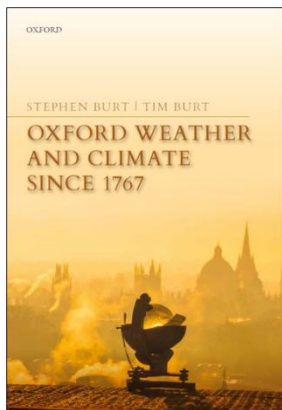
## **Publication 4: Urbanisation in the long Oxford temperature record, 1814 to date**

*Oxford's urban growth and its potential impact on the local climate.* Chapter 3 in *Oxford Weather and Climate since 1767* by Stephen Burt and Tim Burt, 2019: Oxford: Oxford University Press, 544 pp.

*Bibliography #14. Word count 3220 excluding references.*

*Authorship statement:* This chapter, 95% (chapter structure and outline, multi-site record access and retrievals, database preparation and analysis, chapter content): TB 5% (critical review). For the book as a whole contributions were SB 70% (proposal, structure, chapter outlining and content creation, publisher and University of Oxford liaison, database creation, QC and analysis, data digitisation from manuscript originals, photograph research, sub-editing and submission): TB 30% (chapter content creation, data digitisation from manuscript originals, database analysis, publisher and University of Oxford liaison, critical review).

---



The Radcliffe Observatory in Oxford (**Figure 6**), where meteorological records commenced in 1772, possesses the longest continuous single-site weather record in the British Isles. The daily temperature record is (almost) unbroken from November 1813, the daily rainfall record from January 1827 and the daily sunshine record from February 1880 – the rainfall and sunshine series are the world's longest daily same-site records. Original manuscript records dating back to 1760 and archival published summaries held in the University of Oxford and the Bodleian Library were digitised and combined with more recent computerised records (including current observations which are still made at 0900 GMT daily by the University of Oxford School of Geography) during a three year private (i.e. unfunded) research project leading to the preparation of *Oxford Weather and Climate since 1767*, a book written jointly by the author with Tim Burt and published by Oxford University Press in June 2019 (Burt & Burt 2019 – bibl. #14). This work digitised and published the complete Radcliffe Observatory daily, monthly, seasonal and annual temperature, rainfall and sunshine series for the first time, in both book form and freely-available open-access online datasets, a considerable volume of work now in one place. (Resource and funding are sought to rescue thrice-daily barometric pressure data, available in handwritten manuscript registers held in Oxford University for the period 1811-1924, as set out in Chapter 3).

A key consideration for any long-term temperature series relates to the urbanisation of the site where the records were or are made. If and when development occurs in the vicinity of the observing site, its effects can be complex – they may vary with season, with hour of day (day maximum and night minimum may show very different influences), they are unlikely to be linear





**Figure 6.** *The morning observation being taken at the Radcliffe Meteorological Station, Oxford. Photograph by the author*

over the period of record, and so on. On a global scale, Oxford is a relatively small city (population in 2015 168,000), and as such the record integrity seemed likely to suffer less than the case for larger cities such as London (see, for example, Chandler 1965, Oke 2017). The issue was first publicly raised in a famous exchange between Gordon Manley and Gordon Smith, then the Director of the Radcliffe Meteorological Station, in 1974/75 following the former's publication of the extended Central England Temperature series (Manley 1974, Smith 1975), when Smith cast doubt upon Manley's assertion of a small urban effect on the record ( $\sim 0.1$  K since 1815). Recent developments in Oxford, particularly the redevelopment of the Radcliffe Infirmary complex close to the observatory buildings, mandated qualification and quantification of urban influence on the continuing record of air temperature at the Radcliffe Observatory site.

This chapter, from *Oxford Weather and Climate since 1767*, compared the Radcliffe Observatory record with other long-period sites to assess long-term trends, and also with the relatively close and mostly rural site at Wallingford to assess site characteristics on maximum and minimum temperatures.

*Long-period urbanisation.* The very length of the Oxford record means that there are few temperature records of comparable length in the British Isles. It would seem obvious to compare the record against Manley's Central England Temperature series (dating from 1659), but to do so would introduce a circular argument, as the CET series itself is heavily based upon the Oxford record from 1815 to 1879. In the end, comparisons against the long temperature record from Rothamsted (a rural site about 65 km east of Oxford, with daily maximum and minimum temperatures available from 1878 to 2017) and against CET both suggest that Oxford's urban effect is now about 0.2 K of the 1.7 K rise in mean temperatures seen since 1814 (annual mean temperature 1814-1840 9.33 °C, 1991-2020 11.07 °C). Both minimum and maximum temperatures have risen over the 200 years, but the evidence suggests a more rapid increase in maximum temperatures in recent decades, arising from a combination of less frequent cold winter weather together with warmer summer days.

*Urban heat island (UHI).* Comparison was made with three years of daily maximum and minimum temperatures recorded at Wallingford (22 km south-east of the Radcliffe Observatory site, where the Centre for Ecology and Hydrology, CEH, has maintained weather records at a rural site some



distance outside the town since 1961). There is a slight altitude difference (Wallingford 48 m, Oxford 63 m) which would be expected to result in Oxford being about 0.1 K cooler on average. As expected, there is a clear difference between day and night temperatures. Oxford's mean minimum temperature averages 0.93 K above Wallingford, with a slight seasonal variation (summer higher) and a marked positive skew. By daytime, the magnitude of Oxford's UHI is reduced - the mean maximum temperature at Oxford averaging just 0.27 K higher than at Wallingford. There is also a very marked seasonal variation related to solar angle – differences are close to zero at the midwinter solstice, but around +0.7 K at midsummer. This seasonal variation can be accounted for by a combination of shading of the site by the Observatory buildings in midwinter, and stored heat within the urban fabric in summer (the observing site is located in a large enclosed quadrangle within Green-Templeton College). Oke (1973) examined maximum urban heat island effects as a function of settlement size, suggesting a *peak* urban heat island effect in a city of Oxford's size of up to 5 K in favourable conditions, which vary diurnally and seasonally. More recently, and locally within the UK, the urban heat islands of London (Wilby, 2003), Birmingham (Tomlinson et al, 2012), Manchester (Levermore et al, 2018) and Reading (Nicholson, 2020) have been examined. Using a land-use model, Bassett et al (2020) estimated the contribution of urban warming within Great Britain (England, Wales and Scotland) to average 0.04 K, with the rider that about half the population currently live in urban areas where the average daily mean warming is closer to 0.4 K.

In summary, this chapter shows clear quantitative evidence for a slight urban heat island affecting the Radcliffe Observatory site, with the magnitude of this effect greater by night (i.e. on minimum temperatures) than by day (maximum temperatures), and in daytime greater in summer than in winter. Since the start of the record, the Radcliffe Observatory site has warmed by about 0.2 K relative to a hypothetical nearby rural exposure.

The original aspects of this publication, and the wider book, can be summarised as follows:

- (i) The digitisation, quality control, analysis and publication of the entire Radcliffe Observatory record, the first publication of records since 1935, making the entire dataset available freely available online to the meteorological community for the first time;
- (ii) Quantifying the long-term and local heat-island effects on the Radcliffe Observatory record, a matter of some dispute prior to publication, by 'unpicking' the impact of urbanisation on the record from the warming trend due to climate change;
- (iii) Unearthing from original archives, analysing and publishing comprehensive site and instrumental metadata for the entire instrumental series at Oxford.

## Paper 5: A 200-year record of thunderstorms in Oxford

**Two hundred years of thunderstorms in Oxford**, by Stephen Burt. *Weather*, 2021, online publication 9 February 2021: <https://doi.org/10.1002/wea.3884>

*Bibliography #6. Word count 4665 excluding references.*

*Authorship statement:* Sole authorship.

---

The previous publication outlined the long instrumental records at Oxford's Radcliffe Observatory. Oxford is fortunate in that records of other non-instrumental or eye observations survive, in addition to the daily instrumental values of temperature, precipitation and sunshine. Most of these sources were catalogued during the preparation of *Oxford Weather and Climate since 1767*, and some were published in monthly and annual summary form up to 1935. Much remains in hardcopy manuscript format awaiting funding to establish the substantial scanning and digitisation effort required to extract all of the available record into computer-accessible form.

A key publication series consulted frequently during this work were the volumes entitled *Astronomical Observations made at the Radcliffe Observatory in the year [xxxx]*. These volumes, usually abbreviated as *Radcliffe Results* and containing mainly astronomical data, were first published in 1840, and mostly annually thereafter. Although meteorological observations had been made at the Observatory since 1772, with numerous breaks until late 1813, comprehensive meteorological data tables were not included in *Radcliffe Results* until the 1853 volume. Eventually the meteorological tables were published separately, in multi-year volumes some years in arrears, until 1935 when the (astronomical) Observatory relocated to the sunnier skies of South Africa, when publication ceased.

The *Radcliffe Results* tables also include notes of the dates of occurrence of fog, snowfall, thunderstorms, aurora and suchlike. From manuscript records starting in 1828 and then from the *Radcliffe Results* tables from 1853 to 1935, the author digitised the dates of every thunderstorm noted at the Observatory to assemble a century-long record of thunderstorms in the city. Unfortunately, the daily records from 1936 onwards are no longer retained within the University, although monthly frequencies were summarised until 1985. From 1971 to 1985 inclusive, dates of thunderstorms could be extracted from the Met Office MIDAS dataset (Met Office, 2019). Records of thunderstorms and snowfall, etc. were not kept by the University after 1985, but fortunately a high-quality local record was, and is, maintained by a local amateur meteorologist. After checks with local sites to ensure consistency, the continuity of the record appears sound. The complete series was presented and analysed in *Two Hundred Years of Oxford Thunderstorms* in a University of Reading, Department of Meteorology seminar in April 2020 and subsequently published in *Weather* (online publication 9 February 2021) – Paper No. 5, bibliography #6.

This work was stimulated by research by Valdivieso et al (2019) on national trends in thunderstorm frequency over the period 1884-1993 which included earlier, published records from Oxford up to

1986 (and to which the author contributed towards the end of the project). The improved granularity of the daily Oxford records digitised by the author, and their extension prior to 1884 and forward to 2019, enabled consideration of possible longer cycles in the data, as considered below.

This 200-year record of thunderstorms in a single city (**Figure 7**) is almost certainly unique anywhere in the world. The record is compared to (shorter) records from several sites in west London together spanning almost 150 years, which exhibit evident coherence with the Oxford record. Only with records of this length can long-term cycles of thunderstorm activity be detected: the records suggest there may be a very approximate 20-year interval between peaks. The possible mechanisms for this are as yet poorly understood, but may reflect some influence of the sunspot cycle and the changing polarity of the Sun’s magnetic field (which has a 22-year cycle, and has been previously linked with both changes in thunderstorm frequency and circulation changes - Brooks, 1934; Kukoleva et al, 2018; Lavigne et al, 2019) together with possible links with auroral incidence. Publication of the series (including publicly available access to original datasets which have been made available on Figshare) permits wider academic community access to the records.

The metrology aspects of this project were particularly challenging, for a formal definition of a ‘day with thunder’\* did not exist until the second half of the 20th century, and experience-based judgement had to be applied to earlier observations to ensure, as far as was possible, that the criteria for inclusion/exclusion remained broadly comparable. Evidence was provided that records from Oxford previously published in the *Monthly Weather Report*, the source primarily used by Valdivieso et al, were most probably a subset of the true frequency of ‘days with thunder heard’.

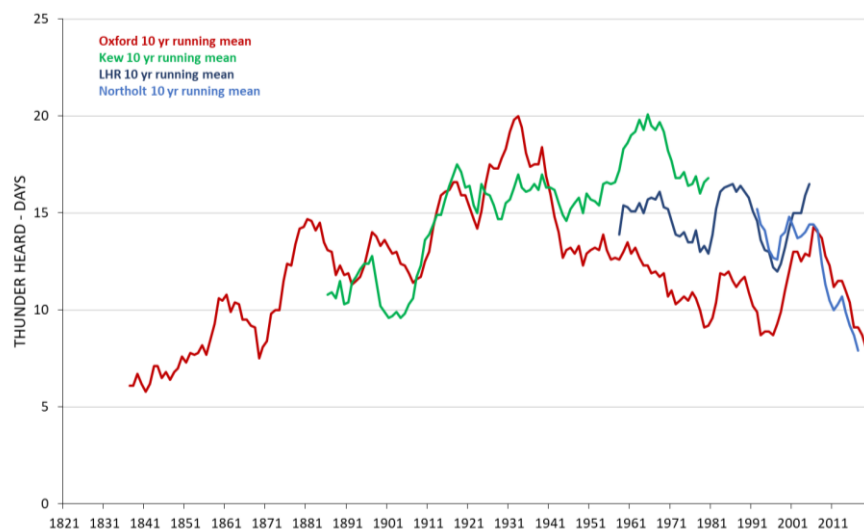


**Figure 7.** Ten-year running means of thunderstorm frequency (plotted at year ending) for Oxford (dark red line) 1828-2019, alongside similar averages for sites in west London – Kew Observatory (1877-1980, green line), Heathrow Airport (LHR, 1949-2005, dark blue line) and Northolt (1984-2019, light blue line). Figure 8 from Burt (2021)

\* “**Thunder heard.** Every day when thunder is heard, at any time from midnight to midnight (GMT), is counted as a day of thunder.” Meteorological Office *Monthly Weather Report*, 1965, Introduction, page (v).

Original elements and ‘new knowledge’ in this paper include digitisation from original sources, dataset assembly and open-access publication of a unique and very long record of thunderstorms in a single city; identification and analysis of thunderstorm occurrence by synoptic regime; and quantitative reasoning applied to synoptic regime changes to suggest possible reasons for the steep decline of thunderstorms in Oxford (and more widely in southern England) in recent decades.

**Planned future work** Whilst researching the Oxford records, a paper from 1897 (Mossman, 1897) was found, containing monthly and annual summaries of various weather elements, including frequency of thunder, snowfall, aurora, gales, etc, for London back to 1713. Numerous original sources are listed, many being manuscript diaries. Mossman (incidentally, one of the Ben Nevis observers) referred to his manuscript working notes for this research as having been deposited in the Royal Meteorological Society’s Library. Eventually I traced these to the Met Office Archives in Exeter, who were kind enough to provide a scanned copy of the originals (untouched for over a century); the original manuscript notes list all events at daily resolution. It is hoped that these will provide the basis of a similar record of thunderstorms for the London area extending back over 300 years, while the existence of a forgotten auroral series of the same length will undoubtedly prove useful for historical ‘space weather’ series (see, for example, Lockwood et al, 2010; Hawkins et al, 2019).

## **Paper 6: Durham’s barometric pressure records, 1843-1960**

**Durham’s barometric pressure records, 1843-1960.** Appendix 5 in *Durham Weather and Climate since 1841* by Tim Burt and Stephen Burt. Oxford: Oxford University Press (in press, to be published spring 2022).

*Bibliography # 2. Word count* 6800 approx. excluding references.

*Authorship statement:* This chapter, 95% (chapter structure and outline, multi-site record access and retrievals, database preparation and analysis, chapter content): TB 5% (critical review). For the book as a whole contributions were SB 50% (proposal, structure, chapter outlining and content creation, publisher liaison, digitisation from manuscript sources, database creation and analysis, photograph research, preparation of synoptic maps, sub-editing and submission): TB 50% (chapter content creation, digitisation from manuscript sources, database analysis, photograph research, publisher and University of Durham liaison, critical review).

A slightly abbreviated version of this chapter has been accepted for a Special Issue of *Geoscience Data Journal*, on **Locating, Imaging and Digitizing Historic Geoscience Data**, to be published in October 2021. The online version of the Durham barometric pressure dataset was published in April 2021.

---

Meteorological records began at Durham Observatory in 1841, as an integral part of astronomical observations. Manuscript records of twice-daily manual instrumental and eye observations survive from July 1843 (**Figure 8**) to October 1999, when manual observations ceased upon the installation of a Met Office automatic weather station which remains in operation today. The site has remained almost unchanged since the beginning of the record, with little if any urban influence detectable in the long temperature record. Durham is second only to Oxford's Radcliffe Observatory in record length in England, and is one of the longest single-site meteorological records in Europe. The record includes daily rainfall from 1843, sunshine from 1880 to 1999 (mostly daily), and twice-daily barometric pressure from 1843 to 1960. Gordon Manley (1902-1979; Tooley & Sheail, 1985) was Durham's first Professor of Geography from 1927 to 1939, and in his time as curator of the observatory he began assembling and compiling the temperature, precipitation and sunshine records, publishing an extensive analysis of the temperature record in 1941 (Manley, 1941), foreshadowing his later work on the Lancashire temperature series (Manley, 1946) and the Central England series (Manley 1953, 1974) for which he is best known. It was Manley's dying wish to see the Durham meteorological record elevated to the same status as Oxford.

Day	Bar.	Air	Earth	Sun	Moon	Wind	Rain	Remarks
July 23. 9 A.M.	29.34	14.4	56.6	47.2	---	N.W. 6.	12.2	Rainy
9 P.M.	29.50	15.7	47.8	---	59.8	N.W. 2	---	Fine and Clear
24. 9 A.M.	29.70	15.5	55.5	43.8	---	N.W. 1	3.56	Fine
9 P.M.	29.77	14.6	49.7	---	59.4	N.W. 1	---	Fine & Clear
25. 9 A.M.	29.84	17.1	63.6	45.4	---	W. 2	---	Fine
9 P.M.	29.88	17.8	55.7	---	68.5	S. 2	---	Fine
26. 9 A.M.	29.80	17.4	61.2	57.5	---	S.W. 3	---	Fine
9 P.M.	29.71	17.9	60.5	---	67.8	S.W. 3	---	Cloudy
27. 9 A.M.	29.64	19.1	62.4	53.2	---	N.W. 3	0.05	Cloudy
9 P.M.	29.66	17.3	55.5	---	66	W. 2	---	Cloudy
28. 9 A.M.	29.58	16.8	61.2	51.2	---	W.S.W. 1	---	Cloudy
9 P.M.	29.50	16.3	52.8	---	65.3	W.S.W. 2	---	Rainy
29. 9 A.M.	---	---	---	57.6	---	---	---	---
9 P.M.	29.10	16.1	52.9	---	65.2	W. 3	---	Fine & Clear

**Figure 8.** The first page of surviving manuscript meteorological records from Durham Observatory, showing twice-daily observations for 23-29 July 1843. (Durham University Library)

Most of the original manuscript meteorological records (and some instrumental metadata) from the Durham Observatory have been retained, either in the Department of Geography or in the Durham University library. An initiative funded by the Leverhulme Trust saw many of the manuscript instrumental records from 1850 to 1997 digitised (Kenworthy et al, 1997), although knowledge of this dataset remained almost entirely within Durham University. Once more jointly with Tim Burt, emeritus Professor of Geography at Durham (no relation), the author embarked upon assembling a definitive climatological database for Durham, researching, compiling and assembling records from various sources including the Met Office archives (both digital and physical). The output from this project again takes the form of a book, *Durham Weather and Climate since 1841*, to be published by Oxford University Press in spring 2022. The full dataset will be made freely available online

through Durham University and the major online climatological databases to coincide with the book's publication.

A particularly valuable component of the Durham record is the twice-daily (09h and 21h) observations of barometric pressure which spans 118 years from July 1843 to December 1960, the record ending following reorganisation of the observing resource at the university. Records from January 1850 were digitised in 1997 in the Leverhulme Trust project referred to above, but until very recently the existence of this record was also unknown outside Durham University. Since then, the 1843-49 records have been digitised by the author and Tim Burt between them (in all, almost 15 000 datapoints). This pressure record, which is 98.7% complete between 1843 and 1960, represents by far the longest single-site barometric pressure series in England\*. It fills a very large temporal and spatial gap in the International Surface Pressure Database (ISPD: Cram et al, 2015), which forms the majority of the input to the 20th Century Reanalysis version 3 (20CRv3 – Slivinski et al 2019, 2020). The latter has recently been extended back to 1836, and experimentally back to 1806.

This chapter from *Durham Weather and Climate since 1841* describes the newly-available Durham pressure series, from instrumental metadata through the various stages in the digital recovery to online publication.

Unfortunately, the Leverhulme Trust project record as originally digitised contained a large number of major errors resulting from a combination of mistakes in reading the instrument together with subsequent transcription or digitisation errors, and was unusable in its original form. In the work here referenced, the author describes the record sources, digitisation work and quality control measures to identify and correct the most significant errors in the digitised dataset. This required access to original archival sources relating to the instruments in use, some of which are held in Durham University Library, and others in (previously restricted) Met Office site inspection reports and correspondence retained within the Met Office Library and Archives in Exeter. In what is believed to be the first time this has been attempted, the 20CRv3 reanalysis dataset was itself used, successfully, to provide a measure of underpinning sub-daily quality control to an independent long-period pressure series (i.e. one which was not previously included in the reanalysis assimilation).

The entire Durham pressure series 1843-1960 has since been published (Burt 2021, bibl. #1), and will in due course be included within ISPD and Copernicus datasets. Until very recently, there were no ISPD records from sites in England (and thus none available to 20CRv3 reanalyses) prior to 1925. Before 1925, the only ISPD records within the British and Irish Isles are those from Armagh in Northern Ireland (pressure data from 1796-1826, 1833-1965), Aberdeen in Scotland (1871-1948, 1957-1988), and Valentia Observatory in the Republic of Ireland (1892 to date) (**Figure 9a, 9b**).

---

\* A multi-site series for London extending back to 1692, originally based upon daily means rather than observations at specific hours of the day, was assembled by Richard Cornes (Cornes, R., 2010: *Early Meteorological Data from London and Paris*. PhD thesis - University of East Anglia) – see also Cornes et al (2012) Cornes, R. C., P. D. Jones, K. R. Briffa et al, 2012: A daily series of mean sea-level pressure for London, 1692–2007. *Int. J. Climatol.*, **32**, 641-656.).

Recent work by Hawkins et al (2019) has added to this meagre fare high-quality hourly pressure data from Fort William and Ben Nevis for the period 1883-1904, together with extensive contemporary synoptic observations from British and European sites published in the UK Met Office contemporary *Daily Weather Report* publication between 1860 and 1910 (Craig and Hawkins, 2020), although neither has yet been added to ISPD. Consequently, the accuracy of atmospheric reanalyses over the north-eastern Atlantic prior to 1925 has to date been sub-optimal (see, for example, the comparison of the Ulysses storm of February 1903 in Hawkins et al. 2019) owing to lack of reliable surface pressure records in and around the British and Irish Isles. The newly-available record from Durham has itself already provided confirmation of incorrect bias assumptions in ship data assimilated within 20CRv3 during 1914-19\* (**Figure 10**), and once incorporated within an updated 20CR should therefore result in substantial improvements (reductions in ensemble spread) in future reanalyses.

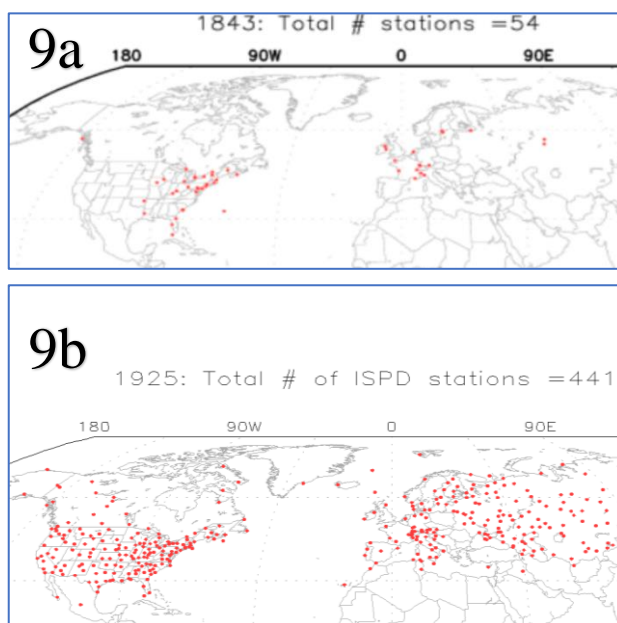


**Figure 9.** Location of pressure observations within the International Surface Pressure Database for (9a) 1843 and (9b) 1925. Twice-daily records from Durham Observatory are available from July 1843 and significantly increase the density of observations in and around the British and Irish Isles, particularly prior to 1925. Plots obtained from NOAA PSL at <https://psl.noaa.gov/cgi-bin/data/ISPD/stationplot.pl>

---

\* This ongoing investigation, which might perhaps be termed *forensic historical meteorology*, involves detailed examination of (often very limited) extant metadata for Royal Navy and Merchant Navy ship barometers for the Arctic Fleet during World War I. It is expected to lead to a future publication.



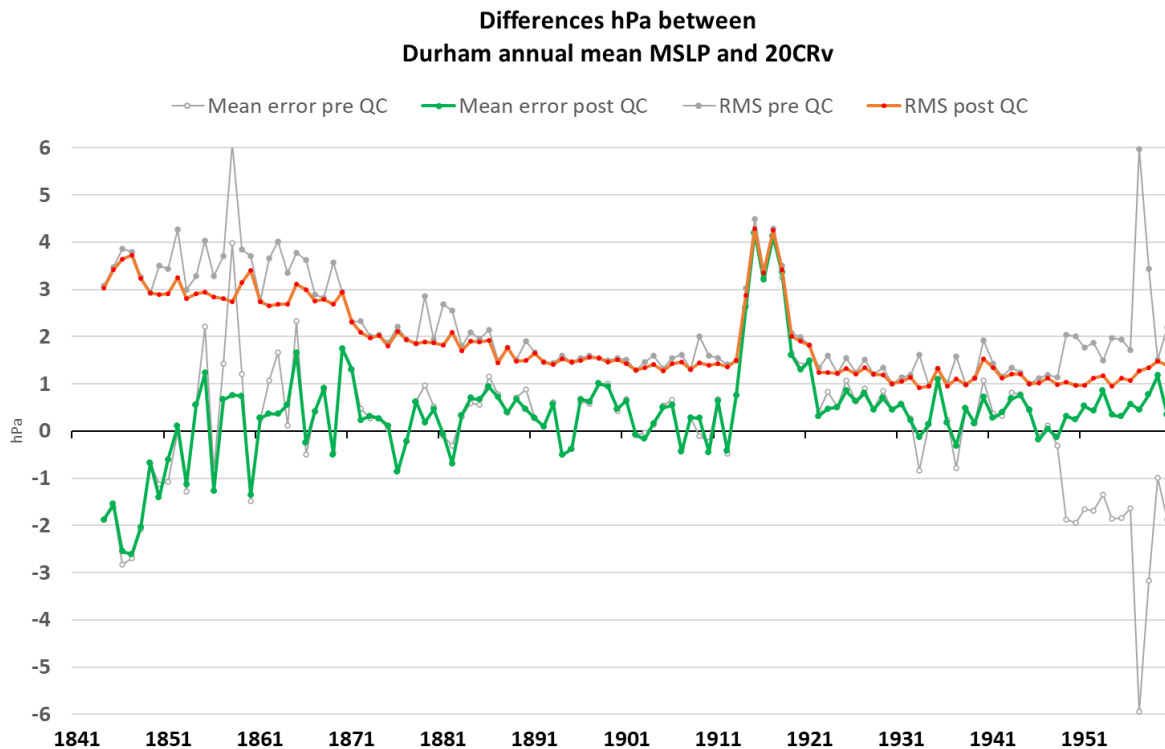
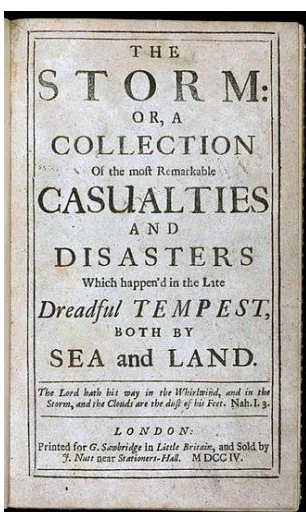


**Figure 10.** Comparison between annual mean MSL pressure (hPa) at Durham Observatory and the 20th Century Reanalysis version 3 (20CRv3) for 1844 to 1960: the green line shows the average arithmetic difference post-QC and the orange line the average root mean square error (RMS) post-QC: the faint grey lines shows their pre-QC values. Digitisation and careful quality control of the Durham record revealed a previously unknown bias in the 20CRv3 reanalysis dataset between 1914 and 1919, which is the subject of ongoing investigation. The large pre-QC bias from 1949 likely resulted from incorrect barometer temperature observations together with several changes in the barometers in use.

## 2.3: Applied historical climatology



The methodical analysis and documentation of significant weather events has a long history, some of the earliest examples being Daniel Defoe's account of the Great Storm in December 1703 (Defoe, 1704, frontispiece shown left: Brooks, 1927; Clow, 1988; Brayne, 2002) and Heinrich Brandes' 1819 analysis of the windflow and circulation of the storm of 6 March 1783, the first synoptic mapping of weather systems (Brandes, 1820; Kington, 2010 chapter 6). Many such event histories have catalysed expansion of knowledge on a wide range of weather and climate processes. Dozens of possible examples include Fitzroy's documentation of the *Royal Charter* storm of October 1859, which led directly to the introduction of coastal storm warnings and the first 'weather forecasts' (Fitzroy's own term) (FitzRoy, 1860), the wind measurement and civil engineering lessons



following the Tay Bridge disaster in December 1879 (Scott, 1880), the deduction of global upper wind patterns following the Krakatoa eruption in August 1883 (Symons, 1888), the unravelling of convective supercell dynamics in the Wokingham hailstorm of 9 July 1959 (Browning and Ludlam, 1962) and the Hampstead storm of 14 August 1975 (Keers and Wescott 1976, Miller 1978), and the seeder/feeder mechanism in orographic rainfall (Hill, Browning and Bader, 1981).

Such analyses serve numerous purposes, the most important of which are the compilation, preservation and dissemination of knowledge relating to the event, for the benefit of both present and future researchers. In particular, the conservation/preservation of collated meteorological information can become increasingly fragmented with the passage of time. Key components include:

- *Why, where and when did these events occur?*
- *What was their impact?*
- *What can we learn from the event/s described? and*
- *What is the longer-term context/climatological frequency of the event/s described?*

The author has published numerous original analyses of specific meteorological events affecting the British and Irish Isles/North Atlantic over the past 40 years, a selection of which are briefly summarised below. All have contributed new knowledge to the meteorological community. Many have resulted in follow-on projects or papers, and some have received dozens of citations or hundreds of downloads. Some events have been re-analysed by others in the light of newer information sources, such as reanalysis datasets and numerical modelling techniques which were not available at the time the paper was written.

**Blizzards and snowstorms** An account of the severe blizzards in south-west England in mid-February 1978, in which over 100 cm of snow fell over higher ground in Devon and Cornwall and in South Wales (Burt 1978 – bibl. # 61; Laing, 1979; Ching, 2008). Together with a major snowstorm affecting central southern England in early January 1982, this was probably the most significant and widespread snowfall event in England during the second half of the 20th Century. Other published work on this topic analysed the widespread heavy snowfalls of winter of 1978/79, the snowiest British winter within the last 50 years (Burt 1980 - bibl. #59), and the synoptic circumstances producing very late spring snowfalls in 1981, where depths exceeded 60 cm in Gloucestershire and Derbyshire during the final week of April (Burt 1982 – bibl. #58). Clearing skies following significant snowfall in northern Scotland towards the end of December 1995 ultimately resulted in the temperature falling to -27.2 °C at Altnaharra in Sutherland on 27 December, equalling the UK's lowest reliably observed air temperature to date (Burt 1997 – bibl. # 46).

**The 'Great Storm' of 15/16 October 1987** A joint-author paper with Doug Mansfield (Met Office) was prepared and submitted within two months of the event, documenting and analysing the events of south-east England's 'Great Storm' of October 1987, the most violent gale in this area since Defoe's storm in 1703 (Burt & Mansfield, 1988 – bibl. # 52). This paper currently has the highest readership and citation statistics of any of the author's papers, with 81 citations on Google Scholar to date, and 57 on Scopus (as at 23 June 2021: see Table 1 in Chapter 3). In particular, the

paper and its analyses of the wind fields during the event were cited by Browning in his work on recognising the sting jet phenomenon and developing the first model to identify and explain such events (Browning 2004), together with other works on modelling such intense and severe cyclonic storms (see, for example, Shutts, 1990; Baker, 2009) and particularly on studies related to windstorm effects and damage (see, for example, Gardiner et al, 2010; Knox et al, 2011; Gibbs and Greig, 2012).

**Intense convective rainstorms** The ‘Boscastle flood’ of 16 August 2004 was a severe flash flood in north Cornwall. It resulted from the repeated development and intensification of, individually, fairly shallow cumulonimbus rainstorms whose rain swathes were both very intense and remarkably localised in extent (**Figure 11**). The event occurred in peak holiday season, and a large number of fatalities were narrowly avoided by the prompt actions of the emergency services, including coastguard helicopters who winched stranded visitors to safety on live television as cars and buildings were washed away by floodwater. The author’s paper (Burt 2004 – bibl. #39) set out the temporal and spatial characteristics of the rainstorms using both the surface raingauge network and radar rainfall estimates, providing detailed and original interpretations of storm intensity from both instrumental and eyewitness observations of the storm and its hydrological impacts, and included quantitative comparisons with previous notable convective rainstorms in the British Isles. Numerous modelling studies of this famous flood have been published over the years, many citing this paper (for example, Golding et al, 2005, Warren et al, 2014; Kendon et al, 2014; Chan et al, 2014; and others). Google Scholar lists 56 citations to this paper, Scopus 43 (Table 1 in Chapter 3).

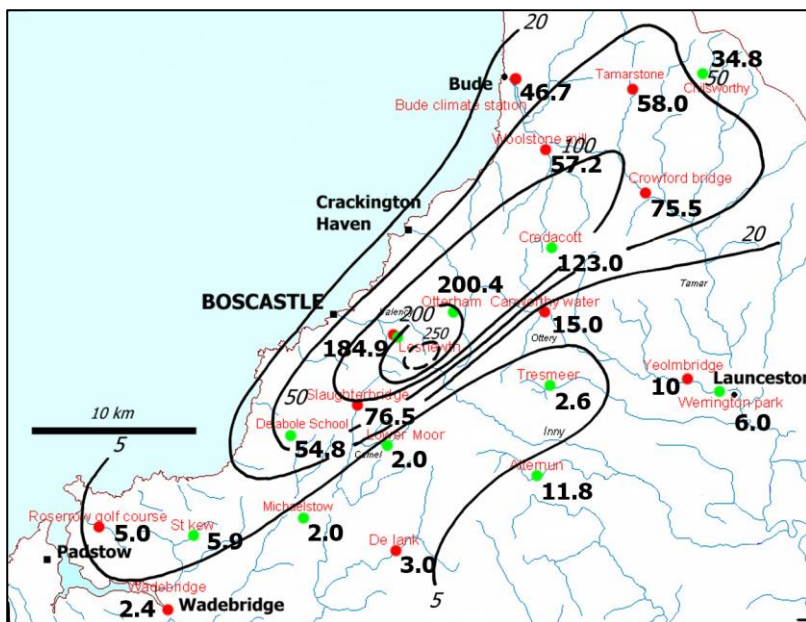


*Figure 11. Approximate distribution of rainfall for the rainfall day of 16 August 2004 in north Cornwall – the Boscastle Storm. Units are millimetres: isohyets are at 5, 20, 50, 100 and 200 mm. Figure 3 from Burt 2005 – bibl. #39.*

**Heatwaves** The Augusts of 1990 and 2003 both included exceptional heatwaves. Both months saw new long-term site records broken, including successive UK record high temperatures to that date (37.1 °C at Cheltenham on 3 August 1990, and 38.1 °C at Kew Gardens on 10 August 2003\*). The heatwave events were methodically analysed by the author (August 1990 in Burt 1992 – bibl. #48:

\* A maximum temperature of 38.5 °C was reported from Faversham in Kent, but the validity of the reading has been questioned owing to gross over-shelter of the Stevenson screen by nearby tall hedging.

August 2003 in Burt 2004a, Burt & Eden 2004, Burt 2004c – bibl. # 40, 41 and 42). All aspects were examined, including high night-time minimum temperatures, now regarded as a major factor in heatwave fatality but rarely considered in the meteorological literature until then (see, for example, Green et al 2016, Basarin et al 2020 and Brimicombe et al 2021).

As Britain's climate warms, heatwaves have become both increasingly common and more intense, particularly in south-east England. Comparative studies of the frequency, intensity and extent of previous heatwaves provide compelling evidence of a warming climate and the decrease in recurrence intervals for various heatwave thresholds (Kendon et al 2020; Christidis et al 2020) and contribute to climatological and societal awareness of past extremes.

## **Paper 7: The extraordinary mildness of December 2015**

**December 2015 – an exceptionally mild month in the United Kingdom**, by Stephen Burt and Mike Kendon (Met Office), 2016. *Weather*, **71**, pp. 314-320.

*Bibliography # 21. Word count 2065 excluding references.*

*Authorship statement:* SB 70% authorship (article structure and drafting, multi-site record access and retrievals, database preparation and analysis, artwork preparation, critical review and journal submission); MK 30% (multi-site record access and retrievals, database preparation and analysis, statistical analysis, long series extremes and critical review)

---

Paper 7 is an example of this type of event analysis, in this case examining the large-scale synoptic environment responsible for the extraordinary warmth of December 2015 – a month which produced the greatest positive departure from normal temperature of any month on the Central England Temperature series dating from 1659. This joint-author paper, written with Mike Kendon from the Met Office, reviewed the circumstances of the month on a daily and monthly basis, and compared and contrasted the circumstances with the exceptionally cold December of 2010, just five years previously, which was the coldest December since 1890. The month was also exceptionally wet: a second paper by the author in the same 'Special Issue' of *Weather* examined the distribution of rainfall (Burt 2016 – bibl. #20). New all-time rainfall amounts, on timescales from 24 hours to three months, were established during the month at locations in the Lake District and North Wales, and in the Republic of Ireland.

**Papers 8 and 9** are considered together in the following section.

## **Paper 8: Extremes of barometric pressure in the British Isles**

*Capstone article as two-part PDF. The Lowest of the Lows ... extremes of barometric pressure in the British Isles, part 1 and The Highest of the Highs ... Extremes of barometric pressure in the British Isles, Part 2 – the most intense anticyclones* by Stephen Burt. Part 1: *Weather*, 2007a, 62, pp. 4-14, Part 2: *Weather*, 2007b, 62, pp. 31-41.

*Bibliography #34 and #35. Word count* Part 1, 6730; Part 2, 4245 (10,975 combined), excluding references. *Authorship statement: Sole authorship*

## **Paper 9: Winter 2020's second pressure extreme – late March 2020**

### **New British Isles late-winter extreme barometric pressure, 29 March 2020**

by Stephen Burt. *Weather*, published online 16 Oct 2020, <https://doi.org/10.1002/wea.3840>

*Bibliography #3. Word count* 2200, excluding references.

*Authorship statement: Sole authorship*

---

The final two papers examine and quantify historical records of extreme barometric pressures in the North Atlantic and the British and Irish Isles, contributing to a coherent and original body of published work now comprising the largest, most detailed and up-to-date analysis on the subject. This body of work consists in all of 16 papers, articles or published correspondence on the topic now spanning almost 40 years in all, the earliest dating from 1983, the two most recent papers covering events in 2020 and published in 2020 and 2021. The events analysed in these publications combine current synoptic observations and numerical forecast model output with published case studies and other original sources including manuscript documents, letters and accounts, many well over 100 years old.

It follows from their categorisation as ‘extreme’ that the events which form the subject matter are infrequent in their occurrence: contemporary contextual documentation is thus necessarily spread over many years, and very often fragmented. **Paper 8** is a two-part ‘capstone’ paper from 2007, summarising known temporal and spatial distributions of barometric pressure extremes over a 200-year period to that date; **Paper 9** is a very recent case study of the intense anticyclone of 29 March 2020. The latter includes descriptions and analysis of the synoptic circumstances and evolution of the systems involved, together with contextual ‘new extremes’ updates to Paper 8, and extends the author’s previous published work on this topic.

The original impetus for work on this subject can be traced to the passage of an exceptionally deep extratropical cyclone (ETC) close to the British Isles in late December 1982, during which MSL pressure fell to 938 hPa at Stornoway in Scotland’s Western Isles (**Figure 12**, and Burt 1983 – bibl. #57). This was the lowest barometric pressure recorded anywhere in the British and Irish Isles for

almost a century. Although the depth and track of the depression had been well forecast by the Met Office numerical models of the time, the event highlighted one unforeseen aspect of aviation flight planning — namely, that the minimum ‘airfield level’ pressure setting (QFE) on aircraft altimeters at the time was 950 millibars (hPa). The depth and extent of this storm was such that, for a time, much of north-west European airspace had to be closed during the passage of the storm, because the requirement for a minimum safety margin for forecast altimeter settings for airfield surface pressures — below 960 hPa — could not be met. As a result, numerous transatlantic flights had to be diverted from their intended destinations, and others cancelled or delayed until the storm system filled and barometric pressure recovered.

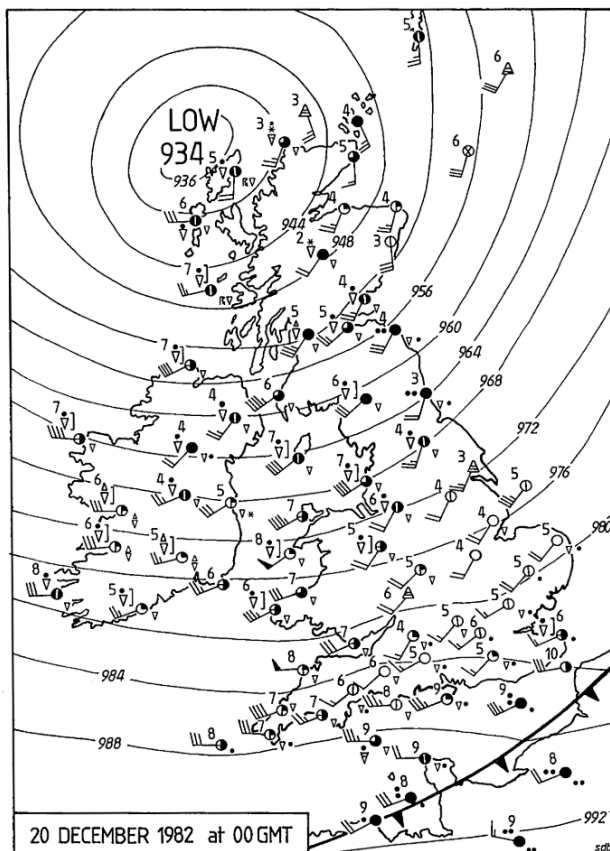


*Figure 12. British Isles surface chart for midnight GMT 20 December 1982, showing cloud, wind, present and past weather and temperature (°C). The isobars are drawn every 4 mbar. Figure 3 from Burt 1983 – bibl. #57.*

The author was in the Met Office’s Special Investigations Branch at the time, and at short notice was tasked with providing a ‘back of the envelope’ climatological assessment of the historical frequency of any previous similar events within and near British airspace for the Civil Aviation Authority. Met Office digital datasets for individual station records extended back only as far as 1957, 25 years, and prior to reanalysis datasets (still 30 years in the future) the only sources of pressure extremes were published case studies in the meteorological literature. I was surprised to find that no comprehensive analysis existed detailing historical extremes of barometric pressure in the north Atlantic and north-west Europe. Fortuitously, several months earlier I had already begun to look into such events on my own account and so could quickly provide preliminary evidence demonstrating that similarly intense extratropical cyclones were ‘rare but not unprecedented’. Scattered historical records and case studies within the available literature back as far as the 1870s indicated that such events had previously occurred in or close to British airspace perhaps ten times

within the previous 100 years, that clusters of increasingly intense systems spanning 10-15 days occurred in a few winters, and provided clear evidence of considerably deeper depressions than the December 1982 event. Such advice to the aviation authorities proved timely, as several other low pressure centres subsequently attained similar depths later that winter, with consequent risks to aviation flight planning and safety margins. Following these incidents, operational recommendations for airlines operating both transatlantic and north-western Europe routes within British and Irish airspace were subsequently amended to reduce minimum altimeter settings from 950 hPa to 925 hPa to ensure an improved safety margin in the event of similarly intense extratropical cyclones in future.

The two-part capstone paper from 2007 (Paper 8) built upon the intervening 25 years of methodical literature searches to uncover previous events, both exceptionally deep extratropical cyclones and intense anticyclones, seeking to establish a definitive climatological analysis of the range and historical frequency of such events, in both temporal and spatial terms. As well as the meteorological journals, the literature search eventually encompassed sources as diverse and obscure as the keepers logs of the Northern Lighthouse Board in Scotland, Irish historical sources (Burt 2006 – bibl. #36) and the Royal Society library. The search for historical events is somewhat complicated by the change in units promulgated in the UK Met Office in 1914 (Gold 1914), from inches of mercury to the millibar (1 mbar = 1 hPa; 1 inHg = 33.864 hPa): inches of mercury continued to be quoted frequently in the literature until the 1950s (and are still used in North American aviation). In addition, the lack of day-to-day familiarity with obsolete units (inHg in particular), which necessitates repeated cumbersome conversions, can make for rather heavy going on older accounts.

It was during this literature review that the oft-cited highest barometric pressure on record within the British Isles was found to have been incorrectly stated, a statement that remained unchallenged for over 80 years. The date and location of the event (Aberdeen Observatory, 2200 GMT on 31 January 1902) were correctly given, but the extreme value was incorrectly quoted as 1054.7 hPa in most collections of ‘extreme weather’ statistics for the British Isles (see, for example, Meteorological Office 1952 page 6; Meteorological Office 1973 Table 2). Only after much checking with original sources, including the hourly barograph tabulations from Aberdeen for 1902, could the correct value be determined, namely 1053.6 hPa. The cause of the error was ultimately a simple conversion error from the original value in inches of mercury to millibars, probably in the 1920s or 1930s, published once and simply cited without checks by all future references (Burt 2006 – bibl. #38). Fortunately, the corrected value now appears in lists of barometric pressure extremes for the United Kingdom; this little example serves as a lesson to us all in checking original sources wherever possible!

Outside British and Irish waters, a scattering of references in the literature to extratropical cyclones of exceptional depth (below about 930 hPa) in the North Atlantic were found, but the rarity of such events together with the fragmented nature of such references as did exist (few surface ships, or their observations, survived such encounters) posed significant challenges to assessing trends in historical frequency, development and growth mechanisms responsible and maximum storm depth

for such extreme cyclonic storms. The changing nature of commercial transport over the North Atlantic during the previous century or so also biased the number and source of observations from the region, as increasing air traffic from the early 1950s acted to reduce the number of surface ships (both passenger and commercial, together with the progressive withdrawal of the Ocean Weather Ships) which formerly provided the majority of surface observations. From the 1980s onwards, significant advancements in data assimilation for increasingly sophisticated numerical forecasting models improved both reliability and robustness of surface analyses in data-sparse areas, particularly over the North Atlantic, and improved surface and upper-air forecast products. Such improvements helped lead to 2-3 days warning of exceptional storms, leading to the great commercial and societal benefit of routing ships away from resulting expected severe weather — although of course this reduced still further ship observations close to the storm track.

One such storm developed from an exceptionally intense thermal gradient off the east coast of the United States and Canada in mid-December 1986, and eventually deepened to about 916 hPa between Greenland and Iceland at 61°N, 32°W at 0000 GMT on 15 December. An account of the development of the storm (Burt 1987 – bibl. # 53) included a preliminary summary of other exceptionally deep ETCs known from literature references.

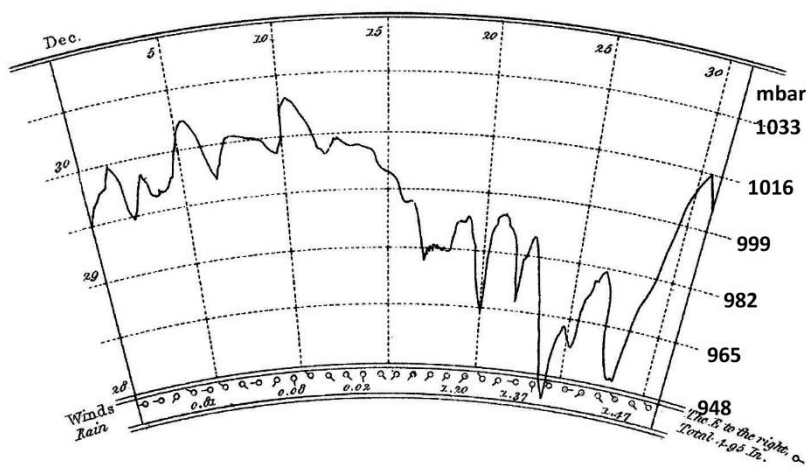
A very similar explosive ETC development in January 1993 spawned a depression whose centre deepened to 912-915 hPa on 10 January 1993 close to 62°N, 15°W, thereby surpassing the depth of the December 1986 storm (Burt 1993 – bibl. # 47). This storm remains today the deepest cyclone yet known in the North Atlantic: for a few hours its central pressure was the lowest yet recorded on the planet outside of tropical storms (and possibly the centres of violent tornadoes). One permanent outcome from the author's investigation of this event was that reporting protocols for pressure sensors on Met Office drifting buoys, deployed in the North Atlantic to report real-time surface wind and weather, were adjusted to avoid an automatic 'quality control' cutoff below 925 hPa, a value which was until then thought to be below any barometric pressure likely to be experienced in these waters. Unfortunately, a number of drifting buoy pressure observations close to the storm centre were lost in this way for several hours, as surface pressure dropped below this value close to peak development of this remarkably intense feature. Following discussions with the Met Office, the threshold 'cutoff' on these and future buoys was reduced to 875 hPa to avoid this happening in future.

In late February 1989, an unusual cyclonic development caused barometric pressure over southern England to fall below 950 hPa at sea level (Burt 1989 – bibl. # 51). In London, this was the lowest barometer reading since Christmas Day 1821, a storm famously documented by Luke Howard, whose account included the world's first published barograph chart (Howard 1822 – **Figure 13**).

The two-part capstone paper in Paper 8 (Burt 2007a, 2007b – bibl. # 34 and 35) consolidated historical and more recently cited events into a coherent and referenced climatology of the deepest ETCs and most intense anticyclones known to affect the British and Irish Isles. This represented the gradual accumulation of 25 years research into the topic, and now extended historical and archive coverage to over 200 years. Using consistent modern-day units, contemporary synoptic analysis and methods of reducing barometric pressures to mean sea level (a practice which began only in the



1860s), details of these events and their temporal and spatial extent were documented in this paper, Part 1 covering the deepest extratropical cyclones and Part 2 the most intense anticyclones. Detailed and up-to-date listings of the highest and lowest barometric pressures at a wide range of observing locations throughout the United Kingdom and the Republic of Ireland, and extremes by month of the year, were also included. This paper continues to be one of the author's most-read (see Chapter 3 for indicative 'read' and 'cited' statistics).



*Autographic Curve of the Variations of the Barometer at Tottenham, in the Months of November, and December, 1821.*

**Figure 13.** The world's first published barograph chart – Luke Howard's 'clockbarometer' (mercury barograph) record from Tottenham, north London, for December 1821, showing the extreme depth of the depression of 25 December. The values are not corrected to MSL (add about 4 hPa) and the original scale is in inches of mercury (inHg) – millibar equivalents are given on the right. From Howard (1822), Plate XIII, reproduced as Figure 3 in Burt 2007a – bibl. #34.

Of course, any event-based climatology of this type requires updating from time-to-time as new events occur. A very strong jet stream in December 2013 spawned a series of notably intense depressions over the North Atlantic which formed and deepened rapidly in quick succession, causing a prolonged spell of stormy and wet weather over the British Isles. The most intense of this sequence of storms passed close to north-western Scotland on 24 December as its central pressure fell to 927 hPa, the deepest depression in the vicinity of the British Isles for almost 130 years (Burt 2014 – bibl. # 25). At Stornoway the MSL barometric pressure fell to 936 hPa, remaining at or below 940 hPa for about 8 hours. This system was marked by widespread severe gales, prolonged heavy rainfall and extensive flooding, both fluvial and coastal, in many parts of the British Isles. At one time, almost 750 000 properties were without power owing to storm damage, although fortunately no fatalities resulted. There was also some disruption to aviation on this occasion, mostly due to strong surface winds or crosswinds at airfields rather than an inability to set aircraft altimeters low enough, as was the case in December 1982.

In contrast, two remarkably intense anticyclones occurred within weeks of each other in January and March 2020. These events were the first instances of MSL pressure exceeding 1050 hPa anywhere in the British or Irish Isles since 1957, and the highest recorded at any British or Irish site since December 1926. The author's previous research and publications enabled timely assessment of the likelihood of a very rare event on the basis of T+72 h forecasts, enabling advance media



briefings to be prepared. In the end, the January event represented the highest barometric pressure recorded in London in over 300 years of records, resulting in considerable media interest with references appearing in *The Times* (Simons 2020) and on BBC News (Amos 2020) during the event itself; an article prepared for *The Conversation* and syndicated worldwide received 23,271 reads within 7 days. A formal synoptic case study was speedily prepared, and subsequently published in *Weather* within three months of the event (Burt 2020 – bibl. # 12).

Paper 9 (Burt 2020 – bibl. # 3) describes the second event in late March 2020: this was, if anything, the more unusual in occurring well outside the existing climatological ‘envelope’ for previous events (**Figure 14**). The two events represented a unique occurrence in the 200-year series first set out in Paper 8 of two 1050 hPa events in the British Isles within a single winter season. Accordingly, substantial updates to the listing of site records and the map of absolute highest barometric pressure since 1948 were included in both papers.

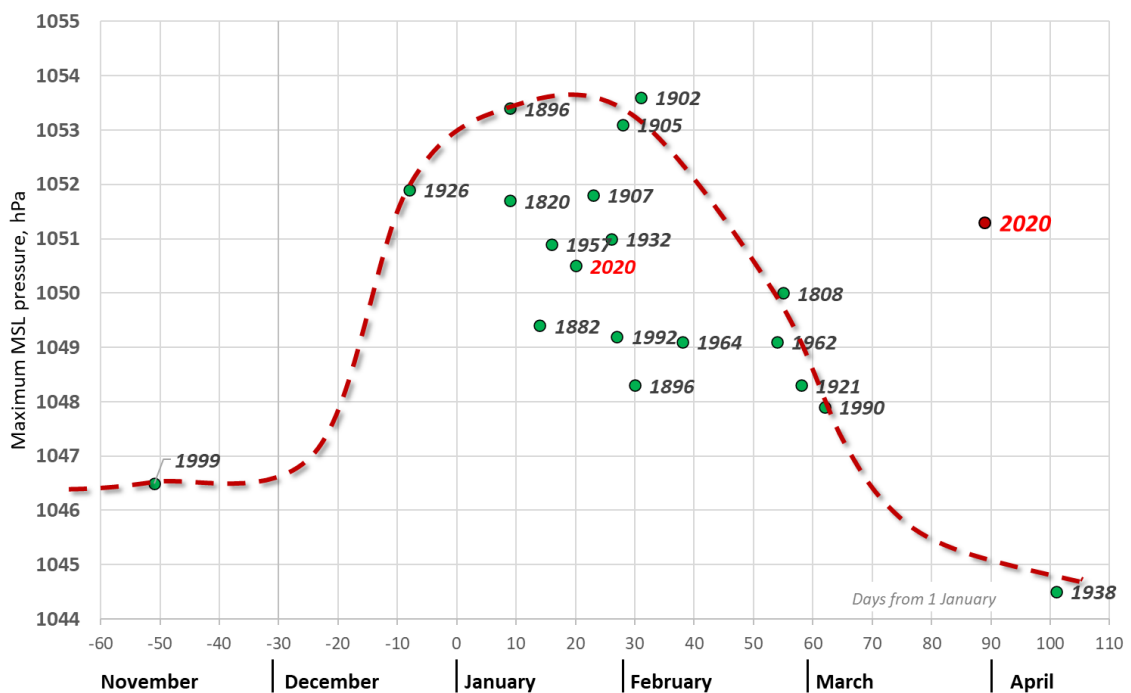


**Figure 14.** The highest MSL barometric pressures observed anywhere in the British and Irish Isles for November to April since about 1800, plotted against the date on which they occurred. The March 2020 event lies well outside the ‘envelope’ of all previous events within the last 200 years or more. The January 2020 event is also highlighted. Expanded version of Figure 11 in Burt 2020b – bibl. #3 – showing the pronounced midwinter ‘bump’ which (until March 2020) clearly delimited all previous occasions on which 1048 hPa was attained or surpassed.

# Chapter 3

## Summary

### 3.1 Summary and conclusions

Returning to the question posed in Chapter 1:

*How does the systematic recovery of old meteorological observations ('data rescue'), together with better awareness of past and present instrumental metrology and metadata, improve our knowledge of past and present weather events and climate trends?*

**Paper 1** examined 20 years of hourly temperature, humidity and wind speed records from the Ben Nevis Observatory, data rescued by a citizen science Zooniverse project, for occasions of extremely dry air. The results showed impressive agreement with contemporary mountain-summit measurements elsewhere in Scotland, despite those measurements being made more than a century later and with different instrument types. The investigation also usefully confirmed the 'real world' validity of laboratory-derived psychrometric coefficients, and provided the first independent confirmation of 850 hPa humidity fields from the 20th Century Reanalysis project. The latter point is particularly impressive, as the reanalysis assimilates only surface pressure observations, and in this case none closer than 200 km.

**Paper 2** shone a light on the performance of air temperature sensors, revealing that none of the commercial platinum resistance sensors tested met WMO specifications for response time. This has important implications for the design, procurement and installation phases of new and updated meteorological observation networks. Once incorporated into WMO WIGOS/CIMO guidance to National Meteorological Services, as expected, the performance metrics set out in this paper, along with the fully-developed theoretical work which justifies them, will result in more reliable, more accurate and more consistent present and future measurements of air temperature around the world.

**Paper 3** set out practical and economical methods of establishing and maintaining accurate instrumental calibrations. Based directly upon WMO CIMO recommendations for observing protocols and instrument exposure but with a more user-friendly format, the intended audience is primarily the non-professional community. The increasing proliferation of 'amateur' or 'citizen science' weather stations offers exciting and cost-effective means to increase the density of meteorological observing networks, particularly in urban areas, but only where the calibration and exposure of the instruments involved can approach professional standards. The chapter considered here offers ways and means to fulfil that requirement, and thus to improve and inform present and future measurements of weather and climate.

**Papers 4, 5 and 6** concentrate on the accumulation of new knowledge derived from the data rescue, quality control, analysis and subsequent open access online publishing of extensive daily

datasets from two sites with the longest meteorological records in England, namely the Radcliffe Meteorological Station in Oxford and Durham University Observatory, where unbroken daily records commenced in November 1813 and July 1843, respectively. The majority of these long-series datasets – now made freely available – were previously available only in manuscript format within the universities of Oxford and Durham, respectively, and their publication widens access to two of the longest single-site meteorological records in Europe. Such long series records are particularly valuable for examination of climate trends past and present, and for reliable assessments of the frequency of low-incidence extreme events, such as possible links with solar activity in Oxford’s unique 200-year thunderstorm incidence (Paper 5). In addition, the new twice-daily digital pressure series from Durham Observatory (1850-1960, Paper 6) represents the longest single-site barometric pressure record in England, and has already provided invaluable independent insights into the homogeneity of reanalysis datasets in the north-east Atlantic area. The feasibility of a citizen science digitisation project to rescue a long thrice-daily barometric pressure series from Oxford (broken 1811-1813, continuous 1814-1924) is under active consideration, and could be quickly implemented if funding becomes available.

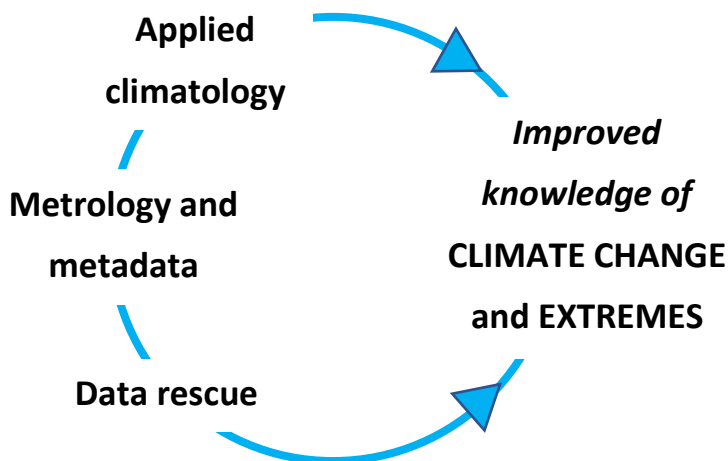
**Papers 7, 8 and 9** presented example case studies of notable events, integrating previous climatology and data rescue efforts (whether long series, manuscript records or previously published case studies) with contemporary synoptic data. Previous case studies by the author have examined many noteworthy weather events and extremes over the past five decades, including the Great Storm of October 1987, the record-setting heatwaves of August 1990 and August 2003, and the Boscastle flash flood of August 2004. Particular emphasis is placed here on a continuing collection of publications, now spanning almost 40 years, of case studies of extremes of barometric pressure in the North Atlantic and the British and Irish Isles, the earliest account from December 1982 and the most recent to date March 2020. These studies collectively compile a coherent and comprehensive climatology of the incidence of such events in the north-east Atlantic and western Europe, and (using a variety of data rescue and archival research methods) document their incidence over more than 200 years.

## **3.2: The broader context – why does it matter?**

Considered together, these nine papers clearly demonstrate the benefits to climate science of meteorological data rescue (particularly papers 1 and 4-9) and the vital importance of meteorological metrology (especially in papers 1 to 6) in both past and current meteorological and climatological measurements. Influences on present and future measurement techniques (papers 2 and 3) make important contributions to improving meteorological records, today and tomorrow. The various long data series described provide quantitative means by which the climate science community can assess present and future changes in climate – for instance, examining changes in the frequency of hot summers in south-east and central England from Oxford’s long records with a view to estimating risks to water supply or human health, or considering recent increases in average annual rainfall in north-east England from the Durham Observatory series and the resulting

downstream implications for the frequency and extent of winter flooding in population centres such as Newcastle and York.

The broader relationship between the three core concepts outlined in chapter 1 and their contribution towards an improved understanding of climate change and climate extremes can be summarised visually as follows:



In addition, three of the papers and projects described in this thesis have contributed to the increasing capability, sophistication and record length of reanalysis datasets – by demonstrating the means reliably to identify occasions of anticyclonic subsidence above the boundary layer well before the commencement of regular upper-air observations, and the use of reanalysis gridpoint pressure data as an underpinning quality control reference for an independent long-period sub-daily pressure series. The methodical review and documentation by the author of extremes of barometric pressure in the North Atlantic and north-west Europe, examples of which are set out in papers 8 and 9, provides a very long baseline (over 200 years) against which changes in frequency or intensity of major cyclonic storms and exceptional anticyclones can be confidently examined, together with a rich source of historical data from which will come important contributions to improving the accuracy and positioning of such features in reanalyses. The winter of 2020 provided a surprise in that two anticyclones surpassed 1050 hPa over the British and Irish Isles within a few weeks of each other — the first such occurrence in over 60 years, and the only winter in at least the past 200 years to have seen *two* such events. There is little doubt that our changing climate will produce more extremes, not all of them temperature related. When will the next 1050 hPa event occur – will it be another 60 years, or will we revert to a once in 10-year recurrence interval, as happened in the early 20th century? What are the underlying changes in atmospheric circulation responsible for such events? The 20th Century reanalysis programme, now extending back to 1806 through combined data rescue efforts over many years, offers us our best chance of answering such questions.

In summary, the author’s cumulative publication history, including the subset listed in this thesis, provides clear evidence in explanation and affirmation of the research question set out at the beginning of this thesis. Across several contexts, the author has clearly demonstrated that the

systematic recovery of old meteorological observations, allied with improved knowledge of relevant instrumental metrology and metadata, continues to extend and enhance our knowledge of past and present weather and climate, placing them within wider research contexts. Such knowledge is increasingly useful for future weather and climate change studies, in which the sum of the whole is often much greater than the sum of the individual components.

### 3.3: Future research directions

#### Data rescue

**OXFORD:** The Oxford climatological series are updated online annually using the continuing daily observations record from the Radcliffe Observatory site. Thrice-daily barometric pressure records from the Radcliffe site from 1811 (broken to 1813) to 1853 have been scanned and are (slowly) being digitised from the original manuscript records; these are being added to the International Surface Pressure Database in five-year tranches as completed. There are opportunities to speed this up substantially using a Zooniverse-type citizen science offering. Thrice-daily records from 1854 to 1924 exist in manuscript archives within the University of Oxford, with hourly pressure tabulations available for many years within this series: these await funding/resource to convert to digital format.

**DURHAM:** The manuscript for *Durham Weather and Climate since 1841* will be delivered to Oxford University Press in July 2021, and publication is expected in spring 2022. The twice-daily Durham pressure series July 1843 to December 1960 is complete and has already been published, and the record metadata submitted for publication (both as a journal paper and a book chapter); the record will be included in the International Surface Pressure Database in due course. The remainder of the meteorological records from Durham (the long temperature, precipitation and sunshine series in particular) will be published online in 2022 to coincide with the book's launch at the University of Durham.

**LONDON:** It seems possible to produce a near 300 year record of daily thunderstorm activity in London, compiled from a variety of published and manuscript sources. This would provide valuable insights into long-term trends, including possible links with the 22-year cycle of solar magnetic field polarity and incidence of aurorae. Ironically, the production of a coherent thunder-day series is more problematic in recent decades than in the 18th century owing to the cessation of observations at long-period London sites in the 1980s and 1990s (Kew Observatory, Greenwich Observatory, London Weather Centre) and the replacement of most manual observations with automatic weather stations at today's main observing locations in west London (London Heathrow Airport and RAF Northolt). The possibility of correlating automated lightning flash counts with 'thunder day' records within a given area or gridbox within the London area over the last two decades or so may offer the opportunity to define a more objective long-term series of thunderstorm activity within the capital (see also Lavigne et al, 2019).

Other useful sources of long period data for London remain under-utilised. The long composite series of ‘daily mean’ barometric pressures from various sites in London, starting in 1692, assembled as part of his PhD by Richard Cornes (Cornes, 2012) could usefully be re-examined (adding observation hours) and combined with the early Oxford record, providing valuable early data to extend European reanalysis back into the early 19th century. The London records may be extended further back still - Robert Hooke noted daily details of wind, temperature and pressure in London in his diary from 1672, with some gaps, until his death in 1703 (Andrade, 1960; Jardine, 2004), while Robert Boyle kept daily records of the ‘baroscope’ and thermometer at his home in London’s Pall Mall in the 1680s (Cornes, 2020).

In 1960, Gordon Manley assembled a list of sources of historical London weather records, extending back to Robert Hooke and the early Royal Society in the 1660s (Manley 1960, 1961, 1963). Other important diaries and manuscript sources of meteorological records have since been discovered, and some have been scanned or otherwise digitised. Of course, most of London’s long-period temperature records have been largely vitiated over time — at least from the perspective of climate trend analysis, if not for urban heat island studies — by the growth of the city itself. However, there remain many unrealised opportunities for the assembly of digital datasets for other meteorological elements for London, such as rainfall — currently the only such composite series being that for Kew from 1697 (Wales-Smith, 1971) — snowfall, cloud cover and sunshine.

### Applied historical climatology: Pressure extremes

An update to the two-part capstone Paper 8 of 2007 is planned, to include summaries of events since the paper was published, along with other historical events that have since come to light, and making full use of reanalysis insights and resources unavailable in 2007. The creation of extensive long-period reanalysis datasets such as the 20th Century Reanalysis version 3 (20CRv3: Slivinski et al 2020), now extended back to 1836, offers numerous exciting opportunities to build on the work thus far:

- To examine performance of reanalysis datasets in the numerous occasions now on record when surface pressures have fallen below 940 hPa or risen above 1048 hPa in the North Atlantic, including the British and Irish Isles, with a view to assessing biases in position, depth/intensity or both in the spread of ensemble means;
- To track the development and progression of these extreme systems, both cyclones and anticyclones, across the Atlantic at 3 hour intervals using modern data assimilation methods. Some event case studies as far back as the 1870s – for example, Toynbee and Harding (1872) – contain very detailed surface pressure observations from the denser networks of ship reports at that time, prior to the introduction of radio communications and predating today’s commercial aircraft traffic. Assimilation of such ‘spot’ observations into model analyses, similar to assimilation methods used for tropical storm or hurricane paths, would be especially beneficial in reducing ensemble spreads in data-sparse areas along the system track, particularly in formation areas and close to the peak intensity of such systems;

- To undertake quantitative interrogation of the reanalysis datasets to generate robust statistical probability distributions of such extreme events by threshold, location, time of year, preferred development and track, and
- To identify any long-term trend or clustering in their occurrence which may be related to climate change, and consider any common factors such as the reduction in polar sea ice.

## Reanalysis

The digitisation of the Oxford and Durham pressure series, and their incorporation into the International Surface Pressure Database and eventually in the next revision of the 20th Century Reanalysis, will have a significant impact on the resolution and veracity of reconstruction of past and present atmospheric circulation patterns over the North Atlantic. In turn, this will inform and improve our estimates of future changes in circulation as a result of anthropogenic climate change.

Further, more detailed comparisons between (observed) Ben Nevis Observatory humidity and (reanalysis) 850 hPa humidity fields in the 20th Century Reanalysis v3 (Slivinski et al, 2020) for the 16 months August 1902 to December 1903 are in hand, using a reanalysis dataset which has been re-run for this period including additional pressure observations assimilated from around the British and Irish Isles, including those taken on Ben Nevis and in Fort William. A particular focus will be on the events of 7-8 December 1902, when the humidity on the summit fell to ~ 0% for 5 hours.

## Meteorological metrology

A second edition of *The Weather Observer's Handbook* is in discussion with Cambridge University Press, and it is hoped this will be published in 2022/23.

## 3.4: Publication metrics

**Table 1** summarises citations and ‘reads’ of the author’s published papers. Data has been extracted from four sources as shown, although the large variations between sources gives little confidence as to accuracy or completeness. The table is shown in publication date order; minor contributions have been omitted (and thus there are some gaps in the numerical sequence). Most recent publications have fewer citations, since the interval since publication has been shorter. Papers included in this thesis subset are highlighted in **bold**.

Total *citations* updated to 23 June 2021:

- Google Scholar **682**;
- Scopus (Elsevier) **375**;
- Web of Science (Clarivate Analytics / Publons) **122**;
- ResearchGate **485**;

Total *reads* on ResearchGate **4582**.

**Table 1** Publication metrics from Clarivate Web of Science, Scopus, ResearchGate and Google Scholar, in publication date order and updated to 14 April 2021. Papers included in this thesis subset are highlighted in **bold**. Minor contributions have been omitted, hence there are some gaps in the numerical sequence; the full author bibliography is given in Section 3.6 below.

<i>Bibliography reference</i>	<i>Publication</i>	<i>Year</i>	<i>Citations Web of Science</i>	<i>Citations Scopus</i>	<i>ResearchGate Reads</i>	<i>Citations Google Scholar</i>
<b>61</b>	The blizzards of February 1978 in south western Britain	1978				13
<b>59</b>	Snowfall in Britain during Winter 1978/79	1980		6	745	8
<b>58</b>	Heavy rainfall and snowstorms, 23–26 April 1981	1982		7	20	4
<b>57</b>	New UK 20th century low pressure extreme	1983		8		21
<b>55</b>	Remarkable pressure fall at Valentia, 17 October 1984	1985		6		6
<b>53</b>	A new North Atlantic low pressure record	1987		17	25	28
<b>52</b>	The great storm of 15–16 October 1987	1988		57	256	81
<b>51</b>	London’s Lowest Barometric Pressure in 167 Years	1989		4	151	5
<b>50</b>	Falls of dust rain within the British Isles	1991		26		34
<b>49</b>	Weather and streamflow in Central Southern England during water year 1989/90	1992		6		4
<b>48</b>	The exceptional hot spell of early August 1990 in the United Kingdom	1992	2	10	184	17
<b>47</b>	Another new North Atlantic low pressure record	1993		16	255	20
<b>46</b>	The Altnaharra minimum temperature of –27.2°C on 30 December 1995	1997		6		6
<b>45</b>	A cluster of intense rainfall events in West Berkshire, summer 1999	2000		4		5
<b>42</b>	The August 2003 heatwave in the United Kingdom: part 3–minimum temperatures	2004		2		7
<b>41</b>	The August 2003 heatwave in the United Kingdom. Part 2 – The hottest sites	2004		12		22
<b>40</b>	The August 2003 heatwave in the United Kingdom: Part 1–Maximum temperatures and historical precedents	2004		37	93	55



**Table 1**  
*continued*

<i>Bibliography reference</i>	<i>Publication</i>	<i>Year</i>	<i>Citations Web of Science</i>	<i>Citations Scopus</i>	<i>ResearchGate Reads</i>	<i>Citations Google Scholar</i>
<b>39</b>	Cloudburst upon Hendrarnick Down: The Boscastle storm of 16 August 2004	2005		43	23	56
<b>38</b>	Britain's highest barometric pressure on record is incorrect	2006		3		4
<b>36</b>	Barometric pressure during the Irish storm of 6-7 January 1839	2006		4		5
<b>33</b>	A comparison of traditional and modern methods of measuring earth temperatures	2006	11		321	1
<b>35</b>	<b>The Highest of the Highs ... Extremes of barometric pressure in the British Isles, Part 2 – the most intense anticyclones</b>	<b>2007</b>		<b>9</b>		<b>15</b>
<b>34</b>	<b>The Lowest of the Lows ... extremes of barometric pressure in the British Isles, Part 1 – the deepest depressions</b>	<b>2007</b>		<b>10</b>	<b>859</b>	<b>15</b>
<b>30</b>	British Rainfall 1860-1993	2010	7	8		12
<b>28</b>	<i>The Weather Observer's Handbook</i>	<b>2012</b>				<b>53</b>
<b>27</b>	An unsung hero in meteorology: Charles Higman Griffith (1830–1896)	2013	2		25	2
<b>25</b>	Britain's lowest barometric pressure since 1886	2014	5	4		6
<b>24</b>	<i>One Hundred Years of Reading Weather</i>	2015				3
<b>21</b>	<b>December 2015 - an exceptionally mild month in the United Kingdom</b>	<b>2016</b>	<b>3</b>	<b>3</b>		<b>3</b>
<b>22</b>	Cumbrian floods, 5/6 December 2015	2016	9	8		15
<b>20</b>	New extreme monthly rainfall totals for the United Kingdom and Ireland: December 2015	2016	6	6	13	9
<b>19</b>	Meteorological responses in the atmospheric boundary layer over southern England to the deep partial eclipse of 20 March 2015	2016	9	11		12
<b>18</b>	Meteorological impacts of the total solar eclipse of 21 August 2017	2018	6	5	122	10
<b>16</b>	Hourly weather observations from the Scottish Highlands (1883–1904) rescued by volunteer citizen scientists	2019	10	9	82	13

**Table 1***continued**Bibliography  
reference**Publication**Year**Citations  
Web of  
Science**Citations  
Scopus**ResearchGate  
Reads**Citations  
Google  
Scholar*

<i>Bibliography reference</i>	<i>Publication</i>	<i>Year</i>	<i>Citations Web of Science</i>	<i>Citations Scopus</i>	<i>ResearchGate Reads</i>	<i>Citations Google Scholar</i>
<b>14</b>	<b>Oxford weather and climate since 1767</b>	<b>2019</b>			<b>42</b>	<b>15</b>
<b>13</b>	Northern Ireland's longstanding record wind gust is almost certainly incorrect	2019	15		17	2
<b>15</b>	<b>Near-zero humidities on Ben Nevis, Scotland, revealed by pioneering 19th-century observers and modern volunteers</b>	<b>2019</b>	<b>4</b>	<b>3</b>	<b>4</b>	<b>5</b>
<b>17</b>	<b>Thunderstorm occurrence at ten sites across Great Britain over 1884-1993</b>	<b>2019</b>	<b>5</b>	<b>5</b>	<b>20</b>	<b>4</b>
<b>12</b>	London's highest barometric pressure in over 300 years	2020	2	2	3	2
<b>5</b>	<b>Response times of meteorological air temperature sensors</b>	<b>2020</b>		<b>1</b>	<b>72</b>	<b>2</b>
<b>6</b>	<b>Two hundred years of thunderstorms in Oxford</b>	<b>2021</b>	<b>1</b>	<b>1</b>	<b>9</b>	<b>1</b>

### 3.5: References

- Amos, J., 2020: Barometric pressure in London 'highest in 300 years' at least. *BBC News Online: Science and Environment*, <https://www.bbc.co.uk/news/science-environment-51180211>.
- Andrade, E. N. D. C., 1960: Robert Hooke, FRS (1635-1703). *Notes and Records of the Royal Society of London*, **15**, 137-145.
- Anon, 1893: Life and work on Ben Nevis. *Quart. J. Royal Meteorol. Soc.*, **19**, 257-258.
- Baker, L., 2009: Sting jets in severe northern European wind storms. *Weather*, **64**, 143-148.
- Barnard, L., A. M. Portas, S. L. Gray *et al*, 2016: The National Eclipse Weather Experiment: an assessment of citizen scientist weather observations. *Philosophical Transactions of the Royal Society A: Mathematical, Physical and Engineering Sciences*, **374**.
- Basarin, B., T. Lukić and A. Matzarakis, 2020: Review of biometeorology of heatwaves and warm extremes in Europe. *Atmosphere*, **11**, 1276.
- Bassett, R., P. J. Young, G. S. Blair *et al*, 2020: Urbanisation's contribution to climate warming in Great Britain. *Environmental Research Letters*, **15**, 114014.
- Brandes, H., 1820: *Beirage zur Witterungskunde [Contributions to Meteorology]*. Breslau.
- Brayne, M., 2002: *The greatest storm: Britain's night of destruction, November 1703*. Stroud, Glos: Sutton Publishing Ltd, 240 pp.
- Brimicombe, C., J. J. Porter, C. Di Napoli *et al*, 2021: Heatwaves: An invisible risk in UK policy and research. *Environmental Science & Policy*, **116**, 1-7.
- Brooks, C. E. P., 1927: An early essay in co-operative meteorology: the Great Storm of 1703 [26-27 November 1703, O.S.]. *Meteorol. Mag.*, **62**, 31-35, p 91.

- , 1934: The variation of the annual frequency of thunderstorms in relation to sunspots. *Quart. J. Royal Meteorol. Soc.*, **60**, 153-166.
- Browning, K. A., 2004: The sting at the end of the tail: Damaging winds associated with extratropical cyclones. *Quart. J. Royal Meteorol. Soc.*, **130**, 375-399.
- Browning, K. A. and F. H. Ludlam, 1962: Airflow in convective storms. *Quart. J. Royal Meteorol. Soc.*, **88**, 117-135.
- Buchan, A., 1890: Meteorology of Ben Nevis. *Trans. Roy. Soc. Edinb.*, **34**, xviii-lxi.
- Buchan, A. and R. T. Omond, 1902: The Ben Nevis observations (1888-1892). *Trans. Roy. Soc. Edinb.*, **42**.
- , 1905: The Ben Nevis observations (1893-1897). *Trans. Roy. Soc. Edinb.*, **43**.
- Burt, S., 1978: The blizzards of February 1978 in south-west Britain. *J. Meteorol. UK*, **3**, 261-278.
- , 1982: Heavy rainfall and snowstorms, 23-26 April 1981. *Weather*, **37**, 108-115.
- , 1983: New UK 20th Century low pressure extreme. *Weather*, **38**, 209-213.
- , 1992: The exceptional hot spell of early August 1990 in the United Kingdom. *Int. J. Climatol.*, **12**, 547-567.
- , 1997: The Altnaharra minimum temperature of  $-27.2^{\circ}\text{C}$  on 30 December 1995. *Weather*, **52**, 134-144.
- , 2004a: The August 2003 heatwave in the United Kingdom: Part 1 - Maximum temperatures and historical precedents. *Weather*, **59**, 199-208.
- , 2004b: The August 2003 heatwave in the United Kingdom: Part 3 - Minimum temperatures. *Weather*, **59**, 272-273.
- , 2005: Cloudburst upon Hendraburnick Down: The Boscastle storm of 16 August 2004. *Weather*, **60**, 219-227.
- , 2006a: Barometric pressure during the Irish storm of 6-7 January 1839. *Weather*, **61**, 22-27.
- , 2006b: Britain's highest barometric pressure on record is incorrect. *Weather*, **61**, 210-211.
- , 2011: Exceptionally low relative humidity in northern England, 2-3 March 2011. *Weather*, **66**, 197-199.
- Burt, S. and P. Eden, 2004: The August 2003 heatwave in the United Kingdom. Part 2 – The hottest sites. *Weather*, **59**, 239-246.
- Burt, S. and M. Kendon, 2016: December 2015 – an exceptionally mild month in the United Kingdom. *Weather*, **71**, 314-320.
- Burt, S. and T. Burt, 2019: *Oxford Weather and Climate since 1767*. Oxford: Oxford University Press 544 pp.
- Burt, S. D. and D. A. Mansfield, 1988: The Great Storm of 15-16 October 1987. *Weather*, **43**, 90-110.
- Cervený, R., 2018: WMO Archive of Weather and Climate Extremes. *WMO Bulletin*, **67(2)**, 52-57.
- Cervený, R. S., J. Lawrimore, R. Edwards *et al*, 2007: Extreme weather records: Compilation, adjudication and publication. *Bull. Amer. Meteorol. Soc.*, **88(6)**, 853-860.
- Chan, S. C., E. J. Kendon, H. J. Fowler *et al*, 2014: The value of high-resolution Met Office regional climate models in the simulation of multihourly precipitation extremes. *J. Climate*, **27**, 6155-6174.
- Chandler, T. J., 1965: *The Climate of London*. Hutchinson, London 292 pp.
- Chapman, L., C. Bell and S. Bell, 2017: Can the crowdsourcing data paradigm take atmospheric science to a new level? A case study of the urban heat island of London quantified using Netatmo weather stations. *Int. J. Climatol.*, **37**, 3597-3605.
- Ching, M., 2008: *The Blizzard of 78: The snowstorm that buried Dorset*. (Self-published) Winfrith Newburgh, Dorset, 178 pp.

- Christidis, N., M. McCarthy and P. A. Stott, 2020: The increasing likelihood of temperatures above 30 to 40 °C in the United Kingdom. *Nature Communications*, **11**.
- Clark, M. R., D. S. Lee and T. P. Legg, 2014: A comparison of screen temperature as measured by two Met Office observing systems. *Int. J. Climatol.*, **34**, 2269-2277.
- Clow, D. G., 1988: Daniel Defoe's account of the storm of 1703. *Weather*, **43**, 140-141.
- Compo, G. P., J. S. Whitaker, P. D. Sardeshmukh *et al*, 2011: The Twentieth Century Reanalysis Project. *Quart. J. Royal Meteorol. Soc.*, **137**, 1-28.
- Craig, P. M. and E. Hawkins, 2020: Digitizing observations from the Met Office Daily Weather Reports for 1900–1910 using citizen scientist volunteers. *Geoscience Data Journal*, doi **10.1002/gdj3.93**.
- Cram, T. A., G. P. Compo, X. Yin *et al*, 2015: The International Surface Pressure Databank version 2. *Geoscience Data Journal*, **2**, 31-46.
- de Podesta, M., S. Bell and R. Underwood, 2018: Air Temperature Sensors: dependence of radiative errors on sensor diameter in precision metrology and meteorology. *Metrologia*, **55**, 229-244.
- Defoe, D., 1704: *The Storm*. Allen Lane
- Diamond, H. J., T. R. Karl, M. A. Palecki *et al*, 2013: U.S. Climate Reference Network after One Decade of Operations: Status and Assessment. *Bull. Amer. Meteorol. Soc.*, **94**, 485-498.
- Doesken, N., 2005: *The National Weather Service MMTS (Maximum-Minimum Temperature System) – 20 years after*. American Meteorological Society conference papers - available online at [ams.confex.com/ams/pdfpapers/91613.pdf](https://ams.confex.com/ams/pdfpapers/91613.pdf) [accessed 8 Oct 2019]. .
- Duncan, C. N. and K. J. Weston, 1983: Ben Nevis observatory, 1883-1983. *Weather*, **38**, 298-303.
- Fitzroy, R., 1860: Notice of 'The Royal Charter Storm' in October 1859. *Proceedings of the Royal Society of London*, **10**, 561-567.
- Gibbs, J. N. and B. J. W. Greig, 1990: Survey of parkland trees after the Great Storm of October 16, 1987. *Arboricultural Journal*, **14**, 321-347.
- Gold, E., 1914: Barometer readings in absolute units and their correction and reduction. *Quart. J. Royal Meteorol. Soc.*, **40**, 185-202.
- Golding, B., P. Clark and B. May, 2005: The Boscastle flood: Meteorological analysis of the conditions leading to flooding on 16 August 2004. *Weather*, **60**, 230-235.
- Green, F. H. W., 1953: A remarkable low humidity. *Weather*, **8**, 182-184.
- , 1965: The incidence of low relative humidity in the British Isles. *Meteorol. Mag.*, **94**, 84-88.
- , 1966: Low air humidities 28 March to 2 April 1965. *Weather*, **21**, 101-104.
- , 1967: Air humidity on Ben Nevis. *Weather*, **22**, 174-186.
- Green, H. K., N. Andrews, B. Armstrong *et al*, 2016: Mortality during the 2013 heatwave in England – How did it compare to previous heatwaves? A retrospective observational study. *Environmental Research*, **147**, 343-349.
- Harrison, R. G. and C. R. Wood, 2012: Ventilation effects on humidity measurements in thermometer screens. *Quart. J. Royal Meteorol. Soc.*, **138**, 1114-1120.
- Hawkins, E., S. Burt, P. Brohan *et al*, 2019: Hourly weather observations from the Scottish Highlands (1883-1904) rescued by volunteer citizen scientists. *Geoscience Data Journal*, **6**, 160–173.
- Hill, F. F., K. A. Browning and M. J. Bader, 1981: Radar and raingauge observations of orographic rain over south Wales. *Quart. J. Royal Meteorol. Soc.*, **107**, 643-670.
- Howard, L., 1822: On the Late Extraordinary Depression of the Barometer. *Philosophical Transactions of the Royal Society of London*, **112**, 113-116.

- International Organization for Standardization (ISO), 2007: ISO 17714 Meteorology — Air temperature measurements — Test methods for comparing the performance of thermometer shields/screens and defining important characteristics. International Organization for Standardization (ISO), Geneva
- Jardine, L., 2004: *The Curious Life of Robert Hooke: The Man Who Measured London*. Harper Perennial London, 448 pp.
- Keers, J. F. and P. Wescott, 1976: The Hampstead storm - 14 August 1975. *Weather*, **31**, 2-10.
- Kendon, E. J., N. M. Roberts, H. J. Fowler *et al*, 2014: Heavier summer downpours with climate change revealed by weather forecast resolution model. *Nature Climate Change*, **4**, 570-576.
- Kendon, M., M. McCarthy, S. Jevrejeva *et al*, 2020: State of the UK Climate 2019. *Int. J. Climatol.*, **40**, 1-69.
- Kenworthy, J. M., N. J. Cox and A. N. Joyce, 1997: *Computerisation and analysis of the Durham Observatory meteorological record: Final Report to the Leverhulme Trust, Reference F/128/Q*. Durham University.
- Kilgour, W. T., 1905: *Twenty years on Ben Nevis*. Reprinted digital edition, 2014 ed. , Cambridge: Cambridge University Press, 155 pp.
- Kington, J., 2010: *Climate and Weather*. Collins London, 484 pp.
- Kirk, P. J., M. R. Clark and E. Creed, 2021: Weather Observations Website. *Weather*, **76**, 47-49.
- Knox, J. A., J. D. Frye, J. D. Durkee *et al*, 2011: Non-convective high winds associated with extratropical cyclones. *Geography Compass*, **5**, 63-89.
- Kukoleva, A. A., N. K. Kononova and A. A. Krivolutskii, 2018: Manifestation of the Solar Cycle in the Circulation Characteristics of the Lower Atmosphere in the Northern Hemisphere. *Geomagnetism and Aeronomy*, **58**, 775-783.
- Laing, J., 1979: The blizzard of 18-19 February 1978 in south-west England and South Wales. *Meteorol. Mag.*, **108**, 119-128.
- Lavigne, T., C. Liu and N. Liu, 2019: How does the trend in thunder days relate to the variation of lightning flash density? *Journal of Geophysical Research: Atmospheres*.
- Levermore, G., J. Parkinson, K. Lee *et al*, 2018: The increasing trend of the urban heat island intensity [in Manchester]. *Urban Climate*, **24**, 360-368.
- Lin, X. and K. G. Hubbard, 2008: What are daily maximum and minimum temperatures in observed climatology? *Int. J. Climatol.*, **28**, 283-294.
- Lin, X., K. G. Hubbard and C. B. Baker, 2005: *Measurement sampling rates for daily maximum and minimum temperatures*. American Meteorological Society: Ninth Symposium on Integrated Observing and Assimilation Systems for the Atmosphere, Oceans, and Land Surface (IOAS-AOLS), San Diego, Jan 2005.
- Lockwood, M., R. G. Harrison, M. J. Owens *et al*, 2011: The solar influence on the probability of relatively cold UK winters in the future. *Environmental Research Letters*, **6**, 034004.
- Manley, G., 1941: The Durham meteorological record, 1847-1940. *Quart. J. Royal Meteorol. Soc.*, **67**, 363-380.
- , 1946: Temperature trend in Lancashire, 1753–1945. *Quart. J. Royal Meteorol. Soc.*, **72**, 1-31.
- , 1953: The mean temperature of central England, 1698–1952. *Quart. J. Royal Meteorol. Soc.*, **79**, 558-567.
- , 1960: Bibliography of the principal sources of daily meteorological observations for the London area. Typescript notes of sources, 7 pp PDF OCR. Source material for Manley's 1961 Met Mag paper on the same topic, qv ed., Met Office Library and Archive, bibliography no 285232, Library Collection.
- , 1961: A preliminary note on early meteorological observations in the London region, 1680-1717, with estimates of the monthly mean temperatures, 1680-1706. *Meteorol. Mag.*, **90**, 303-310.

- , 1963: Seventeenth-century London temperatures: Some further experiments. *Weather*, **18**, 98-105.
- , 1974: Central England temperatures: Monthly means 1659 to 1973. *Quart. J. Royal Meteorol. Soc.*, **100**, 389-405.
- Merlone, A., 2021: Thermal metrology for climate: a review of projects, activities and open issues. *Measurement Science and Technology*, **32**, 102001.
- Merlone, A., G. Lopardo, F. Sanna *et al*, 2015: The MeteoMet project – metrology for meteorology: challenges and results. *Meteorol. Appl.*, **22**, 820-829.
- Met Office, 1973: Averages of mean sea level barometric pressure for the United Kingdom 1941–70. Meteorological Office, 27 pp.
- , 2019: Met Office MIDAS Open: UK Land Surface Stations Data (1853-current). Centre for Environmental Data Analysis (CEDA), <http://catalogue.ceda.ac.uk/uuid/dbd451271eb04662beade68da43546e1>, accessed 14 March 2020. .
- Meteorological Office, 1952: *Climatological Atlas of the British Isles*. HMSO.
- Miller, M. J., 1978: The Hampstead storm: A numerical simulation of a quasi-stationary cumulonimbus system. *Quart. J. Royal Meteorol. Soc.*, **104**, 413-427.
- Mossman, R. C., 1897: The non-instrumental meteorology of London, 1713–1896. *Quart. J. Royal Meteorol. Soc.*, **23**, 287-298.
- Nicholson, A., 2020: Analysis of the diurnal cycle of air temperature between rural Berkshire and the University of Reading: possible role of the urban heat island. *Weather*, **75**, 235-241.
- Oke, T. R., 1973: City size and the urban heat island. *Atmospheric Environment (1967)*, **7**, 769-779.
- Oke, T. R., G. Mills, A. Christen *et al*, 2017: *Urban Climates*. Cambridge University Press 525.
- Omond, R. T., 1910: The meteorology of the Ben Nevis observatories Part IV, containing the observations for the years 1898-1904. *Trans. Roy. Soc. Edinb.*, **46**, Part I.
- Quayle, R. G., D. R. Easterling, T. R. Karl *et al*, 1991: Effects of Recent Thermometer Changes in the Cooperative Station Network. *Bull. Amer. Meteorol. Soc.*, **72**, 1718-1723.
- Roy, M., 2004: *The weathermen of Ben Nevis 1883-1904*. Royal Meteorological Society Fort William, Scotland, 62 pp.
- Scott, R. H., 1880: Note on the Reports of Wind Force and Velocity during the Tay Bridge Storm, December 28th, 1879. *Quart. J. Royal Meteorol. Soc.*, **6**, 98-100.
- Shutts, G. J., 1990: Dynamical aspects of the October storm, 1987: A study of a successful fine-mesh simulation. *Quart. J. Royal Meteorol. Soc.*, **116**, 1315-1347.
- Simons, P., 2020: Newfoundland blizzard puts Britain under pressure. *The Times*, 24 January 2020.
- Skansi, M. d. L. M., J. King, M. A. Lazzara *et al*, 2017: Evaluating the highest temperature extremes in the Antarctic. *Eos*, **98(5)**, 18-23.
- Slivinski, L. C., G. P. Compo, P. D. Sardeshmukh *et al*, 2020: An evaluation of the performance of the 20th Century Reanalysis version 3. *J. Climate*, 1-64.
- Slivinski, L. C., G. P. Compo, J. S. Whitaker *et al*, 2019: Towards a more reliable historical reanalysis: Improvements for version 3 of the Twentieth Century Reanalysis system. *Quart. J. Royal Meteorol. Soc.*, **145**, 2876-2908.
- Smith, C. G., 1975: Central England Temperatures; monthly means of the Radcliffe Meteorological Station, Oxford (Reply by Gordon Manley follows). *Quart. J. Royal Meteorol. Soc.*, **101**, 385-389.
- Strangeways, I., 2019: The replacement of mercury thermometers in Stevenson screens. *Weather*, **74**, 145-147.
- Symons, G. J., Ed., 1888: *The eruption of Krakatoa and subsequent phenomena*. Royal Society 494 pp.

- Thorne, P. W., H. J. Diamond, B. Goodison *et al*, 2018: Towards a global land surface climate fiducial reference measurements network. *Int. J. Climatol.*, **38**, 2760-2774.
- Tomlinson, C. J., L. Chapman, J. E. Thornes *et al*, 2012: Derivation of Birmingham's summer surface urban heat island from MODIS satellite images. *Int. J. Climatol.*, **32**, 214-224.
- Tooley, M. J. and G. M. Sheail, Eds., 1985: *The Climatic Scene*. George Allen & Unwin 306 pp.
- Toynbee, H. and C. Harding, 1872: A discussion of the meteorology of that part of the Atlantic lying north of 30 degrees N for the eleven days ending 8th February 1870, by means of the synoptic charts, diagrams, extracts from logs, remarks and conclusions. *Meteorological Office Publication No. 13*.
- University of Durham, 2016: Catalogue of the Gordon Manley papers. U. o. Durham, Ed., Durham University Library
- Valdivieso, M., M. J. Owens, C. J. Scott *et al*, 2019: Thunderstorm occurrence at ten sites across Great Britain over 1884–1993. *Geoscience Data Journal*, **6**, 222-233. doi <https://doi.org/210.1002/gdj1003.1075>.
- Venema, V., 2020: *The transition to automatic weather stations. We'd better study it now*. Blog available online at <http://variable-variability.blogspot.com/2016/01/transition-automatic-weather-stations-parallel-measurements-ISTI-POST.html>, accessed 24 April 2020
- Wales-Smith, B. G., 1971: Monthly and annual totals of rainfall representative of Kew, Surrey, from 1697 to 1970. *Meteorol. Mag.*, **100**, 345-362.
- Warren, R. A., D. J. Kirshbaum, R. S. Plant *et al*, 2014: A 'Boscastle-type' quasi-stationary convective system over the UK Southwest Peninsula. *Quart. J. Royal Meteorol. Soc.*, **140**, 240-257.
- Weidner, G., J. King, J. E. Box *et al*, 2020: WMO evaluation of northern hemispheric coldest temperature: -69.6 °C at Klinck, Greenland, 22 December 1991. *Quart. J. Royal Meteorol. Soc.*, Online, published 24 Sept 2020.
- Wilby, R. L., 2003: Past and projected trends in London's urban heat island. *Weather*, **58**, 251-260.
- World Meteorological Organization (WMO), 1973: Commission for Instruments and Methods of Observation: Abridged final report of the sixth session, Helsinki, 6-17 August 1973. WMO-No.363. Available online: [https://library.wmo.int/doc\\_num.php?explnum\\_id=8177](https://library.wmo.int/doc_num.php?explnum_id=8177), 124 pp.
- , 2014: WMO No.8 - Guide to Meteorological Instruments and Methods of Observation (CIMO guide) (Updated version, May 2017). WMO, Geneva, Switzerland. Available online: [http://library.wmo.int/opac/doc\\_num.php?explnum\\_id=4147](http://library.wmo.int/opac/doc_num.php?explnum_id=4147), 1139 pp.
- , 2018: WMO No.8 - Guide to Meteorological Instruments and Methods of Observation (CIMO guide). 2018 edition - Volume I: Measurement of Meteorological Variables. WMO, Geneva, Switzerland. Available online: [https://library.wmo.int/index.php?lvl=notice\\_display&id=12407](https://library.wmo.int/index.php?lvl=notice_display&id=12407), 573 pp.
- , 2019: Manual on the WMO Integrated Global Observing System (WIGOS Guide). WMO, Geneva, Switzerland. Available online: [https://library.wmo.int/doc\\_num.php?explnum\\_id=10145](https://library.wmo.int/doc_num.php?explnum_id=10145), 152 pp.

### 3.6: Author bibliography (ORCID ID 0000-0002-5125-6546)

In reverse chronological order, and updated to 23 June 2021

1. Burt, S., *Accepted 9 June 2021*: Twice-daily barometric pressure observations from Durham Observatory in north-east England, 1843-1960. *Geoscience Data Journal*, accepted for Special Issue on *Locating, Imaging and Digitizing Historic Geoscience Data*, publication date October 2021  
  
Burt, Stephen (2021): A twice-daily barometric pressure record from Durham Observatory in north-east England, 1843-1960. University of Reading Research Data Archive – online dataset  
<http://dx.doi.org/10.17864/1947.295>
2. Burt, T. and S. Burt, In Press: *Durham Weather and Climate since 1841*. Oxford: Oxford University Press: Book manuscript. In press, to be published spring 2022
3. Burt, S., 2021: New British Isles late-winter extreme barometric pressure, 29 March 2020. *Weather*, **76**, 72-78: <https://doi.org/10.1002/wea.3840>. Open Access.
4. Burt, S., 2020: In Praise of Meteorology Field Courses. Chapter in: *Curious about Nature - A passion for fieldwork*, T. Burt, and D. Thompson, Eds., Cambridge University Press, January 2020
5. Burt, S. and M. de Podesta, 2020: Response times of meteorological air temperature sensors. *Quart. J. Royal Meteorol. Soc.*, **146**, 2789–2800. Open Access.
6. Burt, S., 2021: Two hundred years of thunderstorms in Oxford. *Weather*, Published online 9 Feb 2021: <https://doi.org/10.1002/wea.3884>. Open Access.
7. Burt, S., 2021: The UK's highest low-level wind speed re-examined: the Fraserburgh gust of 13 February 1989. *Weather*, **76**, 4-11. Open Access.
8. Burt, S., 2020: The gust that never was: a meteorological instrumentation mystery. *Weather*, In Press, Published online 12 September 2020
9. Harrison, R. G. and S. Burt, 2020: Shall I compare thee to a summer's day? Art thou more temperate? ... Sometimes too hot the eye of heaven shines ... *Weather*, **75**, 172-174.
10. Burt, S., 2020: Reading's tornado fatality remembered. *Weather*, **75**, 161-162.
11. Burt, S., 2020: The Climatological Observers Link (COL) at 50. *Weather*, **75**, 137-144.
12. Burt, S., 2020: London's highest barometric pressure in over 300 years. *Weather*, **75**, 109-116.
13. Aylott, L., S. Burt and M. Saunders, 2020: Northern Ireland's longstanding record wind gust is almost certainly incorrect. *Weather*, **75**, 8-13.
14. Burt, S. and T. Burt, 2019: *Oxford Weather and Climate since 1767*. Oxford: Oxford University Press, 544 pp.
15. Burt, S. and E. Hawkins, 2019: Near-zero humidities on Ben Nevis, Scotland, revealed by pioneering nineteenth century observers and modern volunteers. *Int. J. Climatol.*, **2019**, 1-16.
16. Hawkins, E., S. Burt, P. Brohan, M. Lockwood, H. Richardson, M. Roy and S. Thomas, 2019: Hourly weather observations from the Scottish Highlands (1883-1904) rescued by volunteer citizen scientists. *Geoscience Data Journal*, **6**, 160–173.
17. Valdivieso, M., M. J. Owens, C.J. Scott, E. Hawkins, S. Burt and P. Craig, 2019: Thunderstorm occurrence at ten sites across Great Britain over 1884–1993. *Geoscience Data Journal*, **6**, 222-233. doi <https://doi.org/210.1002/gdj1003.1075>.
18. Burt, S., 2018: Meteorological impacts of the total solar eclipse of 21 August 2017. *Weather*, **73**, 90-95.



19. Burt, S., 2016: Meteorological responses in the atmospheric boundary layer over southern England to the deep partial eclipse of 20 March 2015. *Philosophical Transactions of the Royal Society A: Mathematical, Physical and Engineering Sciences*, **374**.
20. Burt, S., 2016: New extreme monthly rainfall totals for the United Kingdom and Ireland: December 2015. *Weather*, **71**, 333-338.
21. Burt, S. and M. Kendon, 2016: December 2015 – an exceptionally mild month in the United Kingdom. *Weather*, **71**, 314-320.
22. Burt, S., M. McCarthy, M. Kendon, J. Hannaford, 2016: Cumbrian floods, 5/6 December 2015. *Weather*, **71**, 36-37.
23. Burt, S., 2016: The Scarborough storm of August 1857. *Weather*, **71**, 19-21.
24. Brugge, R. and S. Burt, 2015: *One hundred years of Reading Weather*. Climatological Observers Link/University of Reading: Reading, UK, 193 pp.
25. Burt, S., 2014: Britain's lowest barometric pressure since 1886. *Weather*, **69**, 79-81.
26. Burt, S., 2013: Synoptic transport and deposition of Saharan dust to the British Isles. MSc Dissertation, Department of Meteorology, University of Reading: 126 pp.
27. Burt, S., 2013: An unsung hero in meteorology: Charles Higman Griffith (1830–1896). *Weather*, **68**, 135-138.
28. Burt, S., 2012: *The Weather Observer's Handbook*. Cambridge University Press New York, 444 pp.
29. Burt, S., 2011: Exceptionally low relative humidity in northern England, 2–3 March 2011. *Weather*, **66**, 197-199.
30. Burt, S., 2010: British Rainfall 1860–1993. *Weather*, **65**, 121-128.
31. Burt, S., 2009: Long-term variations in extremes of barometric pressure in the British Isles. *Weather*, **64**, 187-189.
32. Burt, S., 2008: Intense anticyclone over north-west Russia, early January 2008. *Weather*, **63**, 174-176.
33. Burt, S., 2007: A comparison of traditional and modern methods of measuring earth temperatures. *Weather*, **62**, 331-336.
34. Burt, S., 2007: The Lowest of the Lows ... extremes of barometric pressure in the British Isles, part 1 – the deepest depressions. *Weather*, **62**, 4-14.
35. Burt, S., 2007: The Highest of the Highs ... Extremes of barometric pressure in the British Isles, Part 2 – the most intense anticyclones. *Weather*, **62**, 31-41.
36. Burt, S., 2006: Barometric pressure during the Irish storm of 6–7 January 1839. *Weather*, **61**, 22-27.
37. Burt, S., 2006: Reduction in atmospheric transparency as a result of the Hemel Hempstead fire, 11–12 December 2005. *Weather*, **61**, 156-158.
38. Burt, S., 2006: Britain's highest barometric pressure on record is incorrect. *Weather*, **61**, 210-211.
39. Burt, S., 2005: Cloudburst upon Hendraburnick Down: The Boscastle storm of 16 August 2004. *Weather*, **60**, 219-227.
40. Burt, S., 2004: The August 2003 heatwave in the United Kingdom: Part 1 - Maximum temperatures and historical precedents. *Weather*, **59**, 199-208.
41. Burt, S. and P. Eden, 2004: The August 2003 heatwave in the United Kingdom. Part 2 – The hottest sites. *Weather*, **59**, 239-246.
42. Burt, S., 2004: The August 2003 heatwave in the United Kingdom: part 3--minimum temperatures. *Weather*, **59**, 272-273.

43. Burt, S., 2002: The Bracknell storm, 7 May 2000. *Weather*, **57**, 422-424.
44. Burt, S., 2001: Low relative humidities in England and Wales, Sunday 18 June 2000. *Weather*, **56**, 197-203.
45. Burt, S., 2000: A cluster of intense rainfall events in West Berkshire, summer 1999. *Weather*, **55**, 356-363.
46. Burt, S., 1997: The Altnaharra minimum temperature of  $-27.2^{\circ}\text{C}$  on 30 December 1995. *Weather*, **52**, 134-144.
47. Burt, S., 1993: Another new North Atlantic low pressure record. *Weather*, **48**, 98-103.
48. Burt, S., 1992: The exceptional hot spell of early August 1990 in the United Kingdom. *Int. J. Climatol.*, **12**, 547-567.
49. Burt, S., 1992: Weather and streamflow in central southern England during water year 1989/90. *Weather*, **47**, 2-10.
50. Burt, S., 1991: Falls of dust rain within the British Isles. *Weather*, **46**, 347-353.
51. Burt, S., 1989: London's lowest barometric pressure in 167 years. *Weather*, **44**, 221-225.
52. Burt, S. D. and D. A. Mansfield, 1988: The Great Storm of 15-16 October 1987. *Weather*, **43**, 90-110.
53. Burt, S., 1987: A new North Atlantic low pressure record. *Weather*, **42**, 53-56; also *Marine Observer*, **57**, 122-126.
54. Burt, S., 1986: High absolute humidities in Ireland, 12-13 July 1983. *Meteorol. Mag.*, **115**, 406-410.
55. Burt, S., 1985: Remarkable pressure fall at Valentia, 17 October 1984. *Weather*, **40**, 48-51.
56. Burt, S., 1983: Summer 1983 in the United Kingdom. *Weather*, **38**, 320-323.
57. Burt, S., 1983: New UK 20th Century low pressure extreme. *Weather*, **38**, 209-213.
58. Burt, S., 1982: Heavy rainfall and snowstorms, 23-26 April 1981. *Weather*, **37**, 108-115.
59. Burt, S., 1980: Snowfall in Britain during winter 1978/79. *Weather*, **35**, 288-301.
60. Burt, S., 1980: Rainfall in the United Kingdom during 1978. *J. Meteorol. UK*, **5**, 37-61.
61. Burt, S., 1978: The blizzards of February 1978 in south-west Britain. *J. Meteorol. UK*, **3**, 261-278.
62. Burt, S., 1976: The Coventry tornado of 5 August 1975. *J. Meteorol. UK*, **1**, 342-346.
63. Burt, S., 1976: The climate of Rugby: Part 2, Rainfall. *J. Meteorol. UK*, **1**, 149-155.
64. Burt, S., 1975: The climate of Rugby: Part 1, Temperature. *J. Meteorol. UK*, **1**, 9-14.

## APPENDIX

### Copies of published works included within this thesis

The nine referenced papers follow in this order, prefaced with a header sheet for ease of reference

Paper or publication no.	Title	Year of publication	Word count approx. excluding references
1	Near-zero humidities on Ben Nevis, Scotland	2019	6115
2	Response times of meteorological air temperature sensors	2020	5510
3	<i>Calibration</i> . Chapter 15 in <i>The Weather Observer's Handbook</i>	2012	8115
4	<i>Oxford's urban growth and its potential impact on the local climate</i> . Chapter 3 in <i>Oxford Weather and Climate since 1767</i>	2019	3220
5	Two hundred years of thunderstorms in Oxford	2021	4665
6	<i>Durham's barometric pressure records, 1843-1960</i> . Appendix 4 in <i>Durham Weather and Climate since 1841</i>	2022	6800
7	December 2015 – an exceptionally mild month in the United Kingdom	2016	2065
8	The Lowest of the Lows ... extremes of barometric pressure in the British Isles, part 1 <i>and</i> The Highest of the Highs ... Extremes of barometric pressure in the British Isles, Part 2 – the most intense anticyclones	2007	10 975
9	New British Isles late-winter extreme barometric pressure, 29 March 2020	2020	2220
		<b>TOTAL</b>	<b>49 685</b>



# Paper 1

## **Near-zero humidities on Ben Nevis, Scotland, revealed by pioneering nineteenth century observers and modern volunteers**

By Stephen Burt and Ed Hawkins. *International Journal of Climatology*, 2019, **39**, pp. 4451-4466.

*Bibliography # 15. Word count 6115, excluding references.*

---

*The following content is reproduced by kind permission of the Publishers, John Wiley and Sons, under the terms of the Copyright Clearance Center's RightsLink® license number 5100130681907 dated 1 July 2021*



## RESEARCH ARTICLE

# Near-zero humidities on Ben Nevis, Scotland, revealed by pioneering 19th-century observers and modern volunteers

Stephen Burt  | Ed Hawkins 

Department of Meteorology, University of Reading, Reading, UK

**Correspondence**

Stephen Burt, Department of Meteorology, University of Reading, Reading, UK.  
Email: s.d.burt@reading.ac.uk

**Funding information**

NERC Advanced Fellowship, Grant/Award Number: NE/I020792/1; National Centre for Atmospheric Science (NCAS); UK Natural Environment Research Council (NERC)

**Abstract**

The weather on Ben Nevis—the highest mountain in the British Isles at 1345 m above mean sea level—sometimes shows episodes of remarkably low relative humidity (RH) with few precedents anywhere else in the British Isles. We are able to quantify this for the first time using a high-quality series of hourly dry- and wet-bulb observations, made on the summit. These observations were made between 1883 and 1904, but have only just become available to modern science, thanks to thousands of volunteers who worked to rescue this unique and exemplary data set from published volumes. Careful examination and analysis of the original observations using modern psychrometric theory revealed several occasions where we are confident that the summit RH fell close to zero as a result of anticyclonic subsidence. Three case histories are examined in some detail. The 19th-century Ben Nevis humidity records are also compared with contemporary automatic weather station data from two high-altitude Scottish mountain sites.

**KEYWORDS**

anticyclonic subsidence, Aonach Mòr, Ben Nevis, Cairngorm, crowdsourcing, psychrometric calculation, relative humidity, Scotland

## 1 | WHY INVESTIGATE OCCASIONS OF VERY LOW HUMIDITY?

Knowledge of the amount of water vapour in the air, whether measured directly or derived from indirect methods, remains one of the most important parameters in meteorology, whether in climatological studies or in forecast models. Determination of both the average and the range of variation in moisture content is essential for many climatological studies, particularly so for extremes, as prolonged periods of very high humidity (saturated air) or very low humidity are disadvantageous to both human and plant health. Occasions of very low relative humidity (RH) (below 20%) are infrequent in temperate climates, and their rarity warrants investigation of the circumstances under which they occur. Low

humidities at mountain sites in the United Kingdom have previously been documented by Green (1953, p. 490, 1965, p. 477, 1966, p. 488, 1967, p. 320) and Burt (2011).

## 2 | THE BEN NEVIS OBSERVATORY: BACKGROUND AND DATA SOURCES

The International Meteorological Congress of Rome in 1879 set out the perceived necessity of establishing weather stations on mountain summits to assist in developing weather forecasting methods: this was of course many decades before upper-air data became routinely available through balloon and radio-sounding methods. The first such high-level mountain observatory was Säntis in north-east Switzerland at 2502 m above mean sea level (AMSL), where



**FIGURE 1** Location of sites referred to in the text. Aonach Mòr is close to Ben Nevis and is not shown separately

records commenced in 1882 (and continue today). A mountain site in western Scotland was seen to be particularly important owing to its position within the main cyclonic storm track affecting north-west Europe, and Ben Nevis was the obvious choice as both the highest mountain in the British Isles and by virtue of relatively easy access to the summit. Funds were quickly raised by public appeal, and a staffed observatory was established on the summit at 1345 m AMSL by the Scottish Meteorological Society in October 1883 (Figure 1). Hourly observations of pressure, screen temperature (dry- and wet-bulb), wind speed and direction, precipitation, sunshine, cloud amount along with regular observations of present weather types, snow depth and other phenomena (such as thunderstorms, aurora, glories, etc..) were made there and communicated by telegraph link to Fort William, less than 10 km north-west of Ben Nevis as the crow flies (Buchan, 1890, Buchan and Omond, 1902, Omond, 1910, Duncan and Weston, 1983, McConnell, 1988a, McConnell, 1988b; for a recent account of the Observatory's history, see Roy, 2004). Contemporary photographs of the observatory are shown in Figures 2 and 3. A similar observatory was established near sea level in Fort William, to provide simultaneous near-vertical observations throughout the depth of the lowest part of the atmosphere.

Summit weather was frequently atrocious, and observations were often made under difficult or even hazardous circumstances by a small team of dedicated observers. The generation of the records and their survival in published volumes remains a lasting tribute to their dedication, and indeed to the Scottish Meteorological Society itself (which amalgamated with the Royal Meteorological Society in 1921).

Throughout its existence, Ben Nevis Observatory received almost no public funding, and following several



**FIGURE 2** Ben Nevis Observatory from the south-west: contemporary photograph. These images are from the Royal Meteorological Society collection, held as part of the Met Office archive at National Records of Scotland, courtesy Royal Meteorological Society

years of financial deficits both observatories were closed in October 1904. The records from both Ben Nevis and Fort William observatories were published in full in the *Transactions of the Royal Society of Edinburgh* in four large volumes (Buchan, 1890; Buchan and Omond, 1902, 1905; Omond, 1910). However, relatively little use has been made of them since the final volume was published in 1910. In 2017, a project to digitize the published records from the two observatories (by now scanned and available online) resulted in the setting-up of a citizen science Zooniverse website [weatherrescue.org](http://weatherrescue.org). The enthusiastic response of more than 3000 volunteers resulted in the creation of a digital database of close to 2 million records in just 10 weeks. The database has been quality-controlled and researcher access is freely available; the creation and structure of the database are set out in Hawkins *et al.* (2019).

The Ben Nevis Observatory records, consisting of more than 20 years of meticulous manned hourly observations from the highest point in the British Isles made with the best available instruments of the period, constitute without doubt the ultimate British mountain weather data set. Modern unmanned automatic weather stations (AWS) on other Scottish mountains such as Cairngorm (1245 m AMSL) have provided valuable insights into upland weather conditions (see, e.g., Curran *et al.*, 1977, Barton, 1984, <http://cairngormweather.eps.hw.ac.uk>), and more recently Kendon and Diggins (2019), but the severity of the climate and frequent riming make for an extremely difficult operating environment and there are occasional breaks in record as a result. Plans are being made to install a modern, severe-weather capable AWS on Ben Nevis, but these are at an early stage, provision of a stable power supply being one of the main obstacles (the output of solar panels being severely reduced





**FIGURE 3** Ben Nevis Observatory from the south-east: contemporary photograph. These images are from the Royal Meteorological Society collection, held as part of the Met Office archive at National Records of Scotland, courtesy Royal Meteorological Society

in the riming conditions which frequently prevail on the mountain).

### 3 | CALCULATING HUMIDITY

During the years when the Ben Nevis Observatory was operational, values of RH were derived by the observers from published humidity tables. Initially, tables prepared empirically for general-purpose use (not specifically for a high-level observatory) from investigative work undertaken at low-level observatories in London (e.g., Glaisher's tables from Greenwich Observatory—Glaisher, 1869—and similar) were used. The tables made no allowance for reduced atmospheric pressure at altitude (resulting in values of RH that were too low<sup>1</sup>), and although adequate for the conditions of near-saturation that often prevailed, the tables were inadequate for the extremes of both low temperature and low humidity occasionally experienced on Ben Nevis. Extrapolation beyond their normal range was frequently resorted to and “extended” tables drawn up. Work was undertaken at the Observatory in 1885 to compare dew point temperatures derived from dry- and wet-bulb readings using such tables with those measured directly using an early mirror-cell hygrometer by Chrystal (Dickson, 1885); the conclusion was that the tables in use were increasingly in error under certain conditions which occurred much more frequently at the high-level observatory than nearer sea level. The lack of agreement with humidity tables was perhaps fortunate in

<sup>1</sup>The psychrometric equations (see following section) show that the difference between calculated and true ambient RH increases with decreasing ambient pressure and decreasing humidity. A 150 hPa decrease in barometric pressure would reduce a derived RH of 10% to close to zero at the typical air temperatures prevailing on Ben Nevis and result in physically impossible sub-zero RH derivations in drier air.

retrospect, in that the decision was made when the records were eventually prepared for publishing to document the observed readings of both dry- and wet-bulb thermometers, rather than the dry-bulb and RH derived from contemporary tables.

Dry- and wet-bulb thermometers (whether traditional liquid-in-glass units, or electrical resistance devices such as platinum resistance thermometers) offer a reliable, tried-and-tested method for determining RH to acceptable accuracy within a wide range of conditions, specifically when the wet-bulb temperature is above 0°C and the RH is greater than about 20–25%. Outside these limits, the use of a modern properly calibrated capacitance sensor generally provides more consistent and repeatable measurements (see, e.g., Burt, 2011 for another case history of an extremely low RH event in Cumbria in 2011), and it is advisable to exercise caution when using records of dry- and wet-bulb temperature to determine RH in such cases. The subject is covered in more detail elsewhere: see Burt (2012) Chapter 8, Harrison (2014) Chapter 6 or World Meteorological Organization (WMO, 2014) for more detail, but briefly:

- It is difficult to maintain a “wet” wet-bulb thermometer at very low RH, because water loss from evaporation can exceed replacement through capillary action to the wet-bulb muslin “sock”;
- The increased response time owing to the insulation of the muslin “sock” on the wet-bulb can lead to significant lag, particularly where temperatures are changing rapidly;
- The bulb and muslin can remain wet for long periods even when the wet-bulb temperature falls below 0°C, if the temperature does not fall very far. Below typically about –3°C, sometimes lower, the muslin will freeze, at which point the wet-bulb temperature will rapidly rise to 0.0°C owing to the release of latent heat, and remain there for several minutes (a useful calibration check) before as quickly falling back to the pre-freezing temperature, now known as the “ice-bulb temperature.” However, it is almost impossible to maintain a continuous “ice-bulb” (a frozen wet-bulb) at low RH, owing to the cessation of capillary action. The published observatory records do, nevertheless, record the care and attention given to establishing and maintaining the “ice-bulb” at and between hourly observations (Buchan, 1890, pp. xxx–xxx), and we can be sure this was managed as closely as was possible in often extreme circumstances;
- The phase change from ice to liquid water when a frozen wet-bulb warms through 0°C often results in the wet-bulb “sticking” at 0.0°C owing to latent heat extraction. If the dry-bulb continues to warm without hindrance, this results in an artificially large depression of the wet-bulb and thus an unrealistic (low) RH until the phase change is

complete—which in conditions close to 0°C can take hours;

- The derived RH is critically dependent upon wet-bulb ventilation—more on this point subsequently, but a minimum ventilation of about 1 m/s is necessary for confidence in the result;
- Solar heating of the Stevenson screen containing the dry- and wet-bulb thermometers can result in slight additional warming relative to the true air temperature, particularly in light winds (Herbertson, 1905). Usually, the increase in the wet-bulb temperature will be greater than that of the dry-bulb, and the derived RH may be substantially higher than the true (ambient) value.

Hourly values of RH were calculated using the following approach. First, the saturation vapour pressure at the dew point  $e$  was calculated from the psychrometric equation (Harrison 2014):

$$e = e_s(T_{\text{wet}}) - A p (T_{\text{dry}} - T_{\text{wet}}) \quad (1)$$

where  $T_{\text{dry}}$  and  $T_{\text{wet}}$  are, respectively the dry- and wet-bulb temperatures,  $e_s(T_{\text{wet}})$  is the saturation vapour pressure at  $T_{\text{wet}}$ ,  $A$  is the psychrometric coefficient,  $p$  is the station-level pressure in hPa/1,000, and  $T_{\text{dry}} - T_{\text{wet}}$  is the difference in K between the readings of the dry- and wet-bulb thermometers (this term is referred to as the “depression of the wet-bulb”).

The saturation vapour pressure  $e_s$  at any particular temperature  $T$ °C was then obtained from the following expression (Bolton, 1980):

$$e_s = 6.112 \exp(17.67T/T + 243.5) \quad (2)$$

for temperatures  $T$ °C above 0°C, and

$$e_s = 6.109 \exp(22.5T/T + 273) \quad (3)$$

for temperatures  $T$ °C below 0°C.

Finally, the RH is given by

$$\text{RH} = e/e_s \quad (4)$$

usually expressed as a percentage.

The Ben Nevis Observatory humidity data set was calculated from observed and published hourly values of  $T_{\text{dry}}$  and  $T_{\text{wet}}$  (converted from °F to °C, and following quality control checks as set out in Hawkins *et al.*, 2019) and station-level pressure (converted from inches of mercury to hPa). The value of  $A$  varies significantly with ventilation, however. Figure 4, from Harrison and Wood (2012), shows that for ventilation  $\geq 1$  m/s,  $A$  is close to 0.7. For ventilation

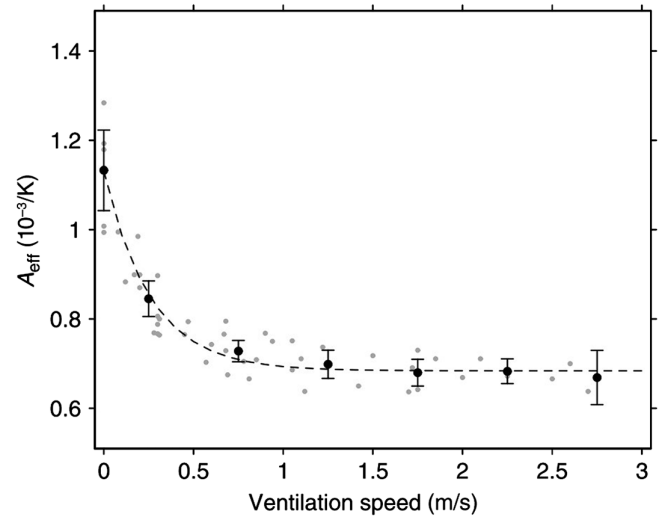


**FIGURE 4** Dependence of psychrometer coefficient  $A$  on ventilation speed. From Harrison and Wood (2012), Figure 3

below about 1 m/s,  $A$  is somewhat higher. The difficulty here is assessing the likely ventilation through the Stevenson-type screens used at the Observatory for each observation; as a proxy (and in the absence of any published studies), it was assumed that screen ventilation was half of the observed hourly wind speeds. At the Ben Nevis Observatory, wind speeds were estimated hourly on the 0–12 Ben Nevis scale (wind speeds were estimated because conventional cup anemometers were unusable in the severe riming conditions prevailing on the summit for much of the year). An equivalence table from the estimated wind force to miles per hour was derived from comparison with cup anemometer records during a few summer months and published (Buchan and Omond, 1905, p. 483). Most often, a range of forces was used—for example, 1–3—and in such cases the average of the two forces is held on the new digital data set. The scale was not linear, and a polynomial expression was used from the published equivalence table to derive observed wind speed in metres per second: more details are given in Hawkins *et al.* (2019). Table 1 gives the values of  $A$  used here for the purposes of the psychrometric equation.

## 4 | THE BEN NEVIS HUMIDITY RECORD

For the entire period of published summit observations, December 1883 to September 1904 inclusive, the RH was calculated using the method above for every hourly observation with a valid dry- and wet-bulb combination—in all, in excess of 180,000 observations. Many wet-bulb observations were missing during the first winter, presumably because it took time to resolve operational difficulties in maintaining ice-bulbs during winter conditions at the

**TABLE 1** Variation of psychrometric coefficient  $A$  used in relative humidity calculations with observed Ben Nevis Observatory wind speed

Ben Nevis Force	Nominal speed in m/s	Assigned value of $A$
0, calm (no wind direction)	0	1.0
0, wind direction given	0.25	1.0
1	3	0.7
2	6	0.7
Range 0–1	Average of force 0 and 1, that is, 1.5 m/s	1.0
Range 0–2	Average of force 0 and 2, that is, 3 m/s	0.7
3 and above	$\geq 10$	0.7

summit; however, after early April 1884 the record is largely complete (including the occasional estimate) until the closure of the Observatory in September 1904. Hourly wind speeds were digitized only for the second half of the record (January 1893 onwards); where a wind speed record was not available, the hourly mean (Ben Nevis Force 2.1, approximately 7 m/s) was used to suggest an appropriate value for  $A$ . Occasional RH values below zero were constrained to 0% RH and (more frequent) values slightly above 100% RH were similarly constrained to 100% (the difficulty of maintaining a “dry” dry-bulb in the high humidity conditions prevalent on the summit are frequently referred to in the published logs). From this, a frequency table was constructed of hourly RH in 5% bins. All observations with a calculated RH less than 10% were re-examined and, where necessary, missing wind speeds added manually from the published observations, and the frequency table recalculated.

**TABLE 2** Frequencies of RH within 5% bins at the Ben Nevis Observatory, April 1884 to September 1904

RH (%)	Frequency	Per mille frequency	RH (%)	Frequency	Per mille frequency
0–5	223	1.2	50–55	1292	7.1
5–10	145	0.8	55–60	1663	9.2
10–15	287	1.6	60–65	1996	11
15–20	395	2.2	65–70	2302	13
20–25	461	2.5	70–75	2675	15
25–30	539	3.0	75–80	3390	19
30–35	666	3.7	80–85	3839	21
35–40	825	4.5	85–90	4884	27
40–45	977	5.4	90–95	6565	36
45–50	1156	6.4	95–100	147 236	811
			Total all obs	181 516	1000

RH calculated using modern psychrometric methods as described in the text and constrained within 0 and 100% RH. All observations of 10% RH or less have a wind speed value associated with them; for other records between 1883 and 1892 inclusive, where hourly wind speeds are not available, the Ben Nevis Observatory mean wind speed of approximately 7 m/s has been assumed in the calculation.

Where station level pressure observations were missing or outside quality control ranges, an average of all the remaining observations (856 hPa) was used in the hourly calculations. Table 2 shows the final table.

The results from Table 2 are plotted on a logarithmic scale in Figure 5 and compared with data for modern records of similar length (from AWS fitted with capacitance humidity sensors) at Aonach Mòr (1130 m AMSL, 3.5 km north-east of the old Ben Nevis Observatory summit site) and on Cairngorm Summit (1237 m AMSL, 91 km east-north-east of Ben Nevis; see Table 3 for site and record details for both locations). The profile of the Ben Nevis historical data in Figure 5 is strikingly similar to the modern records, the higher frequencies close to saturation likely a reflection of the summit being in cloud more frequently than the two slightly lower (and leeward) sites. (The profile agreement also strengthens confidence in the quality and accuracy of the Ben Nevis temperature and humidity data set.) All three sites show a similar frequency of sub-10% RH (2.0 observations per mille at Ben Nevis, 1.2 at Aonach Mòr and 2.6 at Cairngorm), notwithstanding differing record periods, data availability and measurement methods.

The climatological humidity profile for these three high-altitude sites is strikingly different from low-level sites. The fourth profile in Figure 5 is for a low-level site in central southern England (Stratfield Mortimer Observatory in Berkshire, 10 km south-west of Reading, 60 m AMSL) using a 25-year record 1993–2017, mostly from a capacitance RH sensor. Although conditions at high altitude in Scotland remain at or close to saturation for the great majority of observations, RH values below 35% occur more frequently at altitude than at the lowland site,

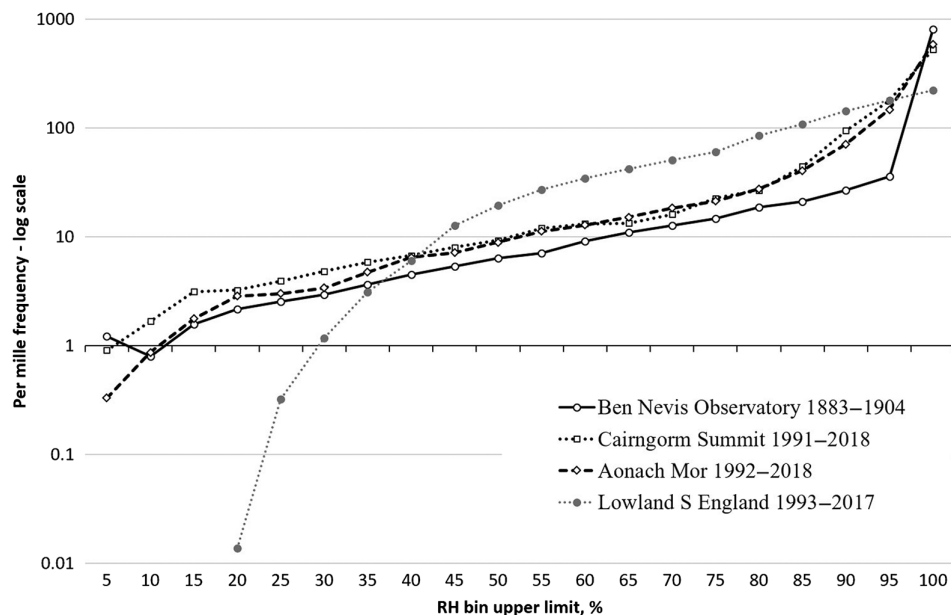


**FIGURE 5** Frequency distribution of hourly relative humidity (per mille, log scale) at the Ben Nevis Observatory, Aonach Mòr and Cairngorm Summit, compared to a lowland site in southern England. Periods of record (20–25 years) and site details are given in Table 3. RH bins are 5% RH ranges plotted to the upper bin limit

**TABLE 3** Location and record details of contemporary high-altitude AWS sites used for comparison with historical Ben Nevis humidity data

	Ben Nevis Observatory	Aonach Mòr	Cairngorm summit
Latitude (°N)	56.80	56.82	57.12
Longitude (°W)	5.00	4.97	3.64
Altitude (m AMSL)	1345	1130	1237
Distance from Ben Nevis summit	-	3.5 km NE	91 km ENE
Record period (within)	12/1883 to 9/1904	2/1992 to 12/2018	12/1991 to 12/2018
No of observations	182,616	197,113	222,469
% availability	100.0	83.3	90.6
No of humidity observations	181,518	178,365	176,910
% observations with humidity data	99.4	90.5	79.5
Mean RH, % (all valid observations)	94.4	90.4	88.9

The Met Office currently operates a network of six mountain stations in the United Kingdom, including Aonach Mòr and Cairngorm Summit. A recent paper by Kendon and Diggins (2019) provides a brief overview of the technology providing records from these very challenging environments. Data for Aonach Mòr and Cairngorm Summit (and the other four UK mountain sites) are now also available online (Met Office, 2019).

the relative frequency increasing with decreasing humidity. On the summit of Ben Nevis, RH values below 25% occurred on average eight times per thousand hours (about 73 hr per annum), compared with a (contemporary) annual average of less than 3 hr at or below 25% in southern England.

## 5 | OCCURRENCES OF VERY LOW RH ON BEN NEVIS

The occurrence of very low humidities on Ben Nevis has been previously documented. The published records themselves contain numerous descriptive accounts and some preliminary steps

towards explanation, although true dynamical understanding in terms of anticyclonic subsidence was still some decades away. Green (1966) investigated several examples from the published record, but the availability of the records only in hardcopy format and the lack of modern digital data-processing methods meant that only a few instances could be examined in detail. The recent digitization of the entire record enables a better understanding of the frequency of such events and a wider examination of the circumstances surrounding them.

From the assembled data set covering April 1884 to September 1904, 49 dates (223 hourly observations in all) were identified when the (recalculated) RH had fallen to 5% or less for at least one hourly observation at the Ben Nevis Observatory. These are listed in Table 4, together with detail

**TABLE 4** All dates when at least one valid hourly observation had a calculated RH 5% or lower, Ben Nevis Observatory December 1883 to September 1904 (see text for calculation method)

Year	Date	Hours RH $\leq$ 5%	Minimum calculated hourly RH (%)	Mean spell (dry-bulb) temperature ( $^{\circ}$ C)	Maximum spell temperature ( $^{\circ}$ C)	Minimum spell temperature ( $^{\circ}$ C)	Mean spell wind speed (m/s)
1886	March 12	3	<0	-6.3	-5.7	-7.1	<1
1888	January 15	2	2	2.2			1
	October 22	1	4	6.4			6
1889	March 27	2	<0	-1.4	-0.7	-2.1	3
1890	February 25	2	<0	7.2	7.2	7.2	2
1892	December 24	1	0	-2.7			12
	December 25	15	<0	-1.9	0.1	-2.7	2
	December 26	6	<0	-1.8	-1.2	-2.2	1
1893	August 29	1	<0	8.4			1
	September 3	1	4	10.9			1
1894	February 14	2	<0	-6.8	-6.4	-7.1	<1
	<b>September 10</b>	8	0	9.5	9.9	9.2	10
	September 16	1	2	9.6			1
	October 4	14	<0	10.9	13.1	8.9	<1
	October 5	3	<0	10.9	10.9	10.6	1
	October 11	2	4	5.6	5.6	5.6	8
1895	<b>February 18</b>	5	<0	-0.1	0.6	-0.9	1
	<b>February 19</b>	17	<0	0.5	3.6	-1.4	<1
	<b>February 20</b>	2	<1	-0.8	-0.6	-0.9	8
	November 25	1	<0	2.6			0
1896	January 9	4	<0	-1.1	-0.4	-1.7	<1
	November 3	1	2	-2.4			0
	November 26	1	3	3.2			0
	November 27	3	<0	3.3	3.9	2.3	<1
1897	February 12	4	<0	-1.7	-1.0	-3.3	0
	April 22	1	<0	-1.0			<1
	April 24	1	4	-0.1			1
	May 20	1	<0	3.5			1
	May 23	3	<0	-2.0	-1.8	-2.2	<1
	November 4	4	<0	9.9	11.1	7.8	1
	November 5	2	2	5.5	6.3	4.7	<1
	December 18	5	<0	0.5	1.0	-0.2	<1
	December 19	4	<0	1.1	1.8	0.5	<1
1898	June 28	2	0	6.9	8.0	5.7	<1
	September 22	5	<0	5.7	6.1	5.1	<1
	September 23	3	<0	5.8	7.1	5.1	<1
	September 24	8	<0	8.8	11.7	6.5	0
	September 25	12	<0	7.7	10.6	5.6	0
	September 26	6	<0	6.0	8.1	5.4	<1
1899	January 28	3	<0	-0.7	-0.3	-1.1	0
	February 19	3	<0	-1.4	-1.0	-2.2	0



TABLE 4 (Continued)

Year	Date	Hours RH $\leq$ 5%	Minimum calculated hourly RH (%)	Mean spell (dry-bulb) temperature ( $^{\circ}$ C)	Maximum spell temperature ( $^{\circ}$ C)	Minimum spell temperature ( $^{\circ}$ C)	Mean spell wind speed (m/s)
	February 20	1	<0	-1.1			1
	May 11	1	1	5.7			1
	May 12	1	5	4.7			0
1900	March 4	1	<0	1.3			1
	March 5	7	<0	1.2	2.1	0.6	<1
	March 6	3	<0	1.3	2.5	0.6	<1
	March 7	1	4	0.4			10
	September 13	1	5	13.9			1
	November 18	1	3	1.9			0
1901	June 6	1	4	5.6			1
	August 20	7	<0	10.8	12.5	9.6	<1
1902	January 30	1	3	-4.9			1
	<b>February 1</b>	8	2	1.1	1.9	-0.3	10
	March 16	2	<0	0.9	1.0	0.7	<1
	December 8	5	<0	-2.9	-2.6	-3.3	1
1904	September 21	2	1	7.9	8.1	7.7	1
	September 23	8	<0	6.9	8.8	6.0	1
	September 24	7	<0	5.4	6.9	5.0	1
	Total hours	223					

All values converted from original units. Observed station level pressures (not shown) used in the calculation. Minimum hourly RH shown as <0 indicates that a negative RH resulted from the calculation and the value was constrained to 0. Mean dry-bulb temperatures and mean wind speeds are also given for the spells listed, and maximum and minimum temperatures where more than a single hour. Multiple hour spells may not all be contiguous within the given date. Dates in bold are examined in more detail in the text.

of mean wind speeds and temperatures for the relevant periods (some are single hour entries). Tables 5–7 provide a breakdown of the frequency (number of observation hours) of RH below 5% by air temperature and wind speed, by month and by hour of day, respectively. During the available period of record, such occurrences were most frequent in late winter and early autumn but are dominated by a few relatively lengthy spells. Very low humidities were not limited to a narrow range of dry-bulb temperatures, events in Table 4 ranging from  $-7$  to  $13^{\circ}$ C. Station level pressure is not shown in Table 4, but the average for the events listed was well above normal (870 hPa, all-events average 856 hPa), indicative of a link with anticyclonic conditions. There is a suggestion of a diurnal variation (afternoon minimum, very broadly similar to the mean diurnal variation of wind speed on the summit), but the effect is small: a possible physical explanation here could involve greater turbulence (and thus entrainment from drier air above the summit) owing to the nocturnal jet. Warming of the screen in sunshine, increasing both dry- and wet-bulb temperatures but with a greater effect on the wet-bulb temperature (thus increasing the calculated RH) may also have some impact.

TABLE 5 Frequency (number of hours) with RH  $\leq$ 5% at Ben Nevis Observatory December 1883 to September 1904, by mean dry-bulb temperature and mean wind speed (for all the RH  $\leq$ 5% hours combined on any given date)

Dry-bulb temperature, $^{\circ}$ C	Mean wind speed $\leq$ 1 m/s	Mean wind speed $\geq$ 2 m/s	Total hours
$\leq -5$	5	0	5
$-5$ to 0	51	9	60
0 to 5	48	9	57
5 to 10	63	12	75
$\geq 10$	26	0	26
Total	193	30	223

## 5.1 | Occurrences at low wind speeds

The majority of the occasions of very low RH (193 of the 223 hourly observations listed in Table 4, 87%) occurred with mean wind speeds during the spell of 1 m/s or less. Unfortunately, the uncertainty associated with such low ventilation rates through the Stevenson screen makes it difficult to assign a firm value to  $A$ , as a result of which the

**TABLE 6** Frequency (number of hours) with RH ≤5% at Ben Nevis Observatory December 1883 to September 1904, by month

	January	February	March	April	May	June	July	August	September	October	November	December	Total
All hours	10	44	19	2	6	3	0	8	62	20	13	36	223
Longest duration on one date, hours	4	20	7	1	3	1	0	7	15	14	4	15	20

The greatest number of hours on any single date in each month is also given.

calculated RH is poorly constrained under those circumstances (this limitation was also pointed out by Townsend (1967), commenting on Green’s 1966 paper). In 124 of these 193 hourly observations (64%) the calculated RH was below zero, a physically impossible result. However, by explicitly assuming that the ambient humidity *was* in low single digits we can evaluate the range of values of *A* necessary to obtain RH = 0% (the minimum value of *A*) or RH = 5% (taken as a nominal low RH value) and compare them with the range of values shown on Figure 4.

By rearranging Equation (3) above, the value of *A* required to produce RH exactly zero (the minimum possible value of *A*, necessarily assuming zero error in thermometer and barometer readings) can be easily calculated, namely

$$A = e_s(T_{wet}) / p(T_{dry} - T_{wet}) \quad (5)$$

at 0% RH and similarly for 5% RH.

The subset of 124 hourly observations with an observed wind speed of 1 m/s or less which resulted in a calculated RH below zero yielded minimum values of *A* (for RH = 0%) and “plausible” values of *A* (RH = nominal 5%) as shown in Table 8. Although this necessarily involves somewhat circular logic, the values of *A* are well within the scope of Figure 4 and are consistent with a mean ventilation through

**TABLE 7** Frequency (number of hours) with RH ≤5% at Ben Nevis Observatory December 1883 to September 1904, by hour of day

Hour GMT	Frequency	Hour GMT	Frequency
01	8	13	7
02	13	14	9
03	9	15	6
04	9	16	6
05	12	17	9
06	9	18	8
07	9	19	6
08	9	20	11
09	10	21	12
10	11	22	9
11	13	23	11
12	9	24	8
		Total	223

**TABLE 8** Minimum values of psychrometric coefficient *A* to attain RH 0% or RH 5% for those occasions when calculated RH fell below 0%, for wind speeds below 2 m/s: Ben Nevis Observatory December 1883 to September 1904

Number of events	124	
	RH = 0%	RH = 5%
Mean	0.903	0.857
Median	0.908	0.863
SD	0.073	0.070
Minimum value	0.636	0.605
Maximum value	0.999	0.949
Mean +2SD	1.049	0.997
Mean -2SD	0.755	0.718

the Observatory screen in light wind conditions of approximately 0.2–0.3 m/s, or about half of the observed mean wind speed during these spells. Within the limits of the century-old data set, the agreement and fit are surprisingly good, and it seems plausible to claim that the summit humidity *was* very close to zero on these occasions. However, a more exact determination would require finer resolution of both surface wind speed and in-screen ventilation during these events, neither of which is ever likely to become available. For this reason, more attention has been focused on occasions when the ventilation was greater than 2 m/s, as this is the approximate lower limit of wind speed sufficient to ensure at least 1 m/s ventilation through a Stevenson screen.

## 5.2 | Occurrences at wind speeds of 2 m/s or more

Of the 223 hourly observations with RH ≤ 5%, only 30 had wind speeds of 2 m/s or greater (Tables 4 and 5). With greater ventilation comes greater confidence in the value of *A*; only one of these 30 hourly observations resulted in a recalculated RH below 0%. These 30 events also ranged across a wide range of air temperatures, although the depression of the wet-bulb required for such low humidities ensured that the wet-bulb was below 0°C in all but one. In the majority of these events the wet-bulb was below -3°C and, as such, would probably consist of an ice-bulb with consequent limitations on the supply of water available through capillary action. Without careful manual attention to

moistening the wet/ice-bulb in good time before the observation, this would result in higher wet-bulb temperatures (i.e., closer to the dry-bulb) and thus artificially highly derived humidity readings; fortunately there is ample evidence in the published accounts (see, e.g., Buchan, 1890, pp. xxx–xxx) that great care was taken in such conditions.

## 6 | CASE STUDIES

Three examples were chosen to illustrate summit conditions during extended periods of low humidity when strong winds provided sufficient ventilation to assume confidence in psychrometric calculations. The three spells detailed here account for one third of the duration of all spells with RH at or below 5%.

### 6.1 | Example 1: September 10, 1894

Scotland lay to the north of an anticyclone centred over the Irish Sea; Figure 6 shows the synoptic situation at 1200 GMT from the 20th Century Reanalysis (Compo et al, 2011) and Figure 7 is a time series of hourly wind speeds and calculated RH from the Ben Nevis Observatory over September 9–10, 1894. This occasion was also one of those examined by Green (1966).

Skies were cloudless throughout September 9 and into the early hours of September 10. Cloudier conditions prevailed from before dawn until late morning (cloud cover was unbroken at 0800 GMT) on September 10, after which cloud cleared to 10% or less until after 1600 GMT; the summit was enveloped in cloud by 2100 GMT. During September 9, winds were light north to north-easterly during the morning, veering

progressively during the day to southerly by late afternoon and westerly by midnight, and freshening somewhat; during September 10 winds were mostly between west and north-west, increasing irregularly during the day to average 16 m/s by evening. The RH began an irregular fall from 2000 GMT on September 9 as the wind became west-south-westerly. This decrease continued through the night and into the following day, the RH remaining at or below 20% for all but one of 16 consecutive hours from 0300 GMT, and below 10% for 10 consecutive hours. Throughout this period, mean winds varied between 6 and 16 m/s, thus providing more than adequate ventilation through the Stevenson screen. At 1600 GMT on September 10, the dry-bulb stood at 9.8°C and the wet-bulb at –0.1°C, leading to a calculated RH of 0.1%. The wind at this time was north-westerly at 14 m/s. Unusually, there are no comments specific to the day's weather or low humidity from the published Observatory logbook entries during this event, although the manuscript log book includes reference to the very dry air (Marjory Roy, Personal Communication, 2018). At Fort William the RH exhibited a simple diurnal cycle, and the lowest observed RH was an unremarkable 57%.

### 6.2 | Example 2: February 17–20, 1895

This spell occurred towards the close of one of the coldest spells in Scotland's recorded history, the temperature on the summit remaining below 0°C continuously from December 26, 1894 to the morning of February 18. Ben Nevis lay close to the centre of an anticyclone on February 20, 1895 (Figure 8). Figure 9 shows the mean wind speed and calculated RH at each hourly observation over the period February 18–20. Aside from more extensive cloud cover during the afternoon of February 18, skies

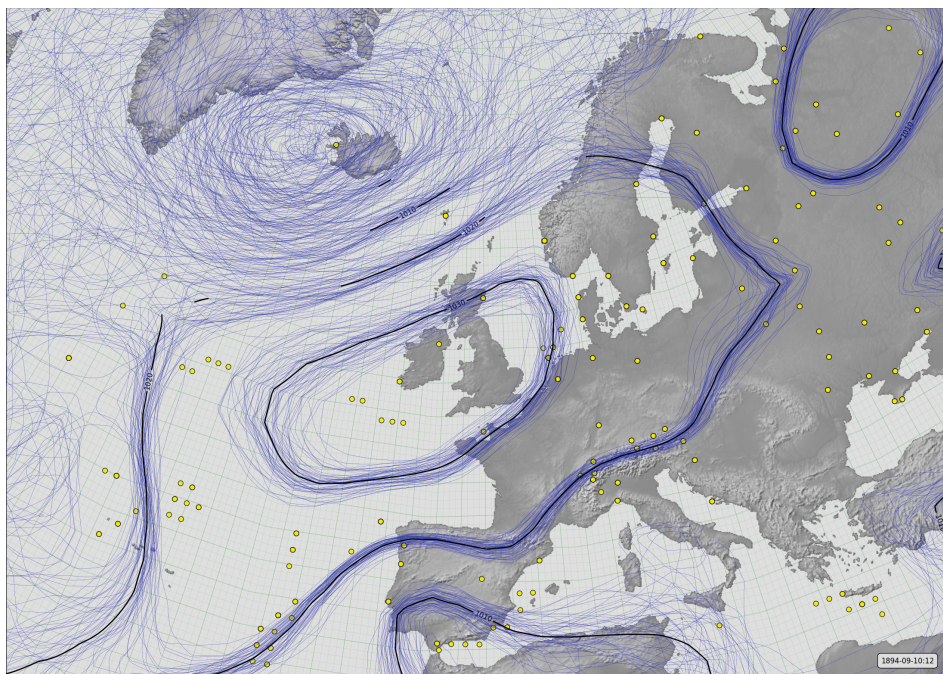


**FIGURE 6** Synoptic situation at 1200 GMT on September 10, 1894. Isobars are shown at 10 hPa intervals from a reanalysis ensemble of multiple members; isobars with high location confidence are shown in black. Small circles mark the locations of sites whose pressure data was used to prepare this reanalysis product. The isobar enclosing most of the British Isles is 1030 hPa. Plot courtesy Philip Brohan, Met Office (Compo et al, 2011) [Colour figure can be viewed at [wileyonlinelibrary.com](http://wileyonlinelibrary.com)]



**FIGURE 7** Time series of hourly wind speed (m/s, grey columns) and calculated RH (%) (solid black line) over September 9–10, 1894 at the Ben Nevis Observatory, Scotland; data set from Hawkins *et al.* (2019). Time is in GMT. At 1600 GMT on September 10, 1894 the calculated RH was 0.1%, surface wind northwesterly 14 m/s

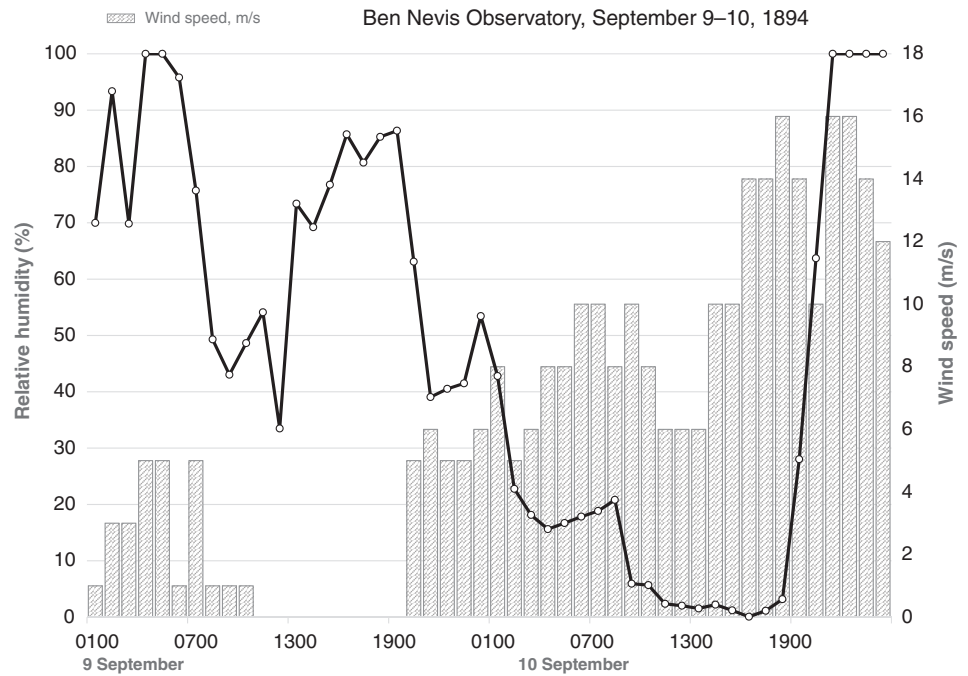
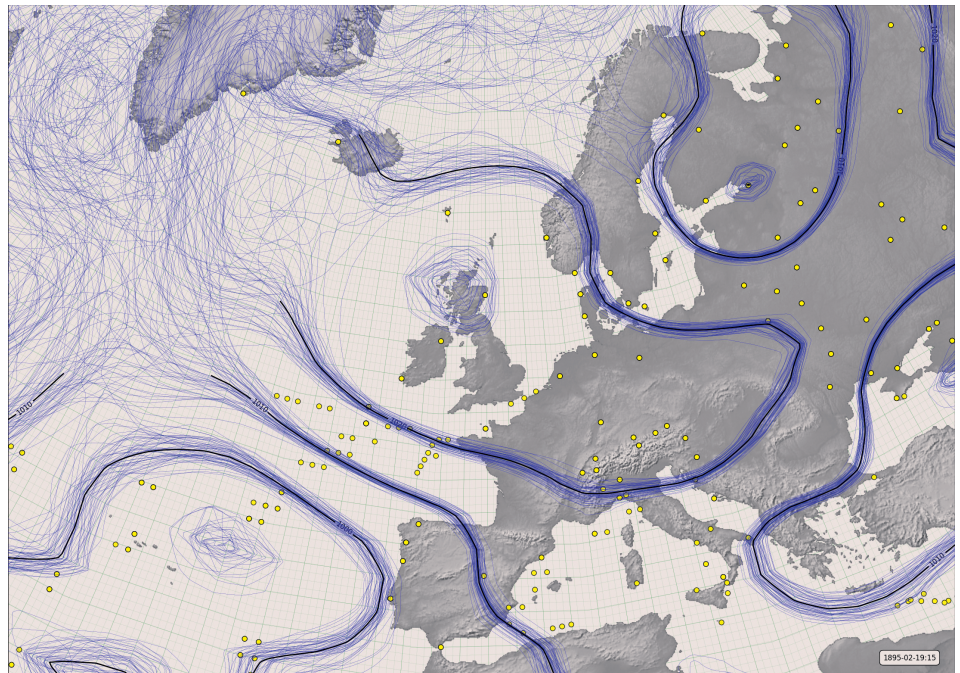


**FIGURE 8** Synoptic situation at 1500 GMT on February 19, 1895. Legend as Figure 6. Plot courtesy Philip Brohan, Met Office (Compo *et al.*, 2011). The central isobar over Scotland is 1030 hPa [Colour figure can be viewed at [wileyonlinelibrary.com](http://wileyonlinelibrary.com)]



were cloudless or nearly so until 1200 GMT on February 20, when the summit became enveloped in cloud for the remainder of the day. Winds were fresh south-easterly on 17th, falling light on 18th then backing north-east by evening before falling calm for long periods on February 19, after which they picked up from the north-west or north during the afternoon of February 19; by late evening mean winds were 6–8 m/s, reaching 12 m/s by 0500 GMT on February 20. The first observation of very low humidity occurred on February 17, when at 1500 GMT the calculated RH stood at 18%, the wind east-south-easterly at 7 m/s; thereafter the RH remained at or below

25% for 63 consecutive hours. Calculated RH values become negative (using  $A = 1$  for winds below 2 m/s) for all but 1 hr in 21 consecutive hours from 2100 GMT on February 18, but as stated above such conclusions are suspect given the very light winds (8 hourly observations during February 19 were “flat calm,” that is, wind speed zero, without a wind direction). Assuming a slightly lower but feasible value of  $A$ , say 0.8, gives RH values mostly in the range from 0 to 10%, as indicated by the dotted grey RH line on Figure 9.

We can have more confidence in the calculated RH from 1800 GMT on February 19, because winds freshened once

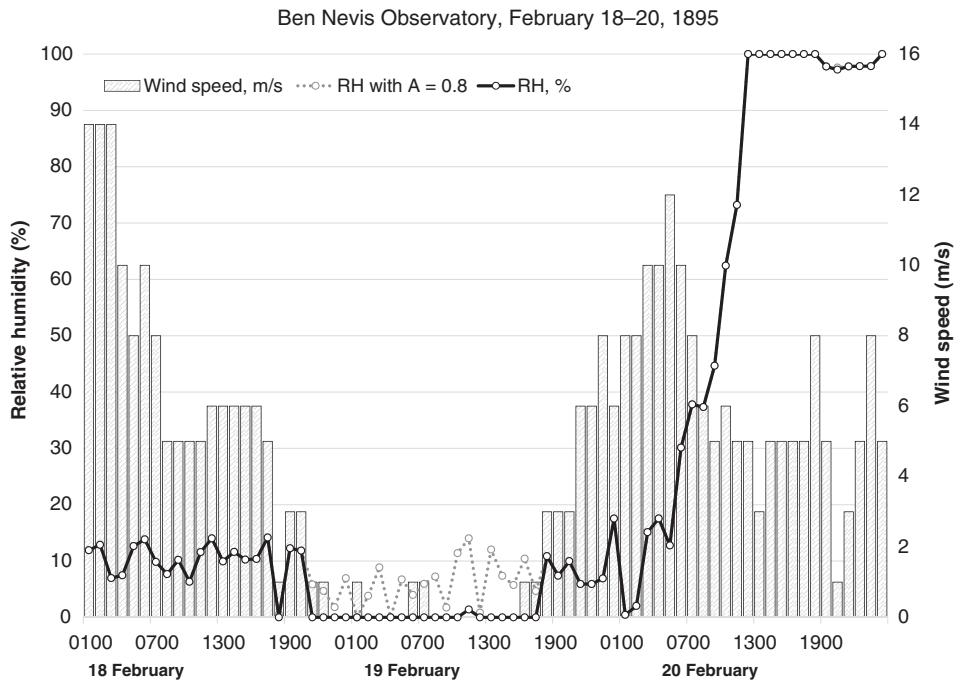


**FIGURE 9** Time series of hourly wind speed (m/s, grey columns) and calculated RH (%) (solid black line) over February 18–20 1895 at the Ben Nevis Observatory, Scotland; data set from Hawkins *et al.* (2019). Time is in GMT. The dotted grey line shows RH values calculated assuming a psychrometric coefficient  $A$  of 0.8 instead of 1.0 during light winds

more from the north–north-west (and thus we can infer that screen ventilation improved). Typical RH values were 5–15% until 0500 GMT, with winds increasing to 6–12 m/s. At 0100 GMT on February 20, with the dry-bulb at  $-0.9^{\circ}\text{C}$  and the wet-bulb (ice-bulb) at  $-6.6^{\circ}\text{C}$ , the wind north-west averaging about 8 m/s, the calculated RH fell to 0.5%. Conditions were almost unchanged the following hour, when the calculated RH was 2%. The values recorded on this date and on September 10, 1894 are probably as close to zero as can be expected, given the limitations of thermometry at such low levels of water vapour content, and remain amongst the lowest reliably recorded RH values on record within the British Isles.

The notes from the Observatory logbook for this event read as follows:

February 17—Not a particle of cloud seen today either above or below summit. Aurora seen till 5 hr and after 20 hr. At the latter hour the zodiacal light was seen. Air exceedingly dry today, humidity being below 20% at 1 hr and 3 hr and from 15 hr till midnight.

February 18—The south-easterly wind that has been blowing since the morning of 13th died out this afternoon. Aurora seen in morning and again at night and the zodiacal light at 20 hr. Air very dry again today, the maximum humidity being only 28%. Today the temperature rose to the freezing point for the first time since 25th December.

February 19—Cloudless, and air very dry all day. Aurora seen in morning and at night, and the zodiacal light at 20 hr.

February 20—Cloudless and air very dry till 1 hr. Fog for the rest of the day. Aurora seen at 1 hr and 2 hr.

### 6.3 | Example 3: January 30 to February 2, 1902

Towards the end of January 1902, barometric pressure rose rapidly in the lee of a deep depression that crossed Scotland on January 28, and an intense anticyclone became established over the Baltic and Scandinavia with a strong ridge westwards towards Scotland during January 31–February 1. The synoptic situation at 1200 GMT on February 1 is shown in Figure 10. This occasion is doubly noteworthy, as the anticyclone in question produced the highest mean sea level barometric pressure yet observed in the British Isles—at 2200 GMT on January 31 the pressure stood at 1053.6 hPa at Aberdeen and 1053.4 hPa at Fort William (Burt, 2007). Occasional examples of low RH are evident in the Ben Nevis Observatory record from January 30, but the main spell of dry air occurred during February 1 (Figure 11), when the calculated RH remained below 20% for 17 consecutive hours from 0300 GMT. The sky was largely free of cloud during this event; the winds were northerly at the beginning of the spell, veering south-easterly during January 30 and remaining south-easterly or east-south-easterly throughout January 31 and February 1, before backing north-easterly on February 2. Except for a few hours late on January 30 winds were brisk throughout, and during the period of lowest RH on February 1 averaged 12 m/s. In the 13 hourly observations commencing 0600 GMT, only one exceeded 10%



**FIGURE 10** Synoptic situation at 1200 GMT on February 1, 1902. Legend as Figure 6. Plot courtesy Philip Brohan, Met Office (Compo et al, 2011). The isobar enclosing Scotland is 1040 hPa. A second reanalysis plot for 850 hPa (not shown) confirmed the existence of very dry air at this level [Colour figure can be viewed at [wileyonlinelibrary.com](http://wileyonlinelibrary.com)]

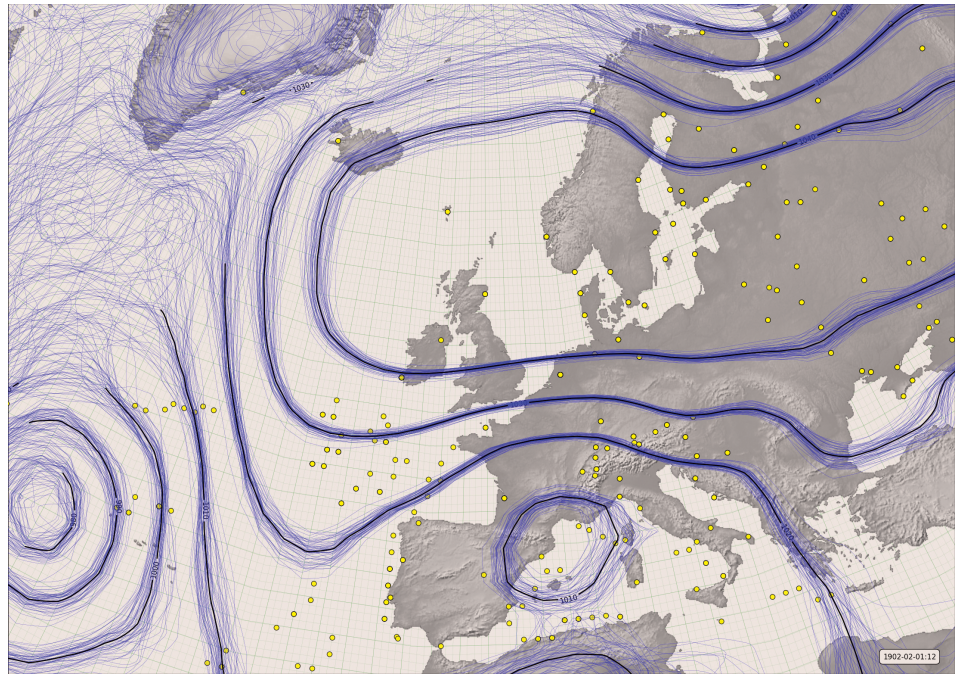
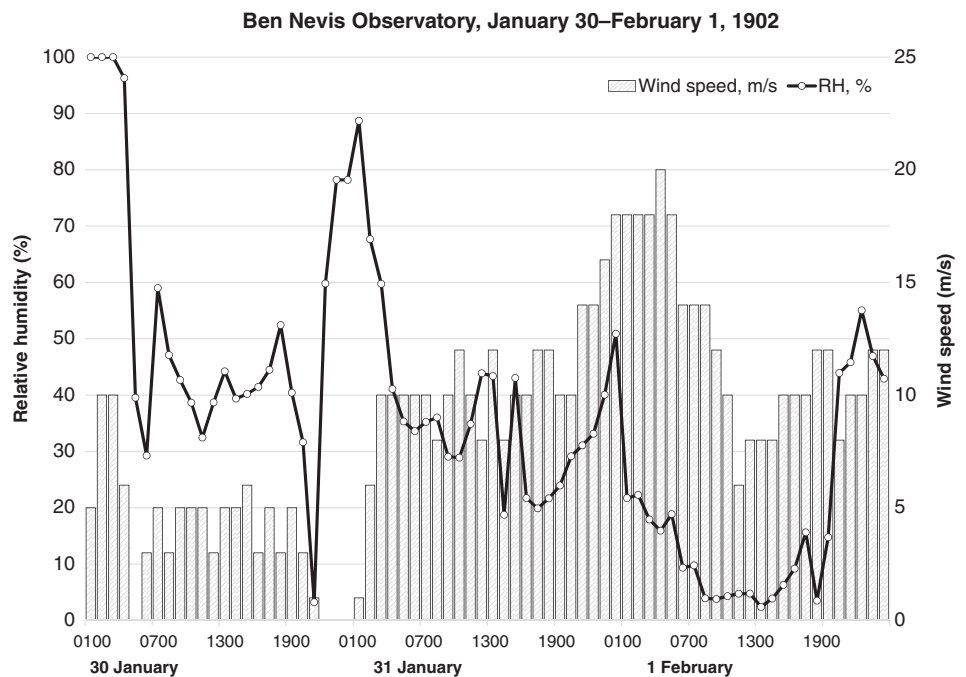


**FIGURE 11** Time series of hourly wind speed (m/s, grey columns) and calculated RH (%), solid black line) over January 30 to February 1, 1902 at the Ben Nevis Observatory, Scotland; data set from Hawkins *et al.* (2019). Time is in GMT



RH, the lowest being 2% at 1300 GMT (dry-bulb 1.2°C, wet/ice-bulb  $-5.0^{\circ}\text{C}$ , wind north-easterly averaging 8 m/s), and 3% at 1800 GMT. This event was written up in the log-book as follows:

January 30—Air exceptionally dry and clear after 4 hr, the lowest humidity being 14% at 21 hr. Sky cloudless all day, except for a little cirrus moving slowly from N. A little fog on hills to E and SE in early morning and over Locheil during the day. The cirrus seen at 5 hr

was ribbed, resembling the shape of an opened fan, the apex being about  $7^{\circ}$  above the southern horizon, and the rays extending to the zenith. January 31—Pressure high all day. The reading at 23h, viz. 26.258 in. [889.2 hPa], is the highest recorded at this Observatory, being 0.003 higher [0.1 hPa] than that in January 1896. The air has been exceptionally dry all day, the lowest humidity being 11% at 17 hr, and the mean for the day 22%. Sky cloudless

and air very clear all day. A little fog in valley to SE in early morning and over Locheil and Loch Lochy during the day.

February 1—Air dry, the humidity ranging from 12 to 53%, and sky cloudless down to horizon all day.

February 2—Air very dry all day, the mean humidity being 39%. A little cirrus on sky in forenoon, but clearing away in the afternoon. Fog below all round most of the day, on which glories were seen in afternoon.

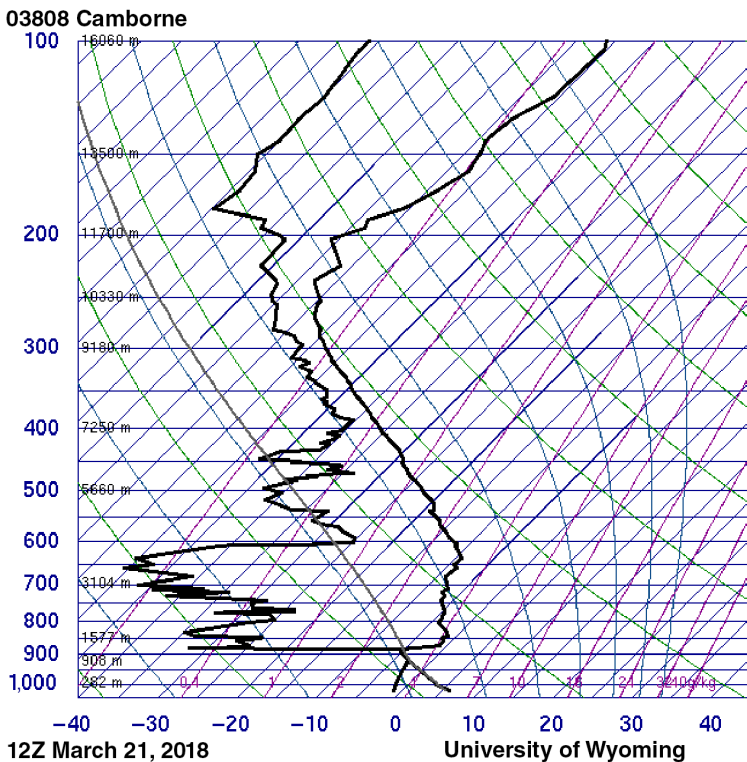
### 6.4 | Discussion and causes

All of the examples listed in the previous section share a common synoptic feature—a nearby anticyclone (corroborated by the mean station-level pressure of the “5% RH events” being 14 hPa above normal). Such instances of dry air at the summit of Ben Nevis are textbook examples of the warming and drying effects of anticyclonic subsidence. Air gently subsides within anticyclones, and as air subsides it warms through compression at or close to the dry adiabatic lapse rate, 10°C per 1,000 m in the lower troposphere. Air descending from considerable heights in the troposphere will be very cold and will contain very little water vapour by virtue of its low temperature. As the air descends and warms within a large anticyclone it will gain little if any additional moisture until it intercepts the planetary boundary layer, at

which point a stable subsidence inversion forms to mark the boundary between moister planetary boundary layer and the warmer, drier subsided air.

Such anticyclonic subsidence inversions are familiar features on upper-air diagrams such as tephigrams or skew-T plots. Figure 12 shows the sounding from Camborne in south-west England for 1200 UTC on March 21, 2018, when a large anticyclone (1038 hPa) lay to the south-west of the British Isles. A pronounced subsidence inversion is present at 883 hPa, the RH decreasing from 100% at 884 hPa (1266 m AMSL) to 9% at 881 hPa (1292 m AMSL)—less than 30 m in altitude separating saturated air from very dry air. On this occasion, had this been a sounding near Ben Nevis, only the topmost reaches of the mountain (summit observatory at 1345 m) would be located within the very dry air, with a sudden fall in RH heralding the “descent” of the subsidence inversion.

Very rapid rises or falls and/or periods of very rapid fluctuations in RH are often symptomatic of the descent of such subsidence inversions over British mountains, as the Ben Nevis Observatory examples in Figures 7, 9 and 11 clearly show. A recent example occurred on Great Dun Fell in Cumbria (857 m AMSL) on March 2–3, 2011 (Burt, 2011), where the 1-min record of a capacitance RH sensor revealed very rapid RH fluctuations between 15 and 70% RH over a 2–3 hr period as the subsidence inversion “settled” over the summit; the RH eventually fell to 5.6%. More recently, the Aonach Mòr site recorded 0% RH at 0900 and 1100 UTC on



SLAT	50.22
SLON	-5.32
SELV	88.00
SHOW	16.11
LIFT	16.28
LFTV	16.27
SWET	48.00
KINX	-42.3
CTOT	-1.80
VTOT	21.20
TOTL	19.40
CAPE	2.93
CAPV	3.33
CINS	0.00
CINV	0.00
EQLV	882.2
EQTV	881.9
LFCT	923.0
LFCV	923.0
BRCH	0.15
BRCV	0.18
LCLT	270.4
LCLP	923.0
MLTH	276.7
MLMR	3.42
THCK	5378.
PWAT	6.65

**FIGURE 12** Skew-T plot of the upper-air sounding from Camborne in south-west England for 1200 UTC on March 21, 2018 showing a very marked anticyclonic subsidence inversion at 883 hPa. Courtesy of the University of Wyoming [Colour figure can be viewed at [wileyonlinelibrary.com](http://wileyonlinelibrary.com)]

June 10, 2015, and the Cairngorm Summit site logged similar values at 0600 GMT on June 5, 2018 and again at 0500 and 0600 GMT on June 6, 2018. Very dry air at summit level on both occasions is supported by Scottish upper-air ascent data. Clearly, the newly digitized 19th-century observations of near-zero humidity on the summits of the highest Scottish mountains, while rare, are fully borne out by modern records.

## 7 | SUMMARY AND CONCLUSIONS

Although the occurrence of spells of such extremely dry air on this notoriously wet mountain summit in western Scotland puzzled contemporary meteorologists, the cause and dynamics of anticyclonic subsidence are well-understood today. Recent digital access to the hourly observation records from the Ben Nevis Observatory, together with improved insights into the parameters used in the psychrometric equation, has allowed the examination of the circumstances surrounding these episodes of near-zero RH to be conducted in greater detail, and with improved confidence in the reliability of the derived humidity values, than previously possible. It is likely that, within the limitations of the thermometry in use at the Ben Nevis Observatory and the assumptions necessarily involved within the psychrometric calculations, on occasions the water vapour content of the air on the summit of this mountain in western Scotland fell as close to zero as could be realistically measured with standard meteorological instruments of the era. The occurrence and frequency of such events are fully supported by contemporary measurements made on two other Scottish mountain summits.

## ACKNOWLEDGEMENTS

This project would not have been possible without the tireless efforts of the thousands of volunteers who donated their spare time to help rescue this unique data set. Marjory Roy provided invaluable assistance in helping get the project off the ground and in tracking down Ben Nevis records and references. Philip Brohan (UK Met Office) kindly contributed reanalysis plots, including 850 hPa humidity ensembles. Data from Cairngorm and Aonach Mòr were kindly provided by Mark McCarthy from the Met Office's National Climate Information Centre under an Open Government Licence (now available online, Met Office, 2019). The UK Natural Environment Research Council (NERC) provided funding through their Public Engagement programme and the National Centre for Atmospheric Science (NCAS) also supported the project. E.H. received funding from a NERC Advanced Fellowship (grant NE/I020792/1). The authors remain grateful to

two anonymous referees who provided numerous useful comments and suggestions on an early version of this paper.

## DATASET ACCESSIBILITY

The full Ben Nevis digitized data set is now available at *Geoscience Data Journal* (Hawkins *et al.*, 2019). The hourly dry-bulb, wet-bulb, pressure, wind speed and direction and calculated RH dataset is available, with documentation, at <https://catalogue.ceda.ac.uk/uuid/1d29816cee7e4fb586b80a3f7debc8e>.

## ORCID

Stephen Burt  <https://orcid.org/0000-0002-5125-6546>

Ed Hawkins  <https://orcid.org/0000-0001-9477-3677>

## REFERENCES

- Barton, J.S. (1984) Observing mountain weather using an automatic station. *Weather*, 39, 140–145.
- Bolton, D. (1980) The computation of equivalent potential temperature. *Monthly Weather Review*, 108, 1046–1053.
- Buchan, A. (1890) Meteorology of Ben Nevis. *Transactions of the Royal Society of Edinburgh*, 34, xvii–lxi.
- Buchan, A. and Omond, R.T. (1902) The Ben Nevis observations (1888–1892). *Transactions of the Royal Society of Edinburgh*, 42.
- Buchan, A. and Omond, R.T. (1905) The Ben Nevis observations (1893–1897). *Transactions of the Royal Society of Edinburgh*, 43.
- Burt, S. (2007) The highest of the highs ... Extremes of barometric pressure in the British Isles, part 2—the most intense anticyclones. *Weather*, 62, 31–41.
- Burt, S. (2011) Exceptionally low relative humidity in northern England, 2–3 March 2011. *Weather*, 66, 197–199.
- Burt, S. (2012) *The Weather Observer's Handbook*. Cambridge University Press, pp. 444.
- Curran, J.C., Peckham, G.E., Smith, D., Thom, A.S., McCulloch, J.S. G. and Strangeways, I.C. (1977) Cairngorm summit automatic weather station. *Weather*, 32, 61–63.
- Dickson, H.N. (1885) The hygrometry of Ben Nevis. *Proceedings of the Royal Society of Edinburgh*, 13, 950–960.
- Duncan, C.N. and Weston, K.J. (1983) Ben Nevis Observatory, 1883–1983. *Weather*, 38, 298–303.
- Glaisher, J. (1869) *Hygrometrical Tables*, Fifth edition. London: Taylor and Francis.
- Green, F.H.W. (1953) A remarkable low humidity. *Weather*, 8, 182–184.
- Green, F.H.W. (1965) The incidence of low relative humidity in the British Isles. *Meteorological Magazine*, 94, 84–88.
- Green, F.H.W. (1966) Low air humidities 28 March to 2 April 1965. *Weather*, 21, 101–104.
- Green, F.H.W. (1967) Air humidity on Ben Nevis. *Weather*, 22, 174–186.
- Harrison, R.G. (2014) *Meteorological Measurements and Instrumentation*. Wiley.

- Harrison, R.G. and Wood, C.R. (2012) Ventilation effects on humidity measurements in thermometer screens. *Quarterly Journal of the Royal Meteorological Society*, 138, 1114–1120.
- Hawkins, E., Burt S., Thomas S., Lockwood M., Brohan P., Richardson H. and Roy M. (2019): Hourly weather observations from the Scottish Highlands (1883-1904) rescued by volunteer citizen scientists. (Submitted to *Geoscience Data Journal*; February 2019)
- Herbertson, A.J. (1905) Comparison of dry and wet-bulb records in Stevenson screen and aspiration-psychrometer under different weather conditions. *Transactions of the Royal Society of Edinburgh*, 43, 529–564.
- Kendon, M. and Diggins, M. (2019) Severe weather and snow conditions on Cairngorm summit in February to March 2018. *Weather*, 74, 98–103. <https://doi.org/10.1002/wea.3390>.
- McConnell, D. (1988a) The Ben Nevis observatory logbooks, part 1. *Weather*, 43, 356–362.
- McConnell, D. (1988b) The Ben Nevis observatory logbooks, part 2. *Weather*, 43, 396–401.
- Met Office. (2019) *Met Office MIDAS Open: UK Land Surface Stations Data (1853-current)*. Centre for Environmental Data Analysis.
- Available at: <http://catalogue.ceda.ac.uk/uuid/dbd451271eb04662beade68da43546e1> [Accessed 22nd February 2019].
- Omond, R.T. (1910) The Meteorology of the Ben Nevis Observatories: Part IV, Containing the Observations for the Years 1898–1904. *Transactions of the Royal Society of Edinburgh*, 46, Part I.
- Roy, M. (2004) *The Weathermen of Ben Nevis 1883-1904*. Royal Meteorological Society, pp. 62.
- Townsend, C.F. (1967) Air humidity on Ben Nevis (letter to the editor). *Weather*, 22, 473–474.
- World Meteorological Organization (WMO), (2014) WMO No.8 – Guide to Meteorological Instruments and Methods of Observation (CIMO guide) (Updated version, May 2017), pp. 1139.

**How to cite this article:** Burt S, Hawkins E. Near-zero humidities on Ben Nevis, Scotland, revealed by pioneering 19th-century observers and modern volunteers. *Int J Climatol*. 2019;1–16. <https://doi.org/10.1002/joc.6084>



# Paper 2

## **Response times of meteorological air temperature sensors**

By Stephen Burt and Michael de Podesta (National Physical Laboratory, Teddington)

*Quarterly Journal of the Royal Meteorological Society*, 2020, **146**, pp. 2789-2800

*Bibliography # 5. Word count 5510, excluding references.*

---

### **Open Access Article**

*This is an open access article distributed under the terms of the Creative Commons CC BY license, which permits unrestricted use, distribution, and reproduction in any medium, provided the original work is properly cited.*





**RESEARCH ARTICLE**

# Response times of meteorological air temperature sensors

Stephen Burt<sup>1</sup>  | Michael de Podesta<sup>2</sup> 

<sup>1</sup>Department of Meteorology, University of Reading, Reading, UK

<sup>2</sup>National Physical Laboratory, Teddington, UK

**Correspondence**

Stephen Burt, Department of Meteorology, University of Reading, RG6 6BB, Reading, UK.

Email: s.d.burt@reading.ac.uk

**Abstract**

Guidelines in the *Guide to Meteorological Instruments and Methods of Observation* (the CIMO guide) of the World Meteorological Organization (WMO, published 2014, updated 2017, section 2.1.3.3, *Response times of thermometers*) recommend that the 63% response time  $\tau$  for an air temperature sensor be 20 s, although – as airflow speed influences response time – the minimum airflow speed at which this applies should also be specified in the document. A 63% response time  $\tau_{63} = 20$  s implies that 95% of a step change be registered within  $3\tau_{63}$  or 60 s, the WMO recommended averaging interval for air temperature: rapid air temperature changes on this time-scale are not uncommon, often associated with convective squalls, frontal systems or sea breeze circulations. An alternative way of expressing the effect of the time constant is that in air whose temperature is changing at  $0.1 \text{ K}\cdot\text{min}^{-1}$  the thermometer would lag by approximately 0.03 K.

To assess whether this response time specification was realistic, we have undertaken an experimental and theoretical study of the time constants of meteorological thermometers. Laboratory wind tunnel tests were undertaken to quantify 63% and 95% response times of 25 commercial  $100 \Omega$  platinum resistance thermometers (PRTs) of various sizes (length and sheath diameter) from five manufacturers. The test results revealed a fourfold difference in response times between different sensors: none of the PRTs tested met the CIMO response time guideline at a ventilation speed of  $1 \text{ m}\cdot\text{s}^{-1}$  assumed typical of passively ventilated thermometer shields such as Stevenson-type thermometer screens. A theoretical model of the sensors was devised which matched the experimental behaviour with regard to the most important contributing factors, namely ventilation rate and sensor diameter. Finally, suggestions and recommendations for operational air temperature sensor adoption and future sensor development are included.

**KEYWORDS**

air temperature, platinum resistance thermometer, response time, thermometer screen, WMO CIMO

## 1 | BACKGROUND AND MOTIVATION

### 1.1 | Meteorological relevance

Although the relative “sensitivity” of meteorological thermometry was first experimentally examined almost 150 years ago (Symons, 1875), it is perhaps surprising how little recent attention has been paid within the meteorological community to determining and optimising the response times of air temperature sensors. This is despite acknowledged recognition of the importance of sensor response time on meteorological temperature measurements, particularly maximum and minimum air temperatures, and the implications of differing sensor response times within a heterogeneous meteorological network are significant. A study by Lin and Hubbard (2008) noted instrumental biases in daily maximum and minimum air temperatures and diurnal temperature range resulting from variations in sampling rates, averaging algorithms and sensor time constants (implying degradation in between-site comparisons, whether in real-time or within long-term records), and recommended that such variations be reduced as far as possible to minimise resulting uncertainties in climatological datasets. More recently, Thorne *et al.* (2016) have included an extensive discussion of inhomogeneities in records of diurnal temperature range, noting that individual  $T_{\text{MAX}}$  and  $T_{\text{MIN}}$  data sets were more sensitive to inhomogeneities than their average. This observation highlights the significance of documenting changes in observational practice (including changes in sensor type or construction) when determining extreme temperatures.

Recent work by the Australian Bureau of Meteorology has quantified differing response times of “traditional” liquid-in-glass thermometry compared to faster-reacting electronic sensors (Benbow *et al.*, 2018) to assess possible lack of record consistency, particularly as “manual” observing sites transition to automatic weather station sensors (see also Box 1). Much of the (rather scant) literature on mercury-in-glass or PRT response times concerns industrial or biomedical temperature sensors, some of which require a much wider or much narrower range of operating temperatures than meteorological applications, lower precision and/or much less demanding requirements in terms of long-term calibration stability (years to decades): examples include Chohan and Hashemian (1989), Mackowiak and Worden (1994), Khorshid *et al.* (2005), Kyriacou (2010) and Niven *et al.* (2015).

Response times in stirred liquids (often water) are more frequently quoted than response times in gases: the relevant British Standards Institution Standard BS

EN 60751:2008<sup>1</sup> (British Standards Institution, 2008) specifies that PRT response times to 50% response should be measured in flowing water (at  $0.2 \text{ m}\cdot\text{s}^{-1}$ ) and flowing air (at  $3 \text{ m}\cdot\text{s}^{-1}$ ), although mandatory performance compliance levels are not set out. Incompletely considered changes in meteorological networks, particularly the wholesale substitution of sensors whose response rate or measuring/sample times differ significantly from historical methods of determination of air temperatures (usually liquid-in-glass thermometry) run the risk of introducing significant inhomogeneities into long-term temperature records: US examples have been given by Hubbard *et al.* (2001; 2004), and Doesken (2005). In Europe, Hannak *et al.* (2020) examined the variable impact of site automation using parallel daily mean temperature series. In addition, the bringing together of meteorology and metrology groups within Europe to work on areas of common importance within recent years has, and continues to bring, both clarity and benefits to meteorological metrology (Merlone *et al.*, 2015) and a forensic examination of environmental extremes (Merlone *et al.*, 2019).

Of course, the pursuit of shorter and shorter time constants to enhance sensor responsiveness in meteorological measurements of air temperatures is desirable only up to a point. Unlike wind speeds, for example, there is little benefit in sampling air temperature every second outside of specific research applications, such as turbulence or eddy-correlation measurements. Very fast-reacting sensors could result in higher fluctuations, increased thermal noise and relatively greater impacts from other environmental factors, such as rapid changes in wind speed or solar radiation. Rapid changes in external conditions in passively ventilated screens or radiation shields fitted with very “fast” sensors would most likely lead to slightly higher maximum and slightly lower minimum air temperatures than those recorded by conventional instruments in otherwise identical exposures, for no reason other than differences in instrumental responsiveness (see also Burt (2012), Chapter 5, *Measuring the temperature of the air*, for a longer discussion regarding operational perspectives). It is for this reason that WMO recommend (WMO, 2014, section 2.1.3.3 and Annex 1E) sampling air temperature every 5–10 s where feasible to do so, and averaging these samples to derive 60 s running means; and further that the highest and lowest (respectively) of the 60 s running average samples be logged as the day's maximum and minimum air temperatures. A consistent approach to sensor time constant and averaging time would improve consistency within and between station networks, as previously noted by Lin and Hubbard (2008), and would over time

<sup>1</sup>This is identical to European Standard EN 60751 of the European Committee for Electrotechnical Standardization, CENELEC.

### BOX 1 PRT response times compared to liquid-in-glass thermometers

In a similar recent laboratory study, Benbow *et al.* (2018) compared the response times for the three most commonly used Australian Bureau of Meteorology standard liquid-in-glass thermometers with a 4 mm diameter PRT as follows (data taken from their appendix A):

Sensor type	Samples	Average response time to 63%, with standard deviation: seconds	
		At 0 m s <sup>-1</sup> airflow	At 3 m s <sup>-1</sup> airflow
Thermometer, mercury-in-glass “ordinary” pattern	9	147 ± 9 s	55 ± 4 s
Thermometer, mercury-in-glass “maximum” pattern	9	211 ± 44	69 ± 10
Thermometer, alcohol-in-glass “minimum” pattern	10	277 ± 12	81 ± 3
PRT, 4 mm diameter	10	95 ± 17	35 ± 5

benefit the consistency of long-term climatological records of maximum and minimum temperatures and diurnal temperature range (Thorne *et al.*, 2016) – albeit at the risk of introducing some inhomogeneity at changeover unless both “old” and “new” records were maintained in parallel for an overlap period. To evaluate their suitability for meteorological air temperature records, measurements of the time constants of representative commercial sensors were determined by laboratory experiment and the results compared with a theoretical model.

## 1.2 | Response time theory

For a sensor with heat capacity  $C$  in thermal contact with air at temperature  $T_{\text{air}}$  through an effective thermal resistance  $R_{\text{th}}$ , the rate of change with time  $t$  of the thermometer temperature  $T$  is given by:

$$\frac{dT}{dt} = \frac{(T_{\text{air}} - T)}{R_{\text{th}}C}, \quad (1)$$

where  $R_{\text{th}}C$  is known as the time constant,  $\tau$ .

Following an instantaneous step change in the air temperature from  $T_0$  to  $T_1$ , a thermometer will respond to the change according to:

$$T(t) = T_0 + (T_1 - T_0)[1 - \exp(-t/\tau)]. \quad (2)$$

For  $t \gg \tau$  the exponential term will diminish and the sensor's temperature  $T$  will approach  $T_1$ . When  $t = \tau$ , the sensor will have registered 63% of the incremental change  $(T_1 - T_0)$ , while after  $3\tau$ , it will have registered 95% of the change. The time constant for a sensor response quoted by manufacturers may be quite different (e.g. time to reach 50% of a step change) and so for clarity we will henceforth refer to this exponential time constant as  $\tau_{63}$ .

Step changes are unusual in meteorological air temperature measurements; instead the effect of the finite sensor time-constant is to cause the sensor to lag behind the actual air temperature by:

$$T(t) = T_{\text{air}}(t) - \tau_{63} \frac{dT_{\text{air}}}{dt}. \quad (3)$$

Thus for a sensor which meets the Commission for Instruments and Methods of Observation (CIMO) guideline of  $\tau_{63}=20$  s, a change of air temperature at  $0.1 \text{ K} \cdot \text{min}^{-1}$  would result in a temperature error of approximately 0.03 K; this would be considered acceptable in most meteorological applications (see Box 2). But for longer time constants and more rapid changes, errors could easily exceed 0.1 K. For a more detailed treatment, see Harrison (2014), section 2.2.

## 2 | EXPERIMENTAL METHOD

Twenty-five PRTs varying in diameter and length from five suppliers were tested. Three samples of each sensor (all rated to IEC60751 Class A specification) were investigated to assess the extent of manufacturing variability. Measurements were also made on a single 2 mm bead thermistor which was expected to have a very short time constant, although in its “bare” form such devices are insufficiently robust for routine operational use. Each PRT was a four-wire sensor (thereby compensating for varying lead lengths and thus resistance) contained within a steel sheath; in one unit the sheath had ventilation holes at its tip, in all others the sheath was continuous. The sheath provides mechanical and chemical protection to the temperature-sensitive element, usually a thin-film chip (platinum deposited on an alumina substrate) typically 2 mm square fixed within the

## BOX 2 Observed rates of air temperature change

How frequently does the air temperature change by more than 0.1 K in 1 minute? There are few published accounts of the rate of change of air temperature over the short intervals considered here, and thus the 2019 records from Stratfield Mortimer Observatory, located 10 km southwest of Reading in southern England, were examined to assess this. The site is an open exposure typical of a midlatitude temperate climate. The observatory logs three closely co-located and carefully calibrated measurements of air temperature – made within a Stevenson screen, an automatic weather station (AWS) “multiplate” radiation shield and a permanently-aspirated shield – using identical PRT sensors. These are polled at 0.1 Hz and the average of the previous six 0.1 Hz values logged every minute, per WMO CIMO recommendations. In laboratory tests, the  $\tau_{63}$  time constants of the  $3 \times 50$  mm commercial PRT sensors in use averaged 26.4 s at  $1 \text{ m}\cdot\text{s}^{-1}$  airflow (more typical of the passively ventilated sensors) and 16.0 s at  $3 \text{ m}\cdot\text{s}^{-1}$  airflow (relevant to the aspirated sensor, and complying with WMO CIMO specification), averaged across 20 samples.

For each of the three screen types, the frequency of temperature changes of magnitude  $|\Delta T|$  (K) from 1 minute to the next within given ranges over a period of 11 months during 2019 were as follows (>99.9% data availability):

### Percentage of records within limits for air temperature change ( $\Delta T$ , K) between consecutive 1 minute logged records: Stratfield Mortimer Observatory, Berkshire, January to November 2019

Magnitude of 1 minute temperature change $ \Delta T $	Exposure		
	Stevenson screen	AWS multiplate shield	Aspirated shield
$ \Delta T  \leq \pm 0.1 \text{ K}$	87.9%	84.6%	65.8%
$0.1 \text{ K} <  \Delta T  \leq 0.25 \text{ K}$	10.3	13.0	23.6
$0.25 \text{ K} <  \Delta T  \leq 0.5 \text{ K}$	1.7	2.2	8.7
$ \Delta T  > 0.5 \text{ K}$	0.1	0.1	1.9
Min. and max. $\Delta T$ , K	-1.53, +0.97	-1.45, +0.89	-1.81, +1.57
Total observations	492,162	492,170	492,101

Of course, the measurements from the Stevenson screen and AWS multiplate shield must be expected to be an underestimate of the truth, owing to a combination of response time, averaging time and screen lag factors. The results from the aspirated shield can be expected to be closer to the truth, owing to the shorter sensor response time at aspirated airflow speeds and the lack of screen lag. Although these results strongly suggest that air temperature changes from minute to minute are more likely within 0.1 K than outside it – at least at this single midlatitude reference site, and of course other sites/climates may differ – there are clear indications that rapid temperature changes occur considerably more frequently than conventional (i.e. screen-based, relatively slow  $\tau_{63}$  sensors) meteorological records would suggest. Thus with a 20 s time constant, even the aspirated sensor may be in error by  $\sim 0.16 \text{ K}$  around 1.9% of the time.

sheath by resin (thermal paste or other “potting compound”) – illustrated schematically in Figure 1. The measured response time will be the “lumped” response time of all the components.

Two PRTs at a time were connected to a Campbell Scientific CR1000 logger using a four-wire configuration and their resistances found, from which their temperature was derived, which was then logged at 2 Hz. Both PRTs were then fitted into dry close-fitting holes drilled within a 2 kg block of aluminium and warmed to 35–40 °C by placing

the aluminium block within a beaker of warm water, and allowed to attain a constant temperature.

Time response evaluations were conducted in the cooling phase using a small laboratory wind tunnel (Figure 2) in which the ventilation provided by an integral axial fan could be adjusted to provide steady airflow at speeds between 0.5 and  $3.0 \text{ m}\cdot\text{s}^{-1}$ . Ventilation speed was measured by a compact thermal anemometer (Testo model 425) located centrally within the wind tunnel, and was held constant for each test within  $\pm 5\%$ . The wind tunnel



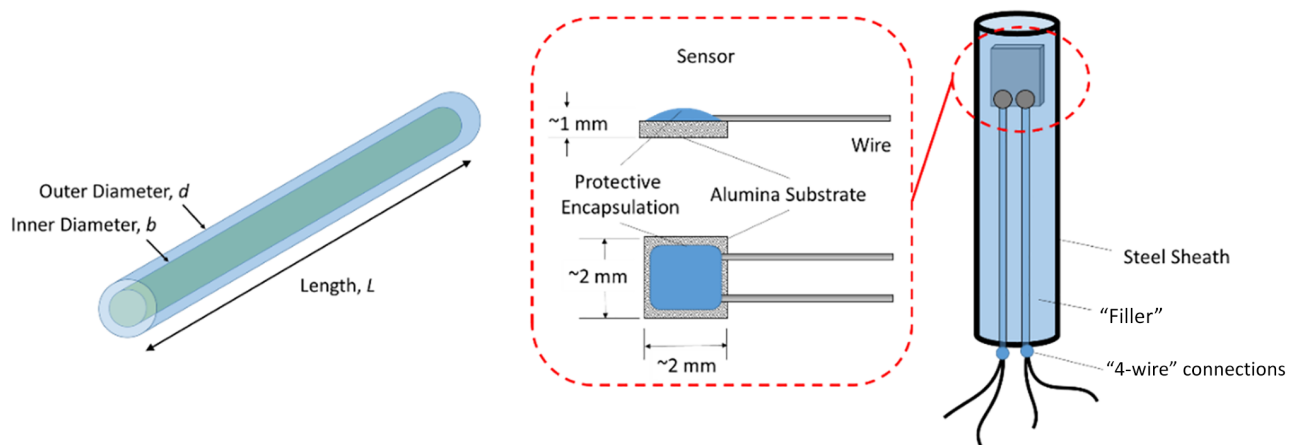


**FIGURE 1** Schematic of typical commercial PRT. The internal diameter of the cylinder,  $b$ , is the external diameter  $d$  less twice the thickness of the steel sheath. Inset: Typical PRT sensor chip detail – based upon MN222 datasheet from Heraeus sensor technology GmbH, [www.heraeus-sensor-technology.com](http://www.heraeus-sensor-technology.com)

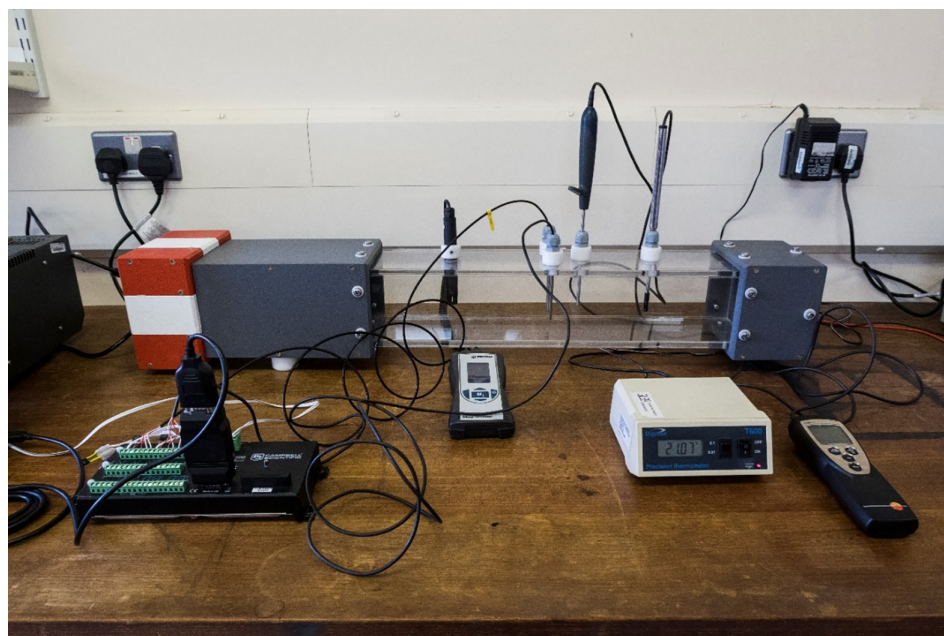


**FIGURE 2** Experimental apparatus used to determine PRT response times: University of Reading, Department of Meteorology main laboratory. The desktop wind tunnel (Perspex) is shown nearest the wall; airflow is controlled by the fan at the left, and ventilation is from left to right. Sensors mounted within the tunnel airflow are (from left to right) a relative humidity (RH) sensor, the two PRTs under evaluation, a reference PRT and the compact thermal anemometer, all mounted within insulated fittings. The three displays on the desktop foreground are, left to right, RH, reference temperature and ventilation speed; the Campbell scientific CR1000 logger appears at left with PRTs connected. The logger is connected to a laptop computer displaying real-time graphical output of temperature from the two PRTs under test (not shown)

instrumentation also included a reference PRT (to monitor changes in ambient temperature) and a relative humidity (RH) sensor. No measurements were made of background irradiance levels, which are likely to have slightly affected the observed temperatures (de Podesta *et al.*, 2018); the occasional cycling of room heating within the laboratory was probably a greater source of error, although both are small in comparison with the 15–20 K cooling cycles used.

In this technique, the time constant deduced from the data is insensitive to key uncertainties affecting the inference of the temperature from the resistance measurement. In particular, the time constant is independent of any resistance offsets or linear calibration errors. Additionally, changes in the starting or finishing temperature are of little consequence as the time constant is derived from a fixed fraction of the temperature difference between the two,

once the rate of temperature fall has slowed to very close to zero.

After ensuring that the wind tunnel was at or very close to room temperature ( $\sim 20^\circ\text{C}$ ), the airflow speed was adjusted to the desired level and allowed to settle for 1–2 minutes. At that point both PRTs were quickly removed from the aluminium block and inserted into the airflow of the wind tunnel, held in place by insulated mounting blocks. The temperature of each PRT was then logged until it fell close to the ambient laboratory temperature, after which it was returned to the aluminium block to warm up once more. This process was repeated for a minimum of four “runs” at each airflow velocity, initially at  $0.5\text{ m}\cdot\text{s}^{-1}$  increments from  $0.5$  to  $3.0\text{ m}\cdot\text{s}^{-1}$  (later streamlined to  $0.5$ ,  $1.0$  and  $3.0\text{ m}\cdot\text{s}^{-1}$ , with intermediate results linearly interpolated) for each PRT. From the logged output, the time to reach 63% and 95% of the difference between the start temperature and steady-state room temperature was objectively evaluated for each sensor to within  $0.25\text{ s}$ , and the mean and standard deviation from each set of runs calculated. In all, 502 individual evaluations were performed.

### 3 | MODELLING THE TIME CONSTANT

#### 3.1 | Overview

The time constant  $\tau_{63}$  depends on the product of the sensor heat capacity  $C$  and the thermal resistance between the sensor and the air  $R_{\text{th}}$  (Equation (1)).

If the sensor construction was homogenous, then we would expect the heat capacity to vary with the sensor volume that is, to vary with diameter and length as  $d^2L$ . However, the sensors have two main components: a stainless steel outer sheath, and an internal insulating filler. The heat capacity can thus be modelled as the sum of two components and the total heat capacity of the sensor  $C$  can be expressed as:

$$C = \pi(d^2 - b^2)L\rho_{\text{steel}}c_{\text{steel}} + \pi b^2L\rho_{\text{filler}}c_{\text{filler}}, \quad (4)$$

where  $\rho$  is the density and  $c$  is the specific heat capacity of the material.

In these experiments the specific heat capacity of the two components, and the relative amounts of each component in the sensor, are unknown but can be plausibly estimated. However, if the specific heat capacities of the two components are similar then we would still expect the heat capacity to scale roughly as  $\sim d^2L$ .

The thermal resistance between the sensor and the air is more difficult to estimate. A simple approach might

assume that the heat transfer was proportional to the exposed area of the cylinder  $\pi dL$  and the rate at which air which flowed past the sensor,  $v$ . However, as discussed in de Podesta *et al.* (2018), the air which flows past a cylinder forms a boundary layer that reduces the effectiveness of heat transfer per unit area for larger cylinders. The full expression for  $R_{\text{th}}$  taken from de Podesta *et al.* (2018) is:

$$R_{\text{th}} = \frac{d}{k \text{Nu}_{\text{cyl}}}, \quad (5)$$

$$\text{Nu}_{\text{cyl}} = 0.3 + \frac{0.62 \text{Re}^{1/2} \text{Pr}^{1/3}}{\left[1 + \left(\frac{0.4}{\text{Pr}}\right)^{2/3}\right]^{1/4}} \left[1 + \left(\frac{\text{Re}}{282000}\right)^{5/8}\right]^{4/5}, \quad (6)$$

where  $\text{Re}$  is the Reynolds number describing the flow and  $\text{Pr}$  is the Prandtl number describing the air. The Reynolds number is given by:

$$\text{Re} = \frac{\rho v d}{\mu}, \quad (7)$$

where  $\rho$  is the air density and  $\mu$  is the air viscosity. The Prandtl number is given by:

$$\text{Pr} = \frac{v}{\alpha} = \frac{\mu c_p}{k}, \quad (8)$$

where  $\alpha$  is the air thermal diffusivity and  $c_p$  is the specific heat capacity of the air. Equation (6) parametrizes an extremely complex process, but over a limited range of air speeds, the thermal resistance  $R_{\text{th}}$  is expected to vary as:

$$R_{\text{th}} \propto \frac{1}{L\sqrt{dv}}. \quad (9)$$

Combining our understanding of the way in which  $R_{\text{th}}$  and  $C$  scale with sensor size, we expect  $\tau_{63}$  to vary roughly as:

$$\tau_{63} = R_{\text{th}}C \propto \frac{1}{L\sqrt{dv}} \times d^2L = \frac{d^{1.5}}{\sqrt{v}}. \quad (10)$$

From this result we expect  $\tau_{63}$  to be independent of length, increase faster than linearly with diameter, and vary inversely as the square root of the air speed. A spreadsheet which encodes these formulae is downloadable from Figshare at <https://tinyurl.com/Burt-dePodesta-spreadsheet>.

#### 3.2 | Model parameters

There are considerable uncertainties in the estimation of both  $R_{\text{th}}$  and  $C$  from first principles. Although there are no adjustable parameters in the estimation of  $R_{\text{th}}$  from

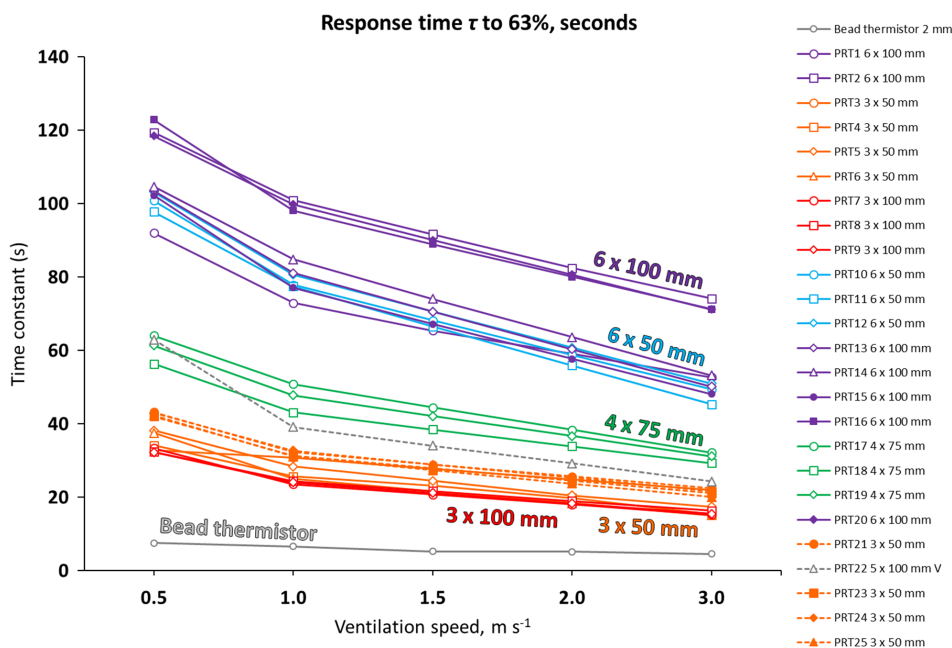


**FIGURE 3** Individual response times (seconds) for the 2 mm bead thermistor and each of the 25 PRTs tested, plotted at each of the ventilation speeds from 0.5 to 3.0 m s<sup>-1</sup> (most of the 1.5 and 2.0 m s<sup>-1</sup> values are interpolations). Values are colour-coded by sensor size as shown in the legend on right. All sensors were sheathed; PRT22's sheath was ventilated (V) around the sensor tip

Equation (5), Çengel and Ghajar (2015) indicate that the uncertainty in Equation (9) is large – roughly 30%. The uncertainty in our estimation of the heat capacity of the sensors arises because we do not know their construction and composition.

We can estimate the overall heat capacity  $C$  by making reasonable assumptions about the sensor construction. We can make rough estimates by considering the sensor as a combination of an “inner cylinder” (containing the PRT chip, connecting leads and potting compound) and an “outer cylinder” (the exterior steel sheath) as illustrated in Figure 1. For a 6 mm diameter sensor 100 mm long, varying the thickness of the steel case from 0.5 to 1 mm, and varying the composition of the inner cylinder from alumina powder to epoxy resin, results in estimates of the sensor heat capacity which vary from 4 to 7.5 J·K<sup>-1</sup> that is, a variation of  $\pm 30\%$  around the mean value. These results strongly suggest that differences in internal filling/potting compound formulation between manufacturers, and perhaps between individual sensors, exert a considerable influence on resulting sensor response times.

Given the large uncertainties in estimates of both  $R_{th}$  and  $C$  we should not expect our first-principles estimates of  $\tau_{63}$  to be accurate to better than roughly  $\pm 40\%$ . However, we would expect  $\tau_{63}$  to scale with sensor diameter  $d$  and length  $L$  in the manner expected from Equation (10).

## 4 | EXPERIMENTAL RESULTS AND DISCUSSION

Derived time constants by ventilation speed are shown for individual sensors in Figure 3, and results aggregated

by PRT form factor in Table 1. Manufacturers have been anonymised. For brevity, only the 63% response times  $\tau_{63}$  are shown because 95% response times were, as expected, close to  $3 \times \tau_{63}$  in all cases.

### 4.1 | Effect of ventilation

As expected (Harrison, 2014; de Podesta *et al.*, 2018) greater airflow speed resulted in increased advective heat transfer and consequently shorter response times. Of particular concern to the meteorological community was the result that the shortest individual  $\tau_{63}$  at 1 m·s<sup>-1</sup> ventilation rate of all sensors tested was  $23.6 \pm 1.9$  s (PRT7, 3 × 100 mm, average of five samples), still some way outside the WMO CIMO recommendation. Ventilation of 1 m s<sup>-1</sup> is the reference value assumed in ISO 17714, *Meteorology – Air temperature measurements – Test methods for comparing the performance of thermometer shields/screens and defining important characteristics* (ISO, 2007). Although there are as yet very few actual measurements of in-screen ventilation with which to compare, this air flow rate approximates to that believed to occur within a Stevenson-type radiation screen with an external wind speed of  $\geq 2$  m·s<sup>-1</sup>.

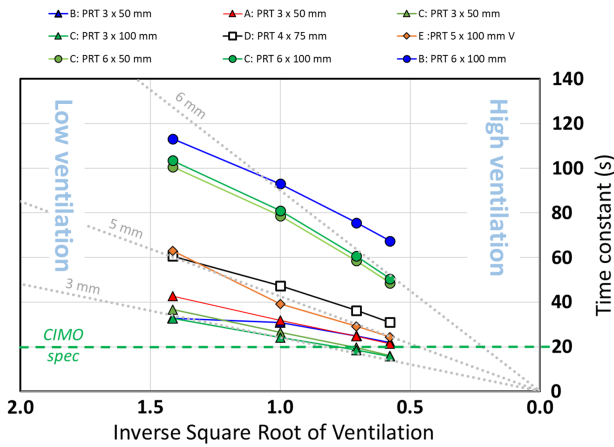
Figure 4 shows experimental response times for various sensor diameters plotted versus the inverse square root of the ventilation speed. If the data are described by Equation 10, then we would expect the data to conform to a straight line through the origin, such as the fitted dotted lines. The fitted lines conform reasonably well to the data for the 3 and 5 mm diameter sensors, but do not describe the ventilation speed dependence of the larger

TABLE 1 PRT response times, grouped by sensor size and manufacturer

Sensor type, size and sample unit IDs	Mfr anonymised	No. of units	No. of samples		$\tau_{63}$ (s) for airflow $v$ , $\text{m}\cdot\text{s}^{-1}$			
					0.5	1.0	2.0	3.0
<b>Thermistor 2 mm bead</b>	A	1	10	Mean	<b>7.6</b>	<b>6.7</b>	<b>5.2</b>	<b>4.6</b>
				SD	0.2	0.3	0.3	0.2
				Max	7.8	7.3	5.8	4.8
				Min	7.3	6.3	4.5	4.3
<b>PRT 3 × 50 mm</b>	B	1	5	Mean	32.8	30.9	<i>24.9</i>	22.0
				SD	1.3	0.6		0.5
				Max	34.3	31.5		22.3
				Min	31.0	29.8		21.0
<b>PRT 3 × 50 mm</b>	A	3	20	Mean	42.7	31.9	<i>24.8</i>	21.4
				SD	0.6	0.5		0.8
				Max	44.5	29.0		24.3
				Min	41.3	23.8		19.8
<b>PRT 3 × 50 mm</b>	C	3	20	Mean	36.7	26.4	<b>19.6</b>	<b>16.0</b>
				SD	1.7	1.0	1.1	0.5
				Max	40.5	29.0	22.5	22.3
				Min	28.8	23.8	18.5	14.5
<b>PRT 3 × 100 mm</b>	C	3	15	Mean	32.7	24.1	<b>18.5</b>	<b>15.7</b>
				SD	1.0	1.4		0.6
				Max	35.3	27.3		17.8
				Min	30.8	20.8		14.8
<b>PRT 4 × 75 mm</b>	D	3	15	Mean	60.6	47.3	36.3	30.9
				SD	1.8	1.2		1.5
				Max	66.8	52.8		34.3
				Min	54.5	41.8		26.8
<b>PRT 5 × 100 mm</b>	E	1	5	Mean	63.0	39.2	29.2	24.4
				SD	2.4	1.7		1.6
				Max	65.3	42.0		26.8
				Min	58.5	37.5		22.0
<b>PRT 6 × 50 mm</b>	C	3	15	Mean	100.6	78.7	58.5	48.6
				SD	1.9	1.6		1.5
				Max	107.3	81.8		53.3
				Min	94.3	75.3		43.0
<b>PRT 6 × 100 mm</b>	C	3	15	Mean	103.5	81.0	<i>60.6</i>	50.5
				SD	2.4	1.7		0.8
				Max	108.3	86.8		54.3
				Min	99.3	74.8		46.8
<b>PRT 6 × 100 mm</b>	B	4	25	Mean	113.2	93.0	75.6	67.4
				SD	2.4	2.7	2.1	1.8
				Max	125.8	107.3	85.0	77.3
				Min	88.3	70.3	53.0	50.8

Note: Average PRT response times (seconds) for 63% change  $\tau_{63}$  by sensor size (sheath diameter  $d \times$  length  $L$ , mm) and for different ventilation rates  $v$ ,  $\text{m}\cdot\text{s}^{-1}$ , aggregated by sensor size and (anonymised) manufacturer. (Figure 3 shows results by individual PRT; this table shows sensor form factor averages). The sensor reference is per Figure 3, the number of sensors and number of samples for each ventilation rate are also shown. Results in *italic* are interpolated. Only the results shown in **bold** meet WMO CIMO specifications for meteorological air temperature sensors.





**FIGURE 4** Mean sensor response times  $\tau_{63}$  (s) from laboratory measurements (average by form factor and manufacturer) plotted versus the inverse square root of the ventilation speed  $1/\sqrt{v}$ . Manufacturers are indicated by letters A to E and by colour, sensor diameter shown by plotted shape (6 mm diameter as a circle, 5 mm diamond, 4 mm square, 3 mm triangle). If the data conform to the expected behaviour (Equation (10)), they should fall on straight lines through the origin shown by pale grey dotted lines for 3, 5 and 6 mm sensors. The CIMO response time  $\tau_{63}$  guideline 20 s is shown by the dashed green line

diameter sensors. The reason for this behaviour is not understood.

The slowest individual sensor response time at  $1 \text{ m}\cdot\text{s}^{-1}$  was  $100.9 \pm 2.8 \text{ s}$  (PRT2,  $6 \times 100 \text{ mm}$ , four samples), more than five times the CIMO recommended specification. Average  $\tau_{63}$  for this particular PRT (PRT2) ranged from  $119.5 \text{ s}$  at  $0.5 \text{ m}\cdot\text{s}^{-1}$  to  $74.2 \text{ s}$  at  $3 \text{ m}\cdot\text{s}^{-1}$ . The measured  $\tau_{95}$  at  $0.5 \text{ m}\cdot\text{s}^{-1}$  for this sensor of  $292 \text{ s} \pm 14 \text{ s}$  (average of five samples) implies that this particular device would be incapable of registering 95% of a step change in air temperature in under 5 minutes in light wind conditions. Alternatively, if the temperature was changing at  $0.1 \text{ K}$  per minute, the sensor would be in error by approximately  $0.2 \text{ K}$ . Clearly such a sensor would be better suited to applications where speed of response is secondary to sensor protection, for example in measurement of soil temperatures.

At  $2 \text{ m}\cdot\text{s}^{-1}$  ventilation, only 20% of the samples (all small sensor diameter), were able to meet the WMO CIMO  $\tau_{63}$  20 s response time specification. Increasing ventilation to  $3 \text{ m}\cdot\text{s}^{-1}$  did not increase this ratio, although one additional sensor lay just outside the specification. A  $3 \text{ m}\cdot\text{s}^{-1}$  airflow is more typical of the minimum ventilation rate in permanently aspirated systems. This low level of compliance with WMO CIMO guideline specifications clearly implies that the majority of the commercial sensors tested would be unsuitable for air temperature measurements in either Stevenson-type thermometer screens or aspirated systems if compliance with WMO CIMO requirements were to become mandatory.

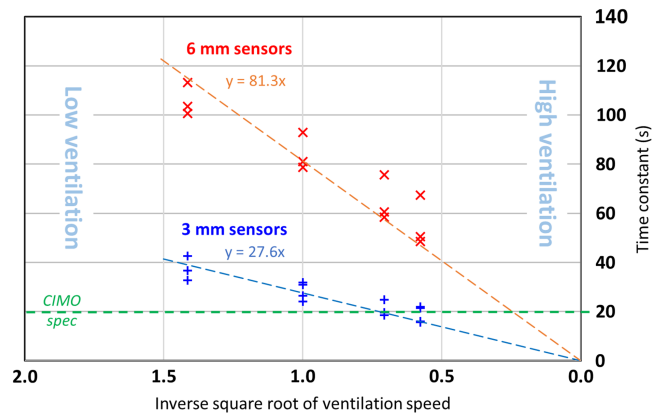


**FIGURE 5** This shows the same data as in Figure 4 but re-plotted to include only 3 and 6 mm diameter sensors which have been lumped together as two datasets grouped by sensor diameter

## 4.2 | Effect of sensor size

Figure 5 shows the data from Figure 4 re-plotted to include only the 3 and 6 mm sensors now grouped together by diameter. The  $\tau_{63}$  values for the sensors in the test are clearly grouped by diameter, rather than length or manufacturer. The ratio of the fitted slopes of the ventilation speed dependence is  $81.3/27.6 = 2.94$ . This can be compared with the expected difference based on the doubling of the sensor diameter of  $2^{1.5} = 2.83$ .

Informal discussions with suppliers suggested that the deviations from the trend are probably due to differences in the composition between the smaller- and larger-diameter thermometers. A typical sensor chip is only about  $2 \text{ mm}$  square, fitting snugly within a  $3 \text{ mm}$  sheath but insulated by a greater thickness of resin within a larger-diameter sheath (Figure 1).

## 4.3 | Rule of thumb

Analysing the data at a ventilation speed of  $1 \text{ m}\cdot\text{s}^{-1}$  only, it was found that within a standard deviation of approximately 10%, the time constant of all the non-ventilated cylindrical sensors could be approximated as  $\tau_{63} \approx 5.6 d^{3/2}$  seconds, where  $d$  is expressed in millimetres. The time constant is expected to scale inversely as the square root of the ventilation speed so as a rule-of-thumb, the time constant in seconds for conventionally constructed PRT sensors can be therefore estimated as:

$$\tau_{63} \approx 5.6 \frac{d^{3/2}}{v^{1/2}}, \quad (11)$$

where  $d$  is expressed in millimetres and  $v$  is expressed in metres per second. The data are re-plotted in this

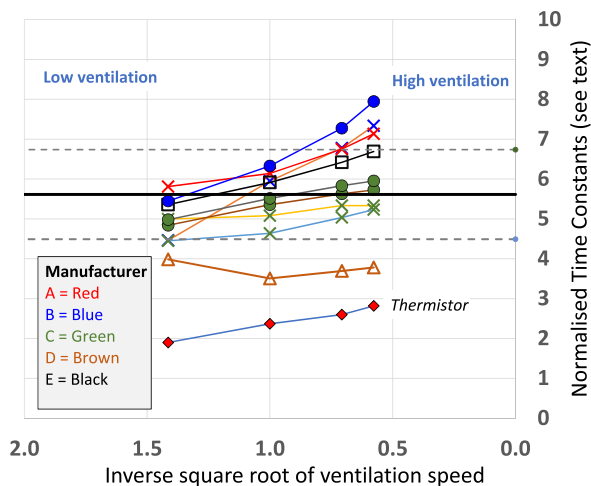


**FIGURE 6** Comparison of experimental data with rule-of-thumb in Equation (11). The measured values of  $\tau_{63}$  have been divided by  $d^{3/2}$  and plotted versus  $1/\sqrt{v}$ . The data lie roughly within  $\pm 20\%$  of the rule of thumb value

way in Figure 6. The rule-of-thumb describes most of the data within roughly  $\pm 20\%$ , but it is clear that it has not quite described the wind-speed dependence. The data indicate that at higher ventilation speeds the time constants are longer than would be expected based on the low-ventilation speed values of  $\tau_{63}$ .

## 5 | SUMMARY AND CONCLUSIONS

This series of laboratory tests showed large variations in response times of commercial PRTs used for meteorological air temperature measurements. Numerical models of a cylinder cooled in horizontal airflow at various ventilation rates provided reasonable approximations to the experimental results and permitted examination of some of the variables affecting sensor performance.

The two most important factors were found to be ventilation rate and sensor diameter, the combination accounting for more than an order of magnitude difference in  $\tau_{63}$ . It was particularly surprising to find that *none* of the PRTs tested met the WMO CIMO  $\tau_{63}$  20 s response time specification at a ventilation speed of  $1 \text{ m}\cdot\text{s}^{-1}$  assumed typical of passively ventilated thermometer shields such as Stevenson-type thermometer screens, where sensor airflow depends nonlinearly upon ambient wind speed. It was found by experiment, and confirmed by modelling, that sub-20 s  $\tau_{63}$  response times were attainable only with small diameter ( $\leq 3 \text{ mm}$ ) PRT probes ventilated at  $> 2 \text{ m}\cdot\text{s}^{-1}$ , an airflow rate more typical of permanently aspirated systems. To attain sub-20 s  $\tau_{63}$  response times at a ventilation speed of  $1 \text{ m}\cdot\text{s}^{-1}$  would require sensors with diameter less

than 3 mm. Although smaller PRTs are available, many commercially available PRTs use a sensor chip which is itself a little over 2 mm in diameter (Figure 1), enclosed in a 0.5 mm thick steel sheath necessary to provide operational robustness and to protect the sensor chip from moisture, dust and atmospheric pollution.

Based upon these findings, the following recommendations are suggested:

1. For meteorological air temperature measurements, in order to meet WMO CIMO guidelines, PRTs no larger than 3 mm diameter should be specified in procurement tenders, particularly where the intended use is within passively ventilated thermometer screens (Stevenson-type or similar, or AWS “multi-plate” radiation shelters). Sensor length is less critical, but should be as short as operationally convenient to minimise sensor mass and unit costs: 25–50 mm for example.
2. Manufacturers and component suppliers should be expected to measure and specify both sensor diameter and  $\tau_{63}$  response times at  $1 \text{ m}\cdot\text{s}^{-1}$  ventilation in air in product specifications and in tender documents for all PRTs intended for meteorological air temperature measurements.
3. Manufacturers should be encouraged to optimise existing PRT design and assembly processes with a view to meeting or exceeding WMO CIMO sub-20 s  $\tau_{63}$  PRT response time at a ventilation rate of  $1 \text{ m}\cdot\text{s}^{-1}$  where this can be achieved without detriment to sensor robustness, calibration stability and conformity to IEC60751. Helpful changes could include changes to sensor placement within the sheath (as near the tip of the sheath as possible), optimising thermal contact between sensor and sheath (and hence with the external environment), and reducing the heat capacity of the potting compound as far as possible. Additionally, polishing or silvering the exterior surface of the sensor will reduce the sensitivity to radiation.
4. Provided they can be mass-produced at similar costs and levels of operational robustness for periods of use lasting a decade or more, smaller PRTs (1–2 mm diameter) should be developed and trialled for future meteorological air temperature measurements. The day-to-day handling requirements for such sensors, once installed, should be negligible, in contrast to fragile conventional liquid-in-glass thermometry.
5. The purpose of the WMO CIMO guide is to ensure that measurements made around the world are ultimately comparable with low uncertainty. We thus recommend updated guidance on response times and sensor selection be included in future revisions of the WMO CIMO guide.

## ACKNOWLEDGEMENTS

The authors are most grateful to Giles Harrison (Department of Meteorology, University of Reading) for his support and inspiration. We are pleased to acknowledge the help of the several manufacturers – who unfortunately must remain anonymous – who provided commercial samples for evaluation in this experiment. We are grateful to Jane Warne (Australian Bureau of Meteorology) for helpful comments on an early draft of this article, and to Paul Copping (Fairmount Weather Systems) who provided material support to undertake the tests (Fairmount does not manufacture PRTs). We also offer thanks to the laboratory technical staff in the Department of Meteorology at the University of Reading, Andrew Lomas, Selena Zito and Ian Read in particular.

A preliminary version of the findings of this experiment was presented at the WMO Technical Conference on meteorological and environmental instruments and methods of observation (CIMO TECO-2018) in Amsterdam, the Netherlands, 8–11 October 2018.

## ORCID

Stephen Burt  <https://orcid.org/0000-0002-5125-6546>

Michael de Podesta  <https://orcid.org/0000-0002-6635-6806>

## REFERENCES

- Benbow, D., Dollery, I. and Warne, J. (2018) *Instrument Test Report 714: Response times of surface thermometers*. Australia: Bureau of Meteorology.
- British Standards Institution (2008) BS EN 60751:2008 – Industrial platinum resistance thermometers and platinum temperature sensors.
- Burt, S. (2012) *The Weather Observer's Handbook*. New York, NY: Cambridge University Press.
- Çengel, Y.A. and Ghajar, A.J. (2015) *Heat and Mass Transfer: Fundamentals and Application*. New York, NY: McGraw-Hill.
- Chohan, R.K. and Hashemian, M. (1989) Response time of platinum resistance thermometers in flowing gases. *Fire and Materials*, 14, 31–36.
- de Podesta, M., Bell, S. and Underwood, R. (2018) Air temperature sensors: dependence of radiative errors on sensor diameter in precision metrology and meteorology. *Metrologia*, 55, 229–244.
- Doesken, N.J. (2005) *The National Weather Service MMTS (Maximum–Minimum Temperature System) – 20 years after*. American Meteorological Society Conference Papers. <http://ams.confex.com/ams/pdfpapers/91613.pdf> Accessed 8 October 2019.
- Hannak, L., Friedrich, K., Imbery, F. and Kaspar, F. (2020) Analyzing the impact of automatization using parallel daily mean temperature series including breakpoint detection and homogenization. *International Journal of Climatology*. <https://doi.org/10.1002/joc.6597>.
- Harrison, R.G. (2014) *Meteorological Measurements and Instrumentation*. Chichester, UK: Wiley.
- Hubbard, K.G., Lin, X.M., Baker, C.B. and Sun, B. (2004) Air temperature comparison between the MMTS and the USCRN temperature systems. *Journal of Atmospheric and Oceanic Technology*, 21, 1590–1597.
- Hubbard, K.G., Lin, X.M. and Walter-Shea, E.A. (2001) The effectiveness of the ASOS, MMTS, Gill, and CRS air temperature radiation shields. *Journal of Atmospheric and Oceanic Technology*, 18, 851–864.
- International Organization for Standardization (ISO). (2007) *ISO 17714 meteorology – air temperature measurements – test methods for comparing the performance of thermometer shields/screens and defining important characteristics*. International Organization for Standardization (ISO); Geneva.
- Khorshid, L., Eşer, İ., Zaybak, A. and Yapucu, Ü. (2005) Comparing mercury-in-glass, tympanic and disposable thermometers in measuring body temperature in healthy young people. *Journal of Clinical Nursing*, 14, 496–500.
- Kyriacou, P.A. (2010) Biomedical sensors: temperature sensor technology. *Sensors Technology Series: Biomedical Sensors*, Chapter 1. New York, NY: Momentum Press
- Lin, X. and Hubbard, K.G. (2008) What are daily maximum and minimum temperatures in observed climatology? *International Journal of Climatology*, 28, 283–294.
- Mackowiak, P.A. and Worden, G. (1994) Carl Reinhold August Wunderlich and the evolution of clinical thermometry. *Clinical Infectious Diseases*, 18, 458–467.
- Merlone, A., Al-Dashti, H., Faisal, N., Cerveny, R.S., AlSarmi, S., Bessemoulin, P., Brunet, M., Driouech, F., Khalatyan, Y., Peterson, T.C., Rahimzadeh, F., Trewin, B., Wahab, M.M.A., Yagan, S., Coppa, G., Smorgon, D., Musacchio, C. and Krahenbuhl, D. (2019) Temperature extreme records: World Meteorological Organization metrological and meteorological evaluation of the 54.0 °C observations in Mitribah, Kuwait and Turbat, Pakistan in 2016/2017. *International Journal of Climatology*, 39, 5154–5169.
- Merlone, A., Lopardo, G., Sanna, F., Bell, S., Benyon, R., Bergerud, R.A., Bertiglia, F., Bojkovski, J., Böse, N., Brunet, M., Cappella, A., Coppa, G., del Campo, D., Dobre, M., Drnovsek, J., Ebert, V., Emardson, R., Fernicola, V., Flakiewicz, K., Gardiner, T., Garcia, C., Izquierdo, E., Georgin, A., Gilabert, A., Grykałowska, E., Grudniewicz, M., Heinonen, M., Holmsten, D., Hudoklin, J., Johansson, H., Kajastie, H., Kaykısızlı, P., Klason, L., Kňazovická, A., Lakka, A., Kowal, H., Müller, C., Musacchio, J., Nwaboh, P., Pavlasek, A., Piccato, L., Pitre, M., de Podesta, M.K., Rasmussen, H.S., Smorgon, D., Sparasci, F., Strnad, R., Szmyrka-Grzebyk, A. and Underwood, R. (2015) The MeteoMet project – metrology for meteorology: challenges and results. *Meteorological Applications*, 22, 820–829.
- Niven, D.J., Gaudet, J.E., Laupland, K.B., Mrklas, K.J., Roberts, D.J. and Stelfox, H.T. (2015) Accuracy of peripheral thermometers for estimating temperature: a systematic review and meta-analysis. *Annals of Internal Medicine*, 163, 768–777.
- Symons, G.J. (1875) On the sensitiveness of thermometers. *Quarterly Journal of the Royal Meteorological Society*, 2(11), 123–129.
- Thorne, P.W., Menne, M.J., Williams, C.N., Rennie, J.J., Lawrimore, J.H., Vose, R.S., Peterson, T.C., Durre, I., Davy, R., Esau, I.,

Klein-Tank, A.M.G. and Merlone, A. (2016) Reassessing changes in diurnal temperature range: a new data set and characterization of data biases. *Journal of Geophysical Research: Atmospheres*, **121**, 5115–5137.

World Meteorological Organization (WMO). (2014) *Guide to Meteorological Instruments and Methods of Observation (CI-MO guide)*. WMO No.8. Updated version, May 2017, p. 1139.

**How to cite this article:** Burt S, de Podesta M. Response times of meteorological air temperature sensors. *QJR Meteorol Soc.* 2020;1–12. <https://doi.org/10.1002/qj.3817>

## Paper 3

***Calibration.*** Chapter 15 in *The Weather Observer's Handbook*, by Stephen Burt.  
Cambridge University Press, New York and London, 2012, 444 pp.

*Bibliography #28. Word count 8115 excluding references.*

---

*The following chapter is reproduced by kind permission of the Publishers,  
Cambridge University Press, under the terms of PLSclear license number 52714  
dated 1 July 2021*



## 15 Calibration

*“The person who has only one watch knows what time it is, but the person who has two is . . . not sure.”*

*A favourite saying of professional metrologists, quoted by Richard Davis, formerly head of the Bureau International des Poids et Mesures (BIPM) mass division, at the Royal Society in London, 24 January 2011*

Instrument calibrations are both one of the most important, and yet also one of the most neglected, areas of weather measurement. We have already seen in Chapter 2 that precision is not the same as accuracy. To make *accurate* weather measurements the instruments themselves need to be accurately calibrated, or at least regularly compared against instruments of known calibration to quantify any differences, or error (which should then be added to, or subtracted from, the observed reading to give the true value). As calibrations can drift over time, the calibration should be checked regularly, and adjusted if necessary. An error of 1 degree Celsius in temperature, or 20 per cent in rainfall, may not seem very significant on a day-to-day basis, but if monthly or annual values are adrift by even half this amount, the readings obtained will not be comparable with other locations, or with historical records. A 1 degree Celsius difference in mean air temperature corresponds on average to about 150 metres difference in altitude, or to the difference in annual mean temperature between London and Paris, or between Boston and New York.

One difficulty that applies to calibrating weather instruments is that, without a duplicate set of instruments, removing the sensor (and sometimes the logger too) for offsite calibration means that the record from that instrument is lost while it is away, which may be for several weeks. Therefore, methods which allow *in situ* calibration of the instruments are preferable. Depending on the instrument type, this can be achieved using an ‘absolute’ or ‘fixed point’ method, or by comparing readings over a period with a portable reference instrument whose calibration is accurately known.

This chapter describes straightforward methods to check and adjust calibrations for the most common weather instruments – precipitation, temperature, humidity, and air pressure sensors.

### Calibrating a recording raingauge

For the reasons outlined in Chapter 6, *Measuring precipitation*, it is always advisable to ensure that the ‘reference’ precipitation measurement is made using a standard



‘manual’ raingauge (a five-inch gauge in the UK and Ireland, eight-inch pattern in the United States). Recording gauges (such as tipping-bucket or weighing raingauges) will almost always read a little lower than the standard gauge, owing to both instrumental and evaporative losses and different exposure. By definition, a standard manual raingauge, when correctly exposed, gives the ‘reference’ rainfall total. Minor differences between the standard gauge and a recording raingauge are therefore to be expected: rarely will two raingauges record exactly the same amount of rainfall. An automatic raingauge should *not* be adjusted merely to attempt exact agreement or near-agreement with the standard gauge – instead, carry out the method below to derive an absolute calibration for the unit by passing a known volume of water through the unit and comparing its measured output.

The method below assumes a tipping-bucket raingauge, but the principle is the same for almost any type of recording gauge.

For the test, the recording raingauge should be connected either to its normal display or logging system, or to a pulse counter, whichever is easier. If a tipping-bucket raingauge is in use, the calibration check can be performed *in situ* on a dry day (remember to delete the calibration test tips from the record afterwards). Ensure the gauge is absolutely level before and during the test.

First, carefully measure out 500 ml of water\* at room temperature. This should be measured as accurately as possible, preferably with a laboratory balance, but with digital scales if not. At room temperature, 1 ml (= 1 cm<sup>3</sup> or 1 c.c.) of water weighs 1 g<sup>†</sup>, so measure 500 g of water, netting off the weight of the container of course.

This needs to be carefully poured through the tipping-bucket raingauge. Pouring it in too rapidly will simply overload the buckets (they will stick in the ‘tipped’ position and the resulting calibration will therefore be inaccurate), so the rate of inflow needs to be reduced to a steady trickle. A large plastic funnel with sufficient capacity to hold at least 500 ml water, obtainable from hardware stores, can be adapted to do this. Push a blob of Blu-Tack, putty or similar material well down into the spout of the funnel so that it blocks it. Using a small screwdriver, carefully make a small hole in the Blu-Tack. Fix the plastic funnel securely in place above the raingauge funnel and tipping-bucket unit (make sure the gauge is perfectly level, and in a position where the water from the emptying buckets can safely drain away). Pour a cupful of water (not the measured 500 ml sample yet) into the funnel and allow it to drip into the raingauge funnel, at a rate to ensure the buckets tip no more often than once per minute or so – simple arithmetic will show that this corresponds to a rainfall rate of 12 mm/h for a 0.2 mm tipping-bucket unit. Adjust the hole size as necessary. (This also serves to pre-wet the surfaces of the funnel and the tipping buckets.) Too rapid a rate of flow risks the buckets overflowing – too slow a rate will simply mean that the test takes hours to complete<sup>‡</sup>.

\* 500 ml is sufficient for most raingauges with funnels of diameter 100–200 mm (4 to 8 inches) or so; larger or smaller funnels may need more or less than this. The exact amount is not critical (although of course it must be accurately known), but it must be sufficient to generate at least 100 tips (of a 0.2 mm tipping-bucket unit) to minimise random counting errors.

<sup>†</sup> Strictly, this applies at a water temperature of 4 °C, but at 20 °C the difference in specific gravity is less than 0.2% (1.000 g/cm<sup>3</sup> at 4 °C, 0.9982 g/cm<sup>3</sup> at 20 °C). The error in the weighing device is likely to be larger than this.

<sup>‡</sup> It is worthwhile to repeat similar calibration ‘runs’ at different flow rates to assess the variation of calibration with rainfall intensity. The resulting matrix of calibration factors versus rainfall intensity becomes a useful aid in the accurate analysis of intense rainstorms. For a 0.2 mm capacity bucket, a



Once the water has completely drained through, remove the raingauge funnel and empty (tip) any partially filled buckets by hand. Replace the raingauge funnel. Note the rainfall reading or pulse count at this point; this is the zero point of the calibration test.

Re-fix the plastic funnel in position and *very carefully* pour the measured 500 ml into it, ensuring that none is spilt and that as little as possible remains in the original vessel. Allow it to flow slowly through the partially obstructed funnel into the tipping-bucket raingauge – this will take an hour or so.

After all the water has passed through – check both the plastic funnel and the raingauge funnel to ensure none remains – note the logged rainfall reading or pulse counter value.

The volume of water  $v$  collected by a cylindrical raingauge funnel is given by the formula

$$v = \pi r^2 h$$

... where  $r$  is the *radius* of the funnel (half the *diameter*) and  $h$  the height of the cylinder (= the measured depth of rainfall). Rearranging in terms of  $h$ :

$$h = \frac{v}{\pi r^2}$$

Measure the radius of the raingauge funnel opening, in millimetres, as accurately as possible.

Using the above equation, and knowing the radius of the raingauge funnel, it is straightforward to calculate the depth of water (= amount of rainfall) that passing through 500 cm<sup>3</sup> of water – or any other amount – should cause the gauge to indicate\*.

*Example:* using a Davis Instruments Vantage Pro2 tipping-bucket raingauge (funnel diameter 165 mm, radius 82.5 mm = 8.25 cm), and working in *centimetres* throughout:

$$\begin{aligned} h &= \frac{500}{3.14 \times 8.25 \times 8.25} \\ &= 2.34 \text{ cm} = 23.4 \text{ mm of rainfall} \end{aligned}$$

Calculate the calibration from the comparison with the measured amount during the test. For example, if the indicated amount shown by the display was 19.8 mm<sup>†</sup> then the calibration is 19.8 / 23.4 = 85 per cent and the tipping-bucket unit reads

simulated 5 mm/h rainfall rate will generate one tip every 2.4 minutes; at 60 mm/h the tip time is 12 sec; at 200 mm/h 3.6 sec; at 500 mm/h 1.4 sec. (Note that the tip rate will slow over time as the hydrostatic pressure of the water head is progressively reduced.) Even assuming the inflow pipe diameter can handle such intensities, above this level splashing, ‘continuous tipping’ or multiple bounce-tips become increasingly significant and repeated calibration runs may generate different results. Where high-intensity rainfall is a regular occurrence, higher capacity tipping buckets matched with wider inflow pipes will yield more reliable intensity profiles, at the cost of decreased resolution for low-intensity rainfall events.

\* This method also applies to checking the calibration of a measuring cylinder for a standard raingauge, for example. For a UK-standard five-inch gauge, 1 mm of rainfall corresponds to 12.7 cm<sup>3</sup> of water; for a U.S.-standard eight-inch gauge, 0.1 inches of rainfall is 82.4 cm<sup>3</sup>.

† If using a pulse counter, multiply the number of tips by the nominal bucket capacity: so, for example, 99 tips of a 0.2 mm unit would give 99 × 0.2 = 19.8 mm.

15 per cent low (a not atypical value ‘out-of-the box’). The nominal 0.2 mm tip capacity in this case is therefore actually 0.17 mm (85 per cent of 0.2 mm).

It is advisable to repeat the test at least once more and compare results. If the two derived calibrations differ by more than 5 per cent, repeat a third time and average the two closest results.

If the derived calibration is more than 5 per cent different from the nominal 0.2 mm (i.e., outside the range 0.19 to 0.21 mm), the tipping capacity of the buckets themselves should be adjusted. The manufacturer’s manual should be checked for the recommended way to do this, but usually this is achieved by adjusting the base-plate upon which the buckets rest in the empty position, by means of an adjusting screw or nut. Lowering the plate increases the bucket capacity (more water required to tip the bucket) and vice versa; the objective should be to adjust the tip capacity to as close to 0.2 mm as possible. It is very important that both buckets are adjusted evenly, and it may be helpful to mark the screw heads or nuts to ensure the same amount of adjustment is made to both sides\*.

Once any adjustments have been made, repeat the calibration process and check results. Calibration within 5 per cent of 0.20 mm is satisfactory: with care, 2 per cent may be achievable on some units.

The calibration test should be repeated at least once every 12 months. The derived calibration may show seasonal variations, particularly with tipping-bucket raingauges using small buckets (the Davis Instruments Vantage Pro2 0.2 mm capacity bucket holds only 4.3 cm<sup>3</sup>, for example)<sup>†</sup> and therefore it is best to perform the calibration test at an air temperature close to the annual mean. Most AWS software will permit the actual bucket calibration, where known, to be substituted for the nominal (and default) 0.2 mm capacity.

### Calibrating temperature sensors

One way to obtain accurate temperature calibrations is to send off the sensors (for electronic sensors, probably the logger too), to a professional calibration facility. As well as being expensive, it is also quite impractical because (except in the case of mercury thermometers) the sensors, wiring and logger will have to be de-installed then re-installed on their return. Unless duplicate equipment is available as a backup, this may mean the loss of several weeks’ records.

For temperature sensors, there are two calibration methods which are easy enough to perform *in situ*: the *absolute* method, using the melting point of ice as a fixed point, and the *comparative* method, comparing results over time against a

\* Particularly on new units, the initial setting of the buckets may be unbalanced. If this is the case, the calibration of the gauge will vary according to which bucket is in use. This can be checked by carefully timing the intervals for 10 or so tip times on each side as the water drips through. If the average tip time for one side is noticeably different from the other, then the bucket tipping capacities differ. If so, both buckets should be adjusted to one end or other of their adjustment and then ‘wound back’ evenly so that they are at the same adjustment position. The calibration test, and the tip timing measures, should then be performed again until the discrepancy between the two has been eliminated and both tip at the equivalent of 0.2 mm ± 5%.

<sup>†</sup> The density of water varies little over normal air temperature ranges, but its viscosity (and thus surface tension) reduces significantly with rising temperature (<http://hyperphysics.phy-astr.gsu.edu/hbase/surten.html#c3>): this may lead to incomplete emptying of small buckets at lower temperatures, an effect which has been observed on Davis Instruments AWSs (see reference [22] in Chapter 5 for details).

sensor of known calibration. Of the two, the absolute method is to be preferred, but as it involves immersing the sensor or sensors to be calibrated in an ice/water mixture, the method is not suitable for some devices. In addition, the design of many consumer AWS models makes it difficult or impossible to access or remove the temperature sensor/s for an immersion calibration test, and the comparative method may be the only option available.

### **Absolute temperature calibration using an ice/water mixture**

This method uses a fixed point, namely the melting point of ice at 0.01 °C, to establish an accurate calibration point. Using a similar approach, calibrations from –5 °C to +40 °C are easy enough to obtain.

This method is easiest to undertake with electrical sensors in steel probes, and with many types of direct-reading mercury thermometer. Unfortunately, this approach cannot be used for many budget or mid-range consumer AWSs, because it requires that the temperature sensors be immersed in the ice/water mixture (as described below). Where access to the temperature sensors is difficult, or they cannot easily be detached from their housing, the method is impractical. It should also **not** be undertaken with combined temperature/humidity sensors, because immersing the humidity element in water will irreparably damage it. It is also unsuitable for certain types of thermometers, such as maximum and minimum thermometers. For these sensor types, the comparative method described below is a better option.

The method is very straightforward. It requires a small, insulated container (a small Thermos-type flask is perfect) and a supply of ice – ice cubes from the freezer are fine (preferably made with distilled water). Partially crush the ice cubes to fit them into the flask, and fill it almost full with crushed ice. Add a little cold water, just sufficient to allow the ice to ‘float’ almost to the brim of the flask, and shake vigorously for a minute or two before carefully inserting the sensors.

Electrical temperature sensors should be connected to a logger (preferably the logger that will be used with the sensor when operational) and logged during the test. Mercury thermometers should be inserted as fully as possible into the flask, although some stem needs to protrude in order to hold and remove them. When inserting mercury thermometers into the ice/water mixture, be very careful not to fracture the bulb or stem by excessive force, or by subsequent stirring. Where two or more devices are being checked at the same time, carefully secure the probes or thermometer stems together with an elastic band so that they can be inserted and removed from the flask as one unit. The temperature sensitive areas (bulbs of mercury thermometers, probe ends on electrical sensors) should be as close to each other as possible.

Carefully insert the sensor or sensors into the flask. Ensure the probe sensors are fully immersed into the ice/water mixture, and as much of the thermometer stem/s as possible is also immersed (make sure the thermometer does not fall into the flask, or it may break).

Gently and continuously shake or stir the flask for several minutes, to ensure an even temperature distribution within the ice/water mixture. Avoid over-energetic shaking or stirring, which may fracture thermometer stems or bulbs. Allow the sensors a few minutes to adjust to the flask temperature and settle to a steady reading.

Over a period of at least 15 minutes, take several readings of each sensor, stirring or gently shaking throughout. The reading from electrical probes should be logged every 30–60 seconds, or read off the displayed output as frequently. If thermometers are being tested, carefully withdraw the stem by the least amount possible to enable a rapid thermometer reading (to 0.1 degC precision) every couple of minutes.

Note and average the ‘steady state’ temperatures, ignoring the highest and lowest values. If the sensor is correctly calibrated, the average should be 0.0 °C. An average of, say, –0.3 °C would indicate that the sensor was reading 0.3 degC too low, and thus the correction to be applied at this temperature would be +0.3 degC.

### Ice point calibration for platinum resistance thermometers (PRTs)

This method is very suitable for checking the calibration of PRTs. If the sensor is an ISO standard unit, its change of resistance with temperature is accurately defined (the world-wide standard for ‘Pt100’ platinum RTDs, DIN/IEC 60751, requires the unit to have an electrical resistance of 100.00  $\Omega$  at 0 °C and a temperature coefficient of resistance of 0.00385  $\Omega$ /degC between 0 and 100 °C). So once the sensor error (if any) at 0.0 °C has been determined, and provided of course the correct temperature coefficient of resistance is used in the logger, then this simple offset correction can be applied to all other temperatures measured by the sensor.

### Establishing other calibration points using this method

The method can easily be extended to establish calibrations at other temperature points. A mixture of crushed ice and salt in the flask can be used to obtain temperatures down to –5 °C, or a little lower. Removing the ice and salt and adding warmer water allows flask temperatures to be obtained at various points up to about +40 °C. An insulated flask and continuous gentle stirring is essential to maintain a steady temperature, particularly where the flask temperature differs considerably from the ambient air temperature.

The method is the same as for the ice-point test, but for all points above 0 °C, an accurate temperature reference is required. If one of the sensors is a PRT, applying the offset determined from the ice point test should give a temperature accurate to 0.1 degC. If no PRT is available, a calibration thermometer (a thermometer with an expanded scale, enabling it to be read to 0.05 degC) or another electrical sensor should be used. Obviously, either must themselves be accurately calibrated before the test. A pre-calibrated Tinytag logger with a flying lead (see Chapter 3) is ideal for this purpose.

Once the ice point and extended point tests have been completed, prepare a calibration table for the sensor similar to that shown in **Table 15.1**. Points between calibration points can be obtained by interpolation. If the calibration is of a manually-read mercury thermometer, calibrations (to 0.1 degC precision only) should be added to the observed reading at every observation prior to recording the value in the observation register. If an electrical sensor is being used, the calibration algorithm should be incorporated into the logger programming or setup configuration.

Note the test date, results and calibrations applied in the site metadata, particularly whether or not corrections have already been included in observations from the site (to avoid mistakenly including them again when the observations are archived). Calibrations on electrical sensors should be checked at least every

Table 15.1. *Simple calibration and correction table, derived from the fixed-point calibration method described in this chapter*

**Dry-bulb thermometer** *Serial no. 12345/12*

Corrections to be applied at various temperatures

*Based on fixed-point calibration tests, October 2012. Calibration introduced 1 Jan 2013*

At observed °C	Add correction to observed reading, degrees C
-15.0	<b>+0.3</b>
-10.0	<b>+0.3</b>
-5.0	<b>+0.2</b>
0.0	<b>+0.2</b>
5.0	<b>+0.1</b>
10.0	<b>+0.1</b>
15.0	<b>0</b>
20.0	<b>0</b>
25.0	<b>-0.1</b>
30.0	<b>-0.1</b>

2 years, or immediately if any sudden change in calibration is suspected. Mercury thermometers should be checked every 5 years.

### Comparative temperature calibration using a sensor of known calibration

The second method is cross-calibration alongside a sensor of known accuracy. For temperature sensor calibrations, this can be done quite easily and accurately (with care, to 0.1 degC) with a calibrated portable reference [1]. The Tinytag loggers made by Gemini Dataloggers (see Chapters 2 and 3, also Appendix 4 for supplier details) are perfect for this purpose; similar units are available from other suppliers. These small, rugged, accurate units can be calibrated to a traceable national standard by the manufacturer, and then exposed alongside existing equipment for an extended comparison period (days to weeks).

There are two types of Tinytag logger – a larger unit which has a built-in sensor package and a digital display of current temperature and humidity (**Figure 3.4**) and a smaller logger which is temperature-only and has no display (**Figure 3.5**). The larger unit is ideally suited to being left in a thermometer screen, but is not weatherproof: the smaller loggers are weatherproof, so can easily be used to check the calibration of exterior sensors, such as grass minimum or earth temperature units (see Chapter 10), as well as sensors exposed in a thermometer screen or a small radiation screen.

This section provides a step-by-step guide to doing this, assuming the smaller logger with a flying lead is being used. Tinytag loggers with built-in sensors are not suitable for this method, as the thermal inertia of the relatively bulky logger unit means response times are too slow – see Appendix 1.

#### 1. Obtain a calibrated datalogger

Required – a temperature logger with a sensitive thermistor on a flying lead, a calibration table from the supplier (specify three calibration points at  $-10^{\circ}\text{C}$ ,  $+10^{\circ}\text{C}$

and +30 °C when ordering the logger), logger software and USB cable to connect the logger unit to a PC\*. The calibration process is undertaken within spreadsheets (it helps to be reasonably spreadsheet-literate, as doing it by hand would be a very tedious task). Sample spreadsheets are available from [www.measuringtheweather.com](http://www.measuringtheweather.com). In the examples below, Microsoft Excel has been used but most spreadsheet packages should be able to duplicate the functions described easily enough.

## 2. Set up the logger

Connect the thermistor to the logger, install the software if not already installed, then launch the datalogger. Check that the battery is fully charged, and that the logger is working satisfactorily by leaving it to log for an hour or two with a short logging interval (say, 1 minute). After this period, check logged data can be downloaded satisfactorily to the PC.

Once everything has been tested and is working satisfactorily, reset the logging interval to be the same as the logging interval on the AWS for the element being monitored (which may be 5 minutes for air temperatures, for example, or perhaps hourly for earth temperatures or for comparing against maximum and minimum thermometers in a Stevenson screen – see Chapter 3 for more on logging intervals). Choose to log either temperature only at the set interval, or maximum and minimum temperatures attained during the logging interval – the latter provides a closer calibration against maximum and minimum observed temperatures logged by the AWS sensor under test, or conventional thermometry. Relaunch the logger. Make a diary note of the date when the logger memory will become full and require downloading.

Choosing more parameters and shorter logging intervals will of course use memory more quickly and so shorten the interval between logger downloads. On current models, selecting 5 minute resolution with spot temperature, maximum and minimum recording permits 4–6 weeks record before the memory becomes full and starts over-writing once more. A few minutes' data will inevitably be lost when the logger is temporarily removed for downloading, so try not to change the logger near a time of maximum or minimum temperature – the morning observation is often a suitable time to do this.

## 3. Expose the temperature sensor adjacent to the equipment to be checked

Expose the small flying-lead thermistor adjacent to the sensor whose calibration is being checked. The sensor comes with 60 cm of lead, so it should be easy enough to locate it exactly where it is required. In a Stevenson screen (or similar), expose the thermistor close to (but not touching) the main air temperature sensor (**Figure 3.4**). Things are a little more complicated with smaller plastic AWS radiation shields as it is more difficult to see where the sensors are, but try to fix the thermistor in place as close as possible to the AWS temperature sensing element without actually touching it. Check that it is not exposed to direct or indirect solar radiation through the

\* The Tinytag units are quite expensive, but within the UK the Climatological Observers Link (COL) operates a loan scheme for members. For a nominal fee plus postage, one of the units can be borrowed for up to a month to conduct cross-calibration tests on your own equipment. Contact details for COL are given in Appendix 4.

'saucers' of the radiation screen (try shining a small torch through them at dusk). Whether in an AWS screen or Stevenson screen, secure the thermistor and its lead with cable clips or weatherproof tape to ensure it cannot work loose. (When removing the unit, ensure you do not accidentally snip through the thermistor lead as well as the cable clips.)

When checking other sensors, for example a grass minimum or earth temperature sensor, locate the unit as close to the sensor to be checked as possible. For the grass minimum sensor, ensure the calibration sensor is not located on top of the unit being checked as this will itself affect outgoing radiation and thus the indicated temperatures.

Finally, connect the calibration thermistor to the Tinytag logger. Minimize any thermal inertia effects from the body of the logger itself by locating it some distance from the sensor/s in use. In small radiation screens, there is unlikely to be sufficient internal space to house the logger, so trail the lead carefully outside the screen and secure the logger to a convenient external mounting point (**Figure 3.5**). Ensure the cable connecting logger to thermistor is not snagged or stretched, as it is easily damaged: the cable connector plug must also be screwed tight into the logger port to avoid moisture ingress. The logger should not be located where it will itself affect the temperature record within the radiation screen (by warming up in sunshine, or blocking ventilation, for example). The logger itself is weatherproof and can safely be left exposed to the elements, provided the risk of theft or vandalism is small.

Allow the sensor and logger to settle to the outside temperature before commencing logging (a delay-start option is available for this purpose), or ignore the first 30 minutes or so of readings to allow for settling. If the logger has been in a centrally heated room and is then taken outside in winter it may be 20 degrees or more warmer than the ambient air temperature, and while cooling down it will affect the readings obtained to a decreasing extent.

#### 4. Log comparison data

Leave the calibration logger to record alongside your existing sensors for as long as possible (at least 2–3 weeks). The logger itself will require removal for downloading to the PC at regular intervals as its memory becomes full, but this need involve only a few minutes loss of record (disconnect the sensor from the logger, and leave the sensor in place). The larger the range of temperature covered during the period, the better, because this provides a better estimate of the calibration curve (see below).

#### 5. Download logger data and apply calibration to logged temperatures

At the end of the logging period, remove the logger, connect to the PC and download the data using the logger software. Export it into a suitable spreadsheet.

The manufacturer's calibration certificate provided with the instrument will give the logger calibration: this is normally linear across the range of calibration temperatures. Plot these on a graph and determine the slope of the calibration curve (a few mouse clicks in Excel will do this). For example, if the calibration values were as follows:

*At -10 °C    Subtract 0.25 degC*  
*At +10 °C    Subtract 0.15 degC*  
*At +30 °C    Subtract 0.05 degC*



... then the calibration offset at any logged value would be given by:

$$\text{Calibration offset} = (\text{Observed temperature } ^\circ\text{C} - 40) \times 0.005$$

The calibrated temperature is then observed temperature + calibration offset

Lay out a spreadsheet something like this (sample calibration spreadsheets in Excel format, including one to determine the slope of the calibration curve with temperature, are available for free download at [www.measuringtheweather.com](http://www.measuringtheweather.com)):

Logger record	Date/time	Logger observed temperature	Calibration offset	Calibrated logger temperature
1	23.2.2014 18:15	10.00 °C	-0.15	<b>9.85 °C</b>
2	23.2.2014 18:20	9.62 °C	-0.15	<b>9.47 °C</b>
3				

## 6. Compare the results to check calibration

The next step depends on whether the requirement is to check the calibration of liquid-in-glass thermometers in a screen, such as maximum and minimum thermometers, or to check sensors on an AWS. Note that for thermometers in a screen it is best to do this check against the readings of self-registering thermometers (i.e., maximum and minimum) rather than an ordinary (dry-bulb) thermometer, because opening the screen door and the proximity of the observer while reading the thermometer is likely to change the observed reading slightly. With self-registering thermometers ‘observer proximity’ effects are less of a problem, unless the maximum or minimum occurs at the time of the observation – if that happens it may be advisable to exclude such observations from the comparison.

To check the calibration on once-daily results (maximum and minimum thermometers in a screen, for example) – go to step 7 below. To check the calibration of logged temperature sensors (air temperature from an AWS, for example) – go to step 8.

## 7. To check maximum and minimum thermometers in a screen

Determine which period your maximum and minimum temperatures refer to (the ‘terminal hours’ – see Chapter 12). For the purposes of this calibration comparison it could be any period, say 0700 to 0700, so long as ‘test’ and ‘reference’ instruments use the same one. Note that the default time period for most AWS extremes is midnight to midnight, so unless screen thermometers are normally read and reset at midnight some adjustment of the period to which the AWS extremes relate will be needed in order to be able to make direct comparisons with the once-daily reading given by the thermometers. Note also that if hourly logging has been selected, then terminal hours will need to be ‘exact hours’ (perhaps 0700 or 0800) rather than fractional hours (such as 0730).

Table 15.2. Sample calibration results for daily maximum and minimum thermometers

Date	Maximum temperature °C			Minimum temperature °C		
	Calibrated logger	Observed thermometer	Difference degC	Calibrated logger	Observed thermometer	Difference degC
23 Feb 14	11.65	11.7	-0.05	2.85	3.1	-0.25
24 Feb 14	8.72	8.9	-0.18	-3.36	-3.2	+0.16
...						

Using the spreadsheet, evaluate the logger-observed daily maximum and minimum temperatures (using the values with manufacturer calibration included, as shown in the table in step 5) over the same time period as the thermometers. Enter these in a second tab on your spreadsheet, looking something like **Table 15.2**.

The ‘difference’ column is (calibrated logger value minus thermometer) – this is the correction to be applied to the thermometer reading to indicate the same temperature shown by the calibrated logger. Don’t worry that logger values are more precise (more than one decimal place), because the thermometers are read only to one decimal place.

It is always best to undertake side-by-side comparisons for as long as possible in order to obtain a wide range of temperatures to derive a good calibration curve. This particularly applies to cross-calibrations where only a single data point per thermometer per day is noted, as is the case with maximum and minimum temperatures. Try to achieve a range of (say) 10 degC or 20 degF on either side of the mean annual maximum and minimum temperature, but even a few days worth of data will quickly identify any gross calibration errors. Note that some results which appear out of line with others may need to be manually excluded. This can happen for various reasons, the most likely of which is due to the differing time constants (response times) of the two sensors (for instance, one day the maximum temperature may occur during a very short spell of sunshine: the response of the mercury thermometer will lag slightly behind that of the smaller, more responsive thermistor, and a relatively lower maximum temperature reading will result: including this in the calibration curve may result in a biased calibration).

Next, for each thermometer separately (as they will probably have differing calibration curves), plot an Excel scatter plot of the observed thermometer value (horizontal  $x$  axis) versus the calibrated logger values (vertical  $y$  axis) – a suitable template is included on the downloadable spreadsheet. Using Excel, evaluate the equation of this line, which may be linear (varies in a straight line with the thermometer reading) or polynomial (a curve which includes more than one term) – see example in **Figure 15.1**.

With a good spread of data points, this trendline equation should provide a robust calibration comparison over a reasonable range of temperatures. These calibrations should then be manually applied to the observed readings of the maximum and minimum thermometers. It is easiest to do this by reading off the ranges for corrections in 0.1 degC increments from the graph – resulting in the small correction table given in **Table 15.3**.

Make a note in the station metadata (see Chapter 16) of the calibrations applied, and the date they were introduced – better still, keep a copy of the calibration tables

Table 15.3. Sample thermometer calibration/correction table

**Minimum thermometer** *Serial no. 23456/11*

Corrections to be applied at various temperatures

*Based on calibration against calibrated Tinytag sensor October 2012. Calibration introduced*

*1 Jan 2013*

At observed °C	True temperature is °C	Add correction to observed
-15.0	-14.2	<b>+0.8</b>
-10.0	-9.2	<b>+0.8</b>
-5.0	-4.3	<b>+0.7</b>
0.0	0.7	<b>+0.7</b>
5.0	5.6	<b>+0.6</b>
10.0	10.5	<b>+0.5</b>
15.0	15.5	<b>+0.5</b>
20.0	20.4	<b>+0.4</b>
25.0	25.4	<b>+0.4</b>
30.0	30.3	<b>+0.3</b>

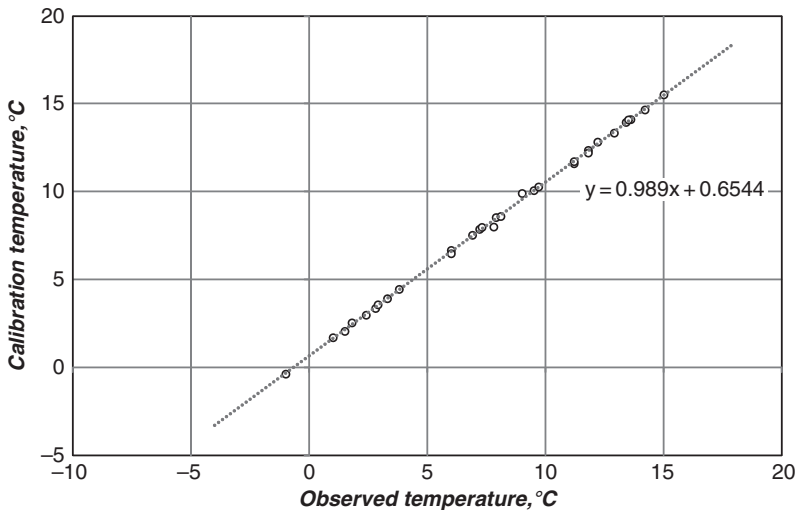


Figure 15.1. Sample scatterplot for a minimum thermometer obtained in a cross-calibration exercise (real data). The plot shows both observed and calibrated temperatures. The dashed line shows the trendline derived using Excel, together with the equation of the line.

within the metadata document. Strictly speaking, the derived calibration is valid only over the observed range of temperatures examined (this is the reason why it is a good idea to undertake one cross-calibration run in winter and another in summer, and combine the results), but when the fit is good (as in **Figure 15.1**) the results can normally be extrapolated using the derived calibration equation for at least a few degrees Celsius above and below the upper and lower observed value. The trendline and the correction table should not be extrapolated too far beyond the observed range of temperatures if the scatter is wide, or the trendline non-linear.

Keep a link to the calibration comparison test results, as these will be useful to refine calibrations if a wider range of temperature data becomes available (if perhaps

the initial calibration run in a winter month can be followed up some months later by a summer comparison).

If the comparison undertaken was against thermometers only, go now to step 9 below.

## 8. To check logged temperature sensors

Ensure the logged values from the calibration logger and the sensor being checked are at the same time interval (5 minutes is ideal) and that both observations are made approximately simultaneously (for example, at 0900, 0905, 0910 and so on).

Check the system documentation as to whether the temperature sensor being cross-calibrated outputs a 'spot' or 'sample' value at the logging interval, or whether all samples are averaged over the logging interval (some AWSs allow toggling between these two options).

If the values are 'spot' values, then these can be compared directly with the 'spot' calibrated logger values as described in section 5 above.

If they are averaged over the logging interval, it is best to compare them with a pseudo-average derived from the calibrated logger data. For short data intervals, the average of (spot value at beginning of logging period + spot value at end of logging period + observed maximum during logging period + observed minimum during logging period) will be very close to the sampled average – and this is very easy to calculate in the Excel table.

Paste into the existing logger spreadsheet the appropriate data from the sensor being checked, taking care to ensure that all data values are coincident in time\*. So the comparison table will now look like this:

Logger record	Date/time	Logger observed temperature	Calibration to be applied	Calibrated logger temperature °C (from Step 5)	Temperature of sensor being checked °C	Difference
1	23.2.2014 18:15	10.00 °C	-0.15	<b>9.85</b>	<b>9.82</b>	<b>+0.03</b>
2	23.2.2014 18:20	9.62 °C	-0.15	<b>9.47</b>	<b>9.45</b>	<b>+0.02</b>
3						

The 'difference' column is (calibrated logger value minus sensor to be checked) and this is the correction to be applied to the sensor being checked to indicate the same temperature shown by the (calibrated) logger.

With logged data at frequent intervals over a period of several weeks, many more observations are available to provide a good comparison and the optimum times to

\* During summer time, ensure both loggers are operating to the same time standard – UTC, local regional time or summer time. If the transition from summer to winter time, or vice versa, happens during the comparison period, check both loggers have handled the transition correctly. (It is much simpler to use one time standard throughout the year, of course.)

check cross-calibrations can be extracted from the record. These are cloudy, windy, dry conditions at night (no solar radiation), when the temperature is stable (from the author's experience, a rate of temperature change less than 1 degC per hour is preferable). Occasions to avoid include times when the temperature is changing rapidly, because relatively large transient differences may arise due to response time/lag effects rather than genuine calibration differences (see Appendix 1). Excluding these occasions enables the construction of a more consistent and thus accurate calibration curve. Here is how to extend the spreadsheet to filter out these specifics:

*Temperature change* In a new column, define a variable that is 1 when the temperature has changed less than 0.25 degC (in either direction) in the previous 15 minutes (i.e., a rate of 1 degC/hour). This value is not critical, and it may be increased a little if too many cells are being excluded from the analysis to obtain representative results.

*Day/Night* Set out a new column that has Day = 1 and Night = 0. Defining day/night periods is easy if pyranometer data are available (day = pyranometer output positive: make the threshold slightly above zero to allow for the slight zero offset of these instruments). If no pyranometer record is available, a table of sunrise/sunset times will provide these (see Chapter 11 for sources); enter 0 or 1 in the column for each observation time.

*Wind speed* If wind speed data are available, set out a third column to indicate 1 if the wind speed at the observation time is above a pre-set value, say 5 knots to start with, else leave it zero. Remember that if the anemometer is located well above screen height, the anemometer-indicated wind speed may not be representative of screen-level wind speeds and a higher threshold may need to be chosen. Again, adjust the value if there remain too few cells in the analysis when the filter is included.

If wind speed data are not available, use only the temperature change and day/night splits. Rainfall is another factor that can make a difference when comparing between screen types (louvred screens tend to stay wetter for longer than the smaller plastic AWS radiation screens, and can therefore appear cooler for a time owing to evaporative cooling effects), but it is difficult to define from recording raingauge data alone how long a surface will remain wet once the rain has stopped.

Next draw a scatter plot of the observed sensor value (horizontal *x* axis) versus the difference from the calibrated logger values (vertical *y* axis), as in the previous example. Using Excel, evaluate the equation of this line, which may be linear (varies in a straight line with the thermometer reading) or polynomial (a curve which includes more than one term). The better the spread of data points, the better the calibration result. Using the Excel Filter function, evaluate the curves for (a) all observations and (b) cloudy, windy nights only with steady temperature – the latter will have far fewer observations (and temperature range) but a smaller range of variance and thus a more accurate derived calibration.

The calibration curve obtained should then be applied to all future logged values – some systems will allow programmed calibrations to be applied as the values are logged, with others it will have to be done in a spreadsheet post-download. Make a note in the station metadata (see Chapter 16) of the calibrations applied, and the date they were introduced. If possible retain a link to the calibration comparison test results, as these will be useful to refine calibrations if a wider range of temperature data becomes available (if perhaps the initial calibration run in a winter month can be followed up some months later by a summer comparison).

Strictly speaking, the derived calibration curve is valid only over the observed range of temperatures examined (this is the reason why it is a good idea to undertake one cross-calibration run in winter and another in summer and pool the results), but in practice the results can normally be extrapolated using the derived calibration equation for at least a few degrees Celsius above and below the upper and lower observed value.

#### 9. Check regularly for calibration drift or sensor malfunction

The calibration of any temperature sensors, whether platinum resistance/thermistor or liquid-in-glass thermometers, can change over time: liquid-in-glass thermometers are susceptible to slow chemical and physical changes in the glass from which they are made, while electrical sensors occasionally go awry for no obvious reason. Whichever type of instrument is in use, it is therefore advisable to repeat this calibration test every 2 years, immediately if the sensor is suspected of malfunctioning.

### Calibrating humidity sensors

Humidity sensors can be calibrated in a laboratory environment using a variety of chemicals which will produce a known relative humidity in an enclosed environment. However, this approach is rarely practical for *in situ* calibration, and a cross-calibration process is more applicable for operational sensors. The process is essentially identical to that for cross-calibrating temperature sensors, with the following provisos:

- No two humidity sensors will agree exactly for very long; agreement to within 2–3 per cent is perfectly satisfactory.
- Avoid using observations where one sensor remains close to saturated while the other begins to fall. These circumstances can give rise to large transient differences owing to time constant/lag effects and hysteresis (see Appendix 1) rather than true differences in calibration. Including them in the calibration curve will bias the results obtained.
- The sensor ‘ceiling’ (maximum indicated humidity) in saturated air may be as low as 94–95% on some sensors. Calibration comparisons at high humidities should be treated with care.
- Best results will be obtained for readings in the range of 50 to 90 per cent humidity, with reasonable sensor ventilation (= screen-level breeze), and when the humidity is not changing too quickly. Afternoon humidity values can vary rapidly by several per cent, and it may be best to smooth both compared and calibrated values by averaging over, say, 15 minute periods, and comparing these results, rather than 5 minute ‘spot’ values.
- Humidity sensors tend to have a shorter lifetime than temperature sensors, and calibration checks should be carried out every 12 months, or if readings become erratic.
- The raw readings should be adjusted in line with the revised calibration as appropriate.

As with other sensors, note any calibrations derived and applied in the site metadata, with the date they were applied.

## Checking calibration drift on pressure sensors, including barographs

Chapter 7 gave details of setting or correcting barometric pressure sensors to mean sea level. Entry-level systems usually provide barometric pressure readings to a precision of only 1 hPa or mbar (although the accuracy may only be  $\pm 5\text{--}10$  mbar), but for accurate meteorological and climatological purposes a precision of 0.1 mbar is required. However, sensor *precision* to 0.1 mbar does not imply *accuracy* to 0.1 mbar, and the calibration should be checked – and regularly rechecked, at least every 6 months – to guard against calibration drift. Drift is inevitable, even in the best sensors: a good electronic sensor should drift by 0.1 mbar per year or less, but a household aneroid barometer or small-scale barograph may drift by much more, perhaps several millibars over a year.

Calibration of pressure sensors in a pressure chamber is expensive, but sensor accuracy (after MSL correction) can be quite easily benchmarked against the synoptic pressure field using essentially a more detailed version of the method given in Chapter 7 (section *MSL pressure corrections – approximate method* page 174). This more accurate method uses more stations, and requires original readings to 0.1 mbar. Unfortunately many state weather service websites list pressure observations only to 1 mbar precision, which is not precise enough for accurately determining calibration drift.

Unless your site is very close to a main reporting synoptic station (within about 10–15 km / 10 miles or so, and at a similar height – in which case a single station is sufficient), select at least four synoptic stations, preferably at similar distances to the north, east, south and west. Locations and maps of observing sites are usually available on state weather service websites. Plot them on a sketch map with your observing location at the centre. On an overlay, plot their reported MSL pressures\*, then draw isobars (lines of equal pressure) at 0.5 mbar intervals. Estimate the pressure at your location from the isobars, and compare this with your own observations made at the same times. (Remember that the synoptic station observations will always be in UTC – see Chapter 12 for more on time standards – so if your observations are in local clock time, or summer time, remember to correct for the difference.) Repeat this at different times of day over a couple of weeks, and keep track of the results in a small spreadsheet. If possible, do the exercise in a period with significant pressure changes as the calibration error may vary with pressure.

Include as many observations as possible to minimize outlier errors – occasional large stray differences may result from showery activity, rapid pressure changes at frontal passages, slight timing differences or even observational error. Check every data point and discard any that are obviously outside the normal range to avoid

\* MSL pressures from synoptic reporting stations to the required 0.1 mbar accuracy, decoded from transmitted observations, can be obtained from several locations on the web – for example, UK and Ireland observations from [www.met.reading.ac.uk/~brugge/latest\\_weather.html](http://www.met.reading.ac.uk/~brugge/latest_weather.html). Numerous synoptic reporting websites, such as [ogimet.com](http://ogimet.com), provide coded observations from reporting stations world-wide – the pressure observation is contained within the coded observations (details of the synoptic codes and how to decode the coded pressure value can be obtained from various meteorological reference sites on the web). The existing method of distributing coded observations using the so-called SYNOP code will be withdrawn at some stage before 2014; at the time of writing it is unclear whether Internet access to coded synoptic observations, including accurate barometer readings, will continue to be available once this code is phased out.



biasing the results obtained. Analyze the results to ascertain how close your barometer readings are to the background field, then adjust future observations accordingly.

When done carefully, this method can easily pick out calibration drift errors down to 0.1 mbar. Once set up in a spreadsheet, it becomes easy to repeat every few months as required.

### Calibrating other sensors

It is possible to cross-calibrate other sensors *in situ* using similar methods to those for temperature, but the relatively high cost of additional sensors for other elements (such as solar radiation) makes this an expensive exercise unless a spare calibrated unit can be borrowed for the duration of the test. Of course, unless the calibration of the 'reference' unit is reliably known, using another instrument to adjust calibrations on existing sensors will almost certainly make matters worse.

For anemometers, the exposure of the instrument is likely to have a greater effect on the readings obtained than any relatively small deficiencies in calibration. Accurate calibration of wind instruments is important, but less important than getting the best possible exposure – see Chapter 9 for details.

### One-minute summary – Calibration

- Instrument calibrations are one of the most important, yet also one of the most neglected, areas of weather measurement. Making accurate weather measurements requires accurately calibrated instruments.
- Recording raingauges can be easily and accurately calibrated by passing a known volume of water through the gauge, and comparing with the indicated measurement. 'Out of the box' errors for some AWS tipping-bucket raingauges of this type can exceed 20 per cent, so this is a vital test for all new instruments at first installation. Recording raingauges should not be adjusted merely to attempt exact agreement, or near-agreement, with a standard raingauge, because instrumental and exposure differences will always lead to slight variations in the amount of rainfall recorded.
- Two calibration methods are described for temperature sensors, whether liquid-in-glass thermometers or electrical units. The first is a quick and easy method based on the fixed point of melting ice at 0.0 °C. An extension of the approach can extend the range of calibration points from –5 °C to +40 °C when used with an accurately calibrated reference thermometer. However, this method is not suitable for certain types of sensor, and on some AWS models the temperature elements may not be accessible to allow this test to be undertaken.
- The second temperature calibration method involves careful comparison over a period with a portable reference unit of known calibration. Both sensors (calibrated reference and test) are exposed in identical adjacent surroundings exposures for a period (days to weeks). Careful comparison of readings can derive an accurate calibration curve, which is then used to apply the corrections obtained to the sensor readings going forward.
- Calibration checks, and checks for calibration drift, on pressure sensors can be made using pressure reports from synoptic sites over a period of a few days or weeks.

- Make a note in the site metadata of all calibrations applied, and the date. Keep a copy of the calibration table or algorithms used in the metadata file. Retain the calibration test results.
- Calibrations can drift over time, so calibrations should be checked (and adjusted if necessary) regularly – at least once every 6 months for pressure sensors, every 2 years for electronic temperature probes and every 5 years for liquid-in-glass thermometers.

## Reference

- [1] Burt, Stephen (2008) Calibration of air temperature sensors. *Climatological Observers Link Bulletin* No. 460, August 2008, pp. 30–32.

# Paper 4

## ***Oxford's urban growth and its potential impact on the local climate.***

Chapter 3 in *Oxford Weather and Climate since 1767* by Stephen Burt and Tim Burt, 2019

Oxford University Press, 544 pp.

*Bibliography #14. Word count 3220 excluding references.*

---

*The following chapter is reproduced by kind permission of Oxford University Press*

*OUP catalogue book website:* <https://global.oup.com/academic/product/oxford-weather-and-climate-since-1767-9780198834632?q=oxford%20weather&cc=gb&lang=en>

*OUP Author Reuse and Self-Archiving site licensing details:*

<https://global.oup.com/academic/rights/permissions/autperm/?cc=gb&lang=en&>



## Oxford's urban growth and its potential impact on the local climate

---

One potentially important source of inhomogeneity in the Oxford meteorological record relates to Oxford's urban development since the Radcliffe Observatory was built in 1772, for it is very likely that this has affected the record to some extent. Close to the site itself, the encroachment of the Radcliffe Infirmary from the south, house-building to the north and west and construction of various University buildings to the east could all have influenced the temperature locally. Looking at the broader situation, it would be surprising if the growth of Oxford more generally did not have some effect upon measured air temperatures at the Observatory, as well as other observations such as visibility. Gordon Manley and Gordon Smith debated the urban heat island (UHI) effect in 1975, without reaching agreement [31]. As with almost any settlement of any size, there is undoubtedly some urban influence. In this chapter, we review the issue and chart its likely development over the last two and a half centuries. To do so, it is first necessary to describe developments immediately adjacent to the Observatory as well as further afield.

When the Observatory was built, the choice of site was very deliberately on the northernmost edge of the built-up area, beyond the Radcliffe Infirmary [20, 32]. Of necessity, the Observatory had to be aligned on an east–west axis and, whilst initially the southern side looked out onto open land, the gardens to the north of the building were the private grounds adjoining the Observer's house, into which Hornsby moved with his family in 1773. According to Michael Pirie (pers. comm.), the wall separating the north lawn and gardens from the open land beyond was built at that time, certainly before 1776. Thus, the sky view from the north lawn has always been a little restricted, even before houses were built north of the Observatory. To the south and west, the aspect remained relatively open until the encroachment of the Radcliffe Infirmary from the early twentieth century onwards [17]. Ironically, as we write this book, the land has been cleared immediately to the south-west of the Observatory, with new building developments soon to follow, no doubt. Already, new buildings to the north of the Infirmary have come very close on the south-east side of the Observatory (Figure 3.1). Michael Pirie [32] notes that the encroachment of the hospital during the First World War coincided with the decline of the astronomical observations. Although the raingauges have remained in exactly the same position on the north lawn since 1850 (aside from a short spell on the



**Figure 3.1** *The view south and south-west from the Radcliffe Observatory tower, April 2018 (Stephen Burt)*

front or south lawn from 1935 to 1939), the screens and their thermometers were located to the south of the main Observatory building from 1878 to 1939 except for 1920 to 1926, when they were located in or close to the current enclosure on the north lawn. They were moved to the north lawn once more in September 1939, where they have remained ever since (Appendix 1 gives more details.) The move of the Observatory to South Africa in 1935 seemed to threaten the continuation of the meteorological observations, but the University wisely insisted on their continuation, whatever use the Observatory itself was put to.

The 1830s saw two important developments close to the Observatory. Oxford University Press was removed from the Clarendon Building to Walton Street in 1830 and its presence there led to the rapid development of small terraced housing in the Jericho district\*. On the other side of the north lawn wall, the terraced houses of Observatory Street were built from 1834 (Figure 3.3). A little further to the west, wharves were gradually opened off Walton Street and Hayfield Road, alongside the Oxford Canal which had opened in 1790; terraced housing was gradually built in this area too. North Oxford grew steadily from the 1850s; most of the land was owned by St John's College, which obtained an Act of Parliament in 1855 enabling it to offer 99-year building leases. Large houses were built on farmland either side of Banbury Road and Woodstock Road. Chance *et al* [33] argue that it is a misconception that north Oxford grew up when the dons were released from celibacy. By the time dons were allowed to marry, following the Royal Commission of 1877, the southern part of north

\* The authors are pleased to draw attention to the strong 'local' link with our publishers, Oxford University Press, which remains in the same buildings in Great Clarendon Street today, barely 2 minutes' walk from the Radcliffe Observatory.





**Figure 3.2** *Google Earth view centred on the Radcliffe Observatory and covering approximately 500 m on each side (0.25 km<sup>2</sup>). The meteorological enclosure can be seen in the grounds of Green Templeton College immediately north of the Observatory building. The grounds and buildings of the Radcliffe Infirmary to the south and south-west, previously the Observatory grounds (compare Figures 2.5 and 2.8), are in the process of extensive redevelopment (see also Figure 3.1) (Google Earth)*

Oxford was already developed, and the movement of dons out of college was, in any case, a gradual process. Professors and readers had always been allowed to live out, and they accounted for the relatively high concentration of families in Norham Gardens and Park Town, to the east of the Observatory. The new houses to the north of the Observatory were mostly taken by tradesmen, for whom the growth of north Oxford was the first opportunity to move from the city centre into suitable middle-class suburbs. Today, the whole area generally to the north of the Observatory, including Summertown, is completely built up, from Port Meadow to the west to the Cherwell floodplain to the east (Figure 1.1). Whilst this has completely changed the view from the uppermost floor of





**Figure 3.3** *View looking north from the Observatory tower, 25 April 2018. The amount of building that has taken place since the 1770s is obvious, starting with Observatory Street immediately to the north of the garden wall in 1834. The Radcliffe Meteorological Station enclosure is clearly visible on the lawn (Tim Burt)*

the Observatory, the sky view of the north lawn, where most of the instruments are now located, is probably not very much different from what it was in the late 1830s.

Two questions therefore come to mind: what is the current magnitude of Oxford's urban heat island (UHI), and how has the UHI evolved since meteorological observations were begun in the 1760s?

Initially, to gauge the current situation, we had hoped to use 'rural' observations from Wytham Woods, some 9 km west of the Observatory on the other side of the Thames floodplain (located on Figure 1.1). There, in a field close to the woodland, the UK Environmental Change Network (ECN) has run an automatic weather station (AWS) since 1992, at 160 m above sea level (ASL). However, the ECN mean temperatures are calculated from hourly averages whereas the Radcliffe Meteorological Station (RMS) means are based upon maximum and minimum temperatures in the usual way. Until we have sufficiently long automatic weather station records from the Observatory, this comparison will have to wait. In any case, the ECN site is on the top of Wytham Hill (c. 160 m ASL), almost 100 m higher than the RMS in a very different topographic situation, hardly an ideal comparison. An additional AWS somewhere on the Port Meadow floodplain might in the future provide a more useful comparison.

Accordingly, we went further afield to the small town of Wallingford, around 22 km south-east of Oxford, where the Centre for Ecology and Hydrology (CEH) has maintained weather records at a rural site some distance outside the town since 1961. The altitude difference is only 15 m (Wallingford 48 m, Oxford 63 m) so, on lapse rate grounds alone, we would expect Oxford to be 0.1 degC cooler on average. We compared daily records over the three most recent years’ record from 2015 to 2017. Figure 3.4 and Table 3.1 show the comparisons for daily maximum and minimum temperatures. As expected, Oxford is somewhat warmer overnight—the mean minimum temperature there averages 0.93 degC above Wallingford, with a slight seasonal variation (summer higher) and a marked positive skew. Oxford is at least 0.2 degC warmer than Wallingford on two nights in three, whereas only one night in five is at least 0.2 degC warmer at Wallingford: 43 per cent of nights are at least 1 degC warmer at Oxford, but only 5 per cent of nights are at least 1 degC warmer at Wallingford. By daytime, the magnitude of Oxford’s UHI is reduced—the mean maximum temperature at Oxford is just 0.27 degC higher than Wallingford on average. The daytime UHI also shows a very marked seasonal variation tied to solar angle—close to zero at the midwinter solstice, around +0.7 degC at midsummer. This seasonal variation can be accounted for by a combination of shading of the site by the Observatory buildings in midwinter, and stored heat within the urban fabric in summer. Nevertheless, almost 60 per cent of daily maxima are at least 0.2 degC higher in Oxford (14 per cent are more than 1 degC warmer), compared with just 23 per cent of days which are more than 0.2 degC warmer at Wallingford.

In conclusion, therefore, and based on the Wallingford comparison, to answer our first question, there is clear evidence that the Radcliffe Observatory site is slightly warmer by day than the surrounding countryside, by around 0.4 degC on average (including the expected lapse rate difference due to the altitude difference), and this is more marked during the summer months. By night, the difference is greater, around 1.0 degC (again including the expected lapse rate difference due to the altitude difference), also more marked in the summer months but less so than for the seasonal variation in daytime temperatures. Averaging the two, we can state that the current magnitude of Oxford’s urban heat island at the Radcliffe Observatory site averages about 0.7 degC.

The second question is more difficult to answer going back as far as the start of the Radcliffe Observatory record, as there are no single-site records of similar length against

**Table 3.1** *Differences in daily maximum and minimum temperatures between Oxford and Wallingford, based on three years data 2015–17*

Difference in max or min temperature	MINIMUM TEMPERATURE		MAXIMUM TEMPERATURE	
	Wallingford warmer	Oxford warmer	Wallingford warmer	Oxford warmer
≥ 0.2 degC	20%	67%	23%	59%
≥ 1.0 degC	5%	43%	5%	14%

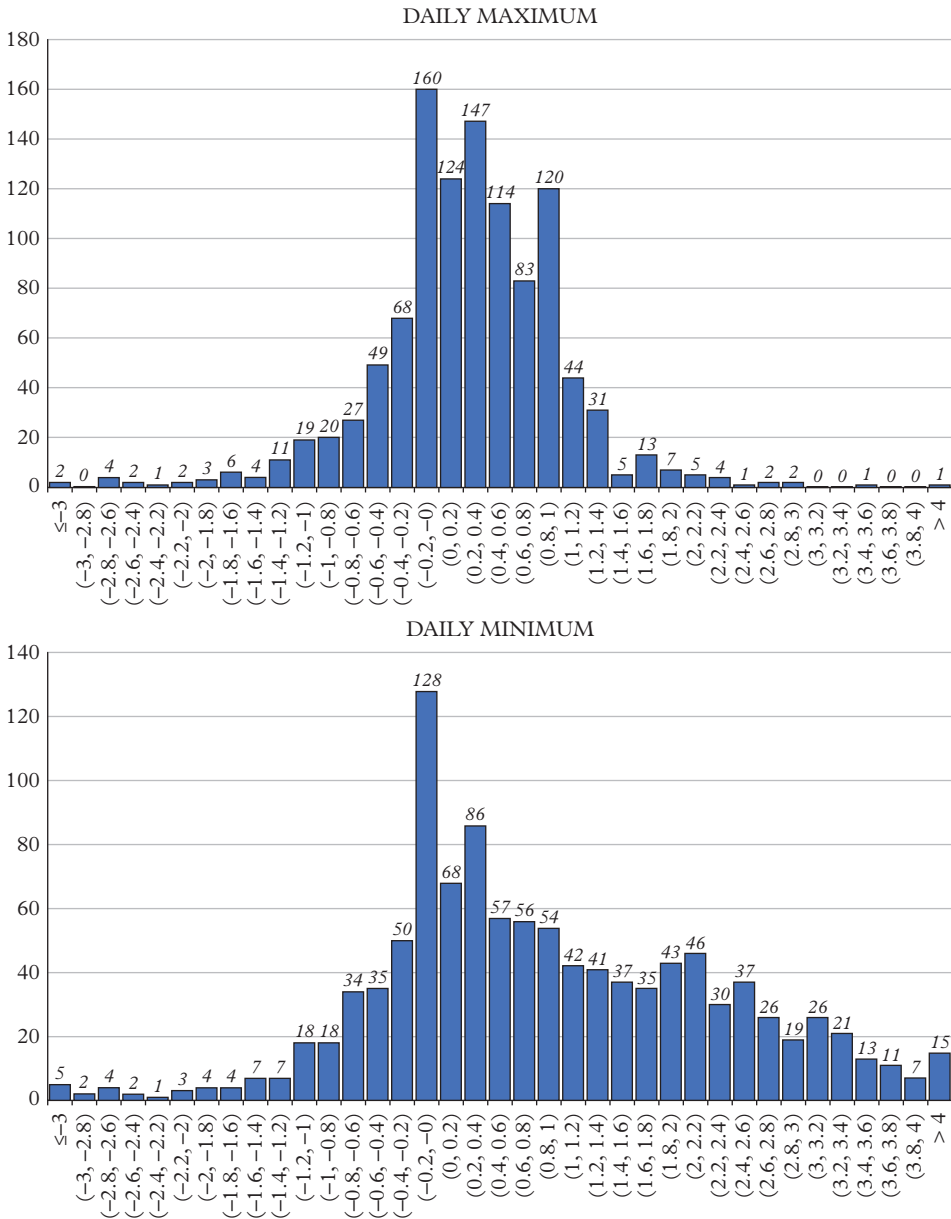


**Figure 3.4** Frequency of differences in daily maximum and minimum temperatures (degC, 0.2 degC bins, positive indicates Oxford warmer) between Radcliffe Meteorological Station Oxford and CEH Wallingford over three years 2015–17

which to compare. The obvious comparator would seem to be Gordon Manley’s Central England Temperature (CET) series [34, 35], but CET data are themselves very dependent on the Oxford record from 1815 to 1841, so this becomes somewhat of a circular argument and meaningful comparisons are accordingly limited. From the mid-nineteenth century, when other weather station data become available, the CET is less dependent on Oxford, so comparisons over time can then be made. Here, we focus on comparisons with the CET daily mean maximum and mean minimum temperature time series which run from 1878 [36, 37], using monthly data downloaded from the Hadley Centre website.

Table 3.2 compares CET mean daily maximum and minimum temperatures with Oxford’s over various 30-year periods since 1901, including the most recent 30 years, 1988–2017 (these are further discussed in Chapter 24). There is no doubt that the urban influence on the long Oxford record continues to increase, although the greatest difference between CET and Oxford is in maximum temperatures\*, and this has increased at a greater rate than the difference in minimum temperatures in the last three decades. Mean air temperatures have also increased by about 0.91 degC compared with 1961–90, 0.20 degC greater than the rise in CET over the same period.

Long-term trends in Oxford maximum and minimum temperatures relative to CET are shown by the solid lines in Figures 3.5 and 3.6, which show ten-year running means of the difference between Oxford and CET mean annual maximum (Figure 3.5) and

**Table 3.2** *Comparison of Central England Temperature (CET) and Oxford mean temperatures over various 30-year periods since 1901*

		1901–30	1931–60	1961–90	1988–2017	Difference
		means	means	means	means	1988–2017 minus 1961–90 degC
<b>Mean maximum °C</b>	CET	12.79	13.24	13.07	13.95	+0.88
	Oxford	13.68	14.10	13.78	14.93	+1.15
	Difference	+0.89	+0.86	+0.71	+0.98	<b>+0.27</b>
<b>Mean minimum °C</b>	CET	5.71	5.97	5.88	6.45	+0.57
	Oxford	5.95	6.21	6.44	7.11	+0.67
	Difference	+0.24	+0.24	+0.56	+0.66	<b>+0.10</b>
<b>Mean air temperature °C</b>	CET	9.28	9.63	9.51	10.22	+0.71
	Oxford	9.81	10.16	10.11	11.02	+0.91
	Difference	+0.63	+0.53	+0.60	+0.80	<b>+0.20</b>

\* This is not surprising and is not related to Oxford’s UHI—it is simply a matter of geography: Oxford is south of the ‘centre of gravity’ of Manley’s CET region, and is therefore slightly warmer as a result.

mean annual minimum temperature (Figure 3.6), in degrees Celsius. Positive values indicate Oxford warmer than CET.

Gordon Manley used the long record from Rothamsted (Hertfordshire) to assess changes in the urban component in the Oxford record up to 1975 [31]; we decided to repeat the comparison, making use of the additional 40+ years of record since Manley's work [38]. The Rothamsted record commenced in 1878; it is a rural site about 65 km almost due east of Oxford, and at a greater altitude (128 m against Oxford's 63 m); the altitude difference alone would be expected to account for about 0.4 degC difference in mean temperature between the two.

Ten-year running means of the differences between Oxford and Rothamsted's mean annual maximum and mean annual minimum temperatures (dotted lines) and Rothamsted and CET mean annual maximum and mean annual minimum temperatures (dashed lines) are also plotted in Figures 3.5 and 3.6. Given that much work has been done to ensure the CET series remains as homogenous as possible and reflects a proper balance of stations across Central England, and that the Oxford and Rothamsted records

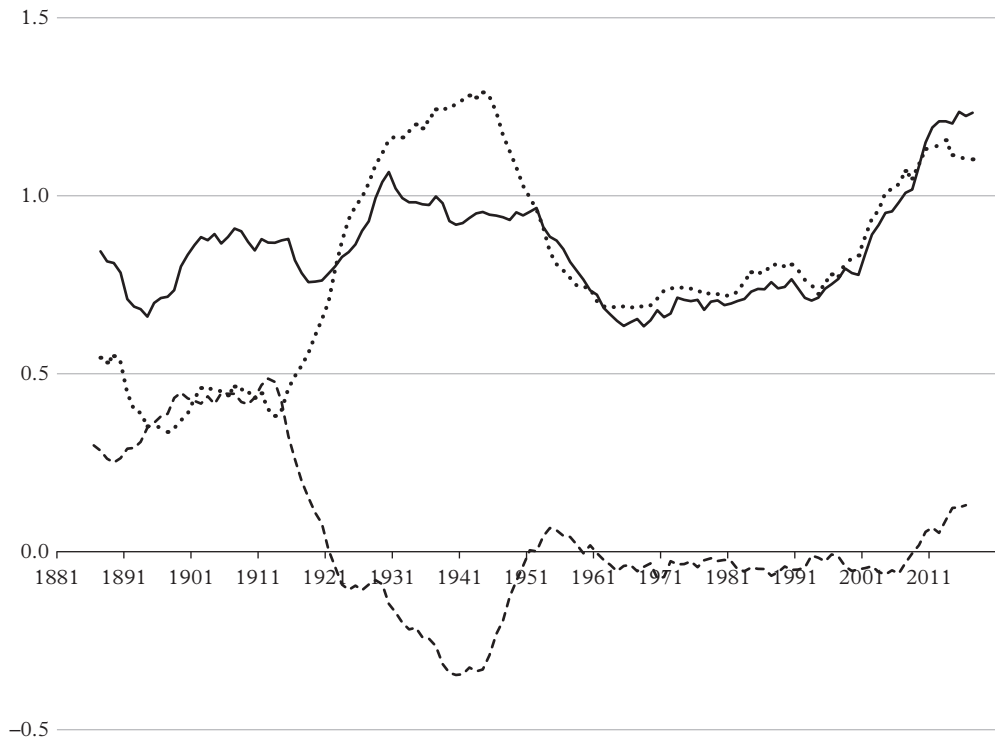


**Figure 3.5** Ten-year unweighted running means, plotted at year ending, of the relative differences (degC) between Oxford, Rothamsted and Central England Temperature (CET) annual mean maximum temperature over the period 1878 to 2017. Solid line shows Oxford minus CET, dotted line Oxford minus Rothamsted, and dashed line Rothamsted minus CET

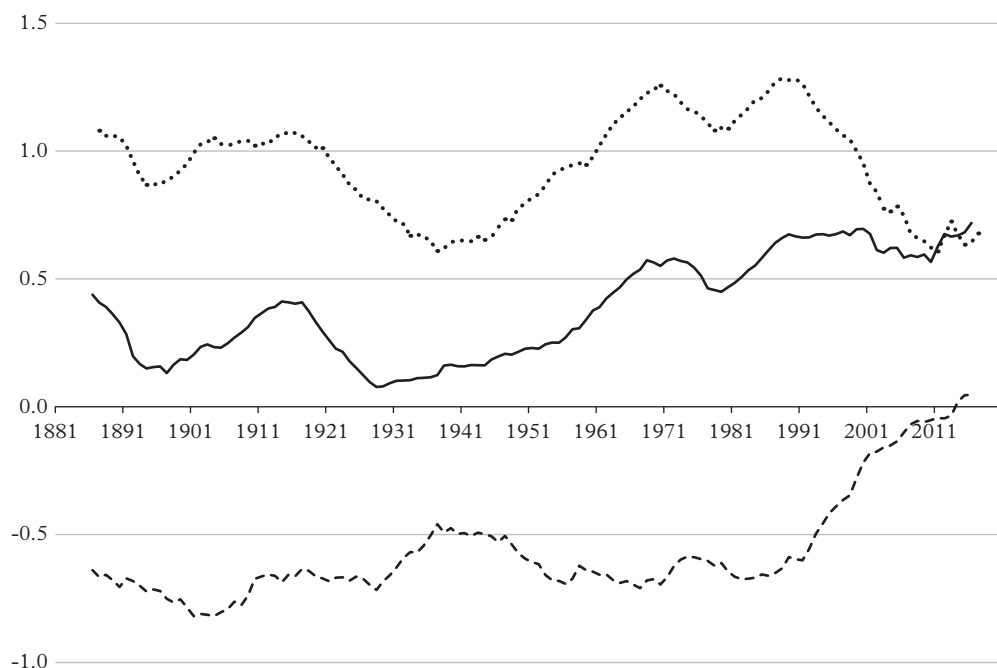


**Figure 3.6** *As for Figure 3.5 but for annual mean minimum temperature. The scales on both plots are identical to facilitate comparison*

reflect much the same regional climate, divergence from the CET and from each other can only arise from changes in observational practice and/or local site factors.

Looking firstly at maximum temperatures (Figure 3.5), there is little overall trend in Oxford's temperatures relative to CET (solid line) until the 1990s, since when the difference has increased quite sharply. The average difference between 1878 and 1990 was 0.76 degC; the last 20 years (to 2017) averaged 1.09 degC and is clearly outside the range of previous inter-decadal variations within the record since 1878. (The significant cooling relative to CET seen in Rothamsted mean maximum temperatures between about 1911 and 1940, dashed line in Figure 3.5, is not reflected in the Oxford record, and may represent an unknown or uncorrected site move or change of observational practice at the former.) There is less evidence at Rothamsted of the relative warming in mean maximum temperatures seen in the Oxford record in recent decades (dashed line), at least until the last decade or so. From this we infer that the increase in Oxford's mean maximum temperatures relative to CET since the mid-1960s is genuine: it most likely relates to an increased urban influence on the Radcliffe Observatory site since then, and particularly since 2000. The observed increase in the duration of bright sunshine in recent decades highlighted in Chapter 24 may also have had some impact on daytime temperatures.

For minimum temperatures (Figure 3.6), the position is simpler—at Oxford there has been a fairly steady warming relative to CET since about 1930 (solid line), averaging about 0.07 degC per decade. Unlike maximum temperatures, there is little evidence of a more rapid warming at Oxford relative to CET over the past two or three decades, although minimum temperatures at Rothamsted (dashed line) appear to have warmed rapidly relative to CET since the 1980s (resulting in a reduction in the mean difference between Oxford and Rothamsted since then, as shown by the dotted line in Figure 3.6). Until about 1990, there is a high degree of similarity between Oxford and Rothamsted mean minimum temperature differences from CET. That this has changed significantly since about 1990 appears to be due to relative warming at Rothamsted rather than Oxford, suggesting that Rothamsted is not itself entirely free of urban effects from the growth of nearby Harpenden.

At a more regional scale, it is possible that synoptic airflow changes may have raised temperatures at both Oxford and Rothamsted more than places further north within the CET area in recent decades. Both sites are in inland south-eastern sites that tend to record larger positive anomalies in generally warm months (Julian Mayes, pers. comm.). Further analysis of the Oxford UHI using rural sites more distant than Rothamsted and further to the north would usefully enhance this picture.

With hindsight, Manley's [31] focus on the difference between Oxford and Rothamsted from the 1950s to the 1960s was prescient, judging by Figure 3.5; he argued for a small urban effect at Oxford of the order of 0.1 degC at that time. To conclude by answering the second question posed at the start of this section, the evidence available 40 years after Smith and Manley's exchange suggests that Oxford's urban effect in comparison to 'background' CET is now 0.2 degC, arising primarily from a more rapid increase in maximum temperatures in recent decades (Table 3.2 and Figure 3.6). The more rapid recent upward trend in Oxford air temperatures is concerning and it may well be that in future some adjustment to Oxford temperature records will need to be made to allow for this more local warming trend: clearly, any inferences regarding climate change at Oxford need to bear this in mind. These increases in urban effects on the long Radcliffe Observatory record are most likely driven partly by changes close to the site itself and partly by wider changes across Oxford's urban area.



# Paper 5

## **Two hundred years of thunderstorms in Oxford**

By Stephen Burt. *Weather*, 2021

Online publication 9 February 2021: <https://doi.org/10.1002/wea.3884>

*Bibliography #6. Word count 4665 excluding references.*

---

### **Open Access Article**

*This is an open access article distributed under the terms of the Creative Commons CC BY license, which permits unrestricted use, distribution, and reproduction in any medium, provided the original work is properly cited.*



# Two hundred years of thunderstorms in Oxford

**Stephen Burt** 

Department of Meteorology,  
University of Reading, UK

The long instrumental meteorological records from the Radcliffe Observatory site in Oxford (where records commenced in 1772) are well known, and have recently been documented to 2018 by Burt and Burt (2019). Less well-known, and still largely in manuscript or paper format, are the non-instrumental records also maintained by the Observatory which documented the occurrence of fog, snowfall, thunderstorms and the like. Records of thunderstorm occurrence at the Radcliffe Observatory, by date, are complete between 1828 and 1986, excluding the years 1936 to 1970 for which only monthly totals are available. Since 1986, a reliable private record of thunder frequency from Oxford, very close to the Radcliffe Observatory site, has been used to extend the record to 2019, forming a record of almost 200 years of thunderstorm frequency for the city – a record probably unique anywhere in the world. This newly digitised record, made available for the first time, is examined for long-term (decadal) trends in thunderstorm frequency, and by Lamb Weather Type. Comparisons are made with other long-period records from west London, around 75km southeast of Oxford. Reasons to account for the marked reduction in thunderstorm frequency in the last decade are suggested.

## The observational record – details and sources

### Sources

Full details of the Radcliffe Observatory site and instrumental records are given in Burt and Burt (2019). An almost unbroken daily temperature record has been maintained since November 1813, although the earliest surviving thunderstorm records are for 1828. The Radcliffe Observatory site is at 51.761°N, 1.264°W, at 63m above mean sea level; the location of the observatory site, known today as the Radcliffe Meteorological Station (RMS) and run by the School of

Geography at the University of Oxford, is shown in Figure 1.

### 1828–1852

The format of the Radcliffe Observatory's meteorological register was expanded in January 1828 to permit more details of the day's weather to be included. For this project, dates with thunder were extracted manually by careful eye examination of the daily weather entries from high-resolution photographic copies of the monthly manuscript observation registers, the originals of which are held in the School of Geography at the University of Oxford. The period 1828–1840 was examined by myself, and 1841–1852 by Tim Burt; a random series of months within each period was checked by us both to minimise the risk of one of us missing an entry, although it is possible that some obscure or illegible entries may have been missed.

### 1853–1935

From 1840, the astronomical observations and tabulations from the Radcliffe Observatory were published in (initially) annual volumes entitled *Astronomical observations made at the Radcliffe Observatory in the year [x]*, volumes hereafter referred to as the *Radcliffe Results*. Some later years were amalgamated into multiyear volumes; from the 1900–1905 volume, the meteorological observations were published in their own binding until the 1931–1935 volume, the last in the series following the move of the (astronomical) observatory to South Africa and the transfer of responsibility for the meteorological records to the University. Meteorological summaries began to be included from the 1853 *Radcliffe Results* volume, and a more-or-less standard format quickly evolved, whereby from 1859 and in most years the dates of various phenomena including thunderstorms were

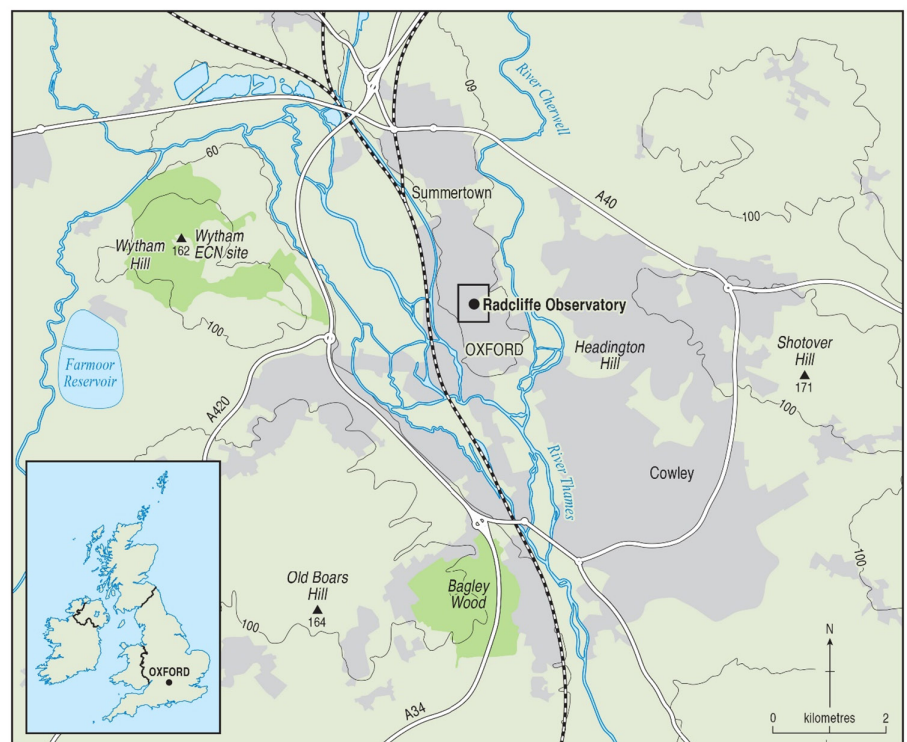


Figure 1. The Oxford area, showing the city, the River Thames and the 60 and 100m contours. The central square shows the Radcliffe Observatory quarter in North Oxford. (Map courtesy of Chris Orton, University of Durham.)

set out by month in a supplementary table entitled 'Summary [or 'Characteristics ...] of the weather and remarkable phenomena, for each month [year]'. An example, for the month of August 1878 (the most thundery month on the record), is included as Figure 2. In addition, the published monthly data tables often include notes of thunder, etc., although the annual 'Summary/Characteristics' table is generally the more complete. Some of the *Radcliffe Results* volumes have already been scanned and a number are available online; the relevant (meteorological) pages from the others were photographed from the partial set held within the School of Geography, the remaining volumes being consulted and photographed in the Bodleian Library to assemble the complete series as PDF files. (These are available on Figshare - <https://www.doi.org/10.6084/m9.figshare.13333925>.) These PDF files were converted to computer-readable text using Optical Character Recognition software, and dates of thunder events were then extracted by searching for the string 'thun' (the abbreviation allowing for hyphenation, abbreviations, etc.). Most entries also carried information on the timing and sometimes the severity of the storms, although these details were not extracted.

For much of the published record, thunderstorm records were separately categorised into 'thunderstorm' (thunder and lightning observed), 'thunder' (thunder heard, presumably without lightning seen) and 'lightning' (only). The first two were counted as a 'thunder day' record, only one per day if both were reported on the same date, while 'lightning only' events were not included in these analyses. The frequency of lightning at the Radcliffe Observatory was surprisingly high, sometimes twice or more the annual frequency of thunder heard; it should be remembered that this was an astronomical observatory with a staff of observers, work-

ing mainly at night, largely in the era before extensive urban street lighting.

Monthly and annual totals of 'days with thunder heard' for Oxford were published in the *Monthly Weather Report (MWR)* 1884–1993 (when the *MWR* ceased publication), and these together with other sites were analysed by Valdivieso *et al.* (2019). However, monthly values extracted from the *MWR* were normally lower than those taken from the *Radcliffe Results*. Examination of the discrepancies suggested that the 'thunder day' totals reported by the Observatory and subsequently published in the *MWR* were (often, but not always) 'thunderstorm days' alone, and days where thunder was heard but no lightning was observed were excluded, resulting in a lower total.

### 1936–1970

Monthly and annual totals of 'thunder days' for this period were extracted from manuscript tabulations held within the School of Geography. Unfortunately, dates of occurrence could not be traced within the School's archive for this period, although the original monthly manuscript climatological returns are believed to exist in the Met Office climatological archive<sup>1</sup>.

<sup>1</sup>The author planned to visit the Met Office archives during spring 2020 to obtain daily thunder day dates for this period and thereby eliminate this gap, but was unable to do so once the facility closed to visitors in mid-March 2020 owing to the coronavirus lockdown. Completion of this paper was delayed for six months awaiting re-opening. Rather than delay publication indefinitely, this paper was resubmitted without the dates for 1936–1970 in late September 2020 as the archive remains closed for the foreseeable future. Monthly and annual totals are complete: the online dataset will be updated with the 1936–1970 dates once access to the Met Office archives is available once more.

### 1971–1986

Dates of 'thunder heard' were extracted from the Met Office Integrated Data Archive System (MIDAS) climate archives held within the Natural Environment Research Council's Data Repository for Atmospheric Science and Earth Observation (CEDA – <http://archive.ceda.ac.uk/>), and monthly and annual totals tabulated.

### 1987–2019

From late 1986, RMS authorities chose not to submit records of snow falling and thunder in their monthly observational returns to the Met Office, because it was felt that the vigilance required for a good record was becoming impossible to maintain. From January 1987 onwards, RMS records of thunder are mostly missing, and the Radcliffe Observatory records effectively cease at this point.

To complete the series to date, a high-quality personal record kept in central Oxford (mostly within 4km of the Radcliffe Observatory) since 1983 by Jonathan Webb, a director of the Tornado and Storm Research Organisation (TORRO), has been used. Accuracy and continuity of record was assessed by comparison with the record from the Met Office staffed airfield at Brize Norton, 21km to the west. Figure 3 shows the annual thunder day totals, and Table 1 the annual averages, from Brize Norton, from the commencement of records in 1968 through to 2019, compared with the record for the Radcliffe site for 1968–1986 and the Webb record for 'central Oxford' for 1987–2019. There is good temporal correlation between Oxford Radcliffe and Brize Norton annual thunder day totals 1968–1986 (correlation coefficient  $R^2 = 0.54$ ) and Brize Norton and central Oxford 1987–2019 ( $R^2 = 0.55$ ), although the more comprehensive Kolmogorov–Smirnov test (Massey, 1951) on the two distributions suggests a difference between the two distributions, probably owing to the 21km separation between the sites. However, the Webb record was chosen for 1987–2019 because it provided spatial continuity with the long Radcliffe record.

### How consistent is the observational record?

A permanent or near-continuous weather watch together with a high level of observer vigilance is essential for accurate counts of thunder(storm) frequencies. Between 1828 and 1924, the Oxford record was from an astronomical observatory maintaining a 24h record, with three or four meteorological observations per day. From January 1925, the formal meteorological observation routine was reduced to once daily, at 0900 GMT, in preparation for the move of the (astronomical) observatory itself to South Africa, and

AUGUST.	
Temp. Highest in sunshine, ..... 13 <sup>h</sup> 2	Fog on the 25th at 16 <sup>h</sup> to 21 <sup>h</sup> .
„ Lowest on grass,..... 4 <sup>h</sup> 5	Solar halos were seen on the 8th at 21 <sup>h</sup> 30 <sup>m</sup> to 22 <sup>h</sup> ; 11th, 23 <sup>h</sup> to 23 <sup>h</sup> 50 <sup>m</sup> ; and 16th, 20 <sup>h</sup> .
Rain fell on Aug. 2, 3, 4, 5, 6, 7, 10, 11, 13, 14, 15, 16, 22, 23, 25, 27, 28, 29, and 30.	Lunar halos were seen on the 10th at 13 <sup>h</sup> 15 <sup>m</sup> ; and 12th, 0 <sup>h</sup> 45 <sup>m</sup> .
Thunderstorms on the 3rd at 0 <sup>h</sup> to 1 <sup>h</sup> ; 4th, 4 <sup>h</sup> 30 <sup>m</sup> to 6 <sup>h</sup> ; 5th, 23 <sup>h</sup> 30 <sup>m</sup> to 0 <sup>h</sup> ; 6th, 0 <sup>h</sup> to 0 <sup>h</sup> 30 <sup>m</sup> ; 23rd, 6 <sup>h</sup> to 6 <sup>h</sup> 45 <sup>m</sup> ; and 28th, 18 <sup>h</sup> 45 <sup>m</sup> to 19 <sup>h</sup> 15 <sup>m</sup> .	Lunar irides were seen on the 10th at 13 <sup>h</sup> 15 <sup>m</sup> ; 12th, 10 <sup>h</sup> 30 <sup>m</sup> ; 14th, 9 <sup>h</sup> 30 <sup>m</sup> ; and 15th, 10 <sup>h</sup> 20 <sup>m</sup> .
Thunder was heard on the 11th at 23 <sup>h</sup> 15 <sup>m</sup> ; 12th, 0 <sup>h</sup> to 0 <sup>h</sup> 30 <sup>m</sup> ; 23rd, 2 <sup>h</sup> 30 <sup>m</sup> to 4 <sup>h</sup> 30 <sup>m</sup> ; 29th, 20 <sup>h</sup> 30 <sup>m</sup> ; and 30th, 1 <sup>h</sup> 30 <sup>m</sup> to 1 <sup>h</sup> 45 <sup>m</sup> .	Dead calms on the 3rd at 10 <sup>h</sup> and 22 <sup>h</sup> ; 6th, 10 <sup>h</sup> ; 9th, 0 <sup>h</sup> to 0 <sup>h</sup> 45 <sup>m</sup> , and 2 <sup>h</sup> ; 18th, 0 <sup>h</sup> ; 20th, 21 <sup>h</sup> 15 <sup>m</sup> ; 22nd, 20 <sup>h</sup> ; 23rd, 2 <sup>h</sup> and 10 <sup>h</sup> ; 24th, 0 <sup>h</sup> to 2 <sup>h</sup> , and 20 <sup>h</sup> ; 25th, 20 <sup>h</sup> to 23 <sup>h</sup> ; and 26th, 0 <sup>h</sup> 45 <sup>m</sup> to 2 <sup>h</sup> , and 10 <sup>h</sup> .
Lightning was seen on the 3rd at 11 <sup>h</sup> ; 15th, 9 <sup>h</sup> to 10 <sup>h</sup> 30 <sup>m</sup> ; and 23rd, 5 <sup>h</sup> 15 <sup>m</sup> to 5 <sup>h</sup> 30 <sup>m</sup> , and 7 <sup>h</sup> 30 <sup>m</sup> to 8 <sup>h</sup> 30 <sup>m</sup> .	Storms of wind on the 27th, and 28th.

Figure 2. An example of the monthly 'Characteristics' data published in the *Radcliffe Results* volumes. This is for August 1878, the most thundery month on the long Oxford record, when 10 days with thunder were noted. Note the differences between 'thunderstorms' and 'thunder heard' and 'lightning' (only) – only the first two are counted as a 'day with thunder heard'.

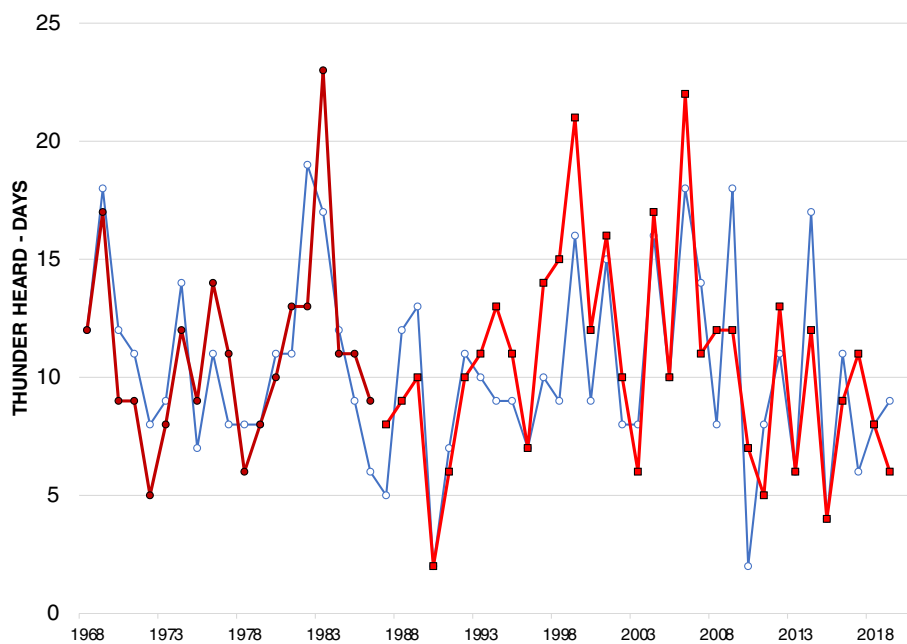


Figure 3. Annual thunder days at Brize Norton, Oxfordshire, 1968–2019 (blue line) compared with Oxford, Radcliffe Meteorological Station (dark red line, round points) 1968–1986 and Oxford City record 1987 to 2019 (red line, square points); see also Table 2.

civil day, midnight to midnight UTC, although thunderstorms occurring overnight are less likely to be noted by most observers (except perhaps by an astronomical observatory), particularly if they consist of only one or two claps of thunder. However, a storm spanning midnight – even if only two claps of thunder, one at 2359 and the other at 0001 UTC – will count as two ‘thunder days’. The timing upon arrival in the south Midlands of summer storms imported on a ‘Spanish plume’ heatwave event will occasionally generate such ‘double counts’, although such events are a minority in the record.

Comparisons of the record using overlapping periods of record with other sites, both nearby (Brize Norton) and regional (west London, discussed subsequently) suggest that the majority of the dataset is remarkably consistent. The early part of the record, perhaps the first two decades, appear slightly ‘light’ when compared with thunder frequency in the London area, but there are few other records with which to compare, and this may simply reflect genuine geographical variation at that time, differing definitions as to what constituted ‘a day of thunder’, or a combination of reasons.

## The observational record 1828–2019

Figure 4 (blue columns) shows the annual totals of ‘days with thunder heard’ in Oxford since 1828, together with a superimposed 10-year running mean (red curve), plotted at year ending. Table 2 gives monthly and annual averages by decade from 1830–1839 to 2010–2019, together with a selection of 30-year average periods including the current standard averaging period<sup>2</sup> (1981–2010) and the most recent 30-year period at the time of writing (1990–2019).

### Averages and extremes

The average number of days with thunder heard in Oxford over the complete period of record (1828–2019) was 11.9 per annum, annual totals varying from zero in 1829 and 2 days in six other years (most recently 1990) to 28 days in 1925. In 1990, there was no thunder recorded until 16 October, and the annual total was the lowest since 1840. Extremes for the record as a whole are listed in Table 3. The three consecutive years 1924 to 1926 were extraordinarily thundery in Oxford (and elsewhere), each recording at least 25 days when thunder was heard. Two particularly thundery spells occurred in 1925 – 6–19 May (14 days, 7 with thunder) and 20–30 July (11 days, 6 with thunder),

Table 1

Oxford and Brize Norton thunder-day records and overlap periods.

Station and location	Period of thunder record	All period average, days	Average 1968–1986, days	Average 1987–2019, days
Oxford, Radcliffe Observatory 51.761°N, 1.264°W	1828–1986	12.0	11.1	–
Brize Norton 51.758°N, 1.576°W	1968–2019	10.3	11.1	9.9
Central Oxford 51.752°N, 1.258°W	1987–2019	10.5	–	10.5

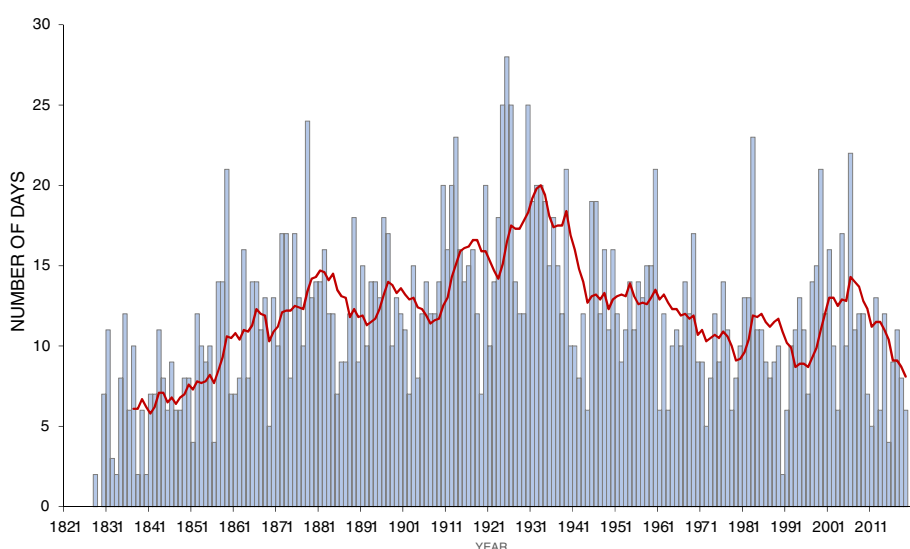


Figure 4. Annual totals of ‘thunder heard’, in days, in Oxford, 1828–2019, with 10-year running mean plotted at year ending: see text for sites and sources.

this routine has continued to the present day, notwithstanding the cessation of reporting of thunder and snowfall from 1987 onwards.

Records of thunder days are inconsistent in other ways. A day of thunder might include a

single weak peal or a day of heavy and prolonged thunderstorms. Background noise (aircraft, traffic, etc.) can make weak thunder difficult or impossible to hear – or may lead to false counts. In addition, records relate to the

<sup>2</sup>The figures quoted here differ slightly from those in *Oxford Weather and Climate since 1767* as additional records have come to light since publication; the data quoted in this paper should be regarded as a more complete set of averages.



**Table 2**

Monthly and annual averages of 'days with thunder heard' in Oxford, by decade 1831–1840 to 2001–2010 and 2010–2019, together with a selection of 30-year average periods including the current standard averaging period (1981–2010), the most recent 30-year period at the time of writing (1990–2019) and the entire dataset (192 years). Totals may differ slightly owing to rounding errors.

<b>Decadal averages</b>	Jan	Feb	Mar	Apr	May	June	July	Aug	Sept	Oct	Nov	Dec	Year	May–Aug	% annual
1831–1840	0.1	0	0.2	0.3	0.8	1.4	1.5	1.4	0.3	0.1	0	0.1	6.2	5.1	82
1841–1850	0.2	0.1	0.1	0.9	1.2	1.0	1.2	1.7	1.0	0.1	0	0.1	7.6	5.1	67
1851–1860	0	0.1	0	0.5	1.1	2.9	3.2	1.5	0.6	0.2	0	0.4	10.5	8.7	83
1861–1870	0.3	0.1	0.2	0.6	1.6	1.8	2.0	1.8	1.9	0.5	0.1	0	10.9	7.2	66
1871–1880	0.2	0	0.1	0.9	1.8	3.3	3.2	3.2	1.1	0.3	0.2	0	14.3	11.5	80
1881–1890	0	0	0	1.2	1.9	3.1	2.6	1.8	0.6	0.4	0.1	0.1	11.8	9.4	80
1891–1900	0	0	0.3	0.7	1.4	3.1	2.8	3.0	1.7	0.3	0.1	0.2	13.6	10.3	76
1901–1910	0.1	0.3	0.2	1.1	1.8	2.6	2.6	2.2	1.1	0.5	0	0	12.5	9.2	74
1911–190	0.3	0	0.6	1.0	3.1	2.5	3.5	2.9	0.7	1.2	0	0.1	15.9	12.0	75
1921–1930	0.1	0.3	0.5	1.5	4.3	1.8	3.7	3.1	1.7	0.5	0.3	0.5	18.3	12.9	70
1931–1940	0.3	0.2	0.3	1.1	2.6	3.4	3.9	2.3	1.6	1.0	0.1	0.1	16.9	12.2	72
1941–1950	0	0.1	0	1.0	2.9	2.1	3.0	2.1	1.2	0.2	0.3	0	12.9	10.1	78
1951–1960	0	0	0.1	0.5	2.1	2.3	3.0	3.0	1.1	0.8	0.4	0.2	13.5	10.4	77
1961–1970	0.2	0.2	0.2	0.9	2.5	1.8	2.6	1.5	0.4	0.2	0.2	0	10.7	8.4	79
1971–1980	0.2	0.1	0.4	0.4	1.3	1.8	1.6	1.9	1.0	0.3	0.1	0.1	9.2	6.6	72
1981–1990	0.3	0	0.5	0.7	1.8	1.6	2.2	2.1	0.8	0.4	0	0.5	10.9	7.7	71
1991–2000	0.2	0.3	0.1	1.1	1.9	1.4	2.5	2.5	1.5	0.4	0	0.1	12.0	8.3	69
2001–2010	0.2	0.2	0.4	0.7	2.2	1.6	2.4	3.0	1.0	0.5	0.1	0	12.3	9.2	75
2010–2019	0	0	0.4	0.8	1.6	1.2	1.5	1.6	0.6	0.4	0	0	8.1	5.9	73
<b>30 year averages</b>	Jan	Feb	Mar	Apr	May	June	July	Aug	Sept	Oct	Nov	Dec	Year	May–Aug	% annual
1831–1860	0.1	0.1	0.1	0.6	1.0	1.8	2.0	1.5	0.6	0.1	0	0.2	8.1	6.3	78
1861–1890	0.2	0.0	0.1	0.9	1.8	2.7	2.6	2.3	1.2	0.4	0.1	0.0	12.3	9.4	76
1901–1930	0.2	0.2	0.4	1.2	3.1	2.3	3.3	2.7	1.2	0.7	0.1	0.2	15.6	11.4	73
1931–1960	0.1	0.1	0.1	0.9	2.5	2.6	3.3	2.5	1.3	0.7	0.3	0.1	14.4	10.9	76
1961–1990	0.2	0.1	0.4	0.7	1.9	1.7	2.1	1.8	0.7	0.3	0.1	0.2	10.3	7.6	74
1971–2000	0.2	0.1	0.3	0.7	1.7	1.6	2.1	2.2	1.1	0.4	0.0	0.2	10.7	7.5	70
1981–2010	0.2	0.2	0.3	0.8	2.0	1.5	2.4	2.5	1.1	0.4	0.0	0.2	11.7	8.4	72
1990–2019	0.1	0.2	0.3	0.9	1.9	1.3	2.1	2.3	1.0	0.5	0.0	0.0	10.6	7.6	72
<b>Entire record, 192 years</b>	Jan	Feb	Mar	Apr	May	June	July	Aug	Sept	Oct	Nov	Dec	Year	May–Aug	% annual
1828–2019	0.1	0.1	0.2	0.8	2.0	2.1	2.6	2.2	1.0	0.4	0.1	0.1	11.9	8.9	75

although the longest spell of consecutive thundery days (period 1828 to 2019, excluding 1936–1970) occurred back in 1859, when thunder was noted on each of five consecutive days, 18–22 July. No thundery spell longer than three consecutive days has occurred since September 1976.

The majority of thundery activity in Oxford occurs during the summer half-year, the four months May to August accounting for around three-quarters of the annual number of days with thunder heard (with little variation across the near 200 years of record – Table 2). Thunderstorms are infrequent (averaging less than one per month using current averages) between September and April (Figure 5). Winter thunderstorms

(particularly November to February) tend to be short-lived and often originate from relatively shallow cumulonimbus, typically associated with narrow frontal rainbands on pronounced cold fronts, while spring storms (March and April) are often associated with showery cyclonic systems. Summer storms tend to be larger in area and depth, and to last longer. During the most recent 30-year period (1990–2019), August was, on average, the most thundery month, averaging 2.3 days with thunder heard, but during the decade 1921–1930, May averaged 4.3 days with thunder heard (Table 2). Notable amongst monthly records are 10 days with thunder heard in August 1878, and 9 days in four months, most

recently in August 2004 (Table 3). During the normally quieter months of the year, 6 days with thunder in April 1998 and 4 days in 10 with thunder in December 1989 are noteworthy.

### *Trends in thunderstorm occurrence*

The main features of Figure 4 and Table 2 are an irregular rise in annual frequency to the 1920s, resulting in an annual average of 20.0 days with thunder heard for the 10 years ending 1933. Since the 1920s and 1930s, very thundery years have become much less common, although in recent years, 1983 (24 days) and 2006 (22 days)

**Table 3***Extremes of thunder frequency in Oxford, 1828 to 2019.*

<b>Most thundery years</b>	28 days, 1925 25 days, 1924, 1926 and 1930 24 days, 1878 and 1983 23 days, 1913
<b>Least thundery years</b>	Nil, 1829 2 days, 1828, 1833, 1838, 1840 and 1990 3 days, 1832 and 1862 4 days, 1851, 1856, 1866 and 2015
<b>Most thundery months</b>	
10 days with thunder heard	August 1878
9 days	July 1925, May 1926, May 1945, August 2004
8 days	June 1883, May 1924, May 1925, July 1947, July 1965, May 1969
<i>The following are notable for particularly high thunder frequency during the normally quiet months:</i>	
6 days	April 1998
5 days	October 1913, April 1925, April 1948
4 days	April 1913, April 1934, October 1960, December 1989
<b>Longest consecutive runs of days with thunder (1828 to 2019 excluding 1936–1970)</b>	
5 days	18–22 July 1859
4 days	3–6 August 1878, 14–17 July 1880, 29 May–1 June 1894, 11–14 June 1900, 7–10 June 1910 <sup>a</sup> , 7–10 August 1912, 14–17 August 1915, 15–18 August 1916, 14–17 June 1920, 18–21 August 1924, 29 August–1 September 1934 and 24–27 September 1976

<sup>a</sup>This notably thundery spell was documented by Webb (2011). LWTs for the four days 7–10 June 1910 were E, SE, CSE and NE, respectively. The spell included, on 9 June, a very violent thunderstorm with hail at Wheatley, just east of Oxford, in which 132mm of rain fell, most of that in an hour, probably the most severe thunderstorm in the Oxford area during the period of record considered here.

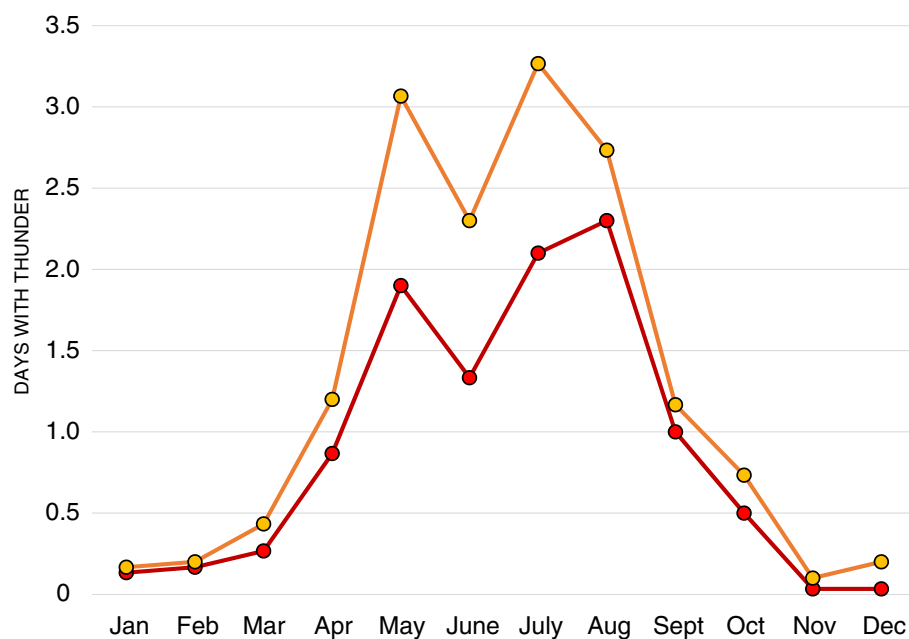


Figure 5. Monthly averages of days with thunder heard in Oxford. The red line shows the most recent 30-year period, 1990–2019 (annual average 10.6 days); the orange line is the average for the most thundery 30-year period 1901–1930 (annual average 15.6 days). See also Table 2.

oppose this trend. Instead, low annual totals have become much more frequent within the last two decades or so, with only 2 days with thunder in 1990 (the lowest annual total since 1840) and 4 days in 2015. The 10-year mean for the period 2010–2019 stands at just 8.1 days (Table 2), the lowest such value on Oxford's records since the

1860s. The possible reasons for this decline are discussed subsequently.

### Local and regional comparisons

There are no other single-location records of thunderstorm frequency of similar length to Oxford in southern England, and

comparisons must necessarily include overlapping records from several sites. A multi-site record for London extending back to 1713 was compiled by Mossman (1897), based mainly on the record from Greenwich (from 1814, Royal Observatory from 1841). An annual record of thunder days exists for Kew Observatory in west London, 73km southeast of the Radcliffe Observatory, from 1877 (Bishop 1947) until the Observatory's closure in December 1980; monthly totals for 1884–1980 were published in the *Monthly Weather Report (MWR)*. Webb (2016) examined decadal trends of thunder frequency using composite records at eight UK sites during the twentieth century, including Kew. Kew Observatory was the Met Office's 'central observatory' for most of this period, with hourly observations made between 0600 and 2100 GMT daily (Galvin, 2003). To extend the 'west London' thunder record since Kew's closure, in this analysis observations from London's Heathrow Airport (10km west of Kew Observatory) and RAF Northolt (12km northwest of Kew Observatory) were used, and averages for overlapping periods calculated (Table 4). Note, however, that Northolt does not maintain 24 × 7 observational coverage, particularly at weekends, and the totals may therefore be slightly low.

The difference in mean annual days of thunder between Kew and Heathrow over the 32-year overlap period 1949–1980 (17.8 vs 14.4 days per annum) is surprisingly large for two permanently manned sites



**Table 4**

'West London' thunder-day records and overlap periods.

Station	Period of thunder record	All period average, days	Average 1949–1980, days	Average 1984–2005, days
Kew Observatory 51.468°N, 0.314°W	1877–1980	15.1	17.8	–
London Heathrow 51.479°N, 0.449°W	1949–2005	14.9	14.4	14.9
RAF Northolt 51.548°N, 0.415°W	1984–2019	12.3	–	14.4

### Lamb Weather Types (LWT)

Hubert Lamb classified the daily synoptic situation over the British Isles from 1861 to February 1997, originally in *Geophysical Memoir 116* (Lamb, 1972). Lamb's original subjective classifications were later objectively reassessed using daily (1200 UTC) grid-point mean sea-level pressure data from reanalysis datasets extending back to 1871 (Jones *et al.*, 2013). The Lamb Weather Types consist of cyclonic (C) and anticyclonic (A) features within the gridded area, together with directional variants – northeasterly (NE) and easterly (E) clockwise through to northerly (N), each with their cyclonic and anticyclonic variants, such that LWT SE represents a southeasterly flow, CSE a cyclonic southeasterly, ASE an anticyclonic southeasterly and so forth. An additional 'unclassifiable' (unc) category is also included for complex or fluid situations. Daily objective UK-centred LWTs are available, only a few days in arrears, courtesy of the Climatic Research Unit, University of East Anglia at <https://crudata.uea.ac.uk/cru/data/lwt/>.

just 10km apart. Differences were unexpectedly high in some years: in 1956, for example, Kew reported 24 days with thunder, Heathrow just 13. The reasons behind these differences remain unclear, whether it be due to a greater background noise level from traffic and aircraft movements at Heathrow, or simply greater vigilance at Kew, but the lack of homogeneity in the series should be noted.

## Characteristics of thunderstorms in Oxford

### Synoptic classification

The Lamb Weather Type (LWT; Jones *et al.*, 2013: see Box) was used to identify the broad-scale synoptic weather pattern for each date on which thunder was heard on the composite Oxford record from 1871 (the first year of the reanalysis dataset upon which the objective LWTs are based), excluding only the years 1936–1970 for which thunder dates were not available. Frequency tables for all LWTs were tabulated for 'thunder days' and all remaining days ('non-thunder days') (Table 5). LWT profiles for 'thunder days' were compared with all 'non-thunder' days in the same analysis period, separately for 'winter' (November to February, just 3.5% of thunder days, Figure 6(a)) and 'summer' (May to August, 75% of thunder days, Figure 6(b)). By their very nature, LWTs provide only a broad-brush picture of the surface synoptic cir-

ulation across the British Isles, and two days with the same classification will inevitably show differences in detail at local or regional scales. Some latitude is therefore necessary in interpreting categorisation of local phenomena by synoptic scale, although for at least those LWTs with reasonable sample sizes, conclusions drawn appear consistent.

It comes as no surprise that Cyclonic (C) weather types dominate thunder days in both seasons, overwhelmingly so in winter – LWT C type accounting for 53% of all thunder days (30 of 57), compared to 13% of non-thunder days (Figure 6(a)). Cyclonic southwesterly CSW, cyclonic westerly CW and cyclonic northwesterly CNW types are similarly over-weighted compared to non-thunder days, although the sample of winter thunderstorms is so small (57 thunder days in total, four in December 1989 alone) that the analysis becomes sensitive to individual events. The broad picture for the winter months is of infrequent short-duration thunderstorms linked with the passage of active cyclonic centres and associated active cold fronts. In contrast, non-cyclonic thunder days occurring in southerly S, southwesterly SW and northwesterly NW LWTs are under-represented by one-third or more in comparison with non-thunder days.

For the summer months, Cyclonic (C) LWTs also accounted for the greatest single category of thunder days – 325 of the 1098 thunder days during the summer months (May to August, just under 30% (Figure 6(b)), a little over twice the C frequency of non-

thunder days. Perhaps surprisingly, the Anticyclonic (A) LWT saw the second-highest frequency of thunder days with individual weather types, with 99 (9%), suggestive of local convective outbreaks on the periphery of an anticyclone. Southeasterly weather types (SE and CSE) are also strongly linked to thundery conditions in Oxford, again suggesting association with Spanish plume events and/or declining hot spells. Of the cyclonic LWTs, cyclonic northerly CN, cyclonic northeasterly CNE and cyclonic easterly CE, as well as CSE, represent an increased likelihood of thunder: storms are relatively less likely in cyclonic southerly CS, cyclonic southwesterly CSW and cyclonic westerly CW situations. Provided the airflow is fairly slack, the relatively long land track of the surface winds in cyclonic CN, CNE or CE situations makes the Oxford area a favourite location for higher day temperatures, helping to increase the likelihood of thunder in favourable conditions. Situations where there is a warm east or northeasterly surface wind, coupled with a veer with height to a broadly southerly mid-level flow, are especially favourable for severe thunderstorms in the area; if the 500hPa flow is relatively light, storm initiation tends to occur over the downlands to the south. Such events in recent years include 24 May 1989, 17 May 1997, 19 May 1999, 3 August 2004 and 29 June 2005. The 1999 and 2004 events occurred in an LWT 'unclassified' situation: by their very nature, unclassified days are likely to be occasions of slack pressure (including classic col situations) and thus favourable days for local convergence zones to develop in the summer (see Figure 6(b)).

In non-cyclonic synoptic situations, LWTs easterly E, southeasterly SE and northerly N are relatively more likely to see thunderstorms in Oxford, and southerly S, southwesterly SW, westerly W and northwesterly NW less likely, particularly SW where that particular LWT accounts for 8.0% of non-thunder days but only 2.6% of thunder days. In such situations, with a surface wind between south and west, the highest temperatures tend to be well to the northeast of Oxford, towards The Wash or East Anglia, and cumulonimbus clouds are often in the developing stage over Oxfordshire with thunder breaking out only as they drift further northeast.

### Relationship with summer maximum temperatures

There remains a strong belief that summer thunderstorms in the south and east of England are most often associated with hot weather, whether resulting from local surface instability during a heatwave or in a more widespread thundery breakdown following a hot spell. To examine the veracity of this belief, a further analysis examined maximum temperatures recorded on thun-

**Table 5**

*Frequencies of Lamb Weather Types (LWTs) for days with and without thunder heard at Oxford, period 1871–2019 excluding 1936–1970, for all months and for the peak thundery months May to August only. Counts and percentage frequency are given within each LWT, together with the ratio of thunder to non-thunder days within each LWT.*

<b>All months</b>	unc	A	ANE	AE	ASE	AS	ASW	AW	ANW	AN	E	SE	S	SW	W	NW	N	C	CNE	CE	CSE	CS	CSW	CW	CNW	CN	Total	
<b>Counts</b>																												
Non-thunder	385	8383	332	425	471	639	1106	1298	738	461	699	735	1206	2312	3916	3747	1959	5414	247	235	369	810	995	901	627	439	40155	
Thunder	53	111	11	11	24	12	14	9	8	7	39	60	110	50	35	48	46	472	29	28	43	37	38	26	40	43	1482	
Total	438	8494	343	436	495	651	1120	1307	746	468	738	795	1316	2362	3951	3795	2005	5886	276	263	412	847	1033	927	667	482	41637	
<b>% by LWT</b>																												
Non-thunder	1.0	20.9	0.8	1.1	1.2	1.6	2.8	3.2	1.8	1.1	1.7	1.8	3.0	5.8	9.8	9.3	4.9	3.3	0.6	0.6	0.9	2.0	2.5	2.2	1.6	1.1	100.0	
Thunder	3.6	7.5	0.7	0.7	1.6	0.8	0.9	0.6	0.5	0.5	2.6	4.0	7.4	3.4	2.4	3.2	3.1	5.3	2.0	1.9	2.9	2.5	2.6	1.8	2.7	2.9	100.0	
Ratio thunder: non-thunder	3.73	0.36	0.90	0.70	1.38	0.51	0.34	0.19	0.29	0.41	1.51	2.21	2.47	0.59	0.24	0.35	0.64	1.62	3.18	3.23	3.16	1.24	1.03	0.78	1.73	2.65		
<b>May to August only</b>	unc	A	ANE	AE	ASE	AS	ASW	AW	ANW	AN	E	SE	S	SW	W	NW	N	C	CNE	CE	CSE	CS	CSW	CW	CNW	CN	Total	
<b>Counts</b>																												
Non-thunder	238	3096	112	157	139	200	302	377	256	176	224	245	365	598	1031	1023	631	405	1855	96	78	121	255	312	267	218	147	12924
Thunder	45	99	7	11	21	10	10	6	6	6	27	46	87	38	28	27	32	56	325	19	23	36	22	25	17	34	35	1098
Total	283	3195	119	168	160	210	312	383	262	182	251	291	452	636	1059	1050	663	461	2180	115	101	157	277	337	284	252	182	14022
<b>% by LWT</b>																												
Non-thunder	1.8	24.0	0.9	1.2	1.1	1.5	2.3	2.9	2.0	1.4	1.7	1.9	2.8	4.6	8.0	7.9	4.9	3.1	14.4	0.7	0.6	0.9	2.0	2.4	2.1	1.7	1.1	100.0
Thunder	4.1	9.0	0.6	1.0	1.9	0.9	0.9	0.5	0.5	0.5	2.5	4.2	7.9	3.5	2.6	2.5	2.9	5.1	29.6	1.7	2.1	3.3	2.0	2.3	1.5	3.1	3.2	100.0
Ratio thunder: non-thunder	2.23	0.38	0.74	0.82	1.78	0.59	0.39	0.19	0.28	0.40	1.42	2.21	2.81	0.75	0.32	0.31	0.60	1.63	2.06	2.33	3.47	3.50	1.02	0.94	0.75	1.84	2.80	

der and non-thunder days during the entire period for which thunder dates were available (157 years 1828–2019, excluding 1936 to

1970). It should be borne in mind, however, that the reported maximum temperature (referring to the 24-hour period com-

mencing 0900 GMT/UTC for the majority of Oxford's record) may not coincide with the time when the thunderstorm occurred: for example, an overnight storm (between midnight and the morning observation) and the afternoon's maximum temperature would both be credited to the same date, although a significant change of air mass may have taken place between the two events.

For every month except August, median maximum temperatures on days with thunder are very slightly higher than on non-thunder days, but outside the winter months, the differences are slight (Table 6). The difference between the two is greatest during the months of December, January and February, when it exceeds 2°C, although it should be noted that sample sizes are very small outside of the summer peak period. Higher temperatures and reduced variation on days when winter thunderstorms were recorded tend to confirm the hypothesis above that winter thunderstorms in Oxford are most likely to occur in mild, unsettled cyclonic conditions, often associated with sharp cold frontal boundaries.

For the summer months May to August, representing around 75% of all thunderstorm days, the boxplots in Figure 7 show the median, interquartile range and extremes of daily maximum temperature for both thunder and non-thunder days. Although both the median (19.8°C non-thunder, 20.3°C thunder days) and the upper quartile (22.4°C vs 23.4°C, respectively) are slightly higher on thunder days, the two groups are statistically indistinguishable. Repeating the analysis using the highest maximum temperature within the previous three days produced a very similar result. The association with summer heatwaves is thus shown to be slight. There may be a greater degree

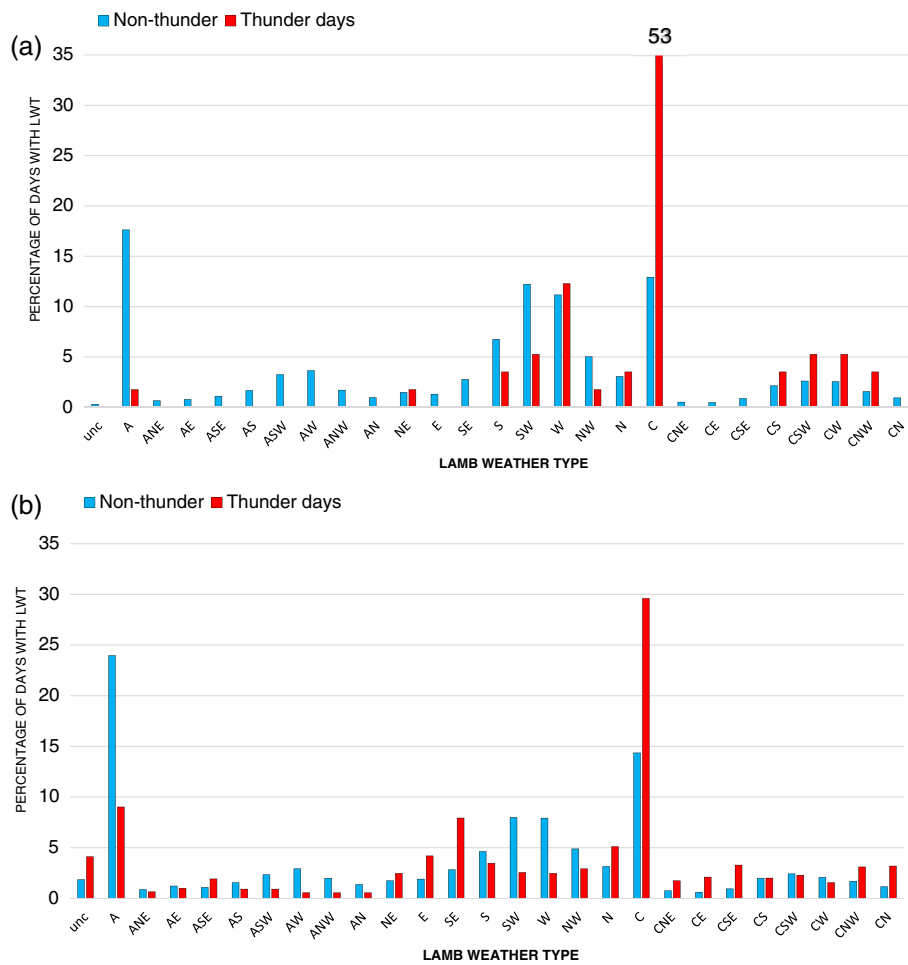


Figure 6. Distribution (percentage of dates) of Lamb Weather Types (LWT) for dates with and without thunder (red and blue columns, respectively) at Oxford, 1871–2019 excluding 1936–1970. Upper plot (a) is for November to February; lower plot (b) is for May to August. The scale is the same on both plots. For LWT details, see text.

Table 6

Comparison of mean maximum temperatures (°C) by month at Oxford on days with and without thunder heard, and the difference, including sample sizes. Period 1828–2019, excluding 1936–1970 – 157 years in total.

Month	Mean maximum temperature °C				Number of days		
	All days	No thunder (noT)	Thunder (T)	T minus noT	No thunder	Thunder	Total
January	6.6	6.5	9.0	2.4	4846	21	4867
February	7.4	7.4	10.4	3.0	4419	15	4434
March	9.9	9.9	10.5	0.6	4828	39	4867
April	13.1	13.1	13.9	0.8	4578	132	4710
May	16.7	16.7	18.3	1.6	4574	293	4867
June	19.9	20.0	20.6	0.6	4380	330	4710
July	21.8	21.7	22.4	0.7	4487	380	4867
August	21.2	21.2	21.2	0.0	4525	342	4867
September	18.4	18.4	18.7	0.3	4547	163	4710
October	14.0	14.1	14.9	0.8	4802	65	4867
November	9.6	9.6	11.6	1.9	4699	11	4710
December	7.3	7.2	10.7	3.4	4843	24	4867
					55 528	1815	57 343

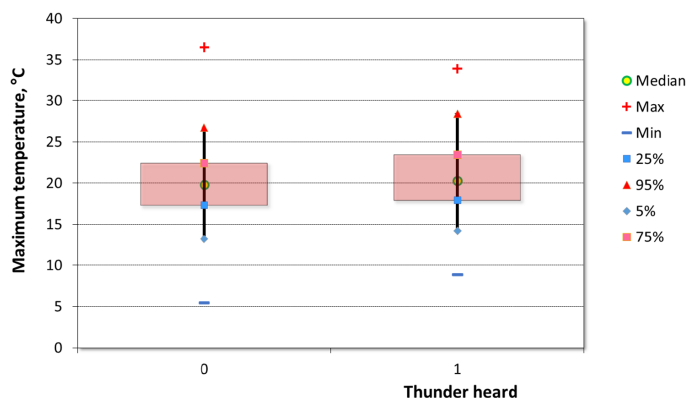


Figure 7. Box-and-whisker plots comparing the distribution of daily maximum temperatures on dates without and with thunder heard (left and right plots, respectively) at Oxford, May to August 1829–2019 excluding 1936–1970. The plotted variables are (from top) maximum value, 95th percentile, 75th percentile (upper box boundary), median (green circle), 25th percentile (lower box boundary), 5th percentile, minimum value.

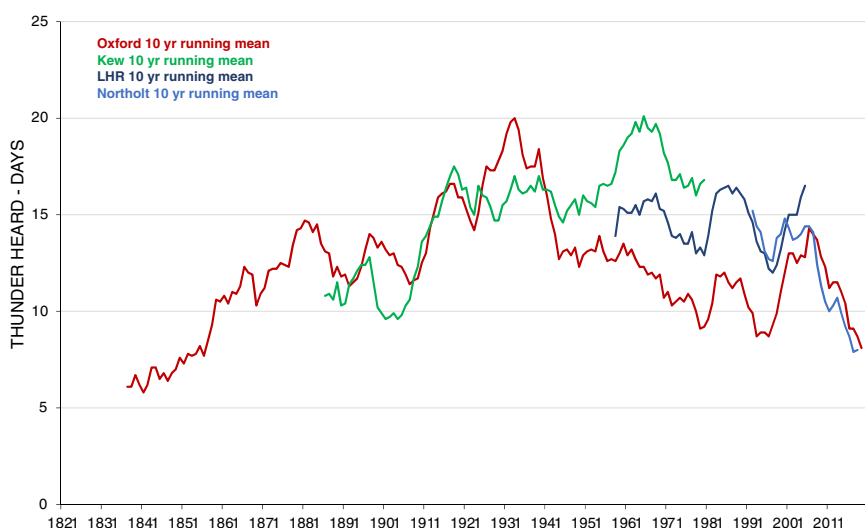


Figure 8. Ten-year running means of thunderstorm frequency (plotted at year ending) for Oxford (dark red line) 1828–2019, alongside similar averages for sites in west London – Kew Observatory (1877–1980, green line), Heathrow Airport (LHR, 1949–2005, dark blue line) and Northolt (1984–2019, light blue line).

of relationship between summer maximum temperatures and heavy or severe thunderstorms, but sample sizes are too small to allow reliable statistical analysis.

## The recent decline in thunderstorm frequency

Figure 8 shows the 10-year running means (plotted at year ending) for Oxford from the commencement of the record in 1828, together with those for Kew Observatory (1877–1980), Heathrow (1949–2005) and Northolt (since 1984). Since at least the 1880s, the peaks and troughs (if not always the relative amplitudes) of decadal thunderstorm incidence in London and Oxford largely coincide, indicative of broader synoptic-scale influence rather than more local factors, although there is a suggestion that thunderstorm frequency in west London has not fallen as far since the peak seen in the Oxford record in the 1920s/1930s. The

possible reasons for this are beyond the scope of this article, but stability changes in the boundary layer and/or urban heat island resulting from extensive urban growth in west London since that time may be involved. There is also an apparent periodicity in the peak years of around 20 years, traceable throughout the record.

Although the thunderstorm record from Oxford is unlikely to be statistically homogeneous throughout the near-200 year series, for reasons already stated, Table 2 and Figures 4, 5 and 8 confirm that the most recent decade has seen a marked reduction in thunderstorm frequency. There is also evidence of an irregular but longer-term decline since the 1960s. Can the decline in frequency be explained, at least in part, by a decline in the frequency of synoptic situations conducive to summertime thundery outbreaks?

If changes in synoptic type over decadal scales are a factor in the observed decline,

we might expect a decrease in conducive or ‘positive’ synoptic conditions and/or an increase in less conducive or ‘negative’ situations. Accordingly, Table 7 and Figure 9 examine the monthly mean frequency of each LWT (pro-rata for a 31 day month) for May to August over 1901–1930, the 30-year period with the greatest mean thunder frequency in Oxford, together with the equivalent data for the most recent 30-year period 1990–2019 (from Table 2).

Comparing the two periods graphically (Figure 9), it can be seen firstly that certain LWTs occurred considerably more frequently than normal during the most thundery months (blue columns – examples C, SE and CSE), and secondly that many of these LWTs occurred less frequently in the last 30 years (red columns) than during 1901–1930 (orange columns).

For a quantitative comparison, the ratios of LWT frequency between thunder days and non-thunder days during May to August (Table 5) were rearranged in Table 7, ranked by the ratio of each LWT, from ‘most conducive’ (greatest relative frequency of thunder days) to ‘least conducive’ (lowest relative frequency of thunder days). For example, the cyclonic southeasterly CSE LWT is 3.5 times more abundant for thunder days than non-thunder days, whereas the anticyclonic westerly AW type is less than one-fifth as common (ratio 0.19). The two 30-year periods were then compared and differences evaluated. Comparing 1990–2019 with 1901–1930, the sum of the difference in ‘conductive’ LWTs (ratio > 0, indicative of an increased frequency of thunder in those synoptic situations) is –0.91 days, and the equivalent for ‘least conducive’ LWTs (ratio < 0) is 0.85 days, suggesting a potential net reduction in conducive thundery synoptic situations between May to August of 1.76 days per 31 day month (–0.91 – 0.85), grossing up to 7.0 days across the four months (123 days). From Table 2, it can be seen that the average frequency of thunder between May and August in Oxford has fallen from 11.4 days in 1901–1930 to 7.6 days in the most recent 30-year period, a reduction of 3.8 days or 34%. Although almost certainly not the only reason for the decline, this analysis is of the right order and suggests that the recent reduction in thunderstorm frequency in Oxford, and by extension a wide area of southern England, can be partly attributed to reductions in the frequency of conducive synoptic environments.

## Summary and conclusions

The long record of ‘days with thunder heard’ in Oxford, commencing in January 1828, is described. Thunder is heard, on average over the entire period of record, on 11.9 days per annum: typically three-quar-

**Table 7**

Ranked relative frequency of Oxford thunder days to non-thunder days by Lamb Weather Type (LWT), for the peak thundery months May to August only, period 1871 to 2019 excluding 1936–1970. From Table 5, the synoptic types more or less conducive to thunder in Oxford are identified, and compared with LWT frequency over the (most thundery) 30-year period 1901–1930 and the (less thundery) most recent 30 years 1990–2019, with the differences between the two shown.

Lamb Weather Type	Non-thunder days %	Thunder days %	Ratio thunder: non-thunder		LWT frequency 1901–1930, days	LWT frequency 1990–2019, days	Days change 1990–2019 versus 1901–1930
CSE	0.9	3.3	3.50	MORE CONDUCTIVE TO THUNDER	0.34	0.27	–0.07
CE	0.6	2.1	3.47		0.28	0.18	–0.10
SE	2.8	7.9	2.81		1.06	0.91	–0.15
CN	1.1	3.2	2.80		0.45	0.40	–0.05
CNE	0.7	1.7	2.33		0.23	0.20	–0.03
Unclassified	1.8	4.1	2.23		0.54	0.70	0.16
E	1.9	4.2	2.21		0.70	0.63	–0.07
C	14.4	29.6	2.06		5.01	4.70	–0.31
CNW	1.7	3.1	1.84		0.65	0.61	–0.04
ASE	1.1	1.9	1.78		0.26	0.40	0.14
N	3.1	5.1	1.63	1.21	0.98	–0.23	
NE	1.7	2.5	1.42	0.63	0.50	–0.13	
CS	2.0	2.0	1.02	0.55	0.52	–0.03	
CSW	2.4	2.3	0.94	LESS CONDUCTIVE TO THUNDER	0.71	0.72	0.01
AE	1.2	1.0	0.82		0.33	0.34	0.01
CW	2.1	1.5	0.75		0.60	0.76	0.16
S	4.6	3.5	0.75		1.46	1.24	–0.22
ANE	0.9	0.6	0.74		0.22	0.20	–0.02
NW	4.9	2.9	0.60		1.45	1.76	0.31
AS	1.5	0.9	0.59		0.40	0.50	0.10
AN	1.4	0.5	0.40		0.45	0.37	–0.08
ASW	2.3	0.9	0.39		0.60	0.63	0.03
A	24.0	9.0	0.38		6.78	6.84	0.06
SW	8.0	2.6	0.32		2.39	2.49	0.10
W	7.9	2.5	0.31		2.30	2.64	0.34
ANW	2.0	0.5	0.28		0.53	0.58	0.05
AW	2.9	0.5	0.19		0.90	0.90	0.00
Totals					31.0	31.0	
Total CONDUCTIVE influence							–0.91 days per month
Total LESS CONDUCTIVE influence							0.85 days per month

ters of these occur in the four months from May to August. The record is examined in terms of the links with particular synoptic types and the day's maximum temperature. Contrary perhaps to popular belief, there is little evidence of a clear relationship between thunder occurrence and high temperatures during the summer months: the incidence of certain weather types, particularly southeasterly variants often indicative of Spanish plume events, is of greater predictive value. By extension and comparison with long multi-site thunder records from London, this synoptic scale relationship is likely to hold over much of

inland southern England. The frequency of thunder in Oxford has declined considerably in the last decade or so, such that the average for the most recent 10-year period 2010–2019 (8.1 days per annum) is the lowest such value in almost 150 years. Although probably not the sole cause of the observed reduction in frequency of thunderstorms in recent decades, a demonstrable decline in synoptic weather types conducive to thunderstorm development in southern England is of the right order to account for the reduction and involves plausible synoptic-scale mechanisms. However, there remains considerable vari-

ability between individual synoptic events and from year-to-year.

## Acknowledgements

Grateful thanks are due to Jonathan Webb for allowing me access to his 33-year personal record of Oxford thunderstorms. I am also grateful to Jonathan, my colleague Mathew Owens and Tim Burt for helpful comments on an earlier draft of this paper. Tim Burt also helped scan the early manuscript Oxford records and jointly review them to extract thunderstorm observations.



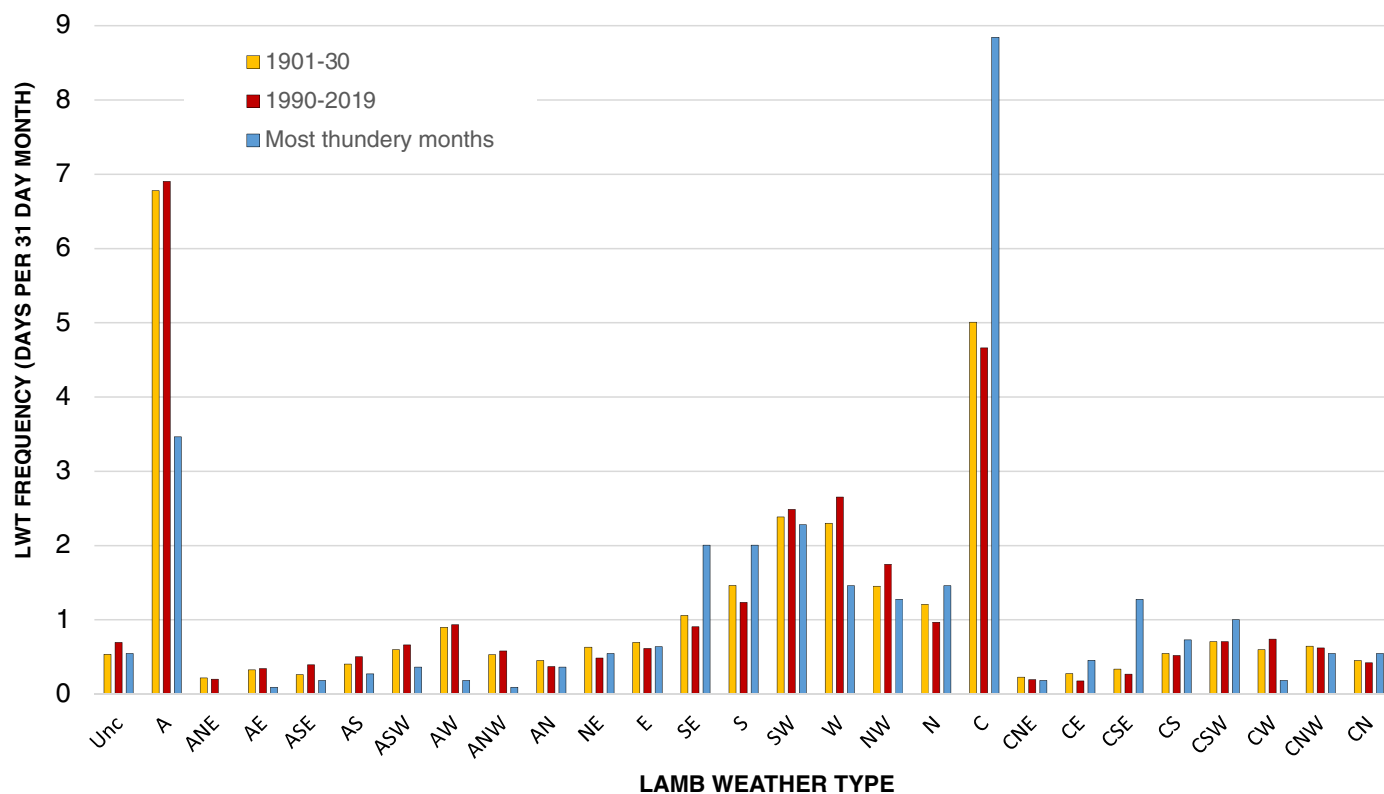


Figure 9. Comparison of LWT frequencies (days in a nominal 31 day month) for May to August 1901–1930 (orange columns) and 1990–2019 (red columns), together with those for the most thundery months on record in Oxford (8 days with thunder or more) listed in Table 3 (blue columns).

## The Oxford Radcliffe Observatory thunder datasets

Two datasets have been placed on Figshare (<https://www.doi.org/10.6084/m9.figshare.13347512.v1>). **Dataset 1** contains the dates upon which thunder was heard in Oxford, January 1828 to December 2019, but note there are no records by date between 1936 and 1970 at present - these will be added post-publication once access to the Met Office archives has been restored.

**Dataset 2** contains monthly and annual totals of the number of days with thunder heard in Oxford, January 1828 to December 2019. This includes monthly totals from 1936 to 1970, and the series is believed complete.

If using either dataset, please include a citation to this paper.

## References

- Burt S, Burt T.** 2019. *Oxford Weather and Climate since 1767*. Oxford University Press: Oxford, UK, 544 p.
- Galvin JFP.** 2003. Kew Observatory. *Weather* **58**: 478–484.
- Jones PD, Harpham C, Briffa KR.** 2013. Lamb weather types derived from reanalysis products. *Int. J. Climatol.* **33**: 1129–1139.
- Lamb HH.** 1972. *British Isles Weather Types and a Register of Daily Sequence of Circulation Patterns, 1861–1971*. Met Office Geophysical Memoir 116. HMSO: London.
- Massey FJ.** 1951. The Kolmogorov-Smirnov test for goodness of fit. *J. Am. Stat. Assoc.* **46**: 68–78.
- Mossman RC.** 1897. The non-instrumental meteorology of London, 1713–1896. *Q. J. R. Meteorol. Soc.* **23**: 287–298.
- Valdivieso M, Owens MJ, Scott CJ et al.** 2019. Thunderstorm occurrence at ten

sites across Great Britain over 1884–1993. *Geosci. Data J.* **6**: 222–233.

**Webb JDC.** 2011. Violent thunderstorms in the Thames Valley and south Midlands in early June 1910. *Weather* **66**: 153–155.

**Webb JDC.** 2016. Decadal trends of thunder in Britain, 1890–2009. *Int. J. Meteorol.* **41**: 88–97.

Correspondence to: Stephen Burt  
s.d.burt@reading.ac.uk

Copyright © Stephen Burt. All rights reserved.

© 2021 Stephen Burt. Weather published by John Wiley & Sons Ltd on behalf of the Royal Meteorological Society

This is an open access article under the terms of the Creative Commons Attribution License, which permits use, distribution and reproduction in any medium, provided the original work is properly cited.

doi: 10.1002/wea.3884





# Paper 6

## **Durham's barometric pressure records, 1843-1960.**

Appendix 5 in *Durham Weather and Climate since 1841* by Tim Burt and Stephen Burt.  
Oxford University Press (in press, to be published spring 2022).

*Bibliography # 2. Word count 6800 approx. excluding references and tables*

A slightly abbreviated version of this chapter has been accepted for a Special Issue of *Geoscience Data Journal*, on **Locating, Imaging and Digitizing Historic Geoscience Data**, to be published in October 2021. This version includes amendments following peer review of the *GDJ* paper, and was updated on 27 June 2021.

The online version of the Durham barometric pressure dataset was published in April 2021 and can be found at <http://dx.doi.org/10.17864/1947.295>.

---

*This is a draft of a chapter that has been accepted for publication by  
Oxford University Press in the forthcoming book detailed above.*

*OUP Author Reuse and Self-Archiving site licensing details:*

<https://global.oup.com/academic/rights/permissions/autperm/?cc=gb&lang=en&>



## **Appendix 5 | Durham's barometric pressure records, 1843 to 1960**

---

### **Summary**

A twice-daily record of barometric pressure exists for Durham Observatory (54.768 °N, 1.584 °W, barometer cistern 107.3 m above mean sea level, MSL) from 23 July 1843 to 31 December 1960. The record, which is 98.7% complete, is by far the longest digital barometric pressure series in northern England, and fills a very large temporal and spatial gap in the International Surface Pressure Database (ISPD: (Cram et al. 2015) ). In what is believed to be the first study of its kind, the record has been independently quality-controlled against the NOAA–CIRES–DOE Twentieth Century Reanalysis version 3, 20CRv3 (Slivinski et al. 2021; Slivinski et al. 2019), which did not include the Durham records in its assimilation set.

This Appendix describes the instruments used and their exposure, the sources of the record, digitisation work undertaken to generate the digital time series (including quality control assessments using 20CRv3), reduction to mean sea level pressure from station level observations, and examines consistency over the period of record against 20CRv3, concluding with a summary of monthly and annual means and extremes over the 117 year series and the details of the new dataset.

Throughout the chapter, the terms millibar (mbar) and hectopascal (hPa) are used interchangeably. For consistency with original sources, the millibar unit has been retained where appropriate.

A slightly condensed version of this Appendix has been accepted for publication in *Geoscience Data Journal*, October 2021 (Burt 2021).

### **Instruments and exposure**

Astronomical observatories such as Durham required observations of barometric pressure and external air temperature to correct star positions for atmospheric refraction (Burt and Burt 2019), and for this purpose high-quality instruments were usually procured from reputable manufacturers. Information on the barometers used, their calibrations and their exposure within Durham Observatory, has been assembled from

original archival records held in Durham University Library together with previously restricted Met Office site inspection reports and correspondence held in the Met Office Library and Archives in Exeter.

The earliest details we have of Durham's barometer are from the monthly climatological return to the Met Office for January 1877, when the barometer's serial number (209) was first stated. The earliest surviving Met Office site inspection record for Durham Observatory, for September 1902, adds the detail that barometer 209 was a Fortin-pattern instrument made by Browning. Brownings were a long-established optician and scientific instrument-maker, trading in London from the early 19th century; Brownings' shop has been suggested as Charles Dickens' model for that of Solomon Gills in *Dombey and Son* (Meliconi 2004). John Browning took over from his father William in 1865 and the business advertised itself as 'Optical and physical instrument-maker to Her Majesty's Government, the Royal Observatory [Greenwich] and Kew Observatory' (Banfield 1991).

At this distance in time, it is impossible to state with certainty whether the Browning barometer noted as being in use in 1877 and 1902 was the original station barometer in use when the Observatory opened in 1840/41, but it is certainly possible; it is equally possible that the Browning barometer replaced an earlier instrument in June 1867, as a very brief comment ('New barometer installed') appears in the observations register at that time, although no equipment receipts or other metadata confirming a possible change of instrument have yet been found (Durham University Library 2016).

Although there were occasional temporary substitutions by other instruments as detailed subsequently, this barometer remained in use between at least January 1877 and termination of the record in December 1960.

In 1910, and probably earlier, the barometer was located at the side of the eastern window on the first floor of the Observatory (Met Office inspection report, 1910) – **Figure A4.1**. The height of the barometer cistern above MSL was stated as 352 ft or 107.3 m throughout the record. Thereafter, only minor relocations of the instrument took place.

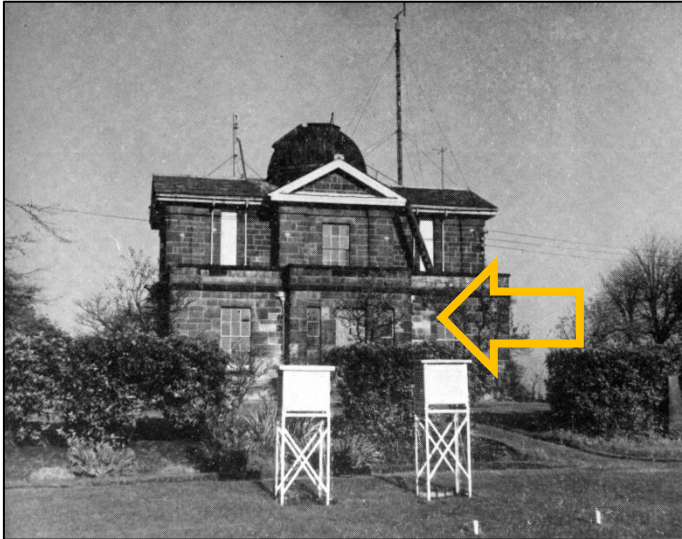


*Figure A4.1 Durham Observatory, photographed in 1955. The observatory's barometer was located behind the eastern window (arrowed).*

*ARTWORK FILE DHM 001*

Until 1949, the barometer was checked against a standard mercury barometer carried by the Met Office inspector at every visit (conducted at typically 2-3 year intervals); errors were found to be small, within  $\pm 0.1$  or  $0.2$  hPa.

From the beginning of the record the observed ('As Read') barometer readings, in inches of mercury, at the morning and evening observation hours are given in the original registers, together with the barometer temperature (the 'Attached Thermometer'), the latter in degrees Celsius to March 1867, thereafter in Fahrenheit until November 1948, after which the 'Att. Therm' entry was omitted from the registers. The 'corrected' reading of the barometer (here referring to correction for the thermal expansion of the mercury column from room temperature to the standard  $0^{\circ}\text{C}$ , rather than the correction to MSL pressure), usually referred to as the 'station level pressure', is also included in the observation registers until November 1948. This correction was made by reference to a local table, not always accurately, and for consistency during the preparation of the series the correction to  $0^{\circ}\text{C}$  was recalculated using the observed Attached Thermometer reading, in preparation for reducing the 'station level pressure' so obtained to 'mean sea level pressure' (as documented below). The 1910 inspection report noted that a minor index correction from the Browning barometer's calibration at

Kew Observatory was included in the table used within the observatory to reduce the barometer reading to 0 °C, and the recalculation of ‘station level’ pressures adopted here will therefore not include this. However, the barometer was recertified on 14 January 1925 following minor cleaning and repair work, after which the corrections applied were all noted as 0.1 hPa or less across the working range of the instrument (1926 inspection report). The effect of the omission of the corrections is therefore probably insignificant.

From early 1948 the barometer readings appear to have given cause for concern, because the mean 0900 and 2100 GMT MSL pressures were not published in the *Monthly Weather Report* after February 1948. It is probably no coincidence that the Browning Fortin barometer was removed for cleaning and repair (by Negretti & Zambra) in December 1948. A Kew pattern barometer, on loan from the Met Office, was read in its place until 31 August 1949 (September 1949 inspection report refers). This barometer was graduated and read in millibars.

The original Browning Fortin barometer returned to Durham in September 1949 and remained in use until the cessation of the record on 31 December 1960, except for the five months 28 August 1957 to 28 February 1958 when it was again away for cleaning. Records during this period were from a temperature-compensated aneroid barometer on loan from the Met Office, and accordingly there are no ‘Attached Thermometer’ readings. The Fortin barometer was recertified by Negretti & Zambra on 5 February 1958 and brought back into use from 1 March 1958.

From September 1949 the barometer readings in the register continue in millibars, suggesting that the Fortin barometer had been refitted with a new scale during its cleaning and repair. The barometer at this date was at least 80 years old, and quite possibly over 100. The reading of the Attached Thermometer was omitted from the observation register from this point, as examined in more detail subsequently.

Unfortunately, there is no record of what happened to the Browning Fortin barometer following the discontinuation of readings in December 1960, and its current whereabouts are unknown.

A Short & Mason open scale barograph was installed in December 1947, on loan from the Met Office, although no chart records from this instrument have survived.

## Instrumental record summary

### OBSERVATION HOURS

From the commencement of record until September 1885, hours were reckoned by local or ‘common’ time, about 6 minutes later than the Greenwich Meridian, but from October 1885 onwards Greenwich Mean Time (GMT) was adopted as the observatory’s standard time. The barometer readings were noted for the majority of the period of record at 09h and 21h daily, the exceptions being as follows:

#### Morning observation:

- At 10h, February 1855 to September 1885
- At 09h Summer Time (07h GMT) during operation of Summer Time, 1916-1918
- At 09h Summer Time (08h GMT) during operation of Summer Time, April to September 1945 (letter in site file, Met Office Archives, dated 30 September 1945)

#### Evening observation:

- No evening observations were made between February 1855 and June 1858; instead, a 14h observation was made during this period
- At 22h, July 1858 to September 1885

Occasional observations at other ‘non-standard’ times such as 2140h have been assumed to be ‘late observations’ from the intended hour and simply included without adjustment along with the other observations for the ‘standard’ hour.

### MISSING DATA

The record is remarkably complete; for the period July 1843 to December 1960, 117 years, 98.7% of observations appear in the database. The main gaps (four or more consecutive missing observations) are shown in [Table A5.1](#).



**Table A5.1** Missing data in the Durham Observatory pressure series, July 1843 to December 1960

<i>Period missing</i>	<i>No. of days</i>	<i>Period missing</i>	<i>No. of days</i>
4-8 August 1845	5	24-31 Dec 1883	8
1 July – 14 Aug 1854	46	6-8 Oct 1908	3
27 Sept – 7 Nov 1854	43	5-16 Feb 1923	12
7-12 Dec 1854	6	9 March – 17 April 1923	39
27 Dec 1854 – 14 Feb 1855	51	10 Oct 1934 – 28 Feb 1935	143
1-11 Feb 1856	11	1 April – 31 May 1935	62
1-6 June 1865	6	1 June – 31 Aug 1936	92
		12-15 June 1960	4

## UNITS

Until November 1948, barometer readings were stated in inches of mercury (inHg), to two places of decimals until 23 March 1846 and thereafter to three places of decimals (0.001 inHg = 0.03 hPa). These have been converted throughout to hectopascals (hPa: 1 hPa = 1 millibar; 1 inHg = 33.86388 mbar) and rounded to 0.1 hPa after the application of any corrections. From December 1948 onwards, observations were noted in millibars. Attached thermometer readings are stated in degrees Fahrenheit or Celsius at various times: all have been converted to degrees Celsius. On the database, both ‘station level pressure reduced to 0 °C’ and the calculated mean sea level (MSL) pressure are given in hPa for each available observation. The method to reduce station level pressures to mean sea level is detailed below.

## Creation of the Durham pressure database

### DIGITISATION OF THE RECORD

Most of the original manuscript meteorological records from Durham Observatory have been retained, either in the Department of Geography or in the Durham University library. An initiative funded by the Leverhulme Trust saw many of the manuscript instrumental records from 1850 to 1997 digitised (Kenworthy et al, 1997), although until recently knowledge of this dataset remained almost entirely limited to Durham University. The barometric pressure observations (which terminated after December 1960) were included in this project – fortunately, for the Durham pressure record now represents by far the longest digital barometric pressure series in northern England, filling a very large gap in the International Surface Pressure Database, ISPD, which forms the majority of the input to the NOAA–CIRES–DOE Twentieth Century Reanalysis version 3 (hereafter 20CRv3; (Slivinski et al. 2021; Slivinski et al. 2019), currently extended back to 1806. The remaining early records, from July 1843 to December 1849, were digitised by the authors in 2021.

## ERRORS IN THE SERIES

Unfortunately, the ‘Leverhulme Trust’ barometric pressure record as originally digitised contained a significant number of major errors, some of which were due to the original observer and some due to mis-digitisation. An understanding of the causes leading to typical errors enables the process of checking and correcting enables to be more efficiently undertaken. Pressure records in inch units tend to exhibit distinct and characteristic errors, which can be briefly summarised as follows:

1. *Observer errors in reading the instrument, or noting the observation.* The typical scale of barometric pressure in the United Kingdom covers the pressure range from below 28 to above 30 inHg. It was very common in manuscript entries in inch pressure registers to omit the inch value until and unless the integer changed, by entering only the values following the decimal point. The transition from one inch integer to another can easily be omitted by the observer, as [Table A5.2](#) indicates:

**Table A5.2** Example of common errors in barometric pressure entries in manuscript register

Observation	Manuscript entry inHg		Digitised as inHg	Conversion to hPa	Correct inch values	Conversion to hPa	Error hPa
1	30	106	30.106	1019.5	30.106	1019.5	
2		062	30.062	1018.0	30.062	1018.0	
3		004	30.004	1016.1	30.004	1016.1	
4	29	994	29.994	1015.7	29.994	1015.7	
5		906	29.906	1012.7	29.906	1012.7	
6		013	29.013	982.5	<b>30.013</b>	1016.4	<b>33.9</b>
7	30	042	30.042	1017.3	30.042	1017.3	
8		981	30.981	1049.1	<b>29.981</b>	1015.3	<b>-33.9</b>

In line 6, the entry ‘30’ has been omitted, implying that the observed pressure is 29.013 inHg rather than 30.013, and this leads to a 1 inHg error (33.9 hPa) in the digitised value. The ‘30’ entry then appears correctly in line 7, but the ‘29’ entry has been omitted from the following entry, leading to a large positive error in the converted inch value. This type of error is particularly common as the average barometric pressure is close to 30 inHg (1015.9 hPa), and thus the changeover of leading digits from ‘29’ to ‘30’ or vice versa happens frequently. Where the observations are close together in time, such as hourly or three hourly records, correction is usually a matter of simple continuity checks to flag as suspect any particularly rapid rises or falls which are immediately followed by a similar magnitude fall or rise. Where observations are spaced 6-12 hours or more apart, as is the case with Durham, great care is required to avoid false corrections as

changes of 30 hPa in 6 hours or more, rises or falls, do occur from time to time, particularly during the winter months.

2. *Incorrect reading of the 0.5 inHg vernier scale.* Most inch barometers have a major division at 0.5 inHg intervals, and it can be easy to misread (say) 29.72 for 29.22 inHg, thereby introducing a 16-17 hPa error. These errors are much harder to spot on a twice-daily or daily record, but comparison with 20CRv3 and manual examination of the relevant synoptic chart, where available, usually helped determine whether the observation value was correct or otherwise.
3. *Incorrect or unclear digits in the observations register.* There are many possible errors here – confusions between 0, 6 or 9; 1, 4 or 7; 2, 4 or 7; and 3, 5 and 8 are typical, and often mistaken for each other at the digitisation stage if the written record is in any way unclear. Any such errors will generally only be obvious where they amount to at least several hPa from the 20CRv3 background, and thus are difficult to identify and correct.
4. *Incorrect entry in the register.* It is very easy to enter, say, 29.852 inHg in the register when the barometer was read as 29.582. Such errors are almost impossible to identify and correct unless the noted observation value differs by at least several hPa from the 20CRv3 background.
5. *Incorrect transcription of any of the above errors during digitisation* will produce similar results. Some are easy to spot by out-of-range checks, especially errors in the inch value itself; digitised values of 20 inHg or 39 inHg are easy to flag and clearly incorrect, but whether the true value in such instances should be 29 inHg or 30 inHg may not be immediately obvious. Such cases require close consideration of the context of the record including, where possible, examination of the original register entry.
6. *Incorrect millibar entries.* For the millibar records (from December 1948 to end of series), occasional errors in reading the scale persist; most appear to be around  $\pm 10$  mbar (hPa), or multiples thereof.

#### CORRECTION TO MEAN SEA LEVEL PRESSURE (MSLP)

For the period 1843 to 1948, reduction of the observed or ‘As Read’ barometer readings to MSL involved a two-stage process; firstly, to correct for the observed temperature of the barometer (the ‘Attached thermometer’ reading) to the standard 0 °C, this value referred to as the ‘station level pressure’; and secondly to correct the derived station

level pressure to mean sea level (MSL), for which the outside air temperature (dry bulb temperature) is also required. From 1949 onwards, the value of the incremental MSL correction was derived at the observatory and noted in the observations register, and thus has been used to correct the ‘As Read’ pressure to MSL. Further details are given subsequently.

A detailed account of the rationale for, and the methods involved in, the reduction of barometric pressure to MSL is beyond the scope of this Appendix, and the reader is referred to specialist texts, such as the *Handbook of Meteorological Instruments, Volume 1: Measurement of atmospheric pressure* (Meteorological Office 1980) and the World Meteorological Organization CIMO observing guide (World Meteorological Organization (WMO) 2018), Chapter 3, *Measurement of atmospheric pressure*. At the Durham Observatory, only the station level pressure was required for astronomical work and MSL pressure was not routinely evaluated until January 1949, and thus is not included in the manuscript observation registers prior to that date.

Throughout, calculations were performed in an Excel spreadsheet.

**Correction to 0 °C** For a Fortin barometer, and for pressure in millibars, the correction in millibars per Kelvin is 0.163 mbar/K at 1000 mbar ‘As Read’ pressure. The correction is proportional to the ‘As Read’ pressure, and is negative for Attached Thermometer readings above 0 °C or 273 K (Meteorological Office, 1956, Chapter 2, *Atmospheric Pressure*). Thus, for ‘As Read’ 1020 mbar and Attached Thermometer 20 °C, the correction is -3.32 mbar and the station level pressure at 0 °C becomes 1016.68 mbar. The calculation is slightly different for a Kew barometer, and is closer to 0.171 mbar/K at 1000 mbar. Normally no correction for barometer temperature is required for aneroid instruments, such as the temperature-compensated aneroid barometer in use at the Observatory during 1957-58.

Prior to 1955, standard corrections for barometer temperature assumed a barometer temperature of 62 °F (17 °C) and standard gravity 9.8062 m/s<sup>2</sup>; correction tables based upon these values (or even earlier standards) would most likely have been used for most of the Durham pressure record. To ensure the application of consistent corrections to modern standards, and to bypass occasional errors in the observation record and the digitised series, the entire Fortin ‘As Read’ record prior to 1949 was corrected to 0 °C using the post-1955 standard.

**Reduction to MSL** The reduction to MSL is computed in two stages. The first is to sum the barometer’s index errors (calibration differences at various pressures) together with

the correction for standard gravity of 9.806 65 m/s<sup>2</sup>, which varies with latitude, then add this to the station level pressure as calculated above. This sum is then added to the MSL correction term to obtain the MSL pressure or MSLP.

The index errors for the barometer in use are not individually known, although inspection reports stated they were small, and accordingly they have been neglected in this calculation. The correction for standard gravity at the Observatory's latitude (54.768 °N) at 1000 mbar is +0.83 mbar (Table LIIA in (Meteorological Office 1956), page 439), and is in proportion to the station level pressure.

The method of reduction to MSL follows that set out by WMO in the CIMO guide, section 3.11.1 (World Meteorological Organization (WMO) 2018) as follows, assuming a constant lapse rate:

$$p_{msl} = p_{stn} \cdot \exp\left(\frac{\frac{g}{R} \cdot H}{T + \frac{L \cdot H}{2} + e_s \cdot C}\right)$$

- where the terms are as follows:

$p_{msl}$  is the MSL pressure (in hPa)

$p_{stn}$  is the station level pressure (hPa)

$g$  is the standard acceleration of gravity (9.806 65 m/s<sup>2</sup>)

$R$  is the gas constant of dry air (287.05 J/kg/k)

$H$  is the station elevation (in geopotential metres – the error in using altitude in metres is insignificant and can be neglected below about 500 m AMSL. For Durham Observatory the barometer cistern height of 107.3 m was used)

$T$  is the outside air temperature (in Kelvin), from observed dry-bulb temperature  $T_C + 273$

$L$  is the assumed lapse rate in the fictitious air column extending from sea level to the level of the barometer cistern, taken as 0.0065 K/gpm

$e_s$  is the station vapour pressure (in hPa)

$C$  is a coefficient (0.12 K/hPa).

In this calculation, the station vapour pressure  $e_s$  is taken as 85% of the saturation vapour pressure  $e_{sat}$  at the outside air temperature  $T_C$  (in °C) – (i.e. the humidity is taken

as 85%, very close to a true mean for Durham<sup>1</sup>).  $e_{sat}$  is calculated using the formula due to Bolton (1980), which is acceptably accurate between -30 °C and 35 °C:

$$e_{sat}(T_c) = 6.112 \exp\left(\frac{17.67 T_c}{T_c + 243.5}\right)$$

The value of the MSL pressure thus obtained was then subjected to quality control measures as set out below.

### **Applying reanalysis data to effect quality control of the Durham MSLP series**

Without some form of independent record, it would be difficult to provide objective assessment of the accuracy and reliability of the new Durham series, particularly at the daily or sub-daily level. Fortunately, the increasing accuracy and lengthening timescale of reanalysis datasets provides an objective means to assess record quality; this is believed to be the first time an underpinning assessment using reanalysis has been applied to verify an independent long-period pressure dataset. Alternative methods include comparisons against gridded MSLP series or weighted comparisons with other sites. Clearly there is the potential for circularity in the correction of the candidate series against 20CR if and when the corrected series is subsequently assimilated into the reanalysis at a later date. However, the risk of circularity in this case is considered to be very small, firstly because the reanalysis series was only used to flag potential errors, which were then followed up wherever possible by scrutiny of the original registers or other sources (such as the online Met Office *Daily Weather Report* and subsequent publications), and secondly because the number of flagged errors is very small, amounting to just 0.42% of the entire series between 1843 and 1960 (Table A5.3). The published database also includes both ‘raw’ and ‘post quality control’ values.

Reanalyses can provide complete and consistent atmospheric fields by objectively combining historical observations with modern numerical weather prediction model forecasts, while accounting for estimated errors in both (Kalnay et al. 1996). The latest version of the Twentieth Century Reanalysis (20CR) has been generated by the University of Colorado Boulder’s Cooperative Institute for Research in Environmental

---

<sup>1</sup> Whilst we do have dry- and wet-bulb temperatures for almost all observations, it would require a great deal of additional computation to calculate relative humidity and vapour pressure for each observation, for no significant benefit to the MSLP calculation. Averaged over a year, the difference between MSLP assuming RH 75% and RH 95% (accounting for the majority of diurnal and seasonal variations) is about 0.01 hPa, which is much lower than instrument and observer errors, and can therefore be safely neglected.

Sciences (CIRES) together with the National Oceanic and Atmospheric Administration (NOAA) and the U.S. Department of Energy (DOE). This NOAA–CIRES–DOE 20CR version 3, 20CRv3, uses a newer, higher-resolution model, assimilates a larger set of observations, and includes an improved data assimilation system relative to its predecessors. The 20CRv3 system further extends the reanalysis period to 1836–2015, with an experimental extension spanning 1806–35. Slivinski et al. (2019) provide an in-depth description of the system that generated the 20CRv3 reanalysis product, which consists of a numerical weather prediction model, an observational dataset, and an assimilation method. Using an 80-member ensemble Kalman filter, the 20CRv3 system assimilates only surface pressure observations (a so-called ‘sparse’ reanalysis) from the open, unrestricted, and publicly available International Surface Pressure Databank (ISPD) version 4.7 (Compo et al. 2019; Cram et al. 2015), into the U.S. National Centers for Environmental Prediction (NCEP) Global Forecast System (GFS) model, with a horizontal resolution of about 60 km at the equator and a vertical atmospheric resolution of 64 levels. Sea surface temperature and sea ice, solar radiation and time-varying atmospheric constituents of volcanic aerosols, stratospheric ozone and atmospheric carbon dioxide (CO<sub>2</sub>) levels are also specified. Output fields are available at 3-hourly resolution.

Until very recently, there were no pressure records from sites in England held on the ISPD (and thus available to the 20CRv3 reanalysis) prior to 1925. Before 1925, the only ISPD records within the British and Irish Isles are those from Armagh in Northern Ireland (pressure data from 1796-1826, 1833-1965), Aberdeen in Scotland (1871-1948, 1957-1988), and Valentia Observatory in the Republic of Ireland (1892 to date). Recent work by Hawkins et al. (2019) rescued pressure data from Fort William and Ben Nevis from 1883-1904 and digitised records from multiple European sites published in the UK Met Office contemporary *Daily Weather Report* publication from 1860 (Craig and Hawkins 2020; Lewis 1982); this work has been completed, although at the time of writing it has not yet been incorporated into ISPD. Consequently, the accuracy of atmospheric reanalyses over the north-eastern Atlantic prior to 1925 has been constrained owing to the dearth of reliable surface pressure records in and around the British and Irish Isles. This newly-available record from Durham should therefore be helpful in assessing both likely errors in gridpoint pressure data from the reanalysis ensemble means, and changes over time, and in improving the accuracy / reducing ensemble spread in future reanalyses once the Durham data are eventually included into ISPD and a future version of 20CR.



## METHOD

A time series of pressure values (ensemble mean pressures) at a given gridpoint can be obtained from the 20CRv3 reanalysis website (<https://psl.noaa.gov/data/timeseries/hour/>), for any period within the main dataset (currently 1836 to 2015). This output, in the form of one or more sub-daily gridpoint ensemble mean pressures at 3 hourly intervals (00, 03, 06 GMT, etc) for the chosen period, was used to provide an independent underpinning quality control measure to the Durham MSLP record (the two series can be regarded as independent since the Durham series was not included in the ISPD datasets from which this version of the reanalysis was built). The nearest 20CRv3 gridpoint to Durham Observatory is at 55°N 2°W, about 36 km north-west of the observatory (54.768 °N, 1.584 °W). Gridpoint ensemble mean pressure values were extracted for 0900 and 2100 GMT<sup>2</sup> throughout the period of record, except for February 1855 to June 1858 when an afternoon observation was made at 1400, for which 1500 GMT gridpoint values were used instead.

An example, from the first winter of the record in December 1843-January 1844 and using observed (i.e., pre-QC) data, is shown in [Figure A4.2](#). The tendency for ensemble averaging to reduce the absolute range in extremes is evident in the plot. This is understandable when it is considered that the assimilation of this version of the reanalysis is based upon only a single site in the British and Irish Isles at this time (viz. Armagh), and consequently the spread of ensemble members is likely to be less constrained than in periods with a denser spread of surface pressure observations.

---

<sup>2</sup> Strictly, GMT as a defined time standard did not exist until 1885, but for convenience times are referred to as GMT for dates prior to 1885 unless otherwise stated.

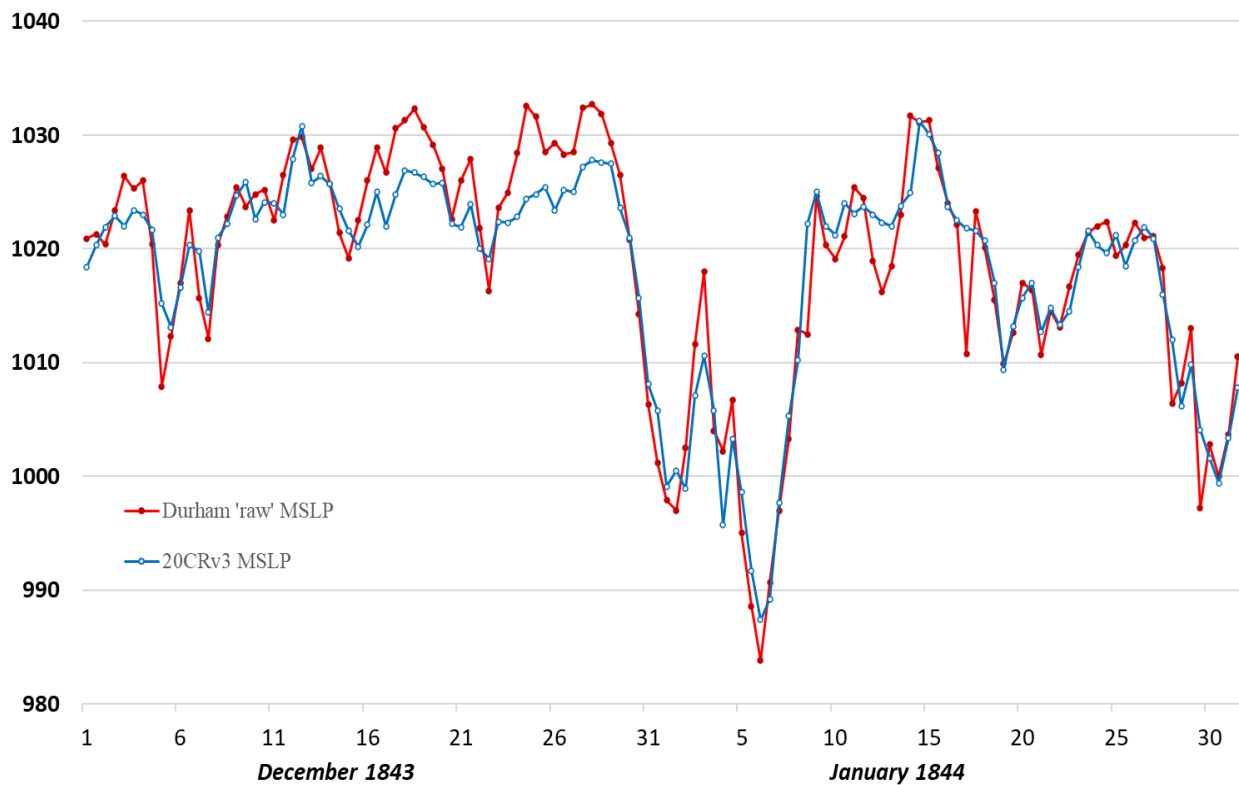


**Figure A4.2.** Comparison of daily ‘raw’ (uncorrected) Durham MSL pressure observations at 09h and 21h solar time (6 minutes later than Greenwich time) (red line) with 20CRv3 nearest gridpoint values at 0900 and 2100 GMT (blue line), for the months of December 1843 to January 1844, the first winter of the record. The very close agreement is evident, and the few significant differences are most likely due to uncertainties in the reanalysis – see text for details [ARTWORK DHM XL 002](#)

When Durham’s observations were made at 10h and 22h, 0900 and 2100 GMT gridpoints were also used as representing the closest point in time. The resulting 20CRv3 twice-daily gridpoint pressure series was then compared against the Durham MSLP record.

Of course, no quality control measure can ever render an imperfect record into a perfect one, and it is important to minimise changes to the original record commensurate with removing at least the most obvious errors. The 20CRv3 daily and sub-daily series are particularly useful where short spells of observations are missing or have been mis-coded with incorrect dates, for pattern-matching (by eye or by algorithm) can quickly suggest a fitting sequence. However, as [Table A5.3](#) shows, the vast majority of the Durham record appears extremely reliable. In turn, the independent Durham dataset provides a useful benchmark to assess the likely accuracy of 20CRv3 within the north-east Atlantic region.

Figure A4.3 shows both the annual mean root-mean-square (RMS) and absolute errors (the arithmetic difference 20CRv3 gridpoint minus Durham) over the period 1844-1960. From this it is evident that the relative accuracy of the reanalysis dataset usually increases over time, as would be expected with increasing density of assimilated surface pressure data. The one significant exception to this fairly smooth trend occurs between 1914 and 1919, when the Durham data provides clear evidence of a previously unknown bias in 20CRv3 over the North Atlantic. This anomaly has been confirmed by examination of other reanalysis products; at the time of writing, the reasons for it remain unclear and under investigation (Ed Hawkins, Clive Wilkinson and Gil Compo, personal communications February-March 2021).

The Durham pressure series is divided into four periods and each discussed in more detail below.

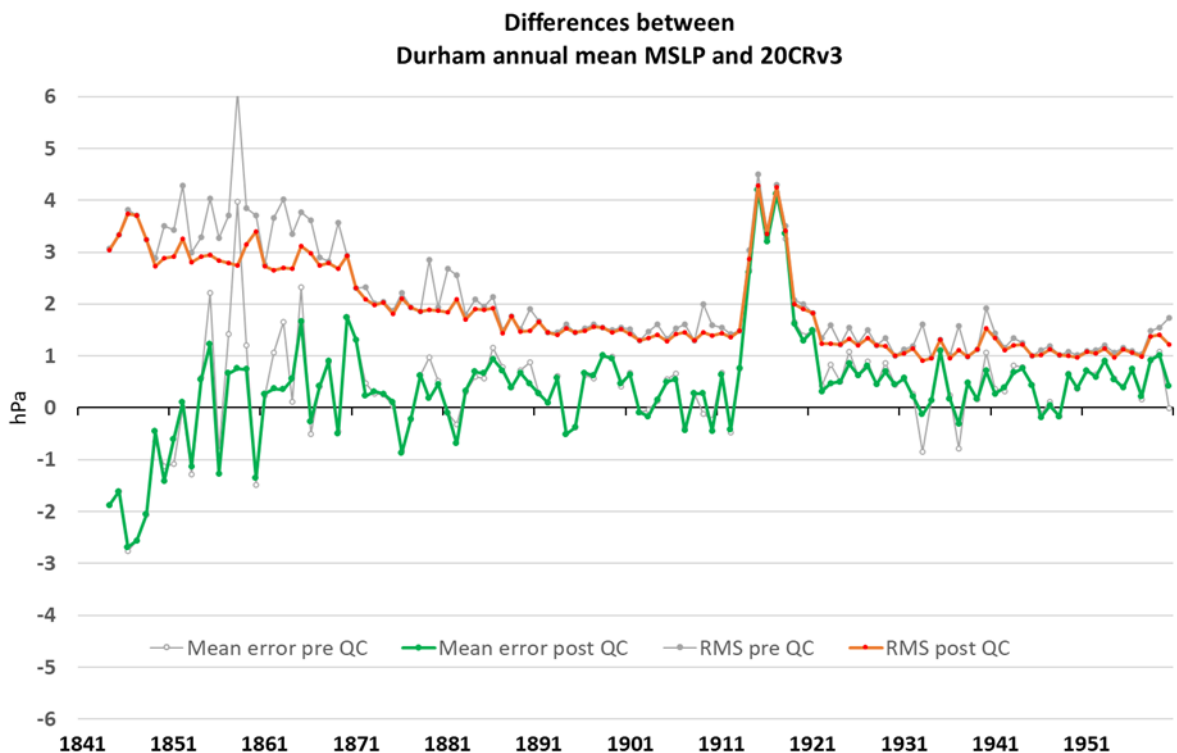


Figure A4.3. Annual mean arithmetic (green line) and root-mean-square RMS errors (orange line) between the quality-controlled Durham pressure series and 20CRv3 nearest gridpoint value, 1844 to 1960. For comparison, the thin grey lines on both series show the arithmetic mean and root-mean-square errors from the uncorrected (pre-QC) series.

JULY 1843 TO NOVEMBER 1948

At just over 105 years in length, this comprises the first and longest subdivision of the Durham pressure series. As far as can be ascertained, the record originates from the same instrument throughout, namely the Browning Fortin barometer. The series is 98.5% complete; most of the gaps after 1883 resulted from periods when the Browning instrument was away for cleaning or repair.

Throughout this period, the twice-daily series appears extremely reliable when compared against the relevant 20CRv3 gridpoint value (Table A5.3 and Figure A4.4). Even prior to the introduction of quality control corrections, between July 1843 and November 1948 64.5 per cent of the available observations lay within  $\pm 2$  hPa of the corresponding 20CRv3 gridpoint value, and 99.0% lay within  $\pm 10$  hPa. Comparisons against 20CRv3 suggested that 319 records (just 0.42% of the total observations) were most likely to be incorrect<sup>3</sup>. Most of these (235, or 73%) were found to be clustered close to 0.5 or 1.0 inHg multiples, thereby suggesting an error in the ‘As Read’ reading as the most likely cause: a few were 9 or 10 inHg errors (i.e. an entry of 20 or 39 inHg instead of 29 or 30 Hg). Such discrepancies are almost certainly due to one or a combination of the reasons outlined earlier. The distribution of errors was Gaussian and almost symmetrically distributed about zero, as is evident from the very minor change in mean MSL pressure (Table A5.3). The post-QC Durham mean pressure is slightly higher than the 20CRv3 gridpoint mean – for the whole 111 year period by 0.37 hPa – as would be expected with the gridpoint being 36 km north-west of the Observatory location and the expected climatological decrease in mean MSL pressure with increasing latitude in the British and Irish Isles.

An automated quality control check against 20CRv3 was successful in flagging most if not all of the major errors during this period, increasing the number of the Durham observations within  $\pm 10$  hPa of the corresponding 20CRv3 gridpoint value from 99.0% to 99.4%. However, objective automated error checking became progressively less reliable with smaller discrepancies. At errors below roughly 17 hPa/0.5 inHg difference, the very high quality of most of the Durham series would suggest that the difference is more likely to arise from errors in the reanalysis field, particularly prior to about 1925 for reasons referred to earlier. The two most likely causes of such errors are timing

---

<sup>3</sup> The term ‘error’ in this sense refers to the difference (20CRv3 gridpoint value minus Durham). Such differences can arise only through an error in the Durham value (whether observer, transcription or subsequent digitisation), or uncertainty in the 20CRv3 reanalysis field. The latter is larger in the early years of the record where fewer surface pressure observations have so far been assimilated.

differences (almost always cyclonic storms moving or developing more quickly than suggested by the reanalysis model), and insufficient deepening of intense cyclonic systems within the reanalysis. In particular, the latter effect clearly resulted in some Durham records being incorrectly flagged as erroneous, when a manual check on the original manuscript records (at present, online files available for 1843-1850 only), or from observations published in the relevant *Daily Weather Report* from September 1860 (and, later, synoptic charts from March 1872), showed that they were almost certainly correct – in which case, the error flags were removed and the original observations reinstated.

**Table A5.3** Durham pressure record QC summary, comparing ‘raw’ (original digital dataset) and ‘Post QC’ (after quality control measures as described in the text). A positive value in the ‘Average arithmetic error’ indicates that the Durham value is higher than the 20CRv3 gridpoint ensemble mean value, and vice versa

Period and number of observations	No of corrected observations	Average arithmetic error 20CRv3 minus Durham, hPa	Error Std Dev'n hPa	Average RMS error 20CRv3 minus Durham	MSLP average, hPa	% values 20CRv3 $\pm$ 2 hPa	% values 20CRv3 $\pm$ 10 hPa	
<b>Fortin barometer July 1843 to Nov 1948</b>								
<i>Raw</i>	75 816 of 76 964 (98.5%)	None	+0.43	11.15	2.21	1013.35	64.5	99.0
<i>Post QC</i>	75 827	319 (0.42%)	+0.34	2.71	1.97	1013.26	64.6	99.4
<b>Kew barometer Dec 1948 to Aug 1949</b>								
<i>Raw</i>	548 of 548 (100%)	None	+0.47	1.38	1.05	1017.53	89.2	99.6
<i>Post QC</i>	548	2 (0.36%)	+0.43	1.22	1.01	1017.49	89.6	100.0
<b>Fortin barometer Sept 1949 to Dec 1960 excl. 28 Aug 1957 to 28 Feb 1958</b>								
<i>Raw</i>	7901 of 7910 (99.9%)	None	+0.59	1.85	1.23	1013.48	85.9	99.4
<i>Post QC</i>	7901	28 (0.35%)	+0.63	1.29	1.13	1013.51	86.7	100.0
<b>Aneroid barometer 28 Aug 1957 to 28 Feb 1958</b>								
<i>Raw</i>	370 of 370 (100%)	None	+0.54	1.76	1.16	1012.66	85.4	99.5
<i>Post QC</i>	370	2 (0.54%)	+0.45	1.34	1.08	1012.58	85.9	100.0
<b>Combined record, Jan 1850 to Dec 1960</b>								
<i>Raw</i>	84 646 of 85 792 (98.7%)	None	+0.45	10.56	2.11	1013.38	66.8	99.1
<i>Post QC</i>	84 646	352 (0.42%)	+0.37	2.60	1.88	1013.30	66.9	99.5

Whilst it would be easy enough automatically to correct all discrepancies larger than, say,  $\pm$  10 hPa by arbitrarily assuming the Durham value was in error and flagging it as ‘incorrect’, and of course doing so would immediately reduce the number of errors larger than 10 hPa from 0.6% to zero, it was felt that such actions would almost certainly result in some valid observations being wrongly flagged as incorrect.

Accordingly, to avoid arbitrary corrections to the Durham series, for this period quality control checks were applied only where the discrepancy was greater than about 15 hPa, or where smaller errors could be investigated by manual checking against other nearby sites (usually from stations included in the *Daily Weather Report*) or by other methods, such as continuity checks in periods of settled weather conditions. Particular attention was paid to records close to or exceeding monthly long-term climatological extremes.

In time, it should be possible to check all discrepancies greater than, say,  $\pm 5$  hPa back against the original manuscript observation registers to identify and correct any mistyped digitisation entries. Unfortunately, coronavirus travel and access restrictions during 2020/21 made this impossible during the preparation of this book, but when this step becomes feasible then it will be possible to re-examine and corrected the Durham series as necessary.

In summary therefore: the first and longest part of the Durham pressure series appears impressively complete, and shows a very high degree of accord with the 20CRv3 reanalysis. Most if not all of the larger errors have been identified and corrected, but it is likely that an unknown number of smaller errors remain in this period of record.

While some uncertainty remains with regard to individual values, monthly and annual means over this 105 year period are believed to be correct to within a few tenths of a millibar.

#### DECEMBER 1948 TO DECEMBER 1960

The barometer in use during the final 12 years of the long Durham record changed several times, as stand-in instruments were used in place of the Browning Fortin unit whilst away for cleaning and refurbishment in 1948-49 and 1957-58 as detailed below.

The period is sub-divided by barometer type in use; the distinction is important because the detail of the corrections applied to the observed value differ somewhat according to the type of barometer, and these have been allowed for in the MSL corrections applied. From December 1948, all barometer readings were made in millibars; with the change of graduation comes a change in the nature of 'major' errors, which are now more likely to be about  $\pm 10$  mbar, or multiples thereof.

Readings of the 'Attached Thermometer' ceased with effect from 1 December 1948.

From January 1949 onwards, the entry in the Att Therm column in the observations register appears to be the incremental MSL correction to the As Read value, presumably derived from a barometer correction card taking the barometer temperature into account

in doing so (the method is explained in the *Handbook of Meteorological Instruments, Volume 1: Measurement of atmospheric pressure* (Meteorological Office 1980)).

Although a different MSL derivation scheme for the final years of the series is unfortunate, the absence of the observed Att Therm reading renders this a necessity and from January 1949 – with exceptions listed below – the MSLP was taken as As Read + MSL correction as given in the observations register. For the few occasions when the correction was missing, estimates based on neighbouring values were used.

#### *DECEMBER 1948 TO AUGUST 1949: KEW BAROMETER*

A loan Kew-pattern barometer replaced the Browning Fortin barometer while the latter was away for repair between December 1948 and August 1949. This barometer was graduated in millibars. Readings of the ‘Attached Thermometer’ ceased with effect from 1 December 1948. For December 1948, MSL values were prepared taking the Att Therm value as the average for December for the previous 10 years 1938-47 and using the calculation as set out in section 3.3. From January to August 1949, the MSL correction is given in the observations register, and the MSLP has been taken as the As Read + MSL correction.

#### *SEPTEMBER 1949 TO DECEMBER 1960: FORTIN BAROMETER*

The Browning Fortin barometer was re-introduced on 1 September 1949, and aside from the six months 28 August 1957 to 28 February 1958, when it was away for cleaning once more, it remained in use until barometric pressure observations were discontinued after 31 December 1960. The barometer was re-certified by Negretti & Zambra (certificate dated 5 February 1958), with errors no more than 0.4 hPa at any point within the calibration range. The August 1958 inspection report states that a handful of comparisons of Durham’s MSL pressure against neighbouring synoptic stations around the date of the inspection indicated that the barometer read up to 1.9 hPa too *low*, although the average of the observatory’s 0900 GMT readings for that month compared with nearby sites would suggest the error was about 1.0 hPa too *high* at that time.

#### *28 AUGUST 1957 TO 28 FEBRUARY 1958: ANEROID BAROMETER*

Daily observations were made with a temperature-compensated aneroid barometer loaned by the Met Office for this five-month period (note on site file dated 28 October 1957). This type of instrument does not require temperature correction and thus no ‘Attached Thermometer’ readings are available for this period.



This instrument appears to have read 27-28 hPa too low – possibly as a result of the MSL adjustment being incorrectly set – but otherwise appears to have indicated daily pressure changes accurately and reliably. During this period, the MSLP was taken as As Read + 27.5 hPa. Two observations during this period required additional corrections for 10 mbar reading errors.

### **The Durham observatory digital pressure record**

The entire Durham twice-daily pressure series 1843-1960 is available on the University of Reading Research Data Archive at <http://dx.doi.org/10.17864/1947.295> as an open access dataset under a Creative Commons Attribution 4.0 International Licence. The file format is Comma Separated Variable (.csv), and the file size is 48 MB. The contents of the file are listed in [Table A5.4](#), as a ReadMe file within the same location.

Three options are available for the Durham MSLP series – the ‘raw’ (as observed) record, including gaps where they occur; the corrected (post QC) record, including gaps where they occur; and a corrected (post QC) record, where gaps have been filled using the 20CRv3 gridpoint data +0.5 mbar to provide an unbroken series. Gaps in the record amount to 1.3% of the record ([Table A5.3](#)) and corrections to 0.42%, distributed fairly evenly throughout the record.

**Table A5.4** Details of the twice-daily Durham Observatory digital pressure series 1843-1960.

Column header	Cell contents
<b>YYYY MM DD</b>	Date as YYYY MM DD character string (two entries per day)
<b>YYYY MM DD HHmm</b>	Date and time as YYYY MM DD HHmm character string (one entry per observation)
<b>DD</b>	Date in month (1-31)
<b>MM</b>	Month (1-12)
<b>YYYY</b>	Year (1843-1960)
<b>HHmm</b>	Observation hour HHmm – mostly 0900 or 2100, GMT from Oct 1885
<b>Missing</b>	Flag: Barometer ‘As Read’ reading missing = 1, else 0
<b>AsRead_inHg</b>	Barometer ‘As Read’ in inches of mercury (inHg) to November 1948, blank thereafter. This is the barometer reading as observed and digitised and includes numerous errors
<b>AsRead_hPa</b>	Barometer ‘As Read’ in millibars (mbar or hPa) throughout – inHg converted by x 33.86388. This is the barometer reading as observed and digitised and includes numerous errors
<b>AttTherm_C</b>	Barometer ‘Attached Thermometer’ in degrees Celsius – converted from °F as necessary. This is the thermometer reading as observed and digitised and includes some errors, particularly from 1949-60
<b>SLP_hPa</b>	Station level pressure – barometer ‘As Read’ reduced to 0 °C using the Attached Thermometer reading (see text for details) corrected for known or suspected errors
<b>Tdry_C</b>	Observed external air temperature (dry bulb in screen) in degrees Celsius. Some are missing; estimates were made using neighbouring values or, occasionally, monthly means over several years
<b>MSLP_RAW_hPa</b>	Calculated MSL pressure in millibars (hPa). MSL calculation details are given in the text. This is the RAW value calculated from the observed As Read and Attached Thermometer with dry bulb temperature, prior to quality control
<b>MSLP_QC_hPa</b>	Calculated MSL pressure in millibars (hPa). This is the CORRECTED value, post quality control (see text for QC details), based upon the SLP_hPa value. Blank cells indicate record gaps
<b>MSLP_QC_gapfilled_hPa</b>	This is identical to <b>MSLP_QC_hPa</b> except that gaps are filled using the 20CRv3 ensemble mean gridpoint value + 0.5 hPa to provide an unbroken series

Missing data are shown blank (empty cell), but note that there are no missing cells in the date/time headers, for the 20CRv3 ensemble mean gridpoint value or for the gapfilled pressure series.

## Record summary

### MONTHLY AND ANNUAL AVERAGES

**Table A5.5** sets out monthly and annual averages of MSLP at Durham over various 30-year periods. These averages are of the *corrected* series, with gaps filled by 20CRv3 gridpoint values +0.5 hPa where necessary. Values are shown minus 1000 hPa.

**Table A5.5** Monthly and annual averages of MSL pressure at Durham Observatory, average of 0900 and 2100 GMT observations, various periods 1851-80 to 1931-60. Units – hPa less 1000.

Period	<i>J</i>	<i>F</i>	<i>M</i>	<i>A</i>	<i>M</i>	<i>J</i>	<i>J</i>	<i>A</i>	<i>S</i>	<i>O</i>	<i>N</i>	<i>D</i>	<i>Year</i>
1851-80	10.8	13.5	12.7	14.6	15.2	14.5	13.8	13.4	13.7	11.2	12.9	12.0	13.17
1861-90	12.4	13.8	12.2	14.0	15.4	15.6	13.3	13.2	13.5	12.0	11.4	12.4	13.24
1871-1900	13.7	14.1	12.7	13.5	15.7	15.6	13.3	12.9	14.1	11.9	12.0	11.6	13.41
1881-1910	14.5	14.0	11.8	13.5	15.6	16.5	14.1	12.9	15.9	12.2	12.6	10.9	13.70
1891-1920	13.9	12.5	10.6	13.8	16.1	16.2	14.9	13.1	16.1	12.3	12.7	9.2	13.43
1901-30	12.9	12.2	11.4	12.8	15.2	15.9	14.4	12.6	16.0	12.3	11.6	9.4	13.06
1911-40	11.6	13.1	12.2	13.0	15.5	15.6	13.3	13.5	14.9	12.1	10.6	10.7	12.99
1921-50	11.6	13.9	14.8	13.0	15.3	15.4	13.0	13.3	14.4	12.6	10.9	12.2	13.36
1931-60	11.9	13.7	14.8	14.7	16.4	15.4	13.1	13.4	14.4	13.5	11.5	11.1	13.68

### EXTREMES ON RECORD

**Daily extremes** **Table A5.6** lists the highest and lowest barometric pressure recorded at Durham Observatory by month (with date and time) and by year, from the *corrected* series (none of these records are from gap-filled missing data). It should be noted that as readings were taken only twice per day, these are almost certainly under-estimates of the range of barometric pressure at the site, since extremes may occur at any hour of the day.

**Table A5.6** Monthly and annual extremes of MSL pressure at Durham Observatory, in rank order, from morning and evening observations only (usually 0900 and 2100 GMT), period July 1843 to December 1960. Units – hPa, omitting initial digit (i.e. 10 for the maximum values, and 9 for the minimum)

Period	J	F	M	A	M	J	J	A	S	O	N	D	Year
Maximum	52.5	48.2	44.9	42.5	42.3	40.7	37.7	35.0	39.3	40.5	42.9	47.4	52.5
Year	1907	1902	1935	1906	1881	1959	1911	1874	1851	1956	1922	1926	1907
Date	23	1	9	8	10	13	10	20	16	31	15	23	23/1
Hour	09	09	09	21*	10	09	09	22	09	09 <sup>†</sup>	09	21	09
Minimum	50.7	59.8	62.3	70.2	72.0	82.4	77.2	68.5	71.9	58.5	64.2	36.2	36.2
Year	1884	1951	1876	1948	1943	1938	1922	1917	1935	1959	1881	1886	1886
Date	26	5	10	1	8	28	6	28	17	27	27	8	8/12
Hour	22	09	10	09	21	21	09	09	09	09	10	21	21
Monthly pressure range	101.8	88.4	82.6	72.3	70.3	58.3	60.5	66.5	67.4	82.0	78.7	111.2	116.3

\* April highest value 1042.5 hPa equalled at 21h on 11 April 1938

<sup>†</sup> October highest value 1040.5 hPa equalled at 09h on 23 October 1958

The ten highest and ten lowest MSL pressure readings at Durham over the period 1843-1960 are listed in [Table A5.7](#), together with the equivalent 20CRv3 gridpoint ensemble mean value closest to that observation time.

**Table A5.7.** The ten highest and ten lowest barometric pressures on the Durham Observatory record 1843-1960, with the date and observation time, in rank order, together with the 20CRv3 gridpoint ensemble mean for that date and time. Units hPa.

<i>Date</i>	<i>Time</i>	<i>Durham QC MSLP hPa</i>	<i>20CRv3 gridpoint ensemble mean hPa</i>	<i>Notes</i>
<b>Highest MSL pressures</b>				
23 Jan 1907	0900	1052.5	1050.8	Slightly high; North Shields 1050.8 hPa at 0800 and 1049.1 hPa at 1800. True maximum probably between 1051 and 1051.5 hPa. See also Chapter 22, Chronology
31 Jan 1902	0900	1050.8	1047.8	
31 Jan 1902	2100	1050.7	1047.7	
22 Jan 1907	2100	1049.9	1047.5	
26 Jan 1932	0900	1049.7	1046.5	
9 Jan 1896	0900	1048.8	1047.1	'Raw' value 1051.2 hPa appears too high
26 Jan 1932	2100	1048.7	1045.1	
1 Feb 1902	0900	1048.2	1046.7	
23 Jan 1907	2100	1048.1	1047.1	
25 Jan 1932	2100	1047.7	1045.4	
<b>Lowest MSL pressures</b>				
8 Dec 1886	2100	936.2	952.8	Reanalysis in error – depth and timing; see also Chapter 22, Chronology
26 Jan 1884	2200	950.7	945.1	Reanalysis system speed too slow
9 Dec 1886	0900	953.7	958.3	
3 Dec 1909	0900	954.7	954.2	
4 Feb 1951	2100	955.4	954.3	
1 Jan 1949	2100	955.7	956.3	
8 Dec 1886	0900	956.3	973.1	
4 Feb 1951	2100	956.4	954.3	
6 Dec 1847	2100	956.9	965.8	Minimum noted as 956.8 hPa at 2025 common time
19 Feb 1900	2100	957.0	962.5	
<b>1 Jan 1949</b>	<b>0900</b>	<b>957.7</b>	<b>957.1</b>	

Details of the circumstances of many of the events listed in [Table A5.7](#), together with synoptic descriptions, can be found in Burt (2007a, 2007b).

**Monthly and annual extremes** [Table A5.8](#) lists the highest and lowest monthly barometric pressure means recorded at Durham Observatory, using the *corrected* series including any gap-fills from 20CRv3 as necessary. The anomaly from the 1931-60 monthly average (from [Table A5.5](#)) is also shown for each entry. The highest monthly mean pressure on the Durham record was in February 1932, when the mean was 1034.6 hPa; only two other months have averaged higher than 1030 hPa, namely February 1959 (1030.4 hPa) and February 1891 (1030.3 hPa); not surprisingly, all three months were very dry in Durham. The lowest monthly mean pressure on the record was in January

1948, when the mean was 994.5 hPa. Other notably cyclonic months include the Decembers of 1868 and 1959, with a monthly mean of 997.0 hPa.

**Table A5.8** Highest and lowest monthly mean MSL pressure (hPa) at Durham Observatory, and the extreme range in monthly means, over the period 1843-1960. The monthly mean is the average of the morning and evening observations (usually 0900 and 2100 GMT). Anomaly from 1931-60 normal also stated. Values omit initial digit (i.e. 10 for values > 1000 hPa, and 9 < 1000 hPa). Highest and lowest values shown in **bold**.

	<i>J</i>	<i>F</i>	<i>M</i>	<i>A</i>	<i>M</i>	<i>J</i>	<i>J</i>	<i>A</i>	<i>S</i>	<i>O</i>	<i>N</i>	<i>D</i>	<i>Year</i>
Maximum	27.4	<b>34.6</b>	29.4	27.0	25.8	24.1	21.8	22.2	24.7	22.2	26.2	24.8	17.0
Year	1880	1932	1953	1938	1896	1865	1955	1947	1865	1947	1867	1926	1921
Anomaly (+)	15.5	20.9	14.6	12.3	9.4	8.7	8.7	8.8	10.3	8.7	14.7	13.7	+3.3
Minimum	<b>94.5</b>	98.8	97.6	05.1	07.7	04.9	05.1	03.4	03.6	00.0	99.4	97.0	07.9
Year	1948	1937	1876	1920	1925	1852	1861	1860	1918	1903	1877	1868 1959	1872
Anomaly (-)	17.4	14.9	17.2	9.6	8.7	10.5	8.0	10.0	10.8	13.5	12.1	14.1	-5.8
Monthly range	32.9	35.8	31.8	21.9	18.1	19.3	16.7	18.8	21.1	22.2	26.8	27.8	9.1

#### ACKNOWLEDGEMENTS

Thanks are due to Richard Higgins, Durham University Library, who kindly arranged for scanning (and, for a few missing pages, re-scanning) of the Observatory registers by the authors covering the period July 1843 to April 1850.

#### REFERENCES

- Banfield, E., 1991: *Barometer makers and retailers 1660-1900*. Baros Books, Trowbridge 246 pp.
- Bolton, D., 1980: The computation of equivalent potential temperature. *Mon. Weather Rev.*, **108**, 1046–1053.
- Burt, S., 2007a: The Lowest of the Lows ... extremes of barometric pressure in the British Isles, part 1 – the deepest depressions. *Weather*, **62**, 4-14.
- , 2007b: The Highest of the Highs ... Extremes of barometric pressure in the British Isles, Part 2 – the most intense anticyclones. *Weather*, **62**, 31-41.
- , 2021: A twice-daily barometric pressure record from Durham Observatory in north-east England, 1843-1960. *Geoscience Data Journal (In Press)*.
- Burt, S. and T. Burt, 2019: *Oxford Weather and Climate since 1767*. Oxford: Oxford University Press 544 pp.
- Compo, G. P., L. C. Slivinski, J. S. Whitaker *et al*, 2019: The International Surface Pressure Databank version 4. Research Data Archive at the National Center for Atmospheric Research, Computational and Information Systems Laboratory: URL <https://doi.org/10.5065/9EYR-TY90>.
- Craig, P. M. and E. Hawkins, 2020: Digitizing observations from the Met Office Daily Weather Reports for 1900–1910 using citizen scientist volunteers. *Geoscience Data Journal*, doi **10.1002/gdj3.93**.
- Cram, T. A., G. P. Compo, X. Yin *et al*, 2015: The International Surface Pressure Databank version 2. *Geoscience Data Journal*, **2**, 31-46.
- Durham University Library, 2016: Catalogue of the records of Durham University Observatory, available at [http://reed.dur.ac.uk/xtf/view?docId=ark/32150\\_s108612n525.xml](http://reed.dur.ac.uk/xtf/view?docId=ark/32150_s108612n525.xml).
- Hawkins, E., S. Burt, P. Brohan *et al*, 2019: Hourly weather observations from the Scottish Highlands (1883-1904) rescued by volunteer citizen scientists. *Geoscience Data Journal*, **6**, 160–173.
- Kalnay, E., M. Kanamitsu, R. Kistler *et al*, 1996: The NCEP/NCAR 40-Year Reanalysis Project. *Bull. Amer. Meteorol. Soc.*, **77**, 437-472.

- Kenworthy, J. M., N. J. Cox and A. N. Joyce, 1997: *Computerisation and analysis of the Durham Observatory meteorological record: Final Report to the Leverhulme Trust, Reference F/128/Q*. Durham University.
- Lewis, R. P. W., 1982: The *Daily Weather Report* and associated publications: 1860-1980. *Meteorol. Mag.*, **111**, 103-121.
- Meliconi, I., 2004: Browning, John (1830/31–1925), scientific instrument maker, in Oxford Dictionary of National Biography. Oxford University Press.
- Meteorological Office, 1956: *Handbook of Meteorological Instruments: Part 1, Instruments for surface observations*. Fifth impression 1969 ed. London: Her Majesty's Stationery Office
- , 1980: *Handbook of Meteorological Instruments: Volume 1, Measurement of atmospheric pressure*. *Handbook of Meteorological Instruments*, Second Edition ed., London: Her Majesty's Stationery Office
- Slivinski, L. C., G. P. Compo, P. D. Sardeshmukh *et al*, 2021: An evaluation of the performance of the twentieth century reanalysis version 3. *J. Climate*, **34**, 1417-1438.
- Slivinski, L. C., G. P. Compo, J. S. Whitaker *et al*, 2019: Towards a more reliable historical reanalysis: Improvements for version 3 of the Twentieth Century Reanalysis system. *Quart. J. Royal Meteorol. Soc.*, **145**, 2876-2908.
- World Meteorological Organization (WMO), 2018: WMO No.8 - Guide to Meteorological Instruments and Methods of Observation (CIMO guide). 2018 edition - Volume I: Measurement of Meteorological Variables. WMO, Geneva, Switzerland. Available online: [https://library.wmo.int/index.php?lvl=notice\\_display&id=12407](https://library.wmo.int/index.php?lvl=notice_display&id=12407), 573 pp.



# Paper 7

## **December 2015 – an exceptionally mild month in the United Kingdom**

By Stephen Burt and Mike Kendon (Met Office), 2016. *Weather*, **71**, pp. 314-320.

*Bibliography # 21. Word count 2065 excluding references.*

---

*The following content is reproduced by kind permission of the Publishers,  
John Wiley and Sons, under the terms of the Copyright Clearance Center's RightsLink®  
license number 5100130020213 dated 1 July 2021*



# December 2015 – an exceptionally mild month in the United Kingdom

Stephen Burt<sup>1</sup> and  
Mike Kendon<sup>2</sup>

<sup>1</sup>Department of Meteorology, University of Reading

<sup>2</sup>National Climate Information Centre, Met Office, Exeter

While the main weather impacts of winter 2015/2016 were those resulting from high winds and extreme rainfall (Burt *et al.*, 2016: references, this issue), an equally remarkable feature was the exceptionally mild weather during the first part of the winter, particularly in December. A persistent southwesterly air flow brought temperatures more typical of April, May or even June; many places in England and Wales remained free of air frost throughout the month. This was, by a very large margin, the mildest December on the long Central England Temperature (CET) record, extending back to 1659 (Manley, 1974; Parker *et al.*, 1992).

This article presents a brief summary of the main weather patterns and notable extreme values during the month, together with an analysis of the monthly anomalies of mean temperature over the United Kingdom. Larger-scale circulation patterns are discussed, and the event is considered in its long-term context, including circulation comparisons with the exceptionally cold December of 2010, just 5 years previously.

## British Isles weather types during December 2015

The month was dominated by unseasonably mild and moist tropical maritime air masses originating far to the southwest of the British Isles, while frequent deep depressions brought strong winds and heavy rain to the north at regular intervals. The energy from the warmth in the moisture-laden atmosphere and associated temperature contrasts helped to invigorate these depressions and greatly increase the rainfall. Following record precipitation totals over Cumbria during the first week, with extensive flooding across northern England and southern Scotland, further heavy rainfall



Figure 1. Places referred to in the text.

during the last week fell on already saturated ground. This led to renewed flooding in the north, and topped up monthly rainfall totals to new record levels in north Wales and in Cumbria (references, this issue).

Figure 1 shows the locations of places referred to in the text. Figure 2 shows daily mean temperatures for each day of December 2015 relative to the 1981–2010 average. Temperatures were occasionally near or below average across parts of Scotland, but the month was dominated by well above-average temperatures, entirely so for southern England and particularly in spells from 1 to 8 and 15 to 30 December. Figure 3 shows the hourly temperature record from two widely-separated sites in southern England (which happen to be located where the two authors are based), namely Exeter (Devon) and Reading (Berkshire); the 1981–2010 mean maximum and minimum tempera-

tures for December are also shown for comparison.

Temperatures reached or exceeded 16°C on several days during the month, most widely on the 16th, 18th and 19th. Amongst the highest temperatures recorded were 17.5°C at Llanfairfechan in north Wales (a COL Grade A site<sup>1</sup>) and 15.5°C at Chivenor (Devon) and Gogerddan (Ceredigion) on 7 December; 17.2°C at Teignmouth (Devon) and at Achnagart and Plockton (both Highland), and 16.7°C at St Athan (South Glamorgan) on 16 December; 16.6°C at Achnagart (Highland) and Prestatyn (Denbighshire) and 16.3°C at Leeming (North Yorkshire) on 18 December (Figure

<sup>1</sup> Climatological Observers Link (COL) Grade A sites are those where instruments, siting and exposure conform to Met Office guidelines, although these do not form part of the official Met Office climate network.

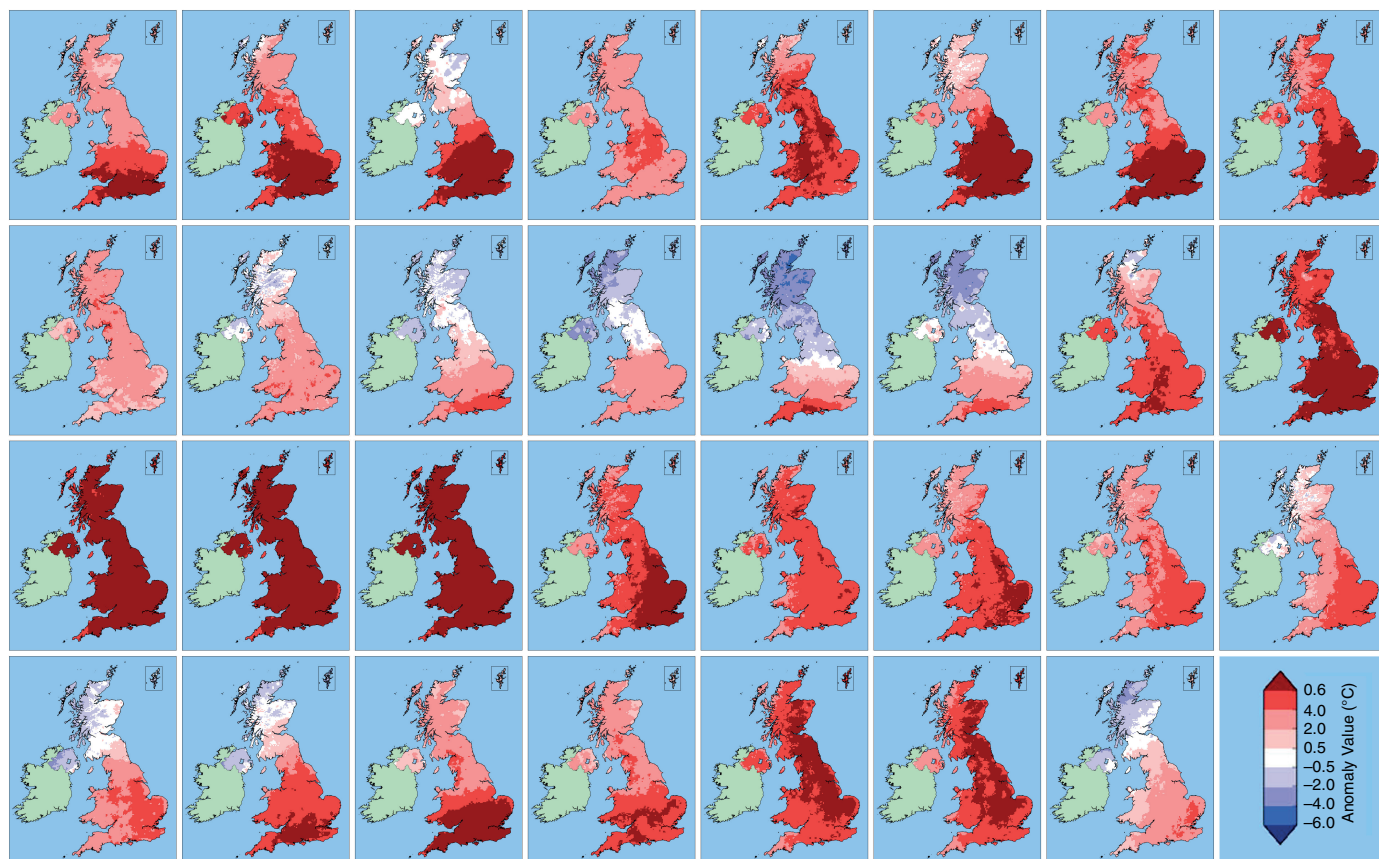


Figure 2. Daily mean temperature anomalies for each day of December 2015 relative to the 1981–2010 average (see last panel for scale). Top row, 1–8 December; second row, 9–16 December; third row, 17–24 December; bottom row, 25–31 December, and scale.

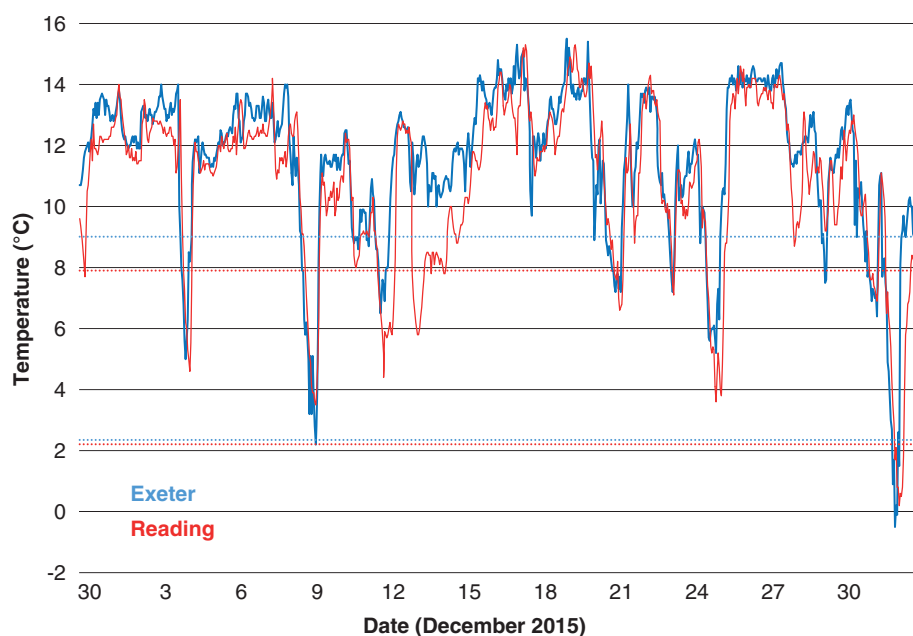


Figure 3. Hourly temperature record ( $^{\circ}\text{C}$ ) from Exeter Airport, Devon (blue line,  $50.74^{\circ}\text{N}$ ,  $3.40^{\circ}\text{W}$ , altitude 27m above mean sea level (AMSL) and Reading, Berkshire (red line, University of Reading Atmospheric Observatory,  $51.44^{\circ}\text{N}$ ,  $0.94^{\circ}\text{W}$ , 66m AMSL) for December 2015. The 1981–2010 December mean daily maximum and mean daily minimum temperatures for each site are also plotted for comparison in dotted lines using the same colour convention. The sharp downward spikes are associated with brief periods of clear skies at night.

4 illustrates the synoptic situation on this date);  $17.1^{\circ}\text{C}$  at Gravesend (Kent),  $16.7^{\circ}\text{C}$  at Prestatyn (Denbighshire) and  $16.5^{\circ}\text{C}$  at Morden (south-west London,

COL A) and Boulmer (Northumberland) on 19 December;  $16.1^{\circ}\text{C}$  at Llandsadwrn (Anglesey, COL A) on 27 December and  $16.1^{\circ}\text{C}$  at Poolewe (Wester Ross) and  $15.6^{\circ}\text{C}$

at Bridgefoot (Cumbria) on 28 December. New maximum December temperature records were established widely, including at Oxford and Durham, where comparable records commenced in 1853 and 1881 respectively (Table 1).

Persistent cloud cover meant that nighttime temperatures were often also unusually high, particularly across England and Wales. Remarkably, almost all locations in England and Wales south of Lincolnshire recorded no air frosts during the month; these districts would expect between 10 and 15 in a normal December. At the University of Reading, where temperature records commenced in 1908, this was the first December on record without a single air frost. Indeed, many places recorded at least one night with a minimum temperature above  $11^{\circ}\text{C}$ , while some nights in southern England remained above  $13^{\circ}\text{C}$  in places. Amongst the highest 0900–0900 UTC minimum temperatures were  $13.2^{\circ}\text{C}$  at Exeter Airport on 17 December and at Heathrow on 27 December. As with maximum temperatures, new record high minimum temperatures for December were established quite widely, including several sites with more than 60 years of records (Table 2). The exceptional mildness of the month brought out many spring-flowering plants weeks or even months early, as illustrated in Figure 5.

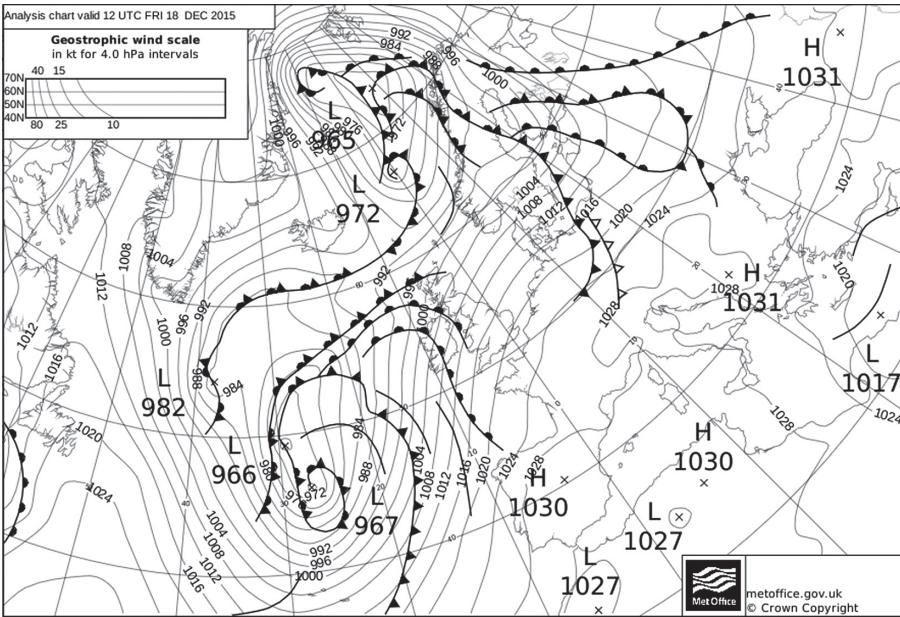


Figure 4. North Atlantic surface analysis chart for 1200 UTC on 18 December 2015, showing a southwesterly airstream bringing humid and exceptionally warm air to the UK. Daily maximum temperatures reached 14–16°C widely across the UK on this date, 7–9 degC higher than might be expected at this time of year: 17.2°C was reached at Teignmouth, Devon. (Source: Met Office; © Crown Copyright.)

## Monthly temperature anomalies during December 2015

Long-term weather records tend to be broken by a narrow margin, but not so for December 2015. In the CET series from 1659, this was not only by far the mildest December on record (Figure 6), but the CET value of 9.7°C was the warmest in the series by a margin of 1.6 degC from the next warmest Decembers (those of 1934 and 1974). In places, the gap was even larger – at the University of Reading observatory site, December 2015 was 2.7 degC milder than the previous mildest Decembers in Reading (also 1934 and 1974), on a record dating back to 1908. Here, December 2015 also saw the largest positive anomaly of mean temperature with respect to the current 1981–2010 normal of *any* month on the record (+5.8 degC), almost 2 degC above the previous highest anomaly (+3.9 degC, in April 2011). In the CET series, the December 2015 mean temperature anomaly of 5.1 degC easily exceeded the previous highest positive

**Table 1**  
A selection of long-period sites where new December 0900–0900 UTC maximum temperature records were established in 2015.

Site	December 2015 highest maximum (°C)	Date of December 2015 highest maximum	Previous December highest maximum (°C)	Date of previous record	Records commenced
Oxford	15.9	18	15.2	2 December 1985	1853
Durham	15.9	19	15.1	22 December 1991	1881
Bradford (West Yorkshire)	15.8	18	15.3	1 December 1985	1908
Buxton (Derbyshire)	13.7	18	13.3	31 December 1925	1914
Rothamsted (Hertfordshire)	15.3	19	14.4	1 December 1939	1914
Balmoral (Aberdeenshire)	14.2	18	13.7	13 December 1998	1914
Woburn (Bedfordshire)	16.0	19	15.7	2 December 1985	1914

**Table 2**  
A selection of long-period sites where new December 0900–0900 UTC minimum temperature records were established in 2015.

Site	December 2015 highest minimum (°C)	Date of December 2015 highest minimum	Previous December highest minimum (°C)	Date of previous record	Records commenced
Bradford (West Yorkshire)	11.6	17	11.5	29 December 1987	1908
Reading (Berkshire)	12.8	27	12.4	3 December 1985	1908
Hastings (East Sussex)	12.3	20	11.9	12 December 1994	1930
Plymouth (Devon)	12.7	27	12.5	3 December 1985	1920
Heathrow (Greater London)	13.2	27	12.9	3 December 1985	1948
Teignmouth (Devon)	13.0	27	12.8	12 December 1961	1914





Figure 5. A very early show of daffodils close to Maidenhead town centre, 13 December 2015. (© Roger Brugge.)

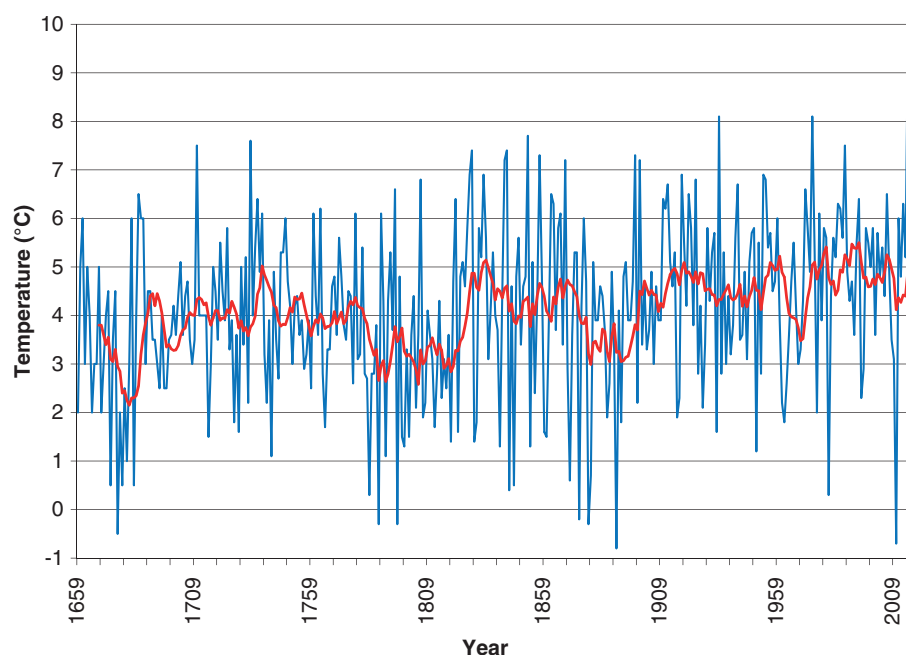


Figure 6. Monthly mean Central England Temperature (CET) series for December from 1659 to 2015 ( $^{\circ}\text{C}$ ). Yearly values are plotted in blue, with a 10-year running mean (plotted against year ending) in red overlay.

anomaly with respect to 1981–2010 for any month (3.7 degC in June 1846): as can be seen from Figure 7, it now represents an extreme positive outlier in this distribution. (Note that the outliers for extreme negative anomalies are dominated by January and February; for example, in the twentieth century, the top-ten lowest include the cold easterly-dominated months of January 1963 and February 1947. This long-tail of the distribution is not present for positive anomalies, making December 2015 a unique outlier).

Not surprisingly, December 2015 was also the mildest in the UK series from 1910 with a mean temperature of 7.9 $^{\circ}\text{C}$ , 4.1 degC above the 1981–2010 long-term average and 1.0 degC milder than the previous mildest December in that series (1934). (UK and national series are based upon 5 km gridded data from the Met Office climate network, using the methods of Perry and Hollis (2005). Monthly temperature and rainfall series are from 1910 and sunshine from 1929). It was also easily the mildest December for the national series for

England, and for Wales, while anomalies for Scotland and Northern Ireland were slightly lower at around 2.5 degC, making this the fifth- and third-mildest December in these series, respectively. The highest anomalies of mean temperature reached 5–6 degC above the 1981–2010 average in southern England (Figure 8), the absolute values being comparable, even a little above, those that might be expected in October, April, or even May. Mean monthly maximum temperature anomalies were highest across central England and East Anglia, whereas minimum temperature anomalies were highest across southern England, with anomalies here widely exceeding 6 degC. At Exeter Airport (Devon), the mean minimum temperature for November 2015 exceeded that for the previous May, but even more remarkably December 2015's mean minimum temperature (8.9 $^{\circ}\text{C}$ ) exceeded that for June 2015 (8.8 $^{\circ}\text{C}$ ), dropping behind only July and August in the annual ranking of monthly mean minimum temperatures for the year.

The month was also particularly dull, with less than 70% of average sunshine widely in the west; the UK recorded 72% of average sunshine in the dulllest December since 1989. Scotland was particularly cloudy, with just 68% of average sunshine: only 9.8h of sunshine was recorded during the month at Eskdalemuir (Dumfriesshire) and 7.2h at Poolewe (Wester Ross).

### Why was the month so mild and wet?

A strong North Atlantic jet stream brought a succession of extratropical cyclones and an almost unbroken feed of warm and moist air from much more southerly latitudes across the British Isles and northwest Europe: the mean axis of the 250 hPa jet lay across the British Isles during December 2015 (Figure 9(a)). At the surface, the mean MSL pressure pattern across the north Atlantic was strongly southwesterly over the British Isles (Figure 10(a)). The surface pressure gradient was much stronger than normal, the Icelandic low being about 12 hPa deeper than December 1981–2010 climatology, while the mean anticyclone over the central Mediterranean was displaced considerably eastwards and intensified with respect to climatology; pressure anomalies over the central Mediterranean were up to 14 hPa above normal as a result (Figure 10(b)). Larger-scale circulation patterns are described in more detail in McCarthy *et al.* (2016), in this issue.

### From one extreme to another – a comparison between the Decembers of 2010 and 2015

Within the space of just 5 years, the December CET has varied from  $-0.7^{\circ}\text{C}$

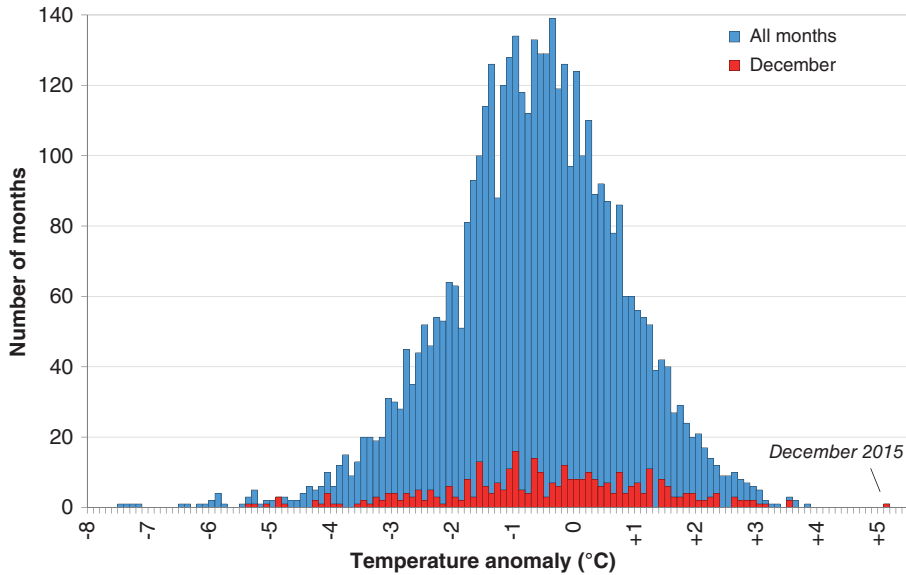


Figure 7. Histogram of CET monthly anomalies relative to the 1981–2010 average for all months from 1659 to 2015. The December 2015 value of +5.1 degC represents the largest positive anomaly relative to current 30 year normals of any month in the entire CET series.

in 2010 (5.3 degC below the 1981–2010 normal and the coldest December since 1890), to 9.7°C (5.1 degC above normal) in 2015, the mildest December in the CET series extending back to 1659. The two months thus differ in mean temperature by 10.4 degC, which is comparable to the difference in long-term average CET between January and July (12.3 degC over 1981–2010), or, looked at another way, the difference in mean December conditions between Stockholm (Sweden) and Lisbon (Portugal). In view of this extreme difference, it is instructive to compare the position of the jet stream and the orientation of the surface pressure field in both months. Figure 9(b) is the same analysis as Figure 9(a), and with the same contours and shading, but for December 2010; similarly, Figures 10(c) and (d) for December 2010 are directly comparable with Figures

10(a) and (b) for December 2015. The contrasting position of the jet stream (far south of the UK during December 2010, permitting a dominant easterly flow, compared with a much stronger southwesterly flow directly across the British Isles during December 2015) is immediately apparent, and with it the enormous difference in surface weather conditions between the two Decembers. A 'normal' climatology would reflect a mixture of both weather types that might be expected in a more typical December, instead of the domination by one or another as occurred in both December 2015 and December 2010. While December 2015 will be remembered as one of the most extraordinary months in the UK's observational records, this huge contrast once again serves to remind us of the very large annual variability which is a key characteristic of the UK's climate.

## Acknowledgements

This analysis builds upon the preliminary monthly summaries prepared by the Met Office's National Climate Information Centre; these summaries are issued routinely a few days after the end of each month. These can be found at <http://www.metoffice.gov.uk/climate>. The contribution of Mike Kendon was written in the course of his employment at the Met Office, UK, and is published with the permission of the Controller of HMSO and the Queen's Printer for Scotland.

## References

- Burt S.** 2016. New extreme monthly rainfall totals for the United Kingdom and Ireland: December 2015. *Weather* **71**: 333–338 (this issue).
- Burt S, McCarthy M, Kendon M et al.** 2016. Cumbrian floods, 5/6 December 2015. *Weather* **71**: 36–37.
- Kalnay E, and Co-authors.** 1996. The NCEP/NCAR reanalysis 40-year project. *Bull. Am. Meteorol. Soc.* **77**: 437–471.
- Manley G.** 1974. Central England temperatures: monthly means 1659 to 1973. *Q. J. R. Meteorol. Soc.* **100**: 389–405.
- McCarthy M et al.** 2016. The meteorology of the exceptional winter of 2015/2016 across the UK and Ireland. *Weather* **71**: 305–313 (this issue).
- Parker DE, Legg TP, Folland CK.** 1992. A new daily Central England temperature series, 1772–1991. *Int. J. Climatol.* **12**: 317–342.
- Perry M, Hollis D.** 2005. The generation of monthly gridded datasets for a range of climatic variables over the UK. *Int. J. Climatol.* **25**: 1041–1054.

Correspondence to: Stephen Burt

[s.d.burt@reading.ac.uk](mailto:s.d.burt@reading.ac.uk)

© 2016 Royal Meteorological Society

doi:10.1002/wea.2800

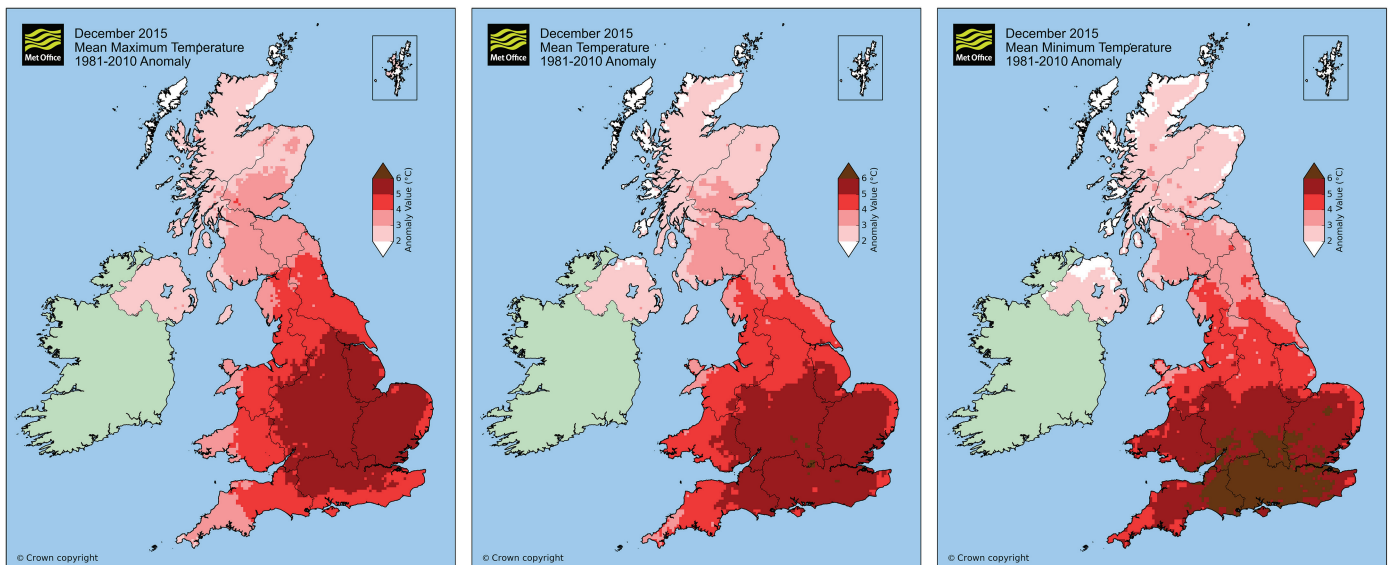


Figure 8. Left to right – anomalies (degC) of monthly mean maximum temperature, mean temperature and mean minimum temperature over the UK for December 2015.



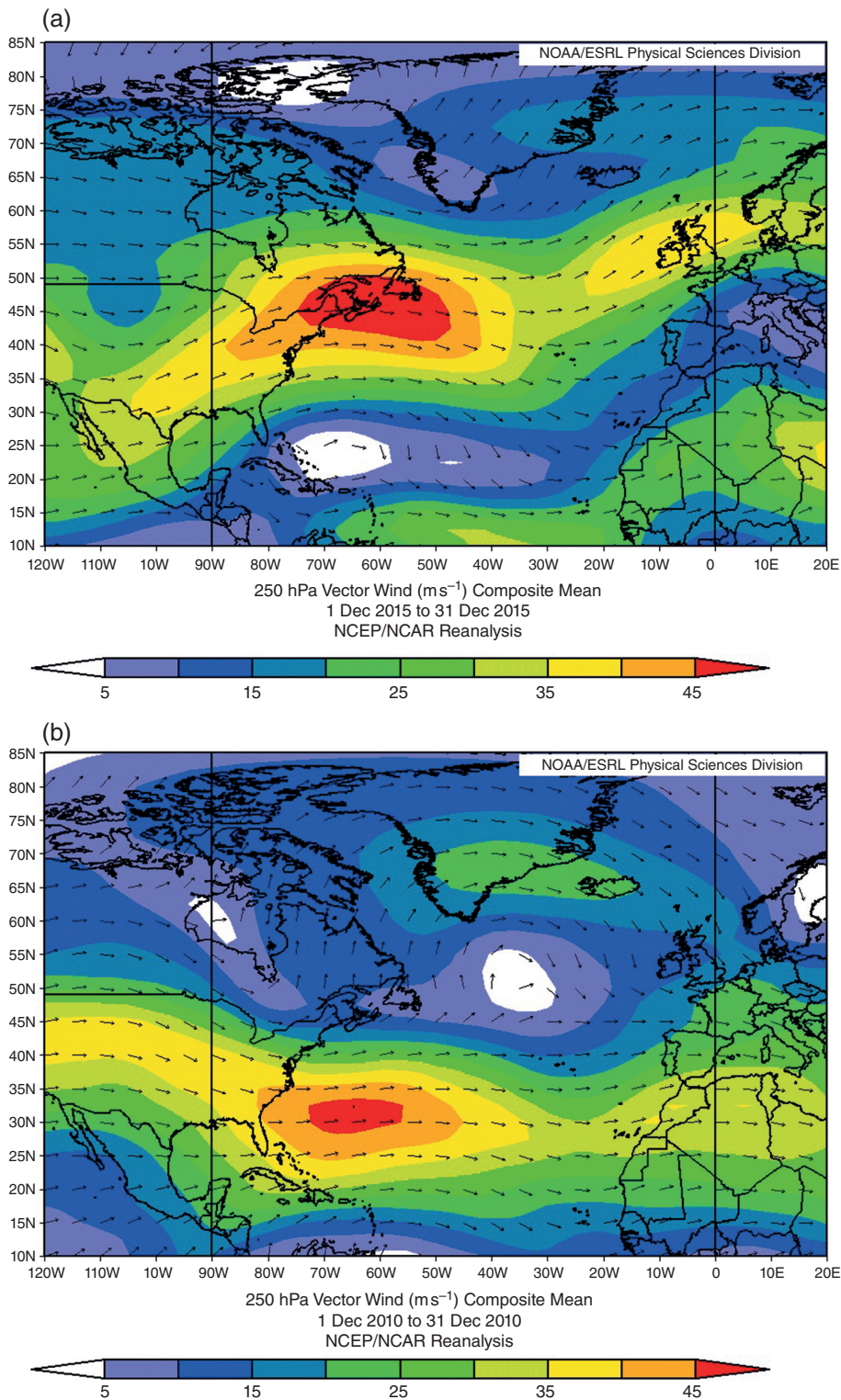


Figure 9. Vector mean winds at 250hPa ( $\text{m s}^{-1}$ ) over North America and the North Atlantic. (a) December 2015, showing a strong jet stream located directly over the British Isles. Compare with (b) – December 2010, showing the jet stream located well south of the British Isles. Scale and shadings are identical in both plots. These plots, and those in Figure 10, are provided courtesy of the NOAA/ESRL Physical Sciences Division, Boulder, Colorado from their website at <http://www.esrl.noaa.gov/psd/> (Kalnay et al., 1996).

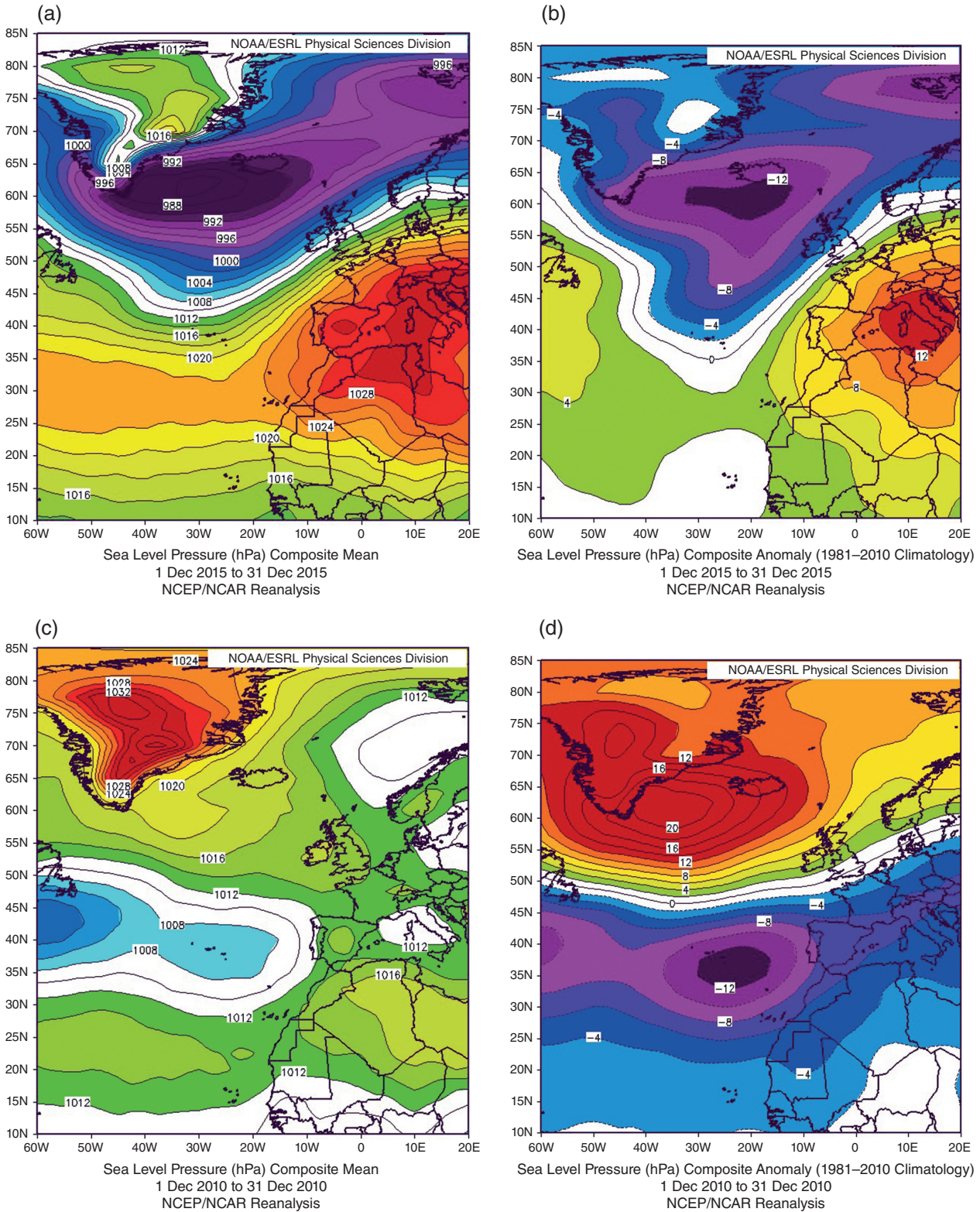


Figure 10. (a) Monthly mean sea-level (MSL) pressure (hPa) over the North Atlantic during December 2015, showing a strong southwesterly gradient across the British Isles. (b) Anomaly of monthly MSL pressure versus 1981–2010 climatology (hPa) during December 2015. (c) As for (a), but for December 2010, showing a broad northerly flow over the British Isles: compare with (a). (Scale and shadings are identical in both plots.) (d) As for (b), but for December 2010; compare with (b).



# Paper 8

*Capstone article as two-part PDF.*

**The Lowest of the Lows ...**  
**Extremes of barometric pressure in the British Isles, Part 1**  
*and*  
**The Highest of the Highs ...**  
**Extremes of barometric pressure in the British Isles,**  
**Part 2 – the most intense anticyclones**

By Stephen Burt. Part 1: *Weather*, 2007a, **62**, pp. 4-14,  
Part 2: *Weather*, 2007b, **62**, pp. 31-41.

*Bibliography #34 and #35. Word count Part 1, 6730; Part 2, 4245 (10,975 combined),  
excluding references.*

---

*The following content is reproduced by kind permission of the Publishers,  
John Wiley and Sons, under the terms of the Copyright Clearance Center's RightsLink®  
license number (Part 1) 5100131143902 and (Part 2) 5100130912336 dated 1 July 2021*





# The Lowest of the Lows . . .

## Extremes of barometric pressure in the British Isles,

### Part 1 – the deepest depressions

#### Stephen Burt

Stratfield Mortimer, Berkshire

Extremes of barometric pressure in the British Isles are reasonably well-known, but the synoptic documentation of many of these events are buried in century-old volumes not readily available. The purpose of this paper is to present brief accounts of several of the deepest depressions known to have crossed the British Isles within the period of instrumental records, together with accounts of associated weather, and where possible 'reconstructing' charts in the light of modern synoptic analyses for the older events.

Prior to about 1914 most measurements of pressure were made in inches of mercury (inHg), but all information in this paper is presented in contemporary units – with pressures reduced to mean sea level unless otherwise stated – and modern synoptic notation as far as possible. A complementary paper, to be published next month, continues the discussion for the most intense anticyclones on record.

#### Historical data

The first step in attempting to follow a sequence of weather events is to draw up a chart of observations made simultaneously over the area of interest. Prior to the first issue of the *Daily Weather Report* on 3 September 1860, there were no routinely published synchronised observations in tabular form covering the British Isles. For a few notable storms before 1860, contemporary writers documented wind, weather and barometric observations from a number of sites, sometimes in reasonably complete 'case history' studies: these can be used to infer the position and movement of the major synoptic features. From 1860 to 1980 (when the publication was discontinued), the British Met Office's *Daily Weather Report* provided a unique and lasting meteorological heritage, on which any account of this kind of necessity draws to a very considerable extent; many of the observations and charts are based upon this source (hereafter

referred to as the *DWR*), often augmented with additional observations from contemporary published accounts. Since 1980 chart data have been obtained from the London Weather Centre *Daily Weather Summary* (*DWS*), from archived Met Office working charts or from online sources.

The references quoted are usually contemporary accounts published shortly after the events to which they refer. Subsequent papers on similar events often refer to the same storm, but unless new information or analyses are presented in the later paper only the original reference is quoted here.

#### How low is low?

The lowest reliably documented sea-level barometric pressures on Earth have all been

recorded close to the centres of intense tropical storms. Lowest on record anywhere in the world is the 870 mbar recorded by a USAF aircraft dropsonde in the eye of typhoon *Tip* about 500 km west of Guam at 16° 44' N, 137° 46' E on 12 October 1979, and there are a handful of other occurrences below 900 mbar on record – for instance 877 mbar at 19° N 135° E in the eye of typhoon *Ida* on 24 September 1958, 882 mbar in the eye of hurricane *Wilma* on 19 October 2005, following a deepening of 88 mbar in 12 hours (National Weather Service 2005) and 885 mbar in the eye of hurricane *Gilbert* west of Grand Cayman Island in the western Caribbean on 13 September 1988 (Eden, 1988).

The lowest sea-level pressures outside of tropical storms occur in intense North



Figure 1. Locations of places referred to in the text

Table 1

Known occurrences of North Atlantic MSL pressures of 930 mbar or lower, last 200 years approximately. This table is probably incomplete.

Date	MSL barometric pressure	Location	Reference
4 February 1824	924 mbar <i>land observation</i>	Reykjavik, Iceland	Met Office, 1975, p. 59
5 February 1870	921.1 mbar <i>ship report</i>	Ship <i>Neier</i> at 49°N 26°W	<i>Shipping Gazette</i> , 9 February 1870, as reported in <i>Q. J. R. Meteorol. Soc.</i> , <b>28</b> , 1902, pp. 39–40 – also Burt, 1987
26 January 1884	925.6 mbar <i>land observation</i>	Ochertyre, near Crieff in Perthshire	This article
8 December 1886	927.2 mbar <i>land observation</i>	Belfast, Northern Ireland	This article
4 December 1929	925.5 mbar <i>ship report</i>	SS <i>Westpool</i> , Atlantic (exact location not stated)	Anon, 1933
3 January 1933	927.2 mbar <i>land observation</i>	Reykjavik, Iceland at 07h	Anon, 1933
19 December 1945	927 mbar approx. <i>central pressure</i>	Between Ireland and Iceland	<i>Daily Weather Report</i>
5 January 1983	930 mbar <i>central pressure</i>	Just south of Iceland	Author's contemporary notes
14/15 December 1986	916 mbar <i>central pressure</i>	South-east of Greenland at 61°N 32°W	Burt, 1987
24 December 1989	A little below 920 mbar <i>central pressure</i>	South-west of Iceland	Author's contemporary notes
2 March 1992	926 mbar <i>central pressure</i>	Off Newfoundland	Author's contemporary notes
10 January 1993	912–915 mbar <i>central pressure</i> NORTH ATLANTIC LOWEST ON RECORD	Between Iceland and Scotland near 62°N 15°W	Burt, 1993
1 February 2002	928 mbar <i>central pressure</i>	Near 60.5°N, 15°W at 1800 UTC	Author's contemporary notes
8 March 2003	928 mbar <i>central pressure</i>	Near 51° N, 39° W at 1200 UTC	Author's contemporary notes

Atlantic mid-winter cyclones. The deepest such depressions known (all those below 930 mbar) are shown in date order in Table 1. Perry (1983) reproduced a map of the lowest surface-level pressures known to have occurred over the North Atlantic over the period 1931–1965. Only the area south-west of Iceland was credited with pressures below 930 mbar, with a small closed isobar indicating 925 mbar or less centred about 60°N 20°W. It is very likely that modern observation and communications networks (including satellite information) and increasingly sophisticated computer models are far more likely to pin down the position and depth of such extreme depressions than would have been the case even half a century ago, but against this increased air traffic has resulted in a great reduction in surface observations from the North Atlantic shipping routes.

Within the period of reasonably reliable instrumental records (approximately 200 years), the barometer at mean sea level (MSL) has fallen to 950 mbar or below over

at least a part of the mainland of the British Isles (the United Kingdom and Ireland) or outlying islands on at least 30 occasions (Table 2): even in southern England MSL values below 950 mbar have been recorded twice. On only five of these occasions have barometric pressures below 940 mbar been reliably documented. Although, for obvious reasons, the majority of the events described affected northern and western districts, for geographical completeness both occasions when the pressure fell below about 950 mbar in southern England are also included. Locations of many of the places referred to in the text are given in Figure 1. Finally, minimum observed pressures within the last few decades are given for a selection of long-period stations and mapped for the British Isles.

### 25 December 1821

A long spell of unsettled weather in December 1821 reached a climax with the passage of an extraordinarily deep depres-

sion close to England's south coast on the morning of the 25th. This exceptional storm was one of the first to be mapped in a recognisable 'synoptic chart' format, and indeed the map of this storm published by Brandes (1826) can be regarded as one of the world's first weather maps (Monmonier, 1999). A student of Brandes, Heinrich Dove, formulated one of the earliest explanations of mid-latitude storms as resulting from the contest between opposing warm and cold air currents in his classic work *The Law of Storms* (Dove, 1828, transl. FitzRoy, 1858) following detailed analysis of this event amongst others. Dove listed wind and barometer observations (the latter as values of 'pressure differences') for 45 places in Europe – five in Britain – for four times (18 h on the 24th, 03 h, 10 h and 20 h on 25th) during this storm. Data for all four hours are available for 17 of the 45 stations, including an unspecified site in 'London'. 'Pressure differences' were quoted rather than actual station values as the accurate determination of station altitudes above mean sea level



Table 2

Known occurrences of MSL pressures below 950 mbar in the British Isles, last 200 years approximately.

This table is probably incomplete. For the dates shown in bold type a brief description follows in the main body of the text.

Date	Lowest known MSL pressure and site	Reference/s
<b>25 December 1821</b>	945.8 mbar North London	See text
<b>28 November 1838</b>	931.2 mbar Limerick (? MSL ?), 941.5 mbar Armagh	See text
<b>7 January 1839</b>	c 931 mbar Sumburgh Head, Shetland	See text
<b>13 January 1843</b>	948-949 mbar Markree, Co. Sligo	See text
27 December 1852	947.6 mbar Culloden, Inverness 1100h	Buchan, 1884
22 November 1865	944.8 mbar Dolgellau, North Wales	<i>British Rainfall</i> , 1865 p. 42
<b>31 December 1865</b>	945.5 mbar Monach Lighthouse, Hebrides	See text
19 January 1872	946.5 mbar Sumburgh 15h	<i>Daily Weather Report</i>
9 March 1876	946.1 mbar Wick 18h	<i>Daily Weather Report</i> , Symons, 1876, Met Office 1973
<b>11 November 1877</b>	939.7 mbar Monach LtHo, Hebrides	See text
<b>26 January 1884</b>	925.6 mbar Ochertyre, nr Crieff <i>BRITISH ISLES RECORD LOWEST</i>	See text
<b>8 December 1886</b>	927.2 mbar Belfast	See text
14 October 1891	946.8 mbar Cawdor Castle, NE Scotland	<i>Daily Weather Report</i>
29 December 1899	950 mbar Lleyn Peninsula, North Wales	Symons, 1900
<b>6 December 1929</b>	950 mbar Valentia, SW Ireland	<i>Daily Weather Report</i>
1 February 1938	948.0 mbar Deerness, Orkney 0915h	<i>Monthly Weather Report Annual Summary</i>
18-19 December 1945	948.6 mbar Valentia 00h 18/19th	<i>Daily Weather Report</i>
<b>4 February 1951</b>	942.3 mbar Midleton, Cork	See text
30 November 1954	947.1 mbar Midleton, Cork 00h 29/30th	<i>Daily Weather Report</i>
<b>1 December 1966</b>	942.6 mbar Carrigans, N Ireland	See text
<b>20 December 1982</b>	937.6 mbar Stornoway	See text
2 January 1984	948 mbar Hebrides	Author's notes
13 January 1984	949 mbar Moray Firth, Kinloss 950.6 mbar 06h	Wheeler, 1984
9 February 1988	944.0 mbar Benbecula, Western Isles	Author's notes
<b>25 February 1989</b>	948.8 mbar Portland, Dorset	See text
<b>16-17 December 1989</b>	942.8 mbar Cork Airport	See text
25 January 1990	949 mbar near Edinburgh, 16h	Author's notes
<b>17 January 1995</b>	943.2 mbar Belmullet, north-west Ireland	See text
25 December 1999	945.6 mbar Aberdeen/Dyce 01h, 944.4 mbar Lerwick 07h	Table 3
11 January 2005	946 mbar North Rona, off NW Scotland, 2300 UTC	Author's notes

(MSL) and the methodology of reducing station-level barometer readings to those at MSL still lay many years in the future. Unfortunately the datum from which the difference has been taken was not specified (it was probably mean annual station-level pressure averaged over several years). For this reconstruction modern MSL pressure normals were used where available (from [www.worldclimate.com](http://www.worldclimate.com)), and for the others a datum of 1016 mbar (representing a reasonable average for Europe in December) was assumed: the noted departure was subtracted to obtain an approximate MSL value for each station. There are obvious sources of error (of up to about 5 mbar) in doing this, but plotting the values so obtained together with the tabulated information on wind

directions yielded a reasonably self-consistent series of charts for western Europe. Some inferences on airmass types can be made from other notes in Dove's paper – for instance, the observations of a shade temperature of 31.4°C on the 24th at Tolmezzo in northern Italy and the fact that at Geneva the temperature at 0130 on the 25th was 15.7°C, together with an “unusual” degree of heat being noted at Paris, Boulogne and Hamburg, would indicate an exceptional temperature contrast over western Europe. A tentative analysis for 03 h is shown in Figure 2; the pressure in London was given by Dove as 66 mbar below datum level at this hour, which by the reasoning above suggests MSL pressure around 948 mbar. This is supported by Luke Howard's

observation\* at Tottenham at 05 h (Howard 1822) of 942.4 mbar (corrected to MSL 945.8 mbar – see also Figure 3) and 948.7 mbar (at MSL) at the same time at

\* Luke Howard, better known for his work on cloud nomenclature (Hamblyn, 2001), made observations with an early self-recording mercury 'clock-barometer' (barograph) in Tottenham from 1814 to 1828 and published many of his observations in *Barometrographia* in 1847. For more details, see Blench (1963). Symons (1892) quotes 945.5 mbar at Ackworth, near Pontefract, on this same date: but this may be a rare location attribution error on his part – Luke Howard owned a small estate at Ackworth, but his observations on 24–25 December 1821 were clearly stated by him as being made in north London.

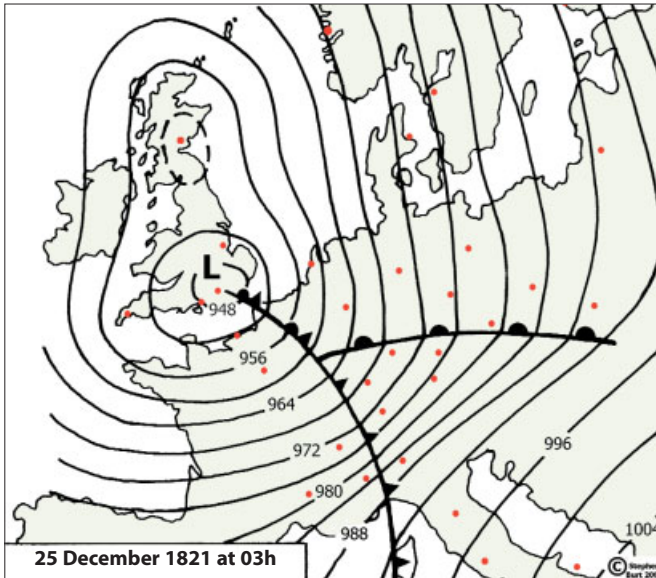


Figure 2. Suggested synoptic situation at 03h on 25 December 1821. Locations of pressure observations are marked by red circles: see text for sources

Greenwich Observatory (Marriott 1884, p.121). At 06h at Epping, Essex (about 25 km north-east of London) it was 951.6 mbar, and at Sion House, Middlesex at 08h 956.7 mbar (Symons 1872, p.10, Marriott 1873). Both values are retrospectively corrected MSL values, although the latter value appears about 5 mbar too high. Hourly station-level pressures were noted at Epping for most of the 24-hour period commencing 16h on 24 December and are given in Howard's *The Climate of London* (1833, pp. 69–70). Howard noted 948 mbar (about 951 mbar at MSL) at 08h, and Dove's data implies about 960 mbar at MSL at 10h. This depression was without doubt the deepest to affect southern England during instrumental history – in London reasonably continuous records extend back almost 250 years. "We had no storm of wind of any consequence after this great depression . . . It appears by the papers, that a like state of the barometer was extensively observed at the same time on the Continent, and that very tempestuous weather attended it, far to the south of our island" (Howard 1833).

After rising 40 mbar by the 27th the barometer fell once more overnight 28/29 December to within 6–8 mbar of the 25 December values, before rising sharply some 65 mbar in the following three days.

### 28 November 1838

Rohan (1975) cites a reading of 931.2 mbar at Limerick in south-west Ireland (probably at Adare, a little south-west of Limerick, the home of the observer, Viscount Adare) as Ireland's lowest November barometer reading. Marriott (1873, p. 220) quoted the lowest reading then on record at Armagh in what is now Northern Ireland as 934.9 mbar

on this date, and stated, "... on this occasion the barometrical readings at the Ordnance Survey Office, Dublin, had ranged below 28 in. (948 mbar) for 24 hours, and, as might be expected with such an extensive depression, there had been no storm." The records from the Armagh Observatory for November 1838 (available online at climate.arm.ac.uk) show that the minimum value of 934.9 mbar was a station level pressure\*: correcting for observed temperature and known site altitude gives an MSL value close to 941.5 mbar. It is very likely that the Limerick value is also a station-level pressure and thus caution is required in accepting the veracity of the reading (although the MSL correction would be small, just 2–3 mbar). In contrast with the Dublin observation, at Armagh, "Gales from ESE" are noted in the observation register. No further details of the event are known.

### 6–7 January 1839

The depression of 6–7 January 1839 is remarkable for being the only known occurrence of a second cyclone below 940 mbar to cross the British Isles in a single winter season, only six weeks after the occasion described above. Rohan (1975, pp. 104–5) describes the havoc caused by this storm, and concludes, "it . . . probably caused more widespread damage in Ireland than any storm in recent centuries. This night has become legendary as 'The Night of the Big Wind'."

A detailed account of the storm was assembled to mark its 150th anniversary by the Irish Meteorological Service (Shields and

\* Ten readings were taken between 3.35 a.m. and 11 a.m.; the minimum was noted at 7.55 a.m.

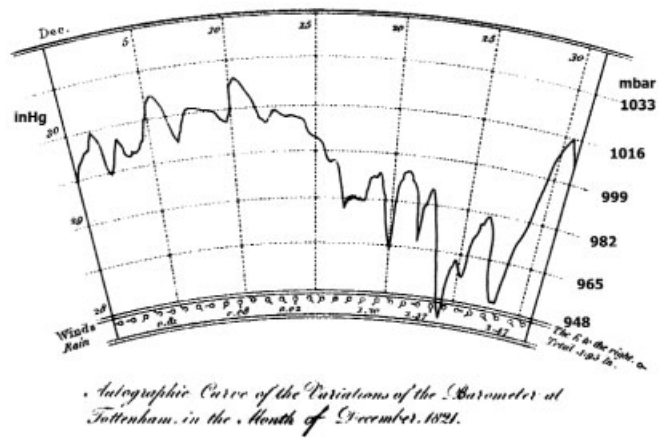


Figure 3. The world's first published barograph chart – Luke Howard's 'clock-barometer' (mercury barograph) record from Tottenham, north London, for December 1821, showing the extreme depth of the depression of 25 December. The values are not corrected to MSL (add about 4 mbar) and the original scale is in inches of mercury (inHg) – millibar equivalents are given on the right. From Howard (1822), Plate XIII

Fitzgerald 1989) to which readers are referred for a full account of the severity of the gale, which caused immense damage and considerable loss of life in Ireland, Scotland and north-west England. More recently Burt (2006) analysed the extant station-level barometer readings from this storm and attempted retrospective corrections to MSL pressures (correcting station-level pressures to MSL did not become normal practice in the British Isles until the late 1850s) and reconstructed synoptic charts. The suggested analysis for 09h on 7 January 1839 is shown as Figure 4 (from the original in Burt 2006, *op. cit.*, Figure 6). The central pressure of the depression probably reached its minimum, around 930 mbar, about this time.

The depression arrived from the Atlantic at 40–50 knots from the west-south-west,

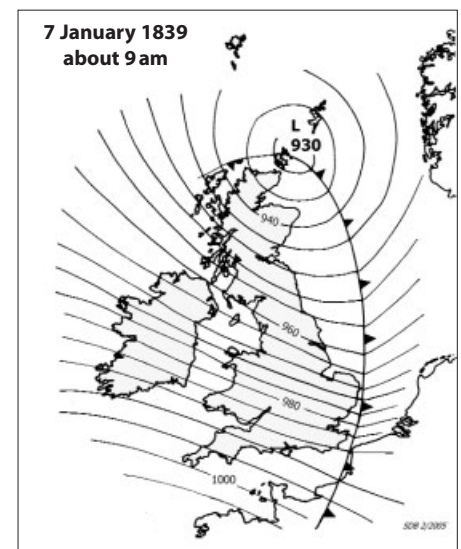


Figure 4. Synoptic situation at 09h on 7 January 1839, from Burt (2006)

slowing considerably as it neared its greatest depth off northern Scotland (Lamb 1991). It passed between Orkney and Shetland before moving out into the North Sea and eventually into the Baltic. The lowest known MSL-corrected barometer reading is 931 mbar at Sumburgh Head at 14h on 7 January 1839: this is the third-lowest barometric pressure yet recorded in the British Isles.

### 13 January 1843

A very deep depression crossed the north of Ireland and southern Scotland during the late morning/early afternoon of Friday, 13th January, 1843, travelling towards the east-north-east at about 30 knots. A number of pressure values, reduced (largely retrospectively) to MSL, are given in Symons (1892) who reprinted the contemporary account of William Ick of the Birmingham Philosophical Institution. Ignoring the values obviously in error and plotting the observed minima and times of minima we can ascertain that at noon the centre of the depression was located in the Southern Uplands of Scotland, with MSL pressure probably a little below 950 mbar. It was probably filling, for at 0630h the barometer stood at 944 mbar at Markree, Co. Sligo, in north-west Ireland. (The observatory at Markree Castle stood about 37 m above MSL, which would require a barometric correction to MSL of approx 4.5 mbar, and thus the true MSL pressure at this time was probably 948–949 mbar). Ick's account lists 13 pressure readings made at a wide range of locations, but once again it is difficult to be sure of the lowest MSL (rather than station-level) values reached in this storm as the heights of the observing locations are unstated (in all probability, they were not known at the time). The lowest 'indisputable' MSL value accepted by Symons was 950.5 mbar at Makerstown Observatory near Kelso in Roxburghshire (now Borders Region, Scotland) at 1315h. In London, MSL pressures of 956.7 mbar were noted at 1245h at Somerset House, and 957.2 mbar at Greenwich at 1253h. In Cambridge the MSL minimum was 955.4 mbar at 1335h, and in Norwich 955.1 mbar at 1400h (the latter from Marriott 1873). No other details of the weather are available but Ick's contemporary account does not specifically mention storm damage as perhaps might have been expected. At Carlisle, which lay close to the track of the depression, there were "only a few gusts of wind between midnight of 13th and sunrise on 14th".

### 31 December 1865

A long spell of anticyclonic weather during December 1865 – with the barometer reaching 1045.4 mbar at Bodmin on the

15th – gave way to a very unsettled few days late in the month, with a number of deep depressions crossing northern districts from the 27th onwards. At Aberdeen the MSL pressure was 969 mbar at 03h on the 27th, rose to 1003 mbar on 28th then fell to 968 mbar at 21h on the 29th. At Monkstown in Ireland the pressure on the 28th fell from 1007 to 977 mbar during the day (Symons, 1865). During the early hours of 31 December an intense system passed across the northern Hebrides moving north-eastwards, giving a very severe gale and widespread thunderstorms. Since the storm occurred on a Sunday (for which the *DWR* was not issued at that time) virtually the only record we have of the storm is the table of 'lowest readings' given by Cunningham (1866): he did not state, however, which (if any) were true 'minima' and which were merely the 'lowest observed', although it is stated that the readings had been corrected to MSL. Plotting these values given on a map of north-west Scotland shows a number of values clearly in error – in both directions – but a sufficient degree of corroboration exists to permit an educated guess at the maximum depth attained. The value of 935.7 mbar at Hoy Lighthouse in Orkney appears much too low in comparison with readings on other islands in the group (for instance, 949.2 at North Ronaldsay), and the reading of 937.7 mbar at the Butt of Lewis Lighthouse is also much lower than its neighbours. The Hoy Lighthouse reading was also disbelieved by Symons (1884), although he appeared to accept the Butt of Lewis value. The lowest credible MSL values would appear to be the 945.5 mbar at Monach Lighthouse, off the west coast of North Uist, and 948.2 mbar at Ushenish (now Usinish), South Uist. However, there is insufficient extant information to attempt a more detailed synoptic reconstruction of this storm.

### 11 November 1877

An unsettled spell of weather at the beginning of November 1877 culminated in a series of very deep depressions passing close to north-west Scotland and bringing widespread severe gales or storm-force winds. At Stornoway the barometer stood at 968.5 mbar at 08h on 11 November but just 946.2 mbar at 18h, recovering only slowly to 953.6 mbar by 08h next morning. The minimum at Stornoway was 943.4 mbar (*Daily Weather Report*); the lowest observed pressure was 939.7 mbar once again at Monach Lighthouse, west of the Outer Hebrides (Met Office, 1973).

### 26 January 1884

A protracted spell of mild, quiet settled weather in mid-January 1884 (the baro-

meter reaching 1039.8 mbar at Haverfordwest on 15th) gave way on 19th to one of the stormiest periods of weather ever experienced in Britain. A rapidly moving depression passed over the north of Scotland on 19/20th, causing a pressure fall of 32.5 mbar in four hours at Stornoway: in the Orkney Islands hourly mean winds reached 80 knots. This depression was followed by another on the 20th, and by a third on the 21st, pursuing very nearly the same course. On 23 January a deep depression moved east across southern Scotland causing considerable loss of life and damage to property: at Seathwaite in Cumbria 188 mm of rain fell in the three days ending on the 23rd. Another depression, below 960 mbar, passed to the north of Scotland overnight on the 24/25th: this was followed by an exceptionally deep depression on 26 January.

Marriott (1884) gives a detailed account of this storm, and presents three-hourly isobaric charts upon which the analysis presented here is partly based. The storm can be traced to the development of a frontal wave off Newfoundland, with a central pressure around 1010 mbar, on the morning of the 25th, the system then travelling 1500–1600 nautical miles in the following 24 hours (mean forward speed around 65 knots). At noon on 26 January the centre of the depression lay off north-west Ireland, with central pressure about 945 mbar. Thereafter it continued to deepen and move north-eastwards across Northern Ireland and central Scotland at about 25 knots during the afternoon and evening, reaching a maximum depth of about 925 mbar. At midnight the centre lay near Aberdeen, at 927 mbar. The lowest pressure reported was 925.6 mbar\* at Ochertyre, near Crieff, Perthshire at 2145h (Buchan 1884). Buchan's note in *Nature* does not quote the source, but Ochertyre (56°23'N, 3°53'W, 101 m AMSL – observer Capt. C. M. Dundas, RN) was a second-order station of the Scottish Meteorological Society making observations from 1873 to about 1915. This value, 925.6 mbar, remains the lowest unchallenged MSL pressure reading yet recorded in the British Isles. Corroborative evidence is afforded by the (MSL) readings of 927.2 mbar at Aberdeen at 2330h, 927.3 mbar at Dundee at 2230h, 927.4 mbar at Culloden, near Inverness, at 2300h, 927.5 mbar at Oban at 2100h, 928.8 mbar at Glasgow and 929.6 mbar in Edinburgh (Buchan 1884, Symons 1884). Contemporary sources agree that these were the lowest pressures recorded in Scotland for at

\* The figure is often erroneously quoted as 925.5 mbar (the conversion of 27.33 inHg) whereas Buchan gives the lowest observed value as 27.332 inHg, which converts more precisely to 925.6 mbar.



## The January 1884 storm on Ben Nevis

The Ben Nevis Summit Observatory (Roy 1983, 2004) was in operation during this storm, and features of the weather observed there may be of interest – this account has been taken from Marriott (1884). The observed pressure – corrected for temperature – at station level, 1343 m, fell from 813.8 mbar at noon to 784.7 mbar at 2030, the lowest point reached. This was only 6 mbar above the lowest point on the scale although the instrument had been especially constructed for the Observatory. By midnight it had risen to 790.0 mbar. The sea-level pressure at Fort William, only 7 km away, was 930.1 mbar at 2030. At noon on the summit of Ben Nevis the temperature was  $-9.2^{\circ}\text{C}$ : but thereafter no outdoor observations were possible until 22 h owing to the fury of the gale. At noon the wind was south-east, 60 knots: during the afternoon it increased to above 80 knots. At 19 h it was south-east 65 knots, at 20 h south-east 55 knots, but at 21 h calm: the depression must have passed very close to the observatory. At 22 h it was east-north-easterly, 27 knots. Snow, fog and severe drifting were noted all day. Marriott gives the following description of an eventful day in the observatory:

“In connection with the thermometer readings, it may be mentioned that at 13 h Mr Omond made an attempt to get at the screen. Tying a rope round his waist, the end of which was held by an assistant within the porch, Mr Omond crept cautiously out from the shelter of the Observatory; but so great was the violence of the gale that he could make no headway against it, and was glad to return. At 19 h another attempt was made. The observers got as far as the screen, but found it impossible to read the thermometers owing to the blinding drift lashing in their faces. At 22 h it was calm enough for Mr Omond to go out alone, and the reading of  $22.8^{\circ}\text{F}$  [ $-5.1^{\circ}\text{C}$ ] was obtained.”

26 January 1884  
at 18h

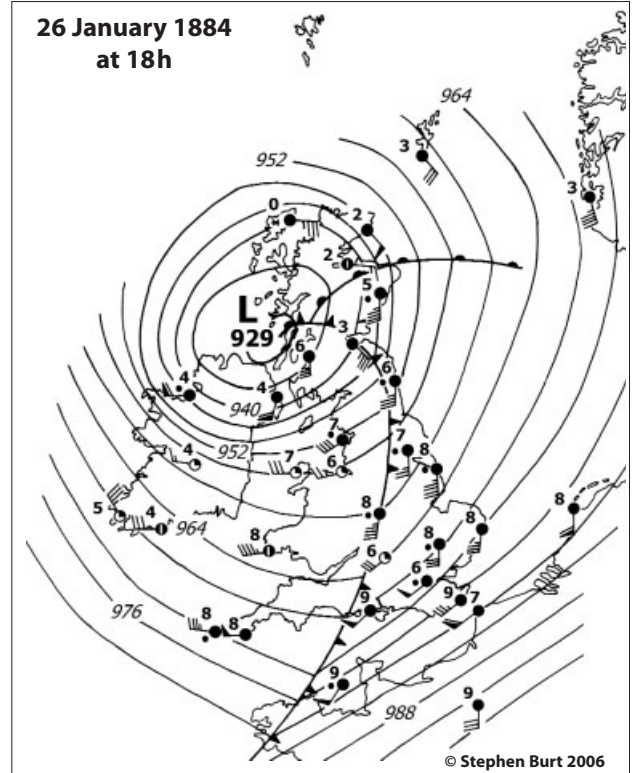


Figure 5. Synoptic situation at 18h on 26 January 1884. See text for sources

© Stephen Burt 2006

least the previous 120 years. The lowest recorded value in Ireland was 936.6 mbar at Markree, Co. Sligo which remains the lowest on record for January in Ireland (Rohan, 1975): however, 933.1 mbar was reported from Waringstown, Co. Down about 50 km south-west of Belfast (Symons 1884, p. 16). The lowest value at Greenwich Observatory on this day was 965.8 mbar at 1935 h (Marriott, 1884, p. 121).

The 1884 accounts of Marriott and Symons contain descriptions of a line of violent thunderstorms, widely accompanied by hail, together with a violent windshift and pressure jump, which would now be recognised as the cold front. (Indeed, some of the comments in the discussion recorded in the Society's *Quarterly Journal* following the presentation of Mr Marriott's paper seem to predate the Bjerknes frontal ideas by 30 years). The chart for 18h (Figure 5) is based on values given in the *DWR*, in Marriott's paper, and such information as time of thunderstorms (indicating the passage of the cold front): 40 values of pressure were available.

A violent gale was experienced in all areas of Britain, but was most severe in northern England, the north of Ireland (where the damage rivalled 1839 in places) and in the south of Scotland – where over a million trees were blown down on one estate alone (Symons, 1884, p. 15). Brodie (1902, p. 150) gives a short account of the storm, and refers to it as having the steepest pressure gradient (15 mbar per 100 km) found over the British Isles to that date. The mean

hourly wind speed reached 66 knots at Alnwick in Northumberland and 61 knots at Holyhead; even at Kew a mean of 46 knots was reached during the evening. There was widespread disruption of services – very few observations appear in the following day's *DWR*, which is annotated 'telegraphic communication interrupted'.

### 8 December 1886

Another very disturbed spell in December 1886 saw a succession of intense depressions cross north-west Europe. A depression forming in an area of marked thermal contrast in mid-Atlantic on 7 December merged with a depression that had formed near south-west Iceland, and the combined storm deepened rapidly to form a single system with a central pressure close to 930 mbar off north-west Ireland on the morning of 8 December (Lamb, 1991). The storm continued to deepen and to slow as it crossed northern Ireland, the barometer falling to 927.2 mbar at Belfast at 1330 h as the depression centre passed nearby. At the peak of the storm, at around 18 h on 8 December, the wind exceeded gale force on all windward coasts between southern Norway and northern and western Spain. At Fleetwood in Lancashire the mean wind speed remained above 30 mph (26 kn) for 65 consecutive hours, the highest hourly mean reaching 69 knots; near the peak of the storm, the lifeboats from Southport and St Anne's were both lost, and 27 of the 29 crew members perished.

An early account of the storm was given by Symons (1886) and a more detailed discussion by Harding (1887). The synoptic situation at 14h on 8 December 1886 shown in Figure 6 is based upon Harding's account together with observations and maps published in the *DWR*. The track of this storm was somewhat to the south of the January 1884 event and as a result new low barometric pressure records were established widely across the north of Ireland, southern Scotland and northern England. The lowest reliable pressure was the 927.2 mbar measured in Belfast at 1330h referred to above; however Harding (*op cit*) stated that he believed the true storm minimum over the north of Ireland was close to 924 mbar\*. The Belfast value is supported by the observations of 928.5 mbar at Mull of Galloway (1430h), 928.9 mbar at Armagh (1230h) and 929.2 mbar at Markree, Co. Sligo (1030h), at Aghalee (Lurgan) at 1230h and at Loch Ryan at 1600h. At Belmullet in north-west Ireland the MSL barometer at 08h stood at 933.9 mbar, having fallen 60 mbar since 18h the previous evening, with the wind at west-south-west Force 12 indicating that the

\* A reading of 922.5 mbar (corrected to MSL) was reported from Omagh in Co. Tyrone, about 90 km west of Belfast, at 13h (Buchanan 1886). Harding (1887, p. 211) stated that "undoubtedly the position of that station was in the direct track of the centre, and at the time when the depression was at its deepest" but that the graduation and calibration of the barometer concerned were not considered satisfactory enough "to quote the reading as trustworthy".

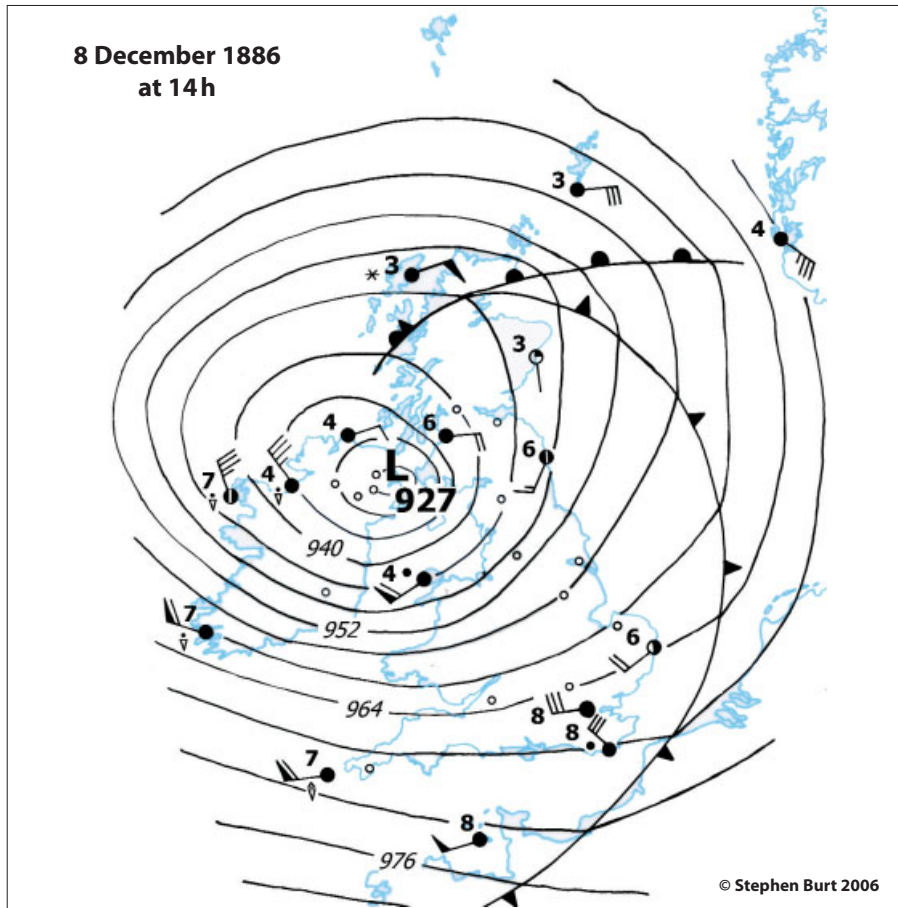


Figure 6. Synoptic situation at 14h on 8 December 1886; from observations in Daily Weather Report and in Harding (1887). Sites with pressure observations only are shown as small open circles.

depression centre lay to the north. At Stonyhurst in Lancashire, where the barometer fell to 940.4 mbar at MSL, the reading was "lower than at any time in the last 40 years" (and it has not been closely approached at any time since). In London the barometer fell to 958.2 mbar at Camden Square at 0445 on 9 December (Symons, 1886, p. 157), the lowest in London since 13 January 1843. This value was not bettered in London until 25 February 1989 (Burt, 1989).

#### 6 December 1929

On 6 December 1929 a deep low was centred not far off south-west Ireland; at Valentia the barometer stood at 966.9 mbar at 13h, 951.3 mbar at 18h and 950 mbar at 22h (by 01h 7 December it had risen 22 mbar in 3 hours, to 971.9 mbar). This depression achieved a notable depth in mid-Atlantic: on 4 December S.S. *Westpool* reported 927.9 mbar, although unfortunately the location of the observation was not stated in the account (*Meteorol. Mag*, **68**, p. 18).

#### 4 February 1951

On 31 January 1951 a depression developed on a very pronounced front in the Gulf of Mexico. By 0600 GMT on 2 February it was centred near the north-east United States at

46°N 71°W with central pressure 996 mbar. By 0600 GMT on 3rd it lay near 53°N 43°W at 985 mbar and after a further 24 hours it lay close to western Ireland with a central pressure about 944 mbar (Shellard and Douglas 1951). It was then occluded 500 km from its centre and its speed and rate of deepening were rapidly decreasing. Throughout its movement from the Gulf of Mexico to Ireland it was in a very strong thermal field which enabled it to combine rapid movement with sustained deepening.

By 1200 on 4 February the depression had temporarily developed two centres, one near Malin Head in the north of Ireland and the other near Cork, with central pressures of 944 and 942 mbar respectively. The depression subsequently filled and drifted north-eastwards. The lowest pressure reported was at Midleton, Co. Cork (about 40 km east of Cork) at 1500 GMT when the barometer stood at 942.3 mbar: this is the lowest on record for February in the British Isles (Met Office, 1973). At Cork the pressure had fallen 62 mbar in 30 hours. The surface synoptic situation at 1800 GMT is shown in Figure 7 (taken from Shellard and Douglas, p. 363). The depression was remarkable for the extent of low barometer readings, but did not produce any exceptional gales. Over the whole of Wales and all parts of England south of 53–54°N the pressure on this date was the lowest on record over the period 1949–88 (see Table 3 and Figure 11); the

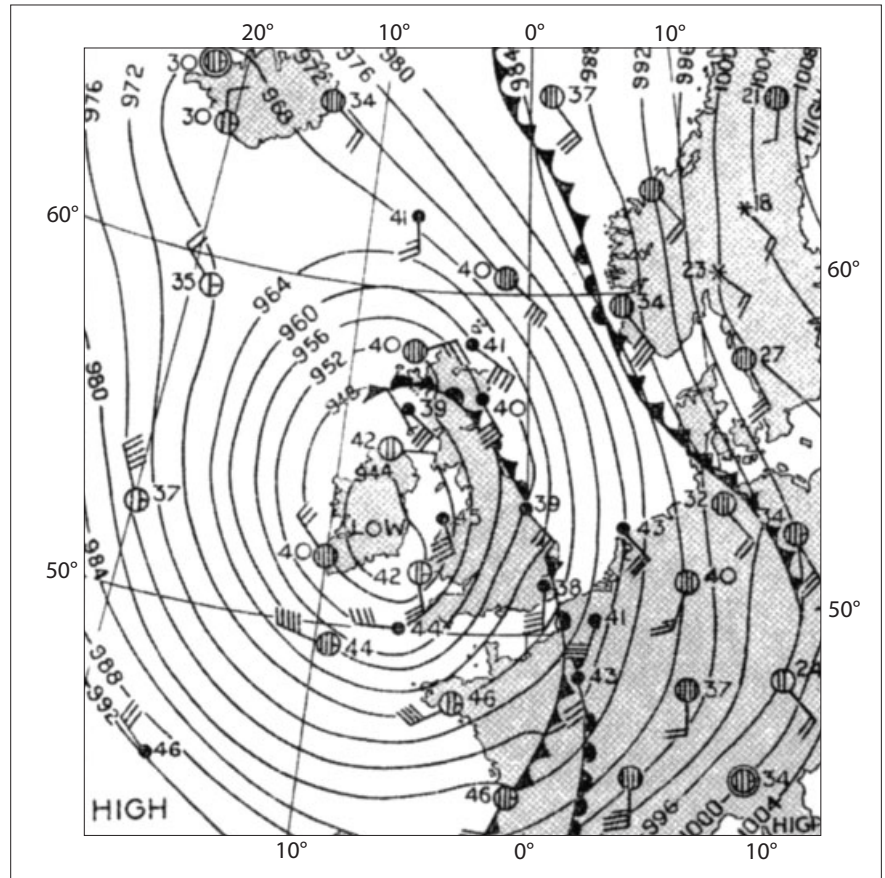


Figure 7. Synoptic situation at 1800 GMT on 4 February 1951, from Shellard and Douglas (1951)



Table 3

Lowest barometric pressure on record at a number of long-period hourly observing sites in the UK and Ireland (typically 40 years or more of computerised hourly or three-hourly observations available in the UK Met Office and Met Éireann data archives; where two or more stations are bracketed together, the lowest value from the combined record has been used). Slightly lower values may have occurred between observations. All times quoted are GMT.

Region and station	Period	Value/date	Source
<b>Northern Scotland</b>			
Lerwick	1957–2005	944.4 mbar 07h 25 Dec. 1999	1
Wick	1957–2005	942.6 04–07h 20 Dec. 1982	1
Cape Wrath	1957–9/1997	} 938.8 03h 20 Dec. 1982	1
Altnaharra	10/1997–2005		
Stornoway	1957–2005	937.6 * 0020h 20 Dec. 1982	1
<b>North-east Scotland</b>			
Kinloss	1959–2005	944.0 03h 20 Dec. 1982	1
Aberdeen/Dyce	1957–2005	945.6 01h 25 Dec. 1999	1
Edinburgh/Turnhouse	1957–10/1999	} 949.1 18h 1 Dec. 1966	1
Edinburgh, Gogarbank	11/1999–2005		
<b>East and north-east England</b>			
Tynemouth	1957–6/2001	} 949.5 00h 2 Dec. 1966	1
Newcastle W Ctr	7/2001–9/2005		
Albemarle	10–12/2005		
Waddington	8/1950–2005	956.7 17h 25 Feb. 1989	1
<b>East Anglia</b>			
Coltishall	11/1962–2005	953.9 23h 25 Feb. 1989, 00h 26 Feb. 1989	1
Marham	1957–2005	954.8 21,22,23h 25 Feb. 1989	1
<b>Midlands</b>			
Birmingham/Elmdon	6/1949–3/1999	} 953.9 00h 5 Feb. 1951	1
Colehill	4/1999–2005		
<b>South-east England</b>			
London/Heathrow	1949–2005	952.3 18,19h 25 Feb. 1989	1
Kew Observatory	1869–1953	959.3 05h 9 Dec. 1886	2
Greenwich Observatory	1814–1884	948.7 05h 25 Dec. 1821	3
South Farnborough	1957–2005	} 951.9 18h 25 Feb. 1989	1
	(no data 1/1974– 11/1983)		
<b>Western Scotland</b>			
Benbecula	1957–7/1996	939.7 23h 19 Dec. 1982	1
Tiree	1957–2005	944.7 13h 9 Feb. 1988	1
Glasgow - Renfrew/ Abbotsinch	1949–4/1966 5/1966–4/1999	} 947.6 18h 1 Dec. 1966	1
Bishopton	5/1999–2005		
Prestwick	1957–1/1997	} 945.2 18h 1 Dec. 1966	1
Prestwick RNAS	2/1997–2005		
<b>Isle of Man</b>			
Ronaldsway	1957–2005	946.5 18h 1 Dec. 1966	1
<b>North-west England and North Wales</b>			
Carlisle	1961–2005	946.5 21h 1 Dec. 1966	1
Manchester/Ringway	1949–10/2004	} 952.5 00h 5 Feb. 1951	1
Woodford	11/2004–2005		
Valley	1957–2005	947.4 07h 17 Dec. 1989	1
<b>South-west England and South Wales</b>			
Aberporth	1957–2005	950.3 05h 17 Dec. 1989	1
Cardiff/Rhoose	1957–1/1998	} 952.4 15h 25 Feb. 1989	1
St Athan	2/1998–2005		
Plymouth	1949–2005	951.1 16h 25 Feb. 1989	1
<b>Northern Ireland</b>			
Aldergrove	1949–2005	943.9 15h 1 Dec. 1966	1
Ballykelly	1957–70, 1995–2005	944.0 15h 1 Dec. 1966	1
<b>Ireland</b>			
Malin Head	5/1955–12/2005	943.6 13h, 14h 1 Dec. 1966	4
Belmullet	9/1956–12/2005	943.2 17h 17 Jan. 1995	4
Clones	1951–2005	943.9 19h 4 Feb. 1951	4
Claremorris	1950–2005	943.9 17h 4 Feb. 1951	4
Mullingar	1950–2005	943.0 17h 4 Feb. 1951	4
Dublin Airport	11/1941–12/2005	944.1 17,18,19h 4 Feb. 1951	4

Table 3 continued on next page

occasion was designated one of 'outstanding interest' by the Met Office. The depression subsequently moved out into the north of the Irish Sea (central pressure 947 mbar at 00h 5 February) then north across the Hebrides, finally becoming stationary and filling between Scotland and Iceland on 6–7 February.

### 1 December 1966

A series of fast-moving and rapidly-deepening depressions crossed northern Britain from the west during late November 1966. One depression formed as an open wave 1002 mbar at 56°N, 35°W at noon on 30 November then deepened rapidly while moving quickly eastwards to be located near 57°N, 18°W just 12 hours later, with central pressure 955 mbar. It subsequently moved more slowly east-south-eastwards across northern Ireland and southern Scotland into the central North Sea by 0600 GMT 2 December. The lowest barometric pressures reported were 942.6 mbar at Carrigans (near Derry/Londonderry) and 943.9 mbar at Belfast/Aldergrove Airport (both at 1500 GMT on 1 December) and 944.3 mbar at the Mull of Galloway at 1800 GMT. The barometric pressure on this occasion remains the lowest on post-war record for Northern Ireland, southern Scotland south of the Great Glen and for all of northern England north of a line Manchester to Hull (Figure 11). Figure 8 shows the synoptic situation at 1800 UTC.

### 20 December 1982

During the early hours of the morning of 20 December 1982 the passage of an intense depression across the north of the British Isles resulted in the lowest barometer readings seen in Britain since December 1886 (see above). At 0020 GMT the sea-level pressure at Stornoway stood at 937.6 mbar, and there is evidence from the pressure gradients to suppose that the pressure on the western side of the Isle of Lewis and at the island of Sule Skerry off northern Scotland may have fallen as low as 936 mbar. A full description of the event was published shortly afterwards (Burt, 1983).

This depression was spawned off the Labrador Coast during the morning of 17 December and subsequently deepened rapidly as it moved swiftly north-eastwards in the very strong jet-stream that had been a persistent feature of the upper-air pattern over the north Atlantic throughout the autumn. It reached a maximum depth of about 931 mbar around 1500 GMT on 19 December near 58.5°N, 15°W and subsequently filled slowly as it moved north-eastwards, passing between the Orkney and Shetland Islands. At Lerwick the barometer remained at or below 965 mbar for 46 consecutive hours, and at Wick for 44.

Table 3 continued

Lowest barometric pressure on record at a number of long-period hourly observing sites in the UK and Ireland (typically 40 years or more of computerised hourly or three-hourly observations available in the UK Met Office and Met Éireann data archives; where two or more stations are bracketed together, the lowest value from the combined record has been used). Slightly lower values may have occurred between observations. All times quoted are GMT.

Region and station	Period	Value/date	Source
<b>Ireland continued</b>			
Casement Aerodrome	1964–2005	945.6 04h 17 Dec. 1989	4
Birr	10/1954–12/2005	944.9 02h 17 Dec. 1989	4
Shannon Airport	9/1945–12/2005	942.8 14h 4 Feb. 1951	4
Valentia Observatory	10/1939–12/2005	942.8 12h 4 Feb. 1951	4
Kilkenny	6/1957–12/2005	944.8 03h 17 Dec. 1989	4
Rosslare	12/1956–12/2005	946.1 04h 17 Dec. 1989	4
Roches Point	12/1955–12/2005	943.2 00h 17 Dec. 1989	4
Cork Airport	1962–2005	942.8 00h 17 Dec. 1989	4
<b>Channel Islands</b>			
Guernsey Airport	1960–2005	952.5 11h 25 Feb. 1989	1
Jersey	1862–2005	953.8 1320h and 1920h 25 Feb. 1989	6
<b>Ocean Weather Ships</b>			
OWS 'A' 62°N, 33°W	1961–70	945.8 15h 21 Sept. 1968	7
OWS 'C' 52.75°N, 35.5°W	1961–70	956.7 09h 23 Feb. 1964	7
OWS 'D' 44°N, 41°W	1961–70	956.0 18h 28 Feb. 1963	7
OWS 'E' 35°N, 48°W	1961–70	978.0 03h 6 Jan. 1963 (+)	7
OWS 'I' 59°N, 19°W	1961–70	931.1 01h 16 Jan. 1962 (+)	7
OWS 'J' 52.5°N, 20°W	1961–70	949.5 16h 17 Nov. 1963	7
OWS 'K' 45°N, 16°W	1961–70	967.5 21h 9 Nov. 1963	7
OWS 'M' 66°N, 2°E	1961–70	948.5 09h 28 Feb. 1967	7

(+) for OWS data indicates the same value occurred at one or more successive hours

#### NOTES

\* Stornoway's minimum is from the barograph record: the lowest at an observation hour was 938.2 mbar at 01h

#### SOURCES

1. UK Met Office hourly and three-hourly observational datasets: courtesy National Climate Information Centre
2. Shellard and Douglas (1951)
3. Marriott (1884)
4. Courtesy of Climatological Division, Met Éireann, January 2006
5. Rohan (1975)
6. Courtesy of Frank le Blancq, Jersey Met Department, January 2006
7. UK Met Office, Special Investigations Branch

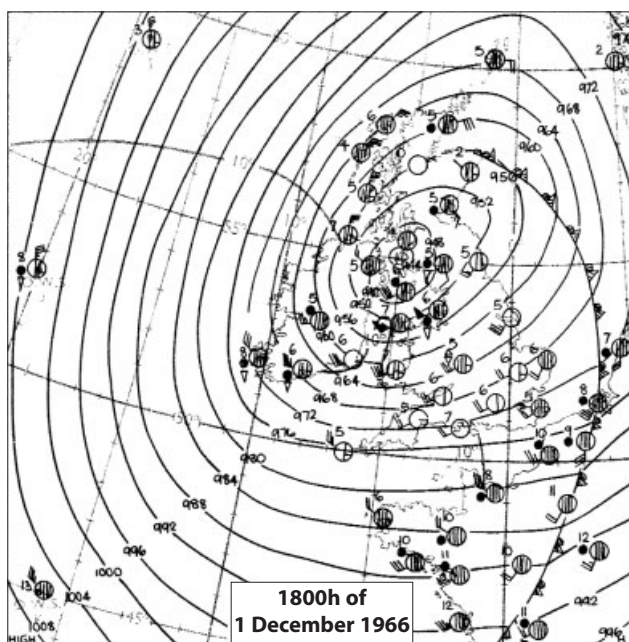


Figure 8. Synoptic situation at 1800 GMT on 1 December 1966, from Daily Weather Report

Severe gales and flooding caused considerable disruption over many parts of Britain, and there were at least nine fatalities in weather-related accidents. The surface synoptic situation at midnight is shown in Figure 9 (Figure 3 of Burt, 1983).

### 25 February 1989

On the afternoon of 25 February 1989, as a large and complex area of low pressure covered the British Isles, the barometric pressure over the southern half of England and Wales fell below 950 mbar. The lowest reported pressure was 948.8 mbar at Portland in Dorset; in London the pressure fell to 952 mbar during the evening – the lowest since December 1821 (Burt, 1989). On Jersey the lowest sea level pressure reported was 953.8 mbar – by more than 4 mbar the lowest value recorded on the island since records commenced in 1862 (Table 3).

As is evident from other accounts above, very low barometric pressure events are usually preceded by a long unsettled spell, with a succession of increasingly deep depressions on similar tracks. In this case, however, the synoptic evolution over the British Isles was very atypical of the preceding four months, which were very strongly anticyclonic over England with an intense anticyclone frequently located over central Europe. Over the north-eastern Atlantic a vigorous south-westerly flow had been maintained between the European high and a deeper-than-normal Icelandic low. The block was broken in mid-February as the dominant anticyclone drifted away allowing frontal systems to cross the British Isles. Secondary depressions circulating around a deep primary system to the north of Scotland maintained low pressure over the whole of the British Isles, although the pressure field itself was slack. The depression ultimately responsible for the lowest pressures developed initially as a wave on the polar front about 1800 GMT on 24 February around 49°N, 18°W. By midnight it was evident as a rather slack system with a closed isobar of 968 mbar to the south-west of Ireland. It continued moving eastwards and deepening (956 mbar well south of Cork at 0600) and then moved east-south-east to cross southern Cornwall during the morning. The centre then tracked across Devon and along the south coast, deepening slowly. At 1500 GMT it was centred over south Dorset, with 948.8 mbar reported at Portland Royal Naval Air Station in Dorset (50° 34' N, 2° 27' W). After this the depression began to fill slowly, drifting further along the south coast before turning north-east during the evening. At 2100 the centre lay inland in East Sussex at 952 mbar, while by midnight it had moved out into the Thames Estuary and filled to 953 mbar.



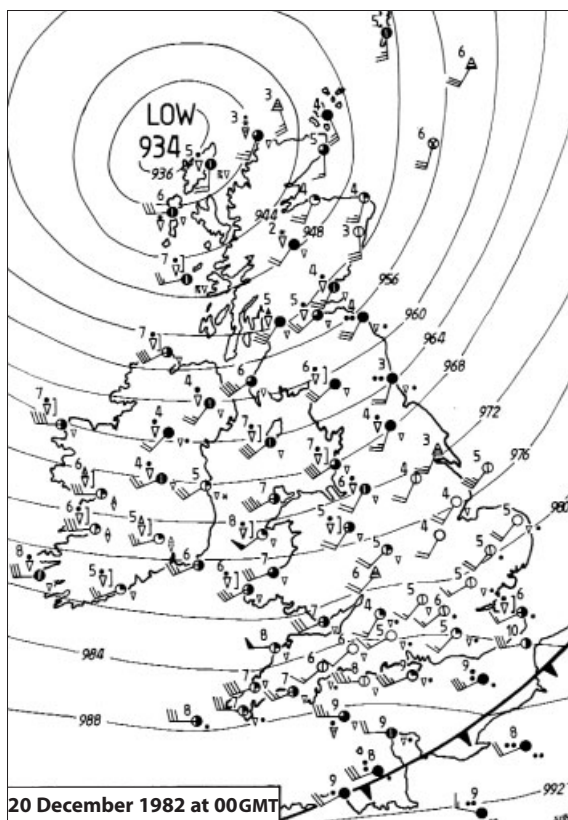


Figure 9. Synoptic situation at 0000 GMT on 20 December 1982 – from Burt (1983)

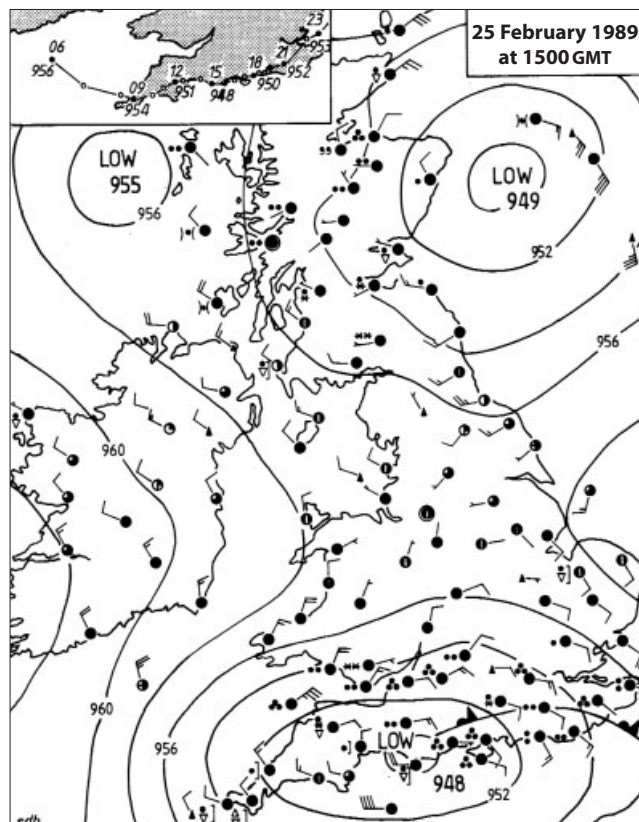


Figure 10. Synoptic situation at 1500 GMT on 25 February 1989 – from Burt (1989)

The synoptic situation over the British Isles at 1500 GMT (when the depression was at about its deepest) is shown in Figure 10 (taken from Figure 2 of Burt, 1989). The track of the depression is shown inset. On this occasion the barometer was exceptionally low over the whole of the British Isles, for in addition to the main low over southern England, at 1500 GMT there was another of 949 mbar off eastern Scotland and another of 955 mbar off western Scotland. The highest pressure at any station in the United Kingdom at this time was 960.4 mbar at Lerwick.

### 17 December 1989

A very strong thermal gradient in mid-Atlantic in mid-December 1989 spawned several intense depressions, one of which had deepened to below 950 mbar near 47°N, 19°W by 0000 GMT on 16 December. The system continued to develop as it subsequently moved quickly north-eastwards, crossing Ireland and Scotland during 17 December. At Cork Airport the barometer stood at 942.8 mbar at 0000 GMT on 17 December, its lowest in more than 40 years on record (Table 3). New site records were established at six other long-period Irish stations on this date, although stations open during the February 1951 event recorded slightly lower barometric pressures on that

occasion. Severe gales and heavy rainfall accompanied the depression as it crossed the British Isles.

### 17 January 1995

A strong baroclinic zone became established across the western and central Atlantic around 13 January 1995 and resulted in a succession of fast-moving, intense cyclonic systems. An open wave on the polar front at 994 mbar around 50°N, 37°W at 1200 UTC on 16 January deepened explosively as it moved very rapidly eastwards and then north-eastwards, passing close to the west coast of Ireland on 17 January. At Belmullet in north-west Ireland the barometer fell to 943.2 mbar at 17 h, the lowest on a record now spanning 50 years at this site (Table 3). Widespread severe gales resulted from this intense and fast-moving storm.

### Common features of notable storms

Most notably deep depressions share a common history, namely the generation of a succession of a series of fast-moving and rapidly deepening cyclonic storms from a greatly intensified polar front. In several cases, the deepest depression was preceded by a series of intense fast-moving and rapidly deepening cyclonic storms along

similar tracks; in others, two already intense systems combined to form a larger and more intense storm. In a few cases, the establishment of a large and very deep complex low pressure area over the British Isles produced very low barometric pressures without the more usual accompaniment of severe gales.

### Extremes of pressure at long-period stations

The lowest observed barometric pressure at a selection of long-period observing sites (most of them hourly synoptic stations) in the British Isles are given in Table 3. In most cases the records have been derived from the period of computerised records. Figure 11 shows the lowest observed MSL pressure observed since approximately 1949 together with the date the lowest value occurred (based on the records in Table 3).

### Summary

Within the last 200 years or so, a barometric pressure of 950 mbar or less at MSL has been reliably recorded at one or more stations within the British Isles on at least 30 occasions. On only three of these has the barometer fallen to 935 mbar or lower, and at the time of writing the most recent occasion of such a low value was 120 years ago. The

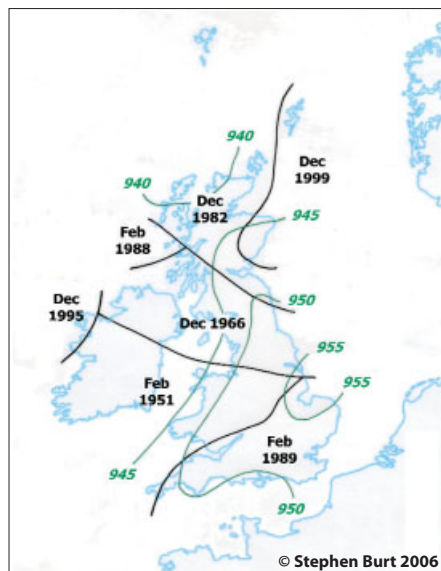


Figure 11. Lowest observed MSL pressure observed since 1949 (smoothed distribution) together with the date of the event

lowest MSL barometric pressure recorded within the British Isles occurred at Ochtertyre, near Crieff, in Scotland on 26 January 1884, when 925.6 mbar was measured. On the morning of 8 December 1886, the barometer may have fallen as low as 924 mbar over northern Ireland. Within the past 100 years, the lowest recorded pressure in the British Isles has been 937.6 mbar at Stornoway on 20 December 1982. In London, the lowest observed in almost 250 years of records has been 946 mbar on the morning of 25 December 1821.

The author would welcome documented examples of other occasions of barometric pressures below 945 mbar in the British Isles which may have been overlooked.

## Data sources and acknowledgements

I am very grateful to a number of people and organisations who have been most helpful in tracking down sometimes very obscure observations or references for this compilation. Frank Le Blancq from the States of Jersey Met Department provided the extremes of barometric pressure on record in Jersey (and generated several useful related discussions on related topics): Howard Oliver kindly drew my attention to and provided a copy of Luke Howard's published 'clock-barometer' chart for the December 1821 storm: Eddie Graham from the University of Fribourg in Switzerland provided helpful comments relating particularly to the Irish extremes: Niall Brooks from the Climatological Division of Met Éireann provided the long-period extremes at the synoptic sites in Ireland used in Table 3, and the UK Met Office's National Climate

Information Centre provided much of the UK content in Table 3. I offer a particular 'thank you' to the National Meteorological Library in Exeter for unearthing many of the references, in particular to Martin Kidds for his unflinching enthusiastic assistance in obtaining copies of numerous *Daily Weather Reports* and additional material from the Met Office archives in Exeter and in Edinburgh.

## References

- Anon.** 1933. The lowest recorded barometric pressures at mean sea level. *Meteorol. Mag.* **68**: 18.
- Blench B.** (1963) Luke Howard and his contribution to meteorology. *Weather*, **18**: 83–93.
- Brandes HW.** 1826. *Dissertatio physica de repentinis variationibus in pressione atmosphaerae observatis* [Published in Latin: *Scientific discussion of rapid changes in atmospheric pressure*]. Leipzig. See also Monmonier 1999.
- Brodie FJ.** 1902. The prevalence of gales on the coasts of the British Isles during the 30 years 1871–1900. *Q. J. R. Meteorol. Soc.*, **28**: 121–157.
- Buchan A.** 1884. The recent storm. *Nature*, London, 31 January 1884.
- Buchanan LM.** 1886. Barometric depression of December 8th–9th [1886]. *Symons's Monthly Meteorol. Mag.* **21**: 172.
- Burt SD.** 1983. New UK 20th century low pressure extreme. *Weather*, **38**: 208–213.
- Burt SD.** 1987. A new North Atlantic low pressure record. *Weather*, **42**: 53–56.
- Burt SD.** 1989. London's lowest barometric pressure in 167 years. *Weather*, **44**: 221–225.
- Burt SD.** 1993. Another new North Atlantic low pressure record. *Weather*, **48**: 98–103.
- Burt SD.** 2006. Barometric pressure during the Irish storm of 6–7 January 1839. *Weather*, **61**: 22–27.
- Cunningham A.** 1866. Barometer during the gale of December 31st 1865. *Symons Monthly Meteorol. Mag.* **1**: 16.
- Dove HW.** 1828. *The law of storms*. Translated by Robert FitzRoy, 1858. London, Board of Trade: Third Number of Meteorological Papers (copy available in National Meteorological Library).
- Eden P.** 1988. Hurricane Gilbert. *Weather*, **43**: 446–448.
- Harding C.** 1887. The storm and low barometer of December 8th and 9th 1886. *Q. J. R. Meteorol. Soc.* **13**: 201–215.
- Hamlyn R.** 2001. *The invention of clouds*. Farrar, Straus and Giroux: New York ISBN 0-374-17715-5.
- Howard L.** 1822. On the late Extraordinary Depression of the Barometer. *Phil. Trans. Roy. Soc. A*, **112**.
- Howard L.** 1833. *The Climate of London*. Second Edition, in 3 volumes.
- Lamb HH.** 1991. *Historic storms of the North Sea, British Isles and northwest Europe*. Cambridge University Press.
- Marriott W.** 1873. On the barometric depression of January 24th 1872. *Q. J. R. Meteorol. Soc.* **1**: 188–203 (1873) – also discussion on pp. 219ff.
- Marriott W.** 1884. The great storm of January 26th 1884. *Q. J. R. Meteorol. Soc.*, **10**: 114–123.
- Met Office.** 1973. *Averages of mean sea level barometric pressure for the United Kingdom 1941–1970*. Climat. Mem. 51A, 27pp.
- Met Office.** 1975. *Weather in home waters, Volume II*. Her Majesty's Stationery Office: Met O 732c.
- Monmonier M.** 1999. *Air apparent: How meteorologists learned to map, predict and dramatize weather*. University of Chicago Press, 309 pp. (The work of Brandes and Dove is covered pp. 18–31, with Brandes' map of the 1821 storm reproduced on p. 21).
- National Weather Service [US].** 2005. Hurricane *Wilma* review, available online at [www.srh.noaa.gov/mfl/events](http://www.srh.noaa.gov/mfl/events).
- Perry AH.** 1983. Extreme surface-level atmospheric pressure values during the 1982/83 winter. *J. Meteorol. (UK)*, **8**: 69–71.
- Rohan PK.** 1975. *The climate of Ireland*. Stationery Office: Dublin. 112 pp.
- Roy MG.** 1983. The Ben Nevis Meteorological Observatory, 1883–1904. *Meteorol. Mag.* **112**: 318–329.
- Roy MG.** 2004. *The weathermen of Ben Nevis 1883–1904*. Royal Meteorological Society: Reading.
- Shellard HC, Douglas CKM.** 1951. Low pressure recorded on February 4 1951. *Meteorol. Mag.* **80**: 362–364.
- Shields L, Fitzgerald D.** 1989. The 'Night of the Big Wind' in Ireland, 6–7 January 1839. *Irish Geography*, **22**: 31–43.
- Symons GJ.** 1865. Barometer in December 1865. *Symons's Rainfall Circular*, December 1865, xxxix.
- Symons GJ.** 1872. The barometric depression of January 24th 1872. *Symons's Monthly Meteorol. Mag.*, **7**: 6–13, 26–27.
- Symons GJ.** 1876. The barometrical depression of March 12th [1876]. *Symons's Monthly Meteorol. Mag.* **11**: 19–22.
- Symons GJ.** 1884. The storms and barometric disturbances January 20–26th [1884]. *Symons's Monthly Meteorol. Mag.* **19**: 1–2, 12–16.
- Symons GJ.** 1886. Barometric depression of December 8th–9th [1886]. *Symons's Monthly Meteorol. Mag.* **21**: 157–161, 180–183.
- Symons GJ.** 1892. The low barometer of January 12th 1843. *Symons's Monthly Meteorol. Mag.* **27**: 164–167.
- Symons GJ.** 1900. Low barometric pressure on December 29th 1899. *Symons's Monthly Meteorol. Mag.* **34**: 177–78.
- Wheeler DA.** 1984. The storm of Friday 13 January 1984 in north-east England. *Weather*, **39**: 152–155.

© Stephen Burt 2007  
doi: 10.1002/wea.20



# The Highest of the Highs . . .

## Extremes of barometric pressure in the British Isles,

### Part 2 – the most intense anticyclones

**Stephen Burt**

*Stratfield Mortimer, Berkshire*

Part 1 of this article, in last month's *Weather* (Burt 2007), discussed the synoptic background to the deepest depressions known to have affected the British Isles within the last 200 years or so. This article continues the discussion for the most intense anticyclones on record.

Prior to about 1914 most measurements of pressure were made in inches of mercury (inHg), but all information in this paper is presented in contemporary units – with pressures reduced to mean sea level unless otherwise stated – and modern synoptic notation as far as possible. As in Part 1, synoptic documentation has mostly been obtained from the British Met Office's *Daily Weather Report* (*DWR*, 1860–1980), with observations augmented where possible from contemporary published accounts. Since 1980 chart data have been obtained from the London Weather Centre *Daily Weather Summary* (*DWS*), from archived Met Office working charts or from online sources.

The references quoted are usually contemporary accounts published shortly after the events to which they refer. Subsequent papers on similar instances often refer to the same event, but unless new information or analyses are presented in the later paper only the original reference is quoted here. In some respects the analysis of the most intense anticyclones is easier than that of the most intense depressions, as the systems are much slower-moving and changes in pressure less rapid: but on the other hand, documentary evidence in terms of published accounts are far fewer, particularly since about 1950.

#### How high is high?

The highest reliably documented sea-level barometric pressures on Earth have all been recorded in intense anticyclones in Siberia or Alaska. Highest on record anywhere in the world is 1083.8 mbar recorded at Agata in Siberia on 31 December 1968\*, and there

are a handful of other occurrences above 1075 mbar on record – for instance 1079.6 mbar at Dawson, Yukon Territories, Canada on 2 February 1989 (Burt, 2004), 1078.9 mbar at Barnaul in Siberia on 23 January 1900, 1078.6 mbar at Northway, Alaska on 31 January 1989 and 1075.2 mbar at Irkutsk, Siberia on 14 January 1893 (US National Weather Service, 1989; Symons, 1899). At low altitude stations in Europe, the highest MSL pressure known to the author was that reported from Pärnu in Estonia and Riga in Latvia on 22–23 January 1907, viz. 1067.1 mbar.

North Atlantic winter anticyclones do not approach these planetary extremes of pressure; probably the most intense systems within the last 100 years or more were those of 28 January 2003 (1057 mbar near 51° N, 27° W, Figure 1) and 27–28 February 1988 (1053 mbar in a mobile high located near 53–54° N, 25–26° W).

Within the period of reasonably reliable instrumental records (approximately 200 years), the barometer at mean sea level (MSL) has risen above 1048 mbar over at least a part of the mainland of the British Isles (the United Kingdom and Ireland) or outlying islands on at least 17 occasions (Table 1). On nine of these occasions a baro-

\* It should be borne in mind that the Siberian sites are located at considerable altitudes in the interior of a vast continental landmass. In mid-winter with air temperatures frequently falling below –50°C the 'MSL correction' can amount to more than 30 mbar. Agata (WMO no. 23383) is at 66° 53' N, 93° 28' E, altitude 278 m; Dawson, Yukon (WMO no. 71966) is at 64° 03' N, 139° 08' W, 370 m; Barnaul (WMO no. 29838) is at 53° 26' N, 83° 31' E, 184 m; Northway, Alaska (WMO no. 70291) is at 62° 58' N, 141° 56' W, 525 m; Irkutsk, Siberia (WMO no. 30710) is at 52° 16' N, 104° 19' E, 469 m.

Higher values have recently been claimed for Tonsontsengel in Mongolia (WMO no. 44225, 48° 44' N, 98° 12' E, altitude 1723 m): 1090.0 mbar on 29 December 2004 (several online sources) and 1085.7 mbar on 19 December 2001 – air temperature at the time was –40°C (online encyclopaedia Wikipedia) – but the great altitude of this site renders barometric correction to mean sea level at low air temperatures (a correction of almost 200 mbar) a rather pointless exercise.

metric pressure at or above 1050 mbar has been reliably documented, although this value has not been reached for almost 50 years at the time of writing. A pressure of 1050 mbar at MSL has been attained at least once in all parts of the British Isles except the south-east of England, although it was closely approached here in January 1882 and January 1905.

Finally, both maximum and minimum observed pressures are given for a selection of long-period stations and mapped for the British Isles, and a table giving the known monthly extremes of pressure in the British Isles is given. Locations of places referred to in the text are given in Figure 2.

#### 8–9 January 1820

Until 1896 the highest barometer readings known for the British Isles occurred in Scotland in January 1820. On this occasion the maximum values attained (reduced retrospectively to mean sea level) were 1051.7 mbar at Kinfauns Castle, near Perth, and 1051.5 mbar at Leith, near Edinburgh, both at 09h on 9 January 1820, and 1051.3 mbar at Gordon Castle, Banff, at 23h on 8 January (Anon, 1820, Wallis, 1882). In London (Royal Society, Somerset House) the highest barometer reading was 1044.1 mbar, also at 09h on 9 January. The surviving details of the event are too limited to attempt a synoptic reconstruction.

#### 18 January 1882

The *Daily Weather Reports* from January 1882 show the intensification and progressive westward movement of an anticyclone located over central Europe on 14 January (central pressure around 1040 mbar) to become located over southern England by the morning of 18 January (central pressure 1049 mbar). It is probable that the anticyclone was already declining from its peak, for at Vienna the barometer had reached 1050.5 mbar at 10h on 16 January – the highest there since 1775. The anticyclone persisted for several days thereafter, declining slowly; the pressure in London did not fall below 1032 mbar until late on 26th, after



Table 1

Known occurrences of MSL pressures above 1048 mbar in the British Isles, within approximately the last 200 years. This table is probably incomplete. For the dates shown in bold type a brief description follows in the main body of the text.

Date	Highest known MSL pressure and site	Reference(s)
24 February 1808	1050.0 mbar Gordon Castle, then in Banff (now Moray), Scotland, 21 h	Wallis, 1882
<b>8–9 January 1820</b>	1051.7 mbar Kinfauns Castle, Perth	See text
<b>14 January 1882</b>	1049.4 mbar St Leonards, East Sussex: 1049.1 mbar London	See text
<b>9 January 1896</b>	1053.4 mbar Ochertyre, Perthshire and Fort William	See text
<b>29–30 January 1896</b>	1048.3 mbar Roches Point, southern Ireland	See text
<b>31 January 1902</b>	1053.6 mbar, Aberdeen <i>BRITISH ISLES RECORD HIGHEST</i>	See text
<b>28 January 1905</b>	1053.1 mbar Falmouth, Cornwall 1051.9 mbar Valentia <i>IRELAND RECORD HIGHEST</i>	Monthly Weather Report February 1921
<b>23 January 1907</b>	1051.8 mbar at Aberdeen, 1015h	Symons's Meteorol. Mag. February 1907
27 February 1921	1048.3 mbar Valentia	Monthly Weather Report Meteorol. Mag. March 1921, p 49
<b>24 December 1926</b>	1051.9 mbar Wick	See text
<b>26 January 1932</b>	1051.0 mbar Stonyhurst, Sheffield and Meltham, West Yorkshire	See text
9 March 1953	1048.6 mbar Tynemouth	Met Office, 1973
<b>16 January 1957</b>	1050.9 mbar Belmullet, NW Ireland	See text
23 February 1962	1049.1 mbar Lerwick	Table 2
<b>7 February 1964</b>	1049.1 mbar Kilkenny 0900 GMT, 1049.1 Mullingar, Co. Westmeath	See text
3 March 1990	1047.9 mbar at Scilly/St Mary's	London Weather Centre Daily Summary
<b>27 January 1992</b>	1049.2 mbar Sennybridge, Powys	See text

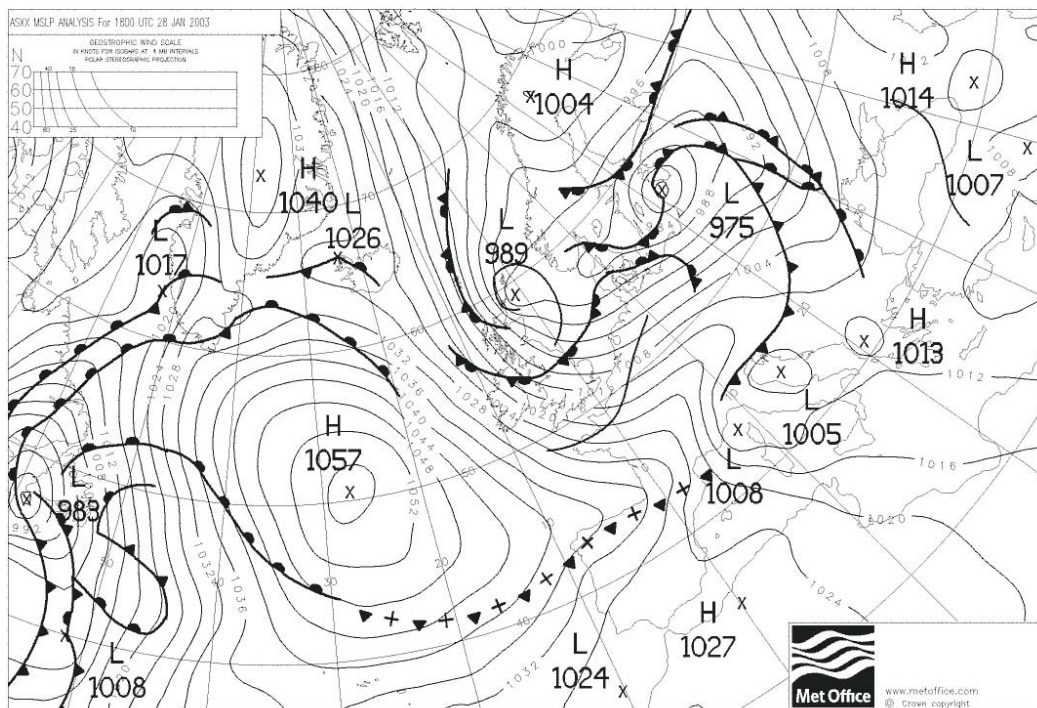


Figure 1. Synoptic situation at 1800 UTC on 28 January 2003. Courtesy UK Met Office © Crown Copyright

remaining at or above this level since early on 14 January.

The synoptic situation at 08 h on 18 January 1882 is shown in Figure 3. At Kew Observatory in west London the highest barometer reading, 1049.1 mbar, occurred at 11 h that morning; this remains the highest barometer reading for the London area on over 200 years records\*. In a slack pressure field 1046 mbar was exceeded across the southern half of Ireland, the whole of Wales and all of England south of a line from Manchester to Hull; 1049 mbar was reached in places as far apart as Brighton, Falmouth, Cheltenham, Banbury and Tonbridge. The highest reading noted by Wallis (1882) was 1049.4 mbar at St Leonards near Hastings in East Sussex at 1030h.

### 9 January 1896

In contrast to the European anticyclone responsible for the high values 14 years earlier, the intense anticyclone of early January 1896 was clearly of Atlantic origin. On the morning of 7 January, the *DWR* showed a high pressure area off western

Ireland, with central pressure close to 1043 mbar; based upon ship reports, this system had been moving eastwards for some days beforehand. By the following evening the centre was located over Scotland: at Stornoway the barometer stood at 1050.1 mbar at 18h, and at Dunrossness in Shetland 1051.1 mbar was recorded at midnight. At 08h 9 January 1896 (Figure 4) the central pressure stood at 1053 mbar: during the morning 1053.4 mbar at MSL was recorded at Ochertyre, near Crieff in Perthshire at 09h<sup>†</sup> and at Fort William in western Scotland at 10h (Scott, 1896), supported by the readings of 1053.0 mbar at Fort Augustus and 1053.1 mbar at Dollar (both at 09h) and 1052.9 mbar at Glasgow (at 0945). In England, 1050 mbar was reached as far south as Bidston (near Liverpool) and as far east as Durham. At Stonyhurst in Lancashire the highest value attained was 1051.9 mbar; this was the highest on record at the site since records commenced there in 1848 (O'Connor, 1932). In

<sup>†</sup> It was of course Ochertyre that 12 years earlier reported the *lowest* barometric pressure recorded in the British Isles, 925.6 mbar at 2145h on 26 January 1884 (see Part 1), thus capturing for six years the unique distinction of holding both the highest *and* lowest barometric pressure records within the British Isles, together with a remarkable range in pressure of 127.8 mbar

London, Kew reached 1047.4 mbar at 2110h on 9 January. The entire system subsequently moved south-westwards and declined, dropping below 1050 mbar during 10 January and disappearing as a separate feature after 15 January, by which time the central pressure had declined to 1034 mbar.

Later in the month another intense anticyclone of Atlantic origin affected the British Isles. On this occasion the highest readings were in southern Ireland (1048.4 mbar at Roches Point at 18h on 29 January, 1048.3 mbar at Valentia at midnight 29/30 January) and as a result barometer readings in southern England and south Wales slightly surpassed those earlier in the month – at Kew the highest was 1047.6 mbar (at 10h on 30 January), at Haverfordwest 1048.2 mbar (at 21h on 29th) and at Falmouth 1047.7 mbar (at 2215h on 29th). From being centred over St George's Channel at 08h on 30 January the high pressure system slipped slowly south-eastwards over France in the following days, with a slow decline in central pressure.

### 31 January 1902

As a depression moved eastwards across Denmark and the southern Baltic on 29–30 January 1902, an intense anticyclone quickly developed in its wake over the



Figure 2. Locations of places referred to in the text

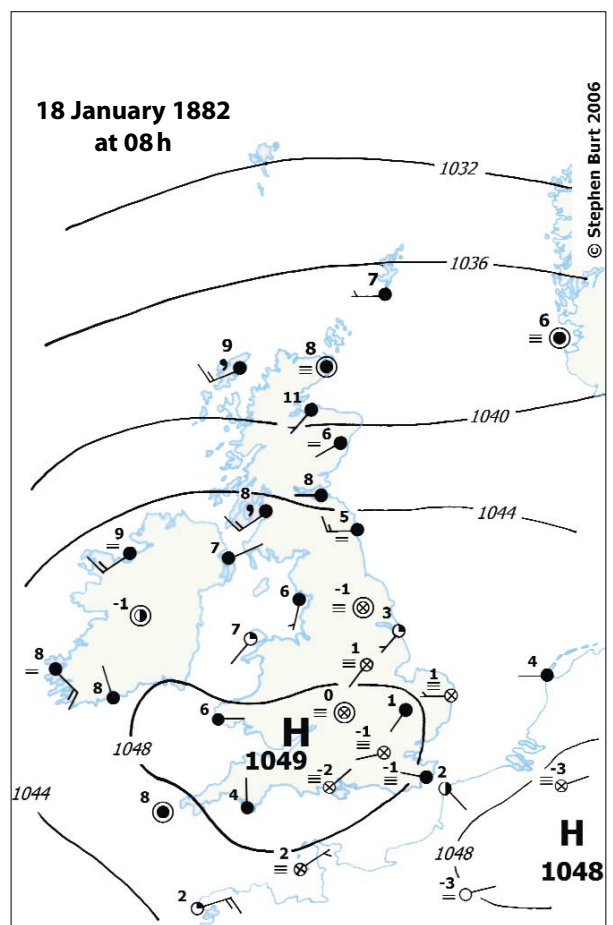


Figure 3. Synoptic situation at 08h on 18 January 1882, from Daily Weather Report

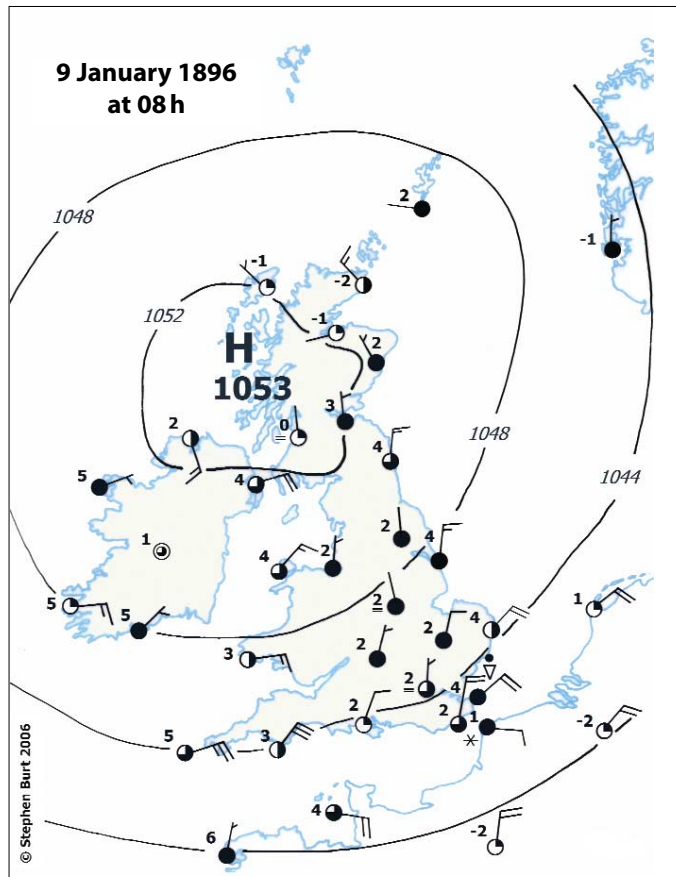


Figure 4. Synoptic situation at 08h 9 January 1896, from Daily Weather Report

northern North Sea. At Aberdeen Observatory the barometer stood just below 985 mbar on the morning of 28 January, thereafter rising almost 70 mbar over the following 3 days (Figure 5). By 0800 GMT on 31 January 1902 the central pressure had risen to 1053 mbar over the northern North Sea: at 1800 GMT the centre lay over eastern Scotland (Figure 6) with little change in central pressure (1053.2 mbar at Aberdeen at this time). Over the following 48 hours the centre of the system migrated a little north or north-eastwards and declined slowly. On this occasion the highest barometric pressure was recorded at Aberdeen Observatory at 2200 GMT, 1053.6 mbar (*Symons's Meteorological Magazine*, **37**, 1902, p. 27), which therefore just exceeded the 1053.4 mbar recorded at Ochtertyre and at Fort William six years previously. This is the highest barometric pressure yet recorded in the British Isles\*. At Fort William, the January 1896 record of 1053.4 mbar was equalled at 2200 GMT†. (The February British Isles record barometric pressure, 1052.9 mbar, was also recorded at Aberdeen at 0000 GMT 1 February, just two hours after the all-time extreme).

In Scotland, the weather was bright but cold, the temperature at Nairn falling to

\*The Aberdeen value has been incorrectly quoted for at least 80 years as 1054.7 mbar, probably owing to the use of a rounded conversion factor from inches of mercury to millibars – see Burt (2006) for details

† There is a note in *Meteorol. Mag.* Vol 37 (1902) p 15 quoting 1054.9 mbar at Coupar Angus, Perth and Kinross (about 18 km north-west of Dundee) on 31 January, but no details of the barometer or time of observation are given to substantiate the validity of the reading

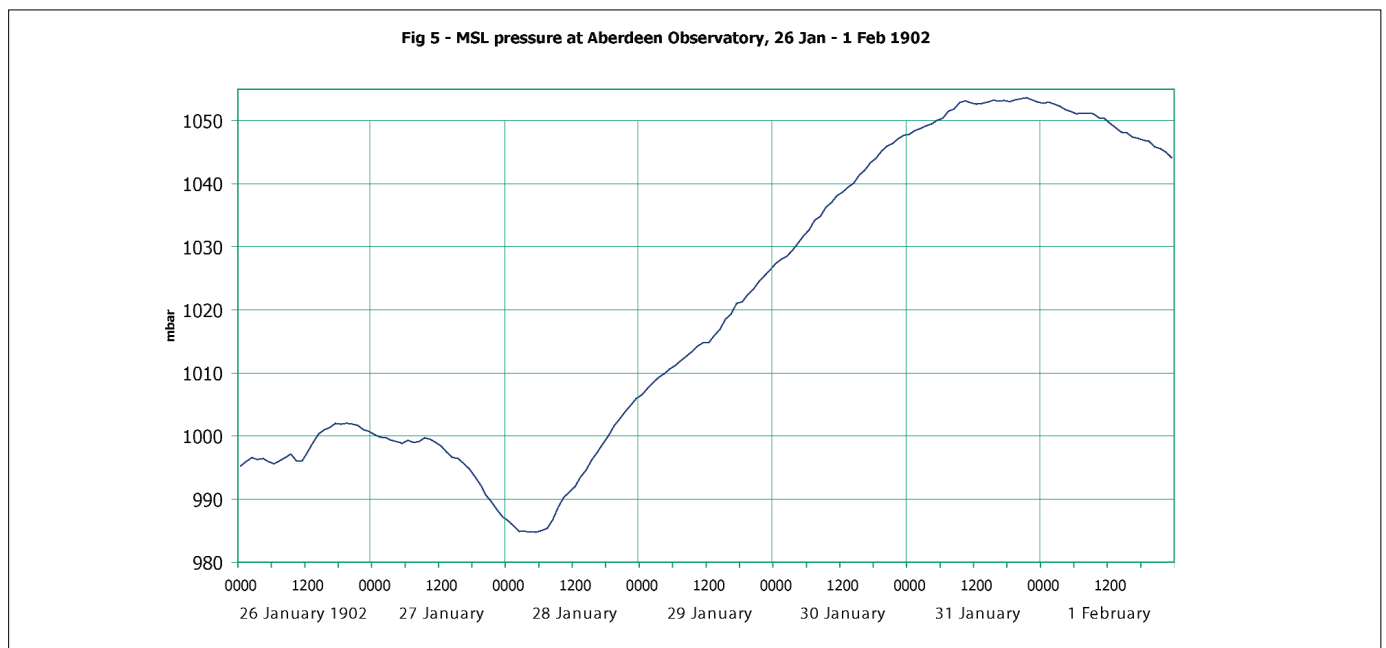


Figure 5. MSL barometric pressure at Aberdeen Observatory 26 January to 1 February 1902, from hourly tabulations of the barograph retained in the Met Office Archives in Edinburgh, showing the strong rise in pressure in the three days leading up to the British Isles record 1053.6 mbar late on 31 January



–13°C on the morning of 31 January and to –11°C at Wick on 1 February; further south, severe easterly gales raged for nearly three days in the southern North Sea and through the English Channel. In London, the highest pressure on this occasion was just under 1040 mbar; 1045.4 mbar had been reached earlier in the month (at 0900 GMT on 15 January).

### 28–29 January 1905

A ridge built over southern Britain on 23–24 January 1905 from an anticyclone located in eastern Europe (itself originally an Atlantic anticyclone). This developed a separate centre over south-west England on 25th and intensified above 1040 mbar on 26th over northern England, retreating south-west once more on 27th, still building. This intense anticyclone reached its peak over the Bay of Biscay on 28–29 January 1905 (Figure 7 shows the synoptic situation at 0800 GMT on 28 January, from the *Daily Weather Report*). This occasion is notable in that the highest barometric pressures on land, around 1052–1053 mbar, occurred in the south of Ireland, the south-west of England and in the Channel Islands: in all three areas the barometric pressure on this occasion remains the highest on historical record. At Falmouth Observatory in Cornwall the barometer reached 1053.1 mbar at 11h on 28 January, the high-

est since records began there in 1870 (Fox 1905) and a value that has not been remotely approached since: it is only 0.5 mbar below the Aberdeen 1902 maximum, the highest on record for England and the third-highest value on record in the British Isles. At Tavistock in Devon the barometer remained at or above 1050 mbar for 39 consecutive hours, the highest value being 1052.1 mbar. At Valentia Observatory, the peak 1051.9 mbar was reached at midnight 28/29 January – this is the highest barometric pressure yet recorded in Ireland (Rohan 1975 – although the date is incorrectly stated there as 20 January). On Jersey 1051.7 mbar was noted at 02h 29 January: this remains the highest barometric pressure observed on Jersey since records began there in 1862. In London, the highest value observed at Camden Square was 1048.3 mbar, at 23h 28 January and 00h 29 January – the third highest on record in the capital (behind January 1882 and January 1825), and the most recent occasion (at the time of writing) to surpass 1048 mbar in the city.

### 23 January 1907

It is easy to assume that any truly intense midwinter anticyclone must be an offshoot of an intense ‘Siberian High’ ridging westwards; however, as these accounts show, the majority are more normally ‘Atlantic’ in

origin. One noteworthy event that was without doubt merely a sideshow to a very intense anticyclone over western Russia occurred in late January 1907. On 23 January 1907, at 1015h, the barometer at Aberdeen reached 1051.8 mbar, and during the morning 1050 mbar was exceeded over all of Scotland except the far north-west, northern England (1050.1 mbar Meltham, West Yorkshire) and the extreme north-east of Ireland (Figure 8). On this occasion the barometer had risen to 1067 mbar at Pernau in Russia (now Pärnu, Estonia) on the Gulf of Riga, at the evening observation on 22 January, and also at Riga (now in Latvia), on the morning of 23 January (Lempfert, 1907). These observations are notable as both cities are on the Baltic coast and therefore the value of the barometric correction to mean sea level is very much smaller than at stations on the higher Siberian or Mongolian plateaux much further east: the current synoptic reporting station in Pärnu is at 8 m AMSL, in Riga 26 m.

### 24 December 1926

An intense anticyclone built over Norway and the northern North Sea on 21–22 December 1926, following the rapid passage south-eastwards across Norway and Denmark of an intense depression on 20 December. At 1800 GMT on 22 December the centre lay near Oslo with a central pres-

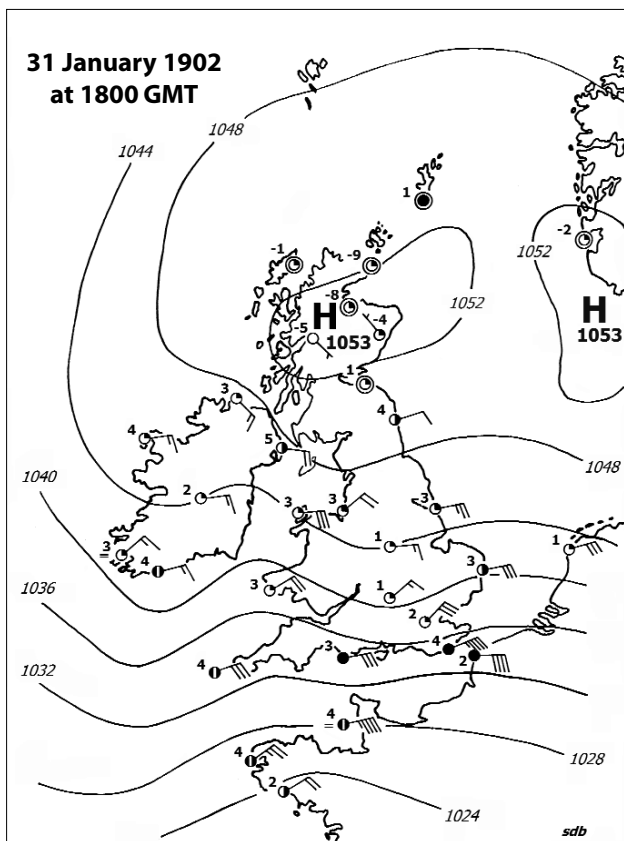


Figure 6. Synoptic situation at 1800 GMT 31 January 1902, from *Daily Weather Report*

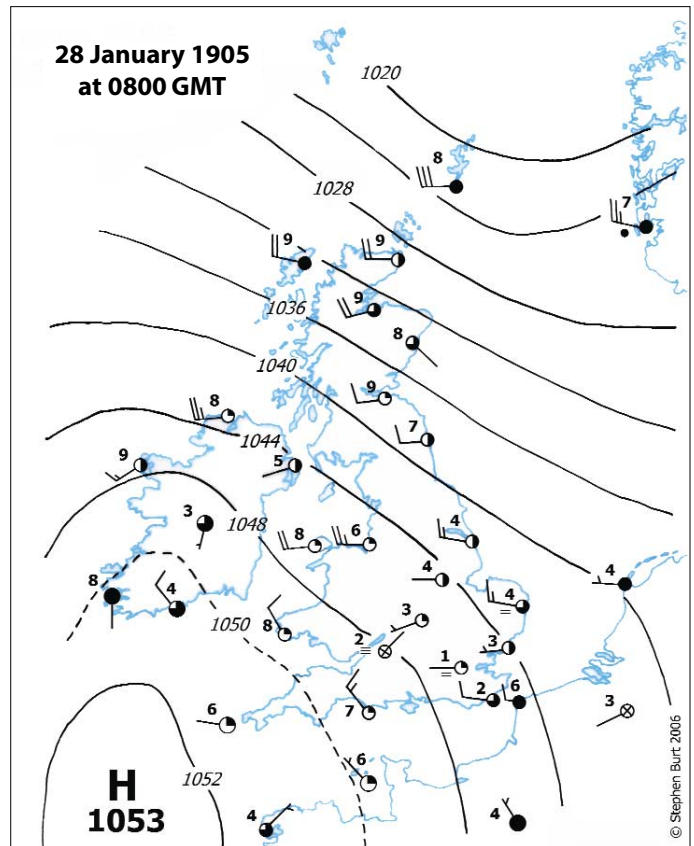


Figure 7. Synoptic situation at 0800 GMT 28 January 1905, from *Daily Weather Report*

sure close to 1049 mbar; the barometer there had risen over 50 mbar in less than 48 hours. A second centre developed over the northern North Sea during 23rd, and by 0700 GMT 24 December the centre had transferred to northern Scotland with central pressure 1050 mbar. The highest values at land stations were attained during the afternoon and evening of 24 December. At 1300 GMT (Figure 9) the barometer stood at 1051.9 mbar at Wick (the highest on record for December in the British Isles), 1050.6 mbar at Stornoway, 1050.4 mbar at Castlebay (Barra) and at Aberdeen and 1050.0 mbar at Leuchars: at 1800 GMT 1051.4 mbar was recorded at Nairn and 1051.1 mbar at Wick. In Ireland, 1049.5 mbar was attained at Malin Head (Rohan, 1975, p 111) which remains the highest on record for December in Ireland.

### 26 January 1932

An intense Siberian anticyclone built westwards into central and then north-western Europe from 18 January 1932, the centre of the system becoming centred over the British Isles on 25–27 January. On 26 January the barometer reached 1051.0 mbar at Stonyhurst, Lancashire, at Sheffield and at Meltham (West Yorkshire), 1050.4 mbar at York and 1050.3 mbar at Sealand, Cheshire (*Monthly Weather Report*: O'Connor, 1932). At both Stonyhurst and Meltham slightly

higher values were reached in January 1896 (1051.9 mbar and 1051.4 mbar, respectively) although the 1048.5 mbar attained at Ross-on-Wye, Herefordshire, was stated as being the highest in more than 60 years records (Morgans, 1932). At the time of writing, this remains the most recent occasion on which the barometer has exceeded 1050 mbar anywhere in England.

Mention should also be made here of the extremely anticyclonic nature of the following month. Although the highest observed pressures during February 1932 were just under the 1048 mbar limit adopted here (1047.4 mbar on 20 February at Inchkeith, Renfrew and Donaghadee – Hawke, 1932), the month was notable for probably the highest monthly mean MSL pressure on record for the British Isles – 1035.4 mbar at Malin Head in the north of Ireland.

### 16 January 1957

Following closely in the wake of an intense depression, an anticyclone developed off the eastern seaboard of the United States on 12 January 1957. As it moved rather quickly east and then north-east it intensified slowly, with central pressure 1043 mbar by 1200 GMT on 14 January in mid-Atlantic near 55° N, 27° W before becoming near-stationary off north-west Ireland by 1800 GMT, absorbing in the process another anticyclone that had lain over the British

Isles for several days previously. As it did so it intensified quickly: its central pressure was first shown as 1050 mbar on the 1200 GMT *Daily Weather Report* Northern Hemisphere map for 15 January, and it remained at or slightly above 1050 mbar with little change in position for about 30 hours. Figure 10 shows the synoptic situation at 0600 GMT on 16 January, close to the time of the highest barometric pressure in Scotland and Ireland. The highest MSL pressures at land stations were 1050.9 mbar at Belmullet at 0800 GMT and at Benbecula at 0900 GMT, and 1050.8 mbar at Claremorris, 1050.6 mbar at Malin Head and 1050.4 mbar at Stornoway, all at 0900 GMT. This occasion is notable for two reasons: firstly, because it resulted in the highest barometric pressure on post-war records at almost all long-period sites in Scotland and Ireland, and secondly because, at the time of writing, it remains the most recent occasion on which 1050 mbar has been reached anywhere in the British Isles.

### 7 February 1964

An anticyclone developed in mid-Atlantic between deep depressions over Newfoundland and Svalbard on 3 February 1964, moving quickly east at first before becoming slow-moving to the north-west of Ireland by 1200 GMT on 5 February, with central pressure about 1042 mbar. Over the following 48 hours the centre slipped slowly

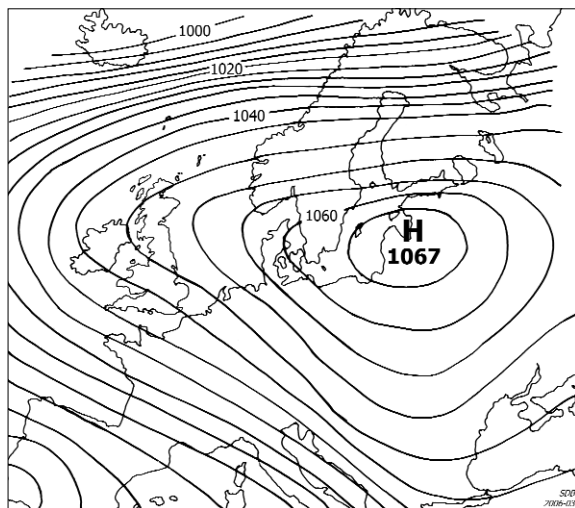


Figure 8. Synoptic situation on the morning of 23 January 1907, based upon Lempfert (1907)

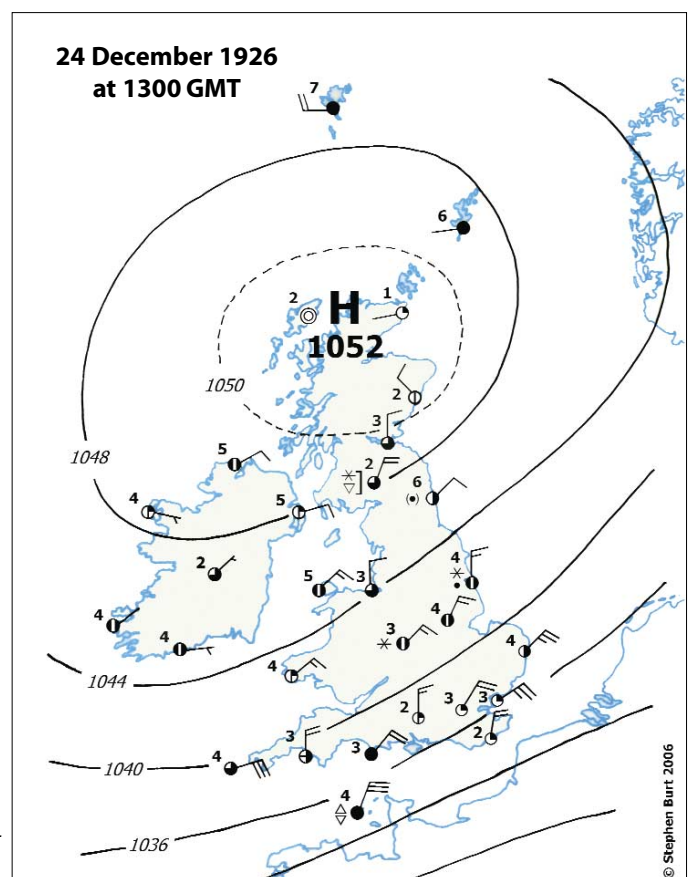


Figure 9. Synoptic situation at 1300 GMT 24 December 1926, from *Daily Weather Report*

south-east to become centred over eastern Ireland at its most intense during the morning of 7 February (Figure 11). The highest values reached on this occasion were all in Ireland: 1049.1 mbar at Kilkenny at 0900 GMT, 1049.1 mbar at Mullingar, Co. Westmeath, 1048.7 mbar at Dublin Airport at 1100 GMT and at Aldergrove (Belfast Airport) at 1200 GMT. Also at 1200 GMT, Cardiff reached 1048.4 mbar and Plymouth 1048.3 mbar. In London, 1047.3 mbar at 0900 GMT at Heathrow was the highest pressure reached in the London area since January 1905 (see above). This occasion established the highest recorded post-WWII barometric pressure over much of south and east Ireland, much of Wales and most locations in south-west, south-east and central southern England. The reading of 1047.9 mbar at South Farnborough at 0900 GMT remains the highest barometric pressure observed in south-east England within the last 100 years.

### 26–27 January 1992

January 1992 was an extremely anticyclonic month, with a mean pressure anomaly of +17 mbar over the Irish Sea and a mean anticyclone 1031 mbar centred close to Switzerland. Late in the month a cell broke away from the main continental anticyclone, moved westwards and then northwards to

sit over the British Isles on 26–27 January. The highest accepted MSL pressures\* were 1049.2 mbar from the AWS at Sennybridge, Powys (altitude 309 m) at 0000 GMT on 27 January, 1049.0 mbar at Cynwyd, Clwyd (228 m) at 1200 GMT on 26 January (*Weather Log*, January, 1992) and 1048.7 mbar at Cilfynydd (194 m) at 2100 GMT on 26 January. Other high values included 1048.5 mbar at Manchester/Ringway, 1048.1 mbar at Eskdalemuir and 1048.0 mbar at Carlisle, Birmingham/Edmond, Watnall and Newcastle Weather Centre. At London's Heathrow Airport the pressure reached 1046.5 mbar at 2300 GMT 26 January and 0000 GMT on 27 January, the highest barometer reading in London since 7 February 1964.

At the time of writing, a barometric pressure of 1048 mbar or more has not been attained in the British Isles since this event. The highest known MSL barometric pressures since then have been 1046.5 mbar at Aviemore on 10 November 1999 and 1046.9 mbar at Castlederg (Co. Tyrone) at 1100 GMT on 13 December 2005.

\* A pressure of 1050.0 mbar was reported at 2100 GMT 26 January and 0000 27 January by the AWS at Trawscoed (52° 21' N, 3° 57' W, 63 m) but at the time the pressure sensor appeared to be about 1 mbar high in comparison with neighbouring stations.

### Common features of notable anticyclones

Intense anticyclones are invariably mid-winter phenomena: of the nine occasions known to have attained 1050 mbar over the British Isles, all but two have occurred in January. Not all notably intense anticyclones in the British Isles are, as might perhaps have been expected, westward offshoots of an intense Siberian or European midwinter high pressure area; in this summary, only the systems in January 1882, January 1907, January 1932 and January 1992 were of this type. The remaining events developed over the Atlantic as travelling anticyclones between intense depressions (January 1896, January 1957, February 1964) or more locally in the wake of a depression plunging south-eastwards across the North Sea (January 1902, December 1926). The system in January 1905 was a hybrid, in that although it presented as a 'Continental' anticyclone, the original high pressure system was of Atlantic origin.

### Extremes of pressure at long-period stations

The highest observed barometric pressure at a selection of long-period observing sites (most of them hourly synoptic stations) in the British Isles is given in Table 2. In most

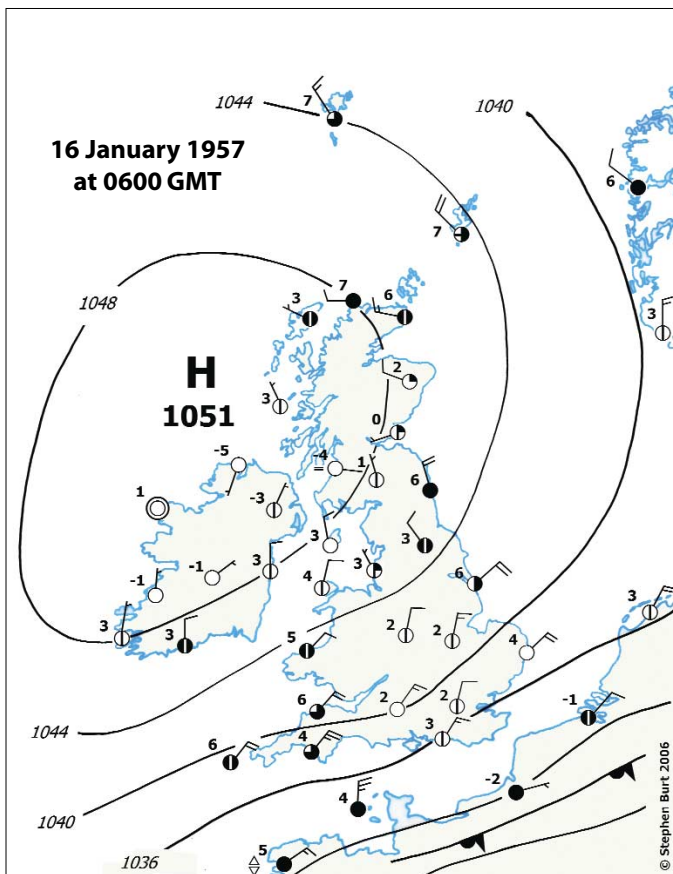


Figure 10. Synoptic situation at 0600 GMT 16 January 1957, from Daily Weather Report

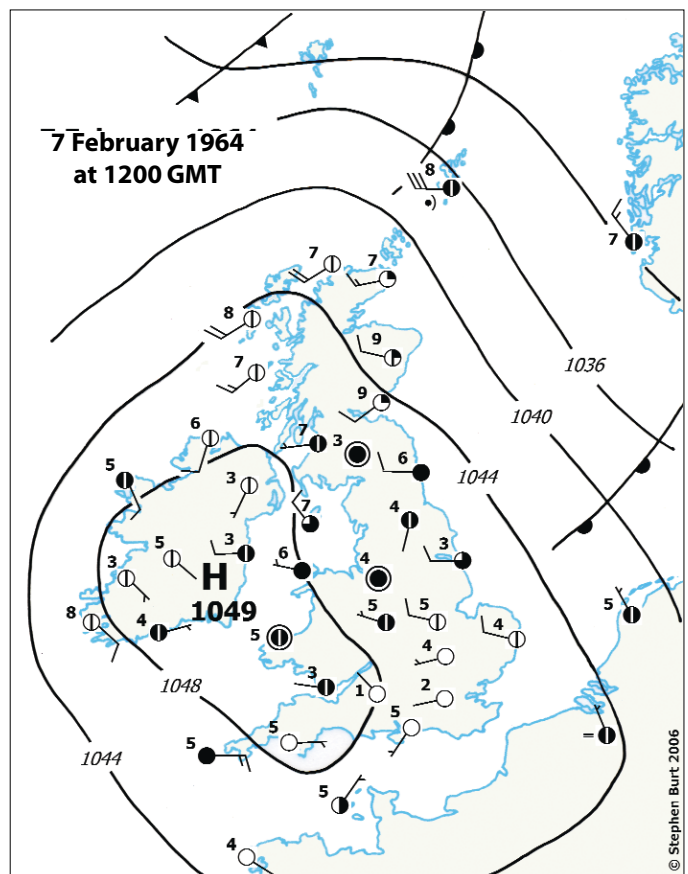


Figure 11. Synoptic situation at 1200 GMT 7 February 1964, from Daily Weather Report



Table 2

Highest and lowest barometric pressures on record at a number of long-period observing sites in the UK and Ireland (typically 40 years or more of computerised hourly or three hourly observations available in the UK Met Office and Met Éireann data archives; where two or more stations are bracketed together, the highest and lowest values from the combined record have been used). Slightly higher or lower values may have occurred between observations. All times quoted are GMT.

Region and station	Period	HIGHEST Value/date	LOWEST Value/date	Range mbar	Source
<b>Northern Scotland</b>					
Lerwick	1957–2005	1049.1 mbar 09h 23 Feb 1962	944.4 mbar 07h 25 Dec 1999	104.7	1
Wick	1957–2005	1047.6 09,12h 16 Jan 1957	942.6 04–07h 20 Dec 1982	105.0	1
Cape Wrath	1957–9/1997	1049.1 09h 16 Jan 1957	938.8	110.3	1
Altnaharra	10/1997–2005		03h 20 Dec 1982		
Stornoway	1957–2005	1050.4 09h 16 Jan 1957	937.6 * 0020h 20 Dec 1982	112.8	1
<b>North-east Scotland</b>					
Kinloss	1959–2005	1047.3 09h 23 Feb 1962	944.0 03h 20 Dec 1982	103.3	1
Aberdeen/Dyce	1957–2005	1048.7 09h 23 Feb 1962	945.6 01h 25 Dec 1999	103.1	1
Edinburgh/Turnhouse	1957–10/1999	1048.5 03h 16 Jan 1957	949.1	99.4	1
Edinburgh, Gogarbank	11/1999–2005		18h 1 Dec 1966		
<b>East and north-east England</b>					
Tynemouth	1957–6/2001	1047.6 21h 7 Feb 1960	949.5	98.1	1
Newcastle W Ctr	7/2001–9/2005		00h 2 Dec 1966		
Albemarle	10–12/2005				
Waddington	8/1950–2005	1047.9 12h 26 Jan 1992	956.7 17h 25 Feb 1989	91.2	1
<b>East Anglia</b>					
Coltishall	11/1962–2005	1047.1 12h 23 Dec 1962	953.9 23h 25 Feb 1989, 00h 26 Feb 1989	93.2	1
Marham	1957–2005	1047.0 22h 26 Jan 1992	954.8 21,22,23h 25 Feb 1989	92.2	1
<b>Midlands</b>					
Birmingham/Elmdon	6/1949–3/1999	1048.1 12h 26 Jan 1992	953.9	94.2	1
Coleshill	4/1999–2005		00h 5 Feb 1951		
<b>South-east England</b>					
London/Heathrow	1949–2005	1047.3 09h 7 Feb 1964	952.3 18,19h 25 Feb 1989	95.0	1
Kew Observatory	1869–1953		959.3 05h 9 Dec 1886		
Greenwich Observatory	1814–1884		948.7 05h 25 Dec 1821	96.0	3
South Farnborough	1957–2005 (no data 1/1974–11/1983)	1047.9 09h 7 Feb 1964	951.9 18h 25 Feb 1989		1
<b>Western Scotland</b>					
Benbecula	1957–7/1996	1050.9 09h 16 Jan 1957	939.7 23h 19 Dec 1982	111.2	1
Tiree	1957–2005	1050.3 09h 16 Jan 1957	944.7 13h 9 Feb 1988	105.6	1
Glasgow – Renfrew/ Abbotsinch	1949–4/1966 5/1966–4/1999	1049.4 03h 16 Jan 1957	947.6	101.8	1
Bishopton	5/1999–2005		18h 1 Dec 1966		
Prestwick	1957–1/1997	1049.4 03h 16 Jan 1957	945.2	104.2	1
Prestwick RNAS	2/1997–2005		18h 1 Dec 1966		
<b>Isle of Man</b>					
Ronaldsway	1957–2005	1047.8 11h 26 Jan 1992	946.5 18h 1 Dec 1966	101.3	1
<b>North-west England and North Wales</b>					
Carlisle	1961–2005	1048.0 23h 26 Jan 1992	946.5 21h 1 Dec 1966	101.5	1
Manchester/Ringway	1949–10/2004	1048.5 11h 26 Jan 1992	952.5	96.0	1
Woodford	11/2004–2005		00h 5 Feb 1951		
Valley	1957–2005		1048.0 12h 7 Feb 1964		

Table 2 continued

Region and station	Period	HIGHEST Value/date	LOWEST Value/date	Range mbar	Source
<b>South-west England and South Wales</b>					
Aberporth	1957–2005	1048.2 09, 12h 7 Feb 1964	950.3 05h 17 Dec 1989	97.9	1
Cardiff/Rhoose	1957–1/1998	1048.4 12h 7 Feb 1964	952.4	96.0	1
St Athan	2/1998–2005		15h 25 Feb 1989		
Plymouth	1949–2005	1048.3 12h 7 Feb 1964	951.1 16h 25 Feb 1989	97.2	1
<b>Northern Ireland</b>					
Aldergrove	1949–2005	1049.6 06h 16 Jan 1957	943.9 15h 1 Dec 1966	105.7	1
Ballykelly	1957–70, 1995–2005	1050.8 09h 16 Jan 1957	944.0 15h 1 Dec 1966	106.8	1
<b>Ireland</b>					
Malin Head	5/1955–12/2005	1050.6 09h 16 Jan 1957	943.6 13h, 14h 1 Dec 1966	107.0	4
Belmullet	9/1956–12/2005	1050.9 08h 16 Jan 1957	943.2 17h 17 Jan 1995	107.7	4
Clones	1951–2005	1050.1 08h, 09h 16 Jan 1957	943.9 19h 4 Feb 1951	106.2	4
Claremorris	1950–2005	1050.8 09h 16 Jan 1957	943.9 17h 4 Feb 1951	106.9	4
Mullingar	1950–2005	1049.9 10h 16 Jan 1957	943.0 17h 4 Feb 1951	106.9	4
Dublin Airport	11/1941–12/2005	1048.7 11h 7 Feb 1964	944.1 17,18,19h 4 Feb 1951	104.6	4
Casement Aerodrome	1964–2005	1048.5 10h, 11h 7 Feb 1964	945.6 04h 17 Dec 1989	102.9	4
Birr	10/1954–12/2005	1049.4 10h 16 Jan 1957	944.9 02h 17 Dec 1989	104.5	4
Shannon Airport	9/1945–12/2005	1049.4 11h 16 Jan 1957	942.8 14h 4 Feb 1951	106.6	4
Valentia Observatory	1894–2005	1051.9 00h 29 January 1905			5
	10/1939–12/2005	1048.4 10h, 11h 16 Jan 1957	942.8 12h 4 Feb 1951		4
Kilkenny	6/1957–12/2005	1049.1 09h 7 Feb 1964	944.8 03h 17 Dec 1989	104.3	4
Rosslare	12/1956–12/2005	1048.4 09h, 10h 7 Feb 1964	946.1 04h 17 Dec 1989	102.3	4
Roches Point	12/1955–12/2005	1048.5 11h 7 Feb 1964	943.2 00h 17 Dec 1989	105.3	4
Cork Airport	1962–2005	1048.4 10,11,12h 7 Feb 1964	942.8 00h 17 Dec 1989	105.6	4
<b>Channel Islands</b>					
Guernsey Airport	1960–2005	1047.7 10h 3 Mar 1990	952.5 11h 25 Feb 1989	95.2	1
Jersey	1862–2005	1051.7 02h 29 Jan 1905	953.8 1320, 1920h 25 Feb 1989	97.9	6
<b>Ocean Weather Ships</b>					
OWS 'A' 62°N, 33°W	1961–70	1050.0 14h 4 Jan 1969 (+)	945.8 15h 21 Sept 1968	104.2	7
OWS 'C' 52.75°N, 35.5°W	1961–70	1045.9 21h 27 Feb 1970	956.7 09h 23 Feb 1964	89.2	7
OWS 'D' 44°N, 41°W	1961–70	1045.0 12h 5 Feb 1970 (+)	956.0 18h 28 Feb 1963	89.0	7
OWS 'E' 35°N, 48°W	1961–70	1038.9 12h 19 May 1969	978.0 03h 6 Jan 1963 (+)	60.9	7
OWS 'I' 59°N, 19°W	1961–70	1048.1 04h 31 Jan 1963 (+)	931.1 01h 16 Jan 1962 (+)	117.0	7
OWS 'J' 52.5°N, 20°W	1961–70	1042.9 13h 6 Feb 1965	949.5 16h 17 Nov 1963	93.4	7
OWS 'K' 45°N, 16°W	1961–70	1045.6 12h 11 Feb 1962	967.5 21h 9 Nov 1963	78.1	7
OWS 'M' 66°N, 2°E	1961–70	1050.3 23h 25 Feb 1962 (+)	948.5 09h 28 Feb 1967	101.8	7

(+) for OWS data indicates the same value occurred at one or more successive hours

**NOTES**

\* Stornoway's minimum is from the barograph record: the lowest at an observation hour was 938.2 mbar at 01h

**SOURCES**

1. UK Met Office hourly and three-hourly observational datasets: courtesy National Climate Information Centre
2. Shellard and Douglas (1951)
3. Marriott (1884)

4. Courtesy of Climatological Division, Met Éireann January 2006
5. Rohan (1975)
6. Courtesy of Frank le Blancq, Jersey Met Department January 2006
7. UK Met Office, Special Investigations Branch

cases the records have been derived from the period of computerised records. (For completeness, the lowest values are also included – these were also given in Table 2 in Part 1 of this article – together with the observed range in barometric pressure.) Figure 12 shows the highest observed MSL pressure observed since 1949 together with the date on which the highest value occurred (based on the records in Table 2).

## Notable ranges in barometric pressure

Table 2 shows that the observed range of barometric pressure during the period 1949–2005 exceeded 90 mbar everywhere in the British Isles, and surpassed 110 mbar in the north-west of Scotland. The site at Ochertyre in Perthshire recorded the remarkable range in pressure of 127.8 mbar in 12 years, from 925.6 mbar on 26 January 1884 to 1053.4 mbar on 9 January 1896.

As noted above, the development of a series of intense depressions can lead to the rapid intensification of travelling anti-cyclones, and where both are embedded in a mobile flow rapid changes in atmospheric pressure can result as the systems pass over a point on the surface. Accounts of notable ranges in barometric pressure are harder to come by, but the following serve as examples:

- In January 1902, Aberdeen Observatory recorded a rise of almost 70 mbar in 88 hours, from 984.8 mbar at 0500 and 0600 GMT on 28 January to the British Isles highest of 1053.6 mbar at 2200 GMT on 31 January;
- In February 1938 Deerness, Orkney recorded 948.0 mbar on 1st followed by 1037.1 mbar on 19th, a range of 89.1 mbar within three weeks;
- In May 1943, Dublin recorded 971.0 mbar on 8 May followed by 1042.2 mbar on 16th, a rise of 71 mbar in eight days;
- In early 1962, Lerwick (Shetland) recorded 954.7 mbar on 11 January followed less than six weeks later by 1049.1 mbar on 23 February, a range of 94.4 mbar;
- In late January 1989, the barometric pressure reached 1045 mbar widely across southern England: on 25 February the pressure fell below 949 mbar at Portland, Dorset (see Part 1 for details), a range of 96 mbar in less than four weeks;
- In November–December 2005, the barometric pressure in parts of south-west England fell from 1038 mbar on 22 November to 964 mbar on 2 December before recovering to 1041 mbar on 11 December – a fall of 74 mbar in 10 days followed by a rise of 77 mbar in 9 days.

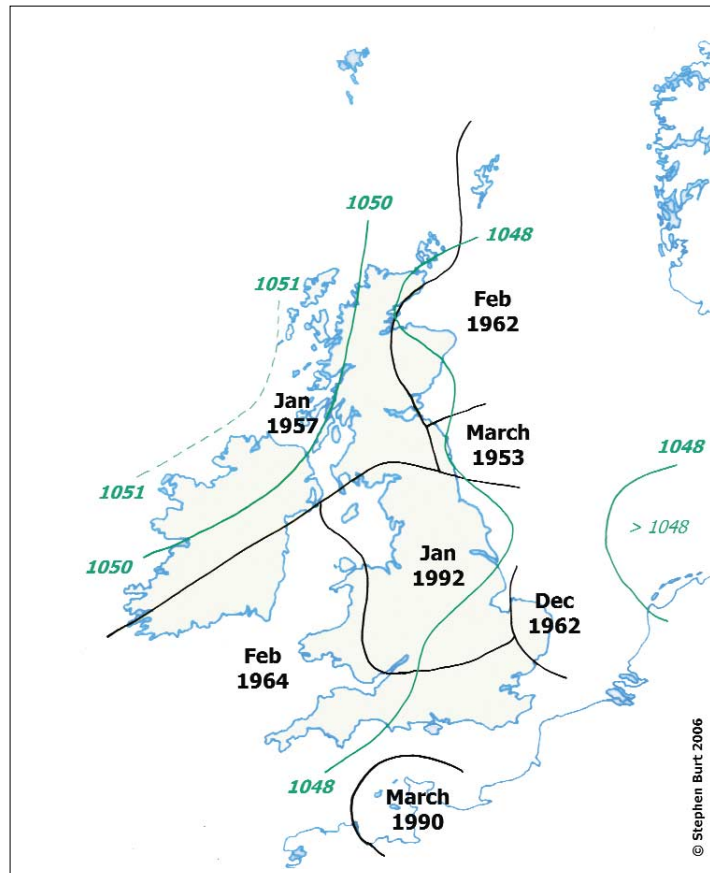


Figure 12. Highest observed MSL pressure observed since 1949 (smoothed distribution) together with the date of the event

## Monthly extremes of pressure

Almost all extremes of atmospheric pressure (below 950 mbar or above 1048 mbar) recorded in the British Isles have occurred between mid-December and mid-February. To provide perspective on other months in the year, Table 3 lists the known monthly extremes of pressure in the British Isles.

## Summary

On at least 17 occasions within the last 200 years, a barometric pressure of 1048 mbar or more has been reliably recorded at one or more stations within the British Isles. On only nine occasions has 1050 mbar or greater been recorded, the most recent occasion of such a high value being 50 years ago. The highest barometric pressure recorded within the British Isles occurred at Aberdeen in Scotland on 31 January 1902, when 1053.6 mbar was measured.

The author would welcome documented examples of other occasions of barometric pressures in excess of 1048 mbar in the British Isles which may have been overlooked in this analysis.

## Data sources and acknowledgements

I am very grateful to a number of people and organisations who have been most helpful in tracking down sometimes very obscure observations or references for this compilation. Frank Le Blancq from the States of Jersey Met. Department provided the extremes of barometric pressure on record in Jersey (and generated several useful related discussions on related topics): Eddie Graham from the University of Fribourg in Switzerland provided helpful comments relating particularly to the Irish extremes: Niall Brooks from the Climatological Division of Met Éireann provided the long-period extremes at the synoptic sites in Ireland used in Table 2, and the UK Met Office's National Climate Information Centre provided much of the UK content in Table 2. I offer a particular 'thank you' to the National Meteorological Library in Exeter for unearthing many of the references, in particular to Martin Kidds for his unflinching enthusiastic assistance in obtaining copies of numerous *Daily Weather Reports* and additional material from the Met Office archives in Exeter and in Edinburgh.



Table 3

Highest and lowest MSL pressures recorded in the British Isles for each month, nominally 1870 to date

Month	HIGHEST VALUE	Site and date	LOWEST VALUE	Site and date	Monthly range mbar
	mbar		mbar		
January	1053.6	Aberdeen Observatory, 2200 GMT 31 Jan 1902 (Note 1)	925.6	Ochertyre, Perthshire, 2145h 26 January 1884	128.0
February	1052.9	Aberdeen Observatory, 0000 GMT 1 Feb 1902 (Note 1)	942.3	Midleton, Co. Cork, 15h 4 February 1951	110.6
March	1048.6	Tynemouth, 9 March 1953	946.2	Wick, 18h 9 March 1876	102.4
April	1044.5	Eskdalemuir, 11 April 1938	952.9	Malin Head, 1 April 1948	91.6
May	1042.2	Dublin Airport, 16 May 1943	968.0	Sealand, Cheshire, 8 May 1943	74.2
June	1043.1	Clones, Co. Monaghan, 14 June 1959	968	Shetland, 27/28 June 1938 (Note 2)	75.1
July	1039.3	Aboyne, Aberdeenshire 0100 GMT 16 July 1996 (Note 3)	967.9	Sule Skerry, 8 July 1964	70.4
August	1036.7	Pembroke, 12 August 1949	967.7	Belmullet, Co Mayo, 14 August 1959 (Note 4)	68.9
September	1041.2	Shawbury, Shropshire, 00 and 01 GMT 19 Sept 1986	957.1	Claremorris, Co. Mayo, 0700 GMT 21 Sept 1953	83.9
October	1045.6	Dyce, Aberdeen, 31 October 1956	946.8	Cawdor Castle, 0115h 14 October 1891	98.8
November	1046.5	Aviemore, 10 November 1999	939.7	Monach LtHo, Hebrides, 11 November 1877	106.8
December	1051.9	Wick, 1300 GMT 24 December 1926	927.2	Belfast, 1330h 8 December 1886	124.7
<b>YEAR</b>	<b>1053.6</b>	<b>Aberdeen Observatory, 2200 GMT 31 Jan 1902</b>	<b>925.6</b>	<b>Ochertyre, Perthshire, 2145h 26 January 1884</b>	<b>128.0</b>

SOURCES and REFERENCES: The table is based upon that given in Met Office *Climatological Memorandum* 51A (1973) with numerous revisions and later additions by the author.

Note 1 – Obtained from the Aberdeen Observatory hourly barograph tabulations, courtesy of the Met Office Archives in Edinburgh, February 2006.

Note 2 – See *Met Mag*, July 1938, p 142: quoted only to 1 mbar. The value was checked from the Lerwick Observatory barograph records (lowest value 970.4 mbar at 0130 GMT on 28 June), courtesy of the Met Office Archives in Edinburgh, February 2006.

Note 3 – *Weather Log*, July 1996.

Note 4 – Rohan (1975), p. 111.

## References

**Anon.** 1820. Account of the remarkable Depression of the Thermometer, and Rise of the Barometer, in January 1820. *Edinburgh Philosophical Journal*. Vol. II: p. 335.

**Burt CC.** 2004. *Extreme weather*. W W Norton & Co: New York.

**Burt S.** 2006. Britain's highest barometric pressure on record is incorrect. *Weather*. **61**: 210–1.

**Burt S.** 2007. The Lowest of the Lows . . . Extremes of barometric pressure in the British Isles, Part 1 – the deepest depressions. *Weather*. **62**: 1–11.

**Fox WL.** 1905. The high barometer of January 1905 at Falmouth. *Symons's Meteorol. Mag.* **40**: p. 6.

**Hawke EL.** 1932. Extreme barometric maxima in pairs. *Meteorol. Mag.* **67**: 40–41.

**Lempfert RGK.** 1907. The high barometer of January 1907. *Symons's Meteorol. Mag.* **42**: 1–3.

**Marriott W.** 1884. The great storm of January 26th 1804. *Q. J. R. Meteorol. Soc.* **10**: 114–123.

**Met Office.** 1973. *Averages of mean sea level barometric pressure for the United Kingdom 1941–70*. Climat. Mem. 51A, 27 pp.

**Morgans WR.** 1932. The high pressure of January 1932. *Meteorol. Mag.* **67**: 18–19.

**O'Connor ED.** 1932. The drought and high pressure of February. *Meteorol. Mag.* **67**: 39–40. [The author quotes the 1896 Stonyhurst extreme as occurring on 26 January; this is certainly a misprint for 9 January – the 1932 extreme occurred on 26 January.]

**Rohan PK.** 1975. *The climate of Ireland*. Stationery Office, Dublin. 112 pp. – also second edition 1986.

**Scott RH.** 1896. Notes on the unusually high barometer readings in the British Isles – January 1896. *Q. J. R. Meteorol. Soc.* **22**: 152–9.

**Shellard HC and Douglas CKM.** 1951. Low pressure recorded on February 4 1951. *Meteorol. Mag.* **80**: 362–4.

**Symons GJ.** 1899. Meteorological extremes. *Symons's Monthly Meteorol. Mag.* **34**: 81–85.

**US National Weather Service.** 1989. National Weather Service Anchorage Alaska telex bulletin, 31 January 1989.

**Wallis HS.** 1882. The high atmospheric pressure in the middle of January 1882. *Q. J. R. Meteorol. Soc.* **8**: 146–154.

Copyright © Stephen Burt 2007.

All rights reserved.

doi: 10.1002/wea.35



# Paper 9

## **New British Isles late-winter extreme barometric pressure, 29 March 2020**

By Stephen Burt. *Weather*, published online 16 Oct 2020, <https://doi.org/10.1002/wea.3840>

*Bibliography #3. Word count 2200, excluding references.*


---

### **Open Access Article**

*This is an open access article distributed under the terms of the Creative Commons CC BY license, which permits unrestricted use, distribution, and reproduction in any medium, provided the original work is properly cited.*



# New British and Irish Isles late-winter extreme barometric pressure, 29 March 2020

**Stephen Burt**   
 Department of Meteorology,  
 University of Reading, UK

During 28–29 March 2020, the rapid development of an anticyclone over the North Atlantic resulted in its central mean sea level (MSL) barometric pressure reaching 1055hPa near 59°N 20°W at 0000 UTC on 29 March. As the anticyclone slipped slowly south-eastwards over the following 12 hours, pressure exceeded 1050hPa in western Scotland and the north of Ireland, establishing new records at several long-running sites. Several factors combine to make this event unique in British climatology. Firstly, this was the second occasion during the winter of 2019/20 when 1050hPa was attained within the British and Irish Isles (the first being 19–20 January 2020), following an interval of more than 60 years since the previous such event. No previous winter in at least the last 200 years has seen two such events occur within one season. Secondly, during this event the previous March pressure record for the British and Irish Isles was exceeded, by over 3hPa: no previous event reaching 1050hPa over the British and Irish Isles has occurred so late in the winter season. Remarkably, between them the January and March 2020 events established new long-term high pressure records in all four capital cities within the United Kingdom – in London and Cardiff on 20 January, and Edinburgh and Belfast on 29 March.

## Causes and development

An anomalously strong and persistent polar vortex remained in place for much of the first 3 months of 2020, and the intense thermal gradients on the periphery of the vortex resulted in powerful jet streams (speeds well in excess of 150kn on occasion) across the North Atlantic. This in turn led to the development of frequent and intense cyclonic activity, the most noteworthy of these being depression centres of 930hPa between Greenland and Iceland on 8 February, followed by another similar system that deepened to

919hPa south of Iceland on 15 February – close to the lowest on record for the North Atlantic (Burt, 1993). The divergent outflow at upper-troposphere levels from these

intense cyclonic systems often accelerated anticyclonic development through convergence at or near the right jet entrance region (for an explanation of why this occurs

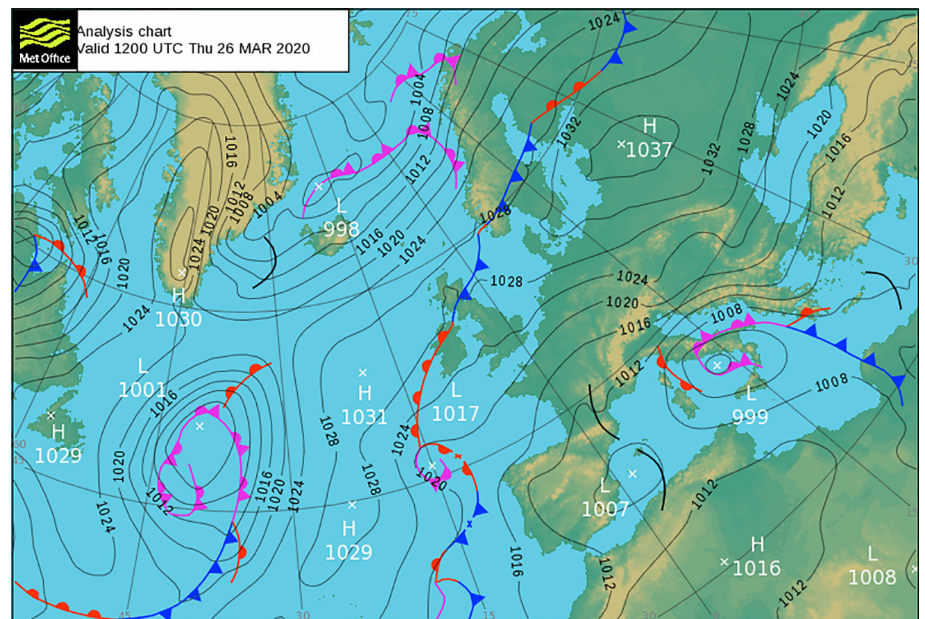


Figure 1. Met Office North Atlantic analysis chart for 1200 GMT 26 March 2020 (Courtesy Met Office: Crown Copyright.)

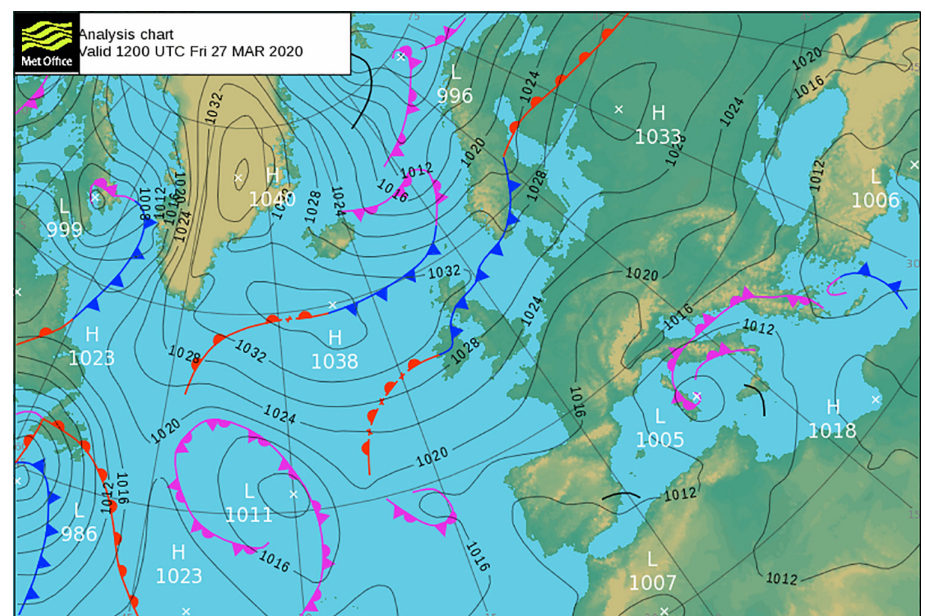


Figure 2. As Figure 1 but for 24 hours later, 1200 UTC 27 March 2020, showing the rapid development of the anticyclone in intensely cold air over Greenland. (Courtesy Met Office: Crown Copyright.)



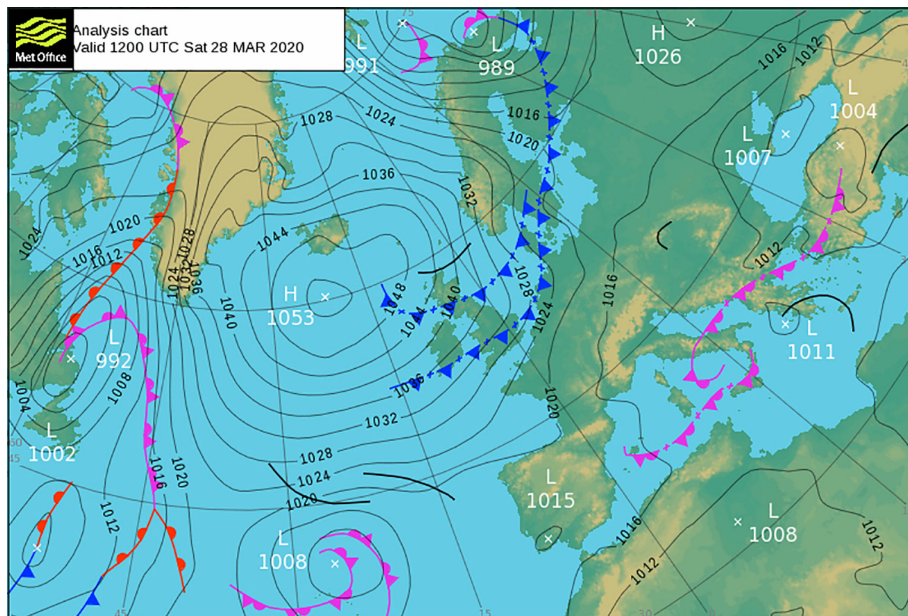


Figure 3. As Figure 2 but for 24 hours later, 1200 UTC 28 March 2020. The anticyclone has continued its rapid development while moving southeast and absorbing an existing area of high pressure, and has now become the dominant synoptic feature over the North Atlantic. (Courtesy Met Office: Crown Copyright.)



Figure 5. Location of places referred to in the text.

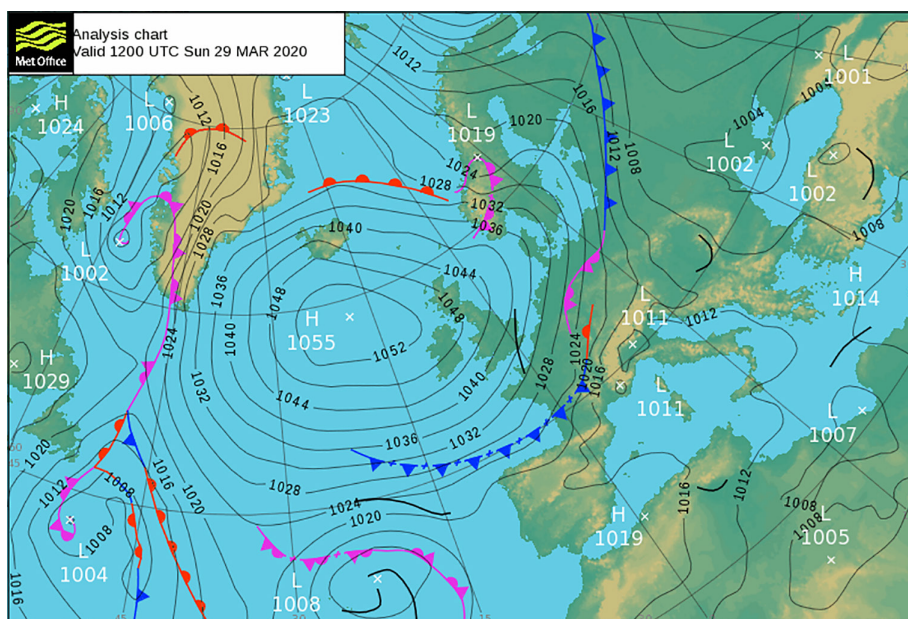


Figure 4. As Figure 3 but for 24 hours later, 0000 UTC 29 March 2020. The anticyclone is almost stationary, with its centre near 59°N 18°W, and has reached its peak central pressure of 1055 hPa. The highest pressures over the British and Irish Isles were reached around the time of this chart. (Courtesy Met Office: Crown Copyright.)

see, e.g. McIlveen, 2010, Chapter 7), and as a result, several North Atlantic anticyclones reached or surpassed 1035–1040 hPa between January and March. This meant that the pressure gradient across the North Atlantic exceeded 100 hPa on several occasions. One such intense anticyclone developed very rapidly over 18–20 January, the barometer surpassing 1050 hPa over southern England, northern France and Belgium on 19–20 January (Burt, 2020), giving London its highest barometric pressure in over 300 years.

On 22–23 March 2020, another intense anticyclone developed off the east coast of the USA and moved rapidly northeast towards the Denmark Strait (between Iceland and Greenland), subsequently deepening to 955 hPa. As this system matured and slowed, the jet stream flow buckled as an upper ridge amplified west of Greenland during 26–27 March, and a surface anticyclone began to build over Greenland in very cold air on the northern side of the upper ridge. The newly formed anticyclone centre first appeared on the UK Met Office North Atlantic anal-

ysis at 1200 UTC on 26 March with a centre of 1030 hPa over southern Greenland (Figure 1). As the upper ridge slowed and became stationary over Greenland, the new anticyclone continued to intensify, and by 1200 UTC on 27 March, the centre lay over central Greenland at 1040 hPa (Figure 2). Pressure continued to build in mid-Atlantic, and over the following 12 hours, the two anticyclonic centres merged as the anticyclone over Greenland built southwards and eastwards, amalgamating with and quickly absorbing the developing mid-Atlantic system. By 0000 UTC 28 March (not shown), the system had become the dominant synoptic feature over the North Atlantic, with twin centres of 1051 hPa located just south of Iceland and close to 60°N 21°W. At 1200 UTC 28 March (Figure 3), the anticyclone centre lay close to 60°N 22°W, with a central pressure of 1053 hPa. Outflow of the very cold air within its circulation is evident from the long double cold fronts over the eastern Atlantic, with strong and cold northerly or northeasterly winds affecting the British Isles; 1000–500 hPa thickness values were just 517 dam at both Thorshavn (Faeroes) and Lerwick (Shetland) at this time.

Over the subsequent 24 hours, the anticyclone continued to drift a little further south and east. At 0000 UTC on 29 March, the centre lay close to 59°N 20°W, its central pressure having reached its maximum of 1055 hPa; at this time, the 1048 hPa isobar extended over the whole of western and northwestern Scotland. At Stornoway, the MSL barometer stood at 1050.2 hPa at midnight. During 29 March, the centre began to migrate slowly westwards, maintaining its peak central pressure at or close to 1055 hPa. The highest barometric pressures over the



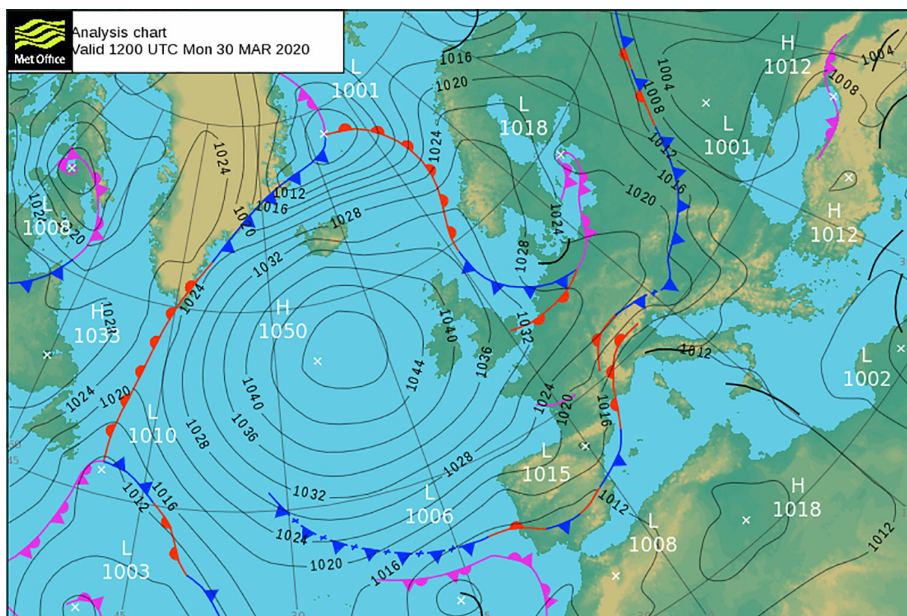


Figure 6. As Figure 4 but for 24 hours later, 1200 UTC 30 March 2020, the anticyclone centre having drifted a little west and south and begun to decline. (Courtesy Met Office: Crown Copyright.)

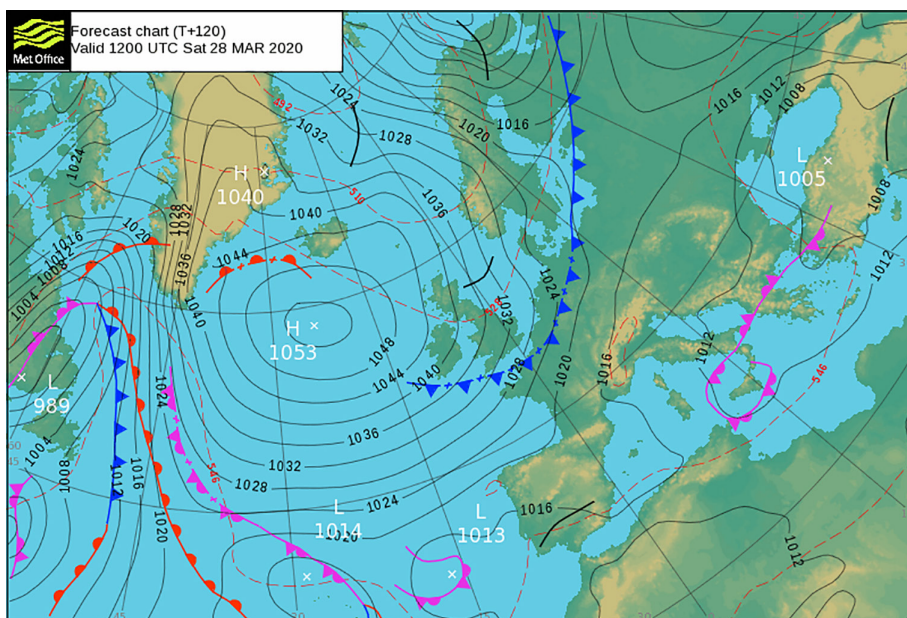


Figure 7. Met Office 120h North Atlantic surface forecast chart for 1200 GMT 28 March 2020, issued more than 60h prior to the synoptic situation depicted in Figure 1. The position and central pressure of the intense anticyclone, and the other surface features including fronts, are in almost perfect agreement with the analysis chart from 5 days later, as shown in Figure 3. (Courtesy Met Office: Crown Copyright.)

British and Irish Isles, namely, 1051.hPa at Tiree at 0900 and 1000 UTC, 1051.2hPa at South Uist at 0900 UTC and 1051.3hPa at Malin Head at 1100 UTC, were recorded about the time of the chart in Figure 4. (Locations are shown on Figure 5.) Cold northerly or northeasterly winds continued to blow across the British Isles, particularly strong on east and northeast-facing coasts, where gusts of 40kn or more occurred widely. Eastern and southeastern England saw showers of sleet, snow and hail during the day, despite the barometer remaining at or above 1040hPa.

Thereafter, the anticyclone continued its slow movement west-southwestwards, and began to weaken; Figure 6 shows the synoptic situation at 1200 UTC on 30 March, by which time the central pressure had declined to 1050hPa. It continued to drift slowly southwestwards, eventually losing its identity in mid-Atlantic on 3–4 April.

### Was the event forecast?

As was the case in the winter's first extreme anticyclone in January 2020 (Burt, 2020), the event was well forecast several days

in advance. Figure 7 shows the Met Office T+120 (5 day) forecast chart valid for 1200 UTC on 28 March 2020 for comparison with the subsequent analysis in Figure 3. This forecast was issued at 2229 UTC on 23 March, well before the anticyclone had begun to form over Greenland. The forecast position and intensity of the anticyclone were extraordinarily close to the subsequent analysis, despite this event being well outside previous North Atlantic climatology for so late in the winter.

### The anticyclone over the British and Irish Isles, 29 March 2020

Figure 4 depicts the Met Office North Atlantic analysis at 1200 UTC on 29 March 2020, at about the closest approach of the centre of the anticyclone to the British and Irish Isles. Table 1 lists MSL pressures for a selection of synoptic stations in Scotland and the north of Ireland, where pressures surpassed 1048hPa, for the period 2100 UTC 28 March to 1500 UTC 29 March 2020. Figure 5 shows the locations of places referred to.

The first report of MSL pressure reaching or surpassing 1050hPa from a station within the British and Irish Isles was from Stornoway at 0000 UTC on 29 March, when 1050.2hPa was reported (Table 1). At South Uist Range, the pressure reached 1050.3hPa at 0100 UTC and 1050.6hPa at 0200 UTC before declining slowly, thereafter rising once more to 1050.4hPa at 0600 and thence to 1051.2hPa at 0900 UTC, the highest value reported from any site in the UK during this event. This represents a new record for the site for the period of the composite digital observation record with nearby Benbecula, extending back to 1957 (Table 1). In Ireland, Malin Head reached 1050.0hPa at 0700 UTC and thereafter rose slowly to 1051.3hPa at 1100 UTC, the highest value attained at any site in the British and Irish Isles on this occasion and a new site record since observations commenced there in May 1955 (and it was within 1hPa of the Irish national extreme, namely, 1051.9hPa recorded at Valentia on 29 January 1905 – Burt, 2007)<sup>1</sup>. At Malin Head, the barometer remained continuously at or above 1050hPa for nine consecutive hours (0700–1500 UTC on 29 March) and at or above 1040hPa for 62 consecutive hours, only falling below this level after 2300 UTC on 30 March. Figure 8 plots the hourly MSL barometric pressures recorded at Malin Head during 24–31 March 2020.

<sup>1</sup>Offshore, the M4 Donegal buoy at 55.0°N 10.0°W (Figure 5) reported 1051.9hPa at 1200 UTC on 29 March according to Met Éireann (<https://www.met.ie/provisional-report-on-new-atmospheric-pressure-records-for-land-and-sea>, accessed 24 April 2020).

Table 1

Reported MSL pressures (hPa), for the period 2100 UTC 28 March to 1500 UTC 29 March 2020, from a selection of synoptic stations, mostly located within the 1049hPa isobar on Figure 9. Values reaching or surpassing 1050hPa are shown in bold; the highest reported hourly pressure at each site is underlined. New site records are indicated; see also Table 2.

	Wick	Kinloss	Aberdeen Dyce	Edinburgh Gogarbank	Stornoway	South Uist Range	Tiree	Islay: Port Ellen	Glasgow Bishopston	Belfast Aldergrove	Malin Head	Claremorris	Belmullet	Mace Head
New site record	X	X	X	X		X	X	X	X	X	X			
WMO Ilii	03075	03066	03091	03166	03026	03023	03100	03150	03134	03917	03980	03970	03976	03963
Time UTC	39m	7m	65m	57m	9m	10m	12m	17m	59m	81m	20m	24m	31m	23m
28 March	1047.3	1047.4	1045.1	1044.7	1049.3	1048.6	1046.7	1045.3	1045.1	1043.6	1045.0	1042.3	1043.7	1041.7
2200	1047.5	1047.8	1045.6	1045.4	1049.7	1049.3	1047.6	1046.0	1045.9	1044.3	1045.8	1042.9	1044.3	1042.2
2300	1047.9	1048.4	1046.2	1045.6	1049.8	1049.5	1048.2	1046.9	1046.4	1045.1	1046.6	1044.0	1045.0	1043.0
0000	1048.0	1048.5	1046.6	1046.2	<b>1050.2</b>	1049.9	1048.7	1047.4	1046.9	1046.0	1047.1	1044.7	1045.7	1043.8
0100	<u>1048.6</u>	1048.8	1046.7	1046.6	<u>1050.3</u>	<b>1050.3</b>	1049.2	1048.1	1047.6	1046.5	1047.9	1045.3	1046.2	1044.4
0200	1048.5	<u>1049.1</u>	1047.0	1046.7	<u>1050.3</u>	<b>1050.6</b>	1049.6	1048.1	1047.7	1046.9	1048.1	1045.9	1046.8	1044.9
0300	1048.3	1049.0	1047.1	1047.0	<b>1050.2</b>	<b>1050.2</b>	1049.8	1048.7	1048.0	1047.0	1048.4	1046.3	1047.2	1045.3
0400	1048.2	1049.0	1047.1	1047.1	<b>1050.0</b>	<b>1050.2</b>	1049.9	1048.8	1048.1	1047.4	1048.6	1046.7	1047.5	1045.7
0500	1047.7	1048.7	1047.1	1047.0	1049.9	1049.9	<b>1050.0</b>	1049.2	1048.2	1047.5	1049.0	1047.3	1047.9	1046.1
0600	1047.5	1048.6	1047.3	1047.4	1049.5	<b>1050.4</b>	<b>1050.2</b>	1049.4	1048.4	1047.9	1049.4	1048.0	1048.4	1047.0
0700	1047.7	1049.0	1047.7	1048.0	1049.7	<b>1050.5</b>	<b>1050.6</b>	1049.9	1048.8	1048.4	<b>1050.0</b>	1048.5	1049.3	1047.8
0800	1047.7	1048.9	<u>1047.8</u>	1048.4	1049.9	<b>1050.9</b>	<b>1050.8</b>	<b>1050.5</b>	1049.5	1048.9	<b>1050.6</b>	1049.0	1049.8	1048.4
0900	1047.3	<u>1049.1</u>	1047.6	1048.5	1049.5	<u>1051.2</u>	<u>1051.1</u>	<b>1050.5</b>	<u>1049.6</u>	1049.4	<b>1050.8</b>	1049.3	<b>1050.1</b>	1048.7
1000	1046.5	1048.8	1047.4	<u>1048.7</u>	1049.3	<b>1050.9</b>	<u>1051.1</u>	<b>1050.6</b>	1049.5	1049.6	<b>1051.0</b>	<u>1049.4</u>	<b>1050.4</b>	1048.8
1100	1045.9	1048.1	1047.2	<u>1048.7</u>	1049.1	<b>1050.8</b>	<b>1050.8</b>	<u>1050.7</u>	1049.2	<u>1049.8</u>	<b>1051.3</b>	1049.3	<b>1050.5</b>	1048.7
1200	1045.2	1047.7	1046.5	1048.3	1048.9	<b>1050.7</b>	<b>1050.7</b>	<b>1050.2</b>	1048.8	1049.7	<b>1051.0</b>	1049.3	<u>1050.6</u>	<u>1048.9</u>
1300	1044.7	1047.0	1046.2	1047.8	1048.3	<b>1050.5</b>	<b>1050.5</b>	<b>1050.0</b>	1048.3	1049.3	<b>1050.8</b>	1049.0	<b>1050.5</b>	1048.8
1400	1044.2	1046.3	1045.4	1047.4	1047.9	1049.8	<b>1050.3</b>	1049.8	1047.9	1049.0	<b>1050.5</b>	1048.5	<b>1050.1</b>	1048.4
1500	1043.5	1046.0	1044.5	1046.5	1047.5	1049.3	1049.7	1049.6	1047.2	1048.6	<b>1050.4</b>	1048.4	<b>1050.3</b>	1048.1

Source: synoptic reports via Oqimet.com.



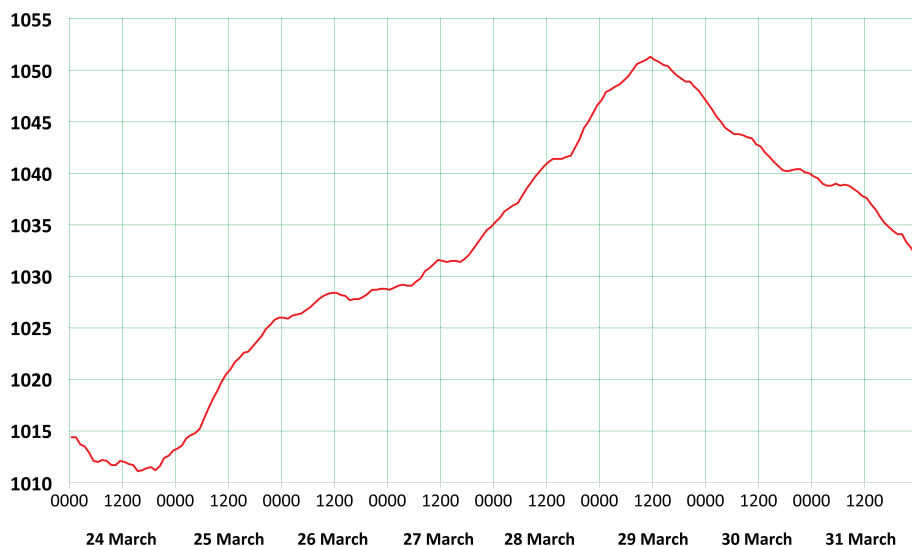


Figure 8. MSL barometric pressure (hPa) at Malin Head (WMO No. 03980) for the period 24–31 March 2020, plotted from hourly synoptic observations. Time is in UTC. The highest value attained, 1051.3hPa at 1100 UTC on 29 March, was the highest barometric pressure recorded anywhere in the British and Irish Isles since December 1926.

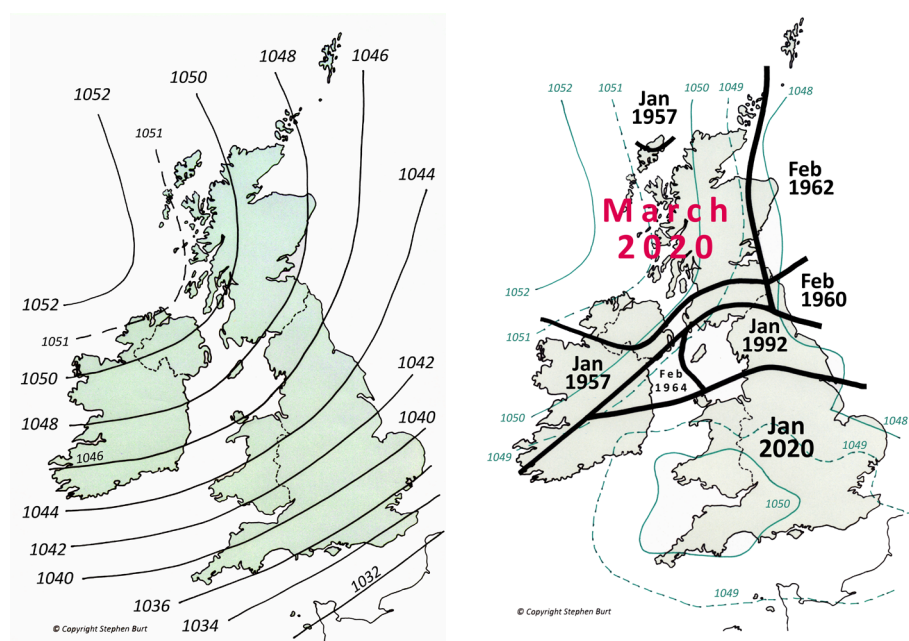


Figure 9. Highest reported MSL barometric pressures on 29 March 2020, in hPa, from hourly synoptic reports. Isobars are plotted at 2hPa intervals.

Figure 10. Dates and areas of highest observed MSL pressure since 1949, with isobars (in hPa). Updated from Figure 12 in Burt (2007) to include January and March 2020 events.

## Climatological significance

Figure 9 shows the highest barometric pressures recorded in the British and Irish Isles on 29 March 2020, based upon hourly synoptic reports: Figure 10 shows both the highest known pressure on post-war record (since 1949) and the date of occurrence of that event<sup>2</sup>. Table 2 compares March 2020

<sup>2</sup>All quoted records for this event are from synoptic pressure observations, mostly hourly and from automatic weather stations, as reported. Slightly higher values may have occurred in between synoptic reports at some sites. There are uncertainties of up to perhaps 0.3hPa in the values tabulated and plotted, particularly for upland sites (see boxed text in Burt, 2020 for a longer discussion).

pressure extremes at several long-period sites in northern, northeastern and western Scotland and Northern Ireland: new extremes were established at nine locations, including 70-year records at Glasgow and Belfast, and also in the Republic of Ireland. Table 2 updates Table 2 in Burt (2007) for these areas to March 2020.

The March 2020 event was exceptional for three reasons: its rarity, the establishment of a new March British and Irish Isles pressure extreme, and for its unprecedented lateness in the winter season.

Although this event was the second occasion on which 1050hPa had been attained in the British and Irish Isles in a 10-week

period, prior to 19–20 January 2020 this level had not been previously reached since January 1957. This was also the first occasion since at least the year 1800 that 1050hPa has been reached in the British and Irish Isles on two separate occasions within a single winter, and it is also notable that new long-term high-pressure records were established in all four capital cities within the UK – in London and Cardiff on 20 January and Edinburgh and Belfast on 29 March. On this occasion, the Malin Head maximum, 1051.3hPa at 1100 UTC on 29 March 2020, also became the highest MSL pressure recorded anywhere in the British and Irish Isles since 24 December 1926, when 1051.9hPa was recorded at Wick (Burt, 2007). Although extremely high, the highest pressures reported on this most recent occasion fell some way short of the highest on record for the British or Irish Isles, namely, 1053.6hPa recorded at Aberdeen Observatory on 31 January 1902 (Burt, 2006, 2007).

This event established a new British and Irish Isles record barometric pressure for March. Prior to March 2020, the highest March pressure on record for anywhere in the British and Irish Isles appears to have been 1047.9hPa, recorded at Scilly on 3 March 1990 (Met Office *Monthly Weather Report*)<sup>3</sup>. This value was comprehensively exceeded by the Malin Head maximum of 1051.3 hPa on 29 March 2020.

Most extraordinary of all is the extreme lateness of this event in the winter season. Figure 11 shows the highest pressure for all occasions since about 1800 when the MSL pressure has risen to 1048hPa anywhere in the British and Irish Isles, plotted against the date on which it occurred (based on the table in Burt, 2007, updated to 2020). Until 2020, the latest date on which 1050hPa has been attained in over 200 years of records has been 24 February, in 1808, in north-east Scotland. The 28–29 March 2020 event clearly sits well outside the ‘envelope’ of all previous events of this nature.

<sup>3</sup>For many years, the highest March MSL pressure recorded in the British and Irish Isles was quoted as 1048.6hPa, recorded at Tynemouth on 9 March 1953. This value originated from the Met Office station data computer archive and is quoted in numerous Met Office publications (e.g. Met Office, 1973: Averages of mean sea level barometric pressure for the United Kingdom 1941–70. Meteorological Office, *Climat. Mem.* 51A and Met Office, 2011: Weather Extremes, National *Meteorological Library and Archive Factsheet 9*) and was duly included in Burt (2007). However, the Tynemouth value has since been found to be incorrect: the online Daily Weather Report available at URL <https://digital.nmla.metoffice.gov.uk> clearly shows the value to have been amended in red ink from 1048.6 to 1043.6hPa, while the highest pressure recorded anywhere on that occasion was just over 1044hPa.

**Table 2**

Sites where the highest barometric pressure in March 2020 approached or surpassed the previous extreme at a number of long-period observing sites in the UK and Ireland (typically 60 years or more of computerised hourly or three-hourly observations available in the UK Met Office and Met Éireann data archives. Where two or more stations are bracketed together, the highest and lowest values from the combined record have been used). Values are in hPa; new extremes are shown in bold type. Slightly higher values may have occurred between hourly or 3-hourly observations. All times quoted are UTC. This is an update to Table 2 in Burt (2007).

WMO station ID (03iii), region and station	Period of record	Previous highest Value/date	March 2020 highest Value/date
<b>Northern Scotland</b>			
005 Lerwick	1957-3/2020	1049.1 09 h 23 Feb 1962	1046.8 00, 01 h 29 March 2020
075 Wick	1957-3/2020	1047.6 09 h, 12 h 16 Jan 1957	<b>1048.6</b> 01 h 29 March 2020
049 Cape Wrath } 044 Altnaharra }	1957-9/1997 10/1997-3/2020	1049.1 09 h 16 Jan 1957	<b>1049.8</b> 01 h 29 March 2020
026 Stornoway	1957-3/2020	1050.4 09 h 16 Jan 1957	1050.3 01, 02 h 29 March 2020
<b>Northeast Scotland</b>			
066 Kinloss	1959-3/2020	1047.3 09 h 23 Feb 1962	<b>1049.1</b> 01 h 29 March 2020
091 Aberdeen/Dyce	1957-3/2020	1048.7 09 h 23 Feb 1962	1047.8 08 h 29 March 2020
049 Edinburgh/Turnhouse } 166 Edinburgh/Gogarbank }	1957-10/1999 11/1999-3/2020	1048.5 03 h 16 Jan 1957	<b>1048.7</b> 10, 11 h 29 March 2020
<b>Western Scotland</b>			
022 Benbecula } 023 South Uist Range }	1957-7/1996 8/1996-3/2020	1050.9 09 h 16 Jan 1957	<b>1051.2</b> 09 h 29 March 2020
100 Tiree	1957-3/2020	1050.3 09 h 16 Jan 1957	<b>1051.1</b> 09, 10 h 29 March 2020
140 Glasgow – Renfrew } 140 Glasgow – Abbotsinch }	1949-4/1966 5/1966-4/1999	1049.4 03 h 16 Jan 1957	<b>1049.6</b> 09 h 29 March 2020
134 Glasgow – Bishopston } 135 Prestwick } 136 Prestwick RNAS }	5/1999-3/2020 1957-1/1997 2/1997-3/2020	1049.4 03 h 16 Jan 1957	1049.3 11 h 29 March 2020
<b>Northern Ireland</b>			
917 Belfast Aldergrove	1949-3/2020	1049.6 06 h 16 Jan 1957	<b>1049.8</b> 11 h 29 March 2020
<b>Republic of Ireland</b>			
980 Malin Head	5/1955-3/2020	1050.6 09 h 16 Jan 1957	<b>1051.3</b> 11 h 29 March 2020
976 Belmullet	9/1956-3/2020	1050.9 08 h 16 Jan 1957	1050.6 12 h 29 March 2020
970 Claremorris	1950-3/2020	1050.8 09 h 16 Jan 1957	1049.4 10 h 29 March 2020

Source: Historical data from Burt (2007), 2020 synoptic reports from Ogimet.com.

## Summary and conclusions

The development and rapid intensification of an intense anticyclone over the North Atlantic, and its close approach to the British and Irish Isles at its maximum extent on 29 March 2020, resulted in the highest MSL barometric pressure recorded anywhere in the British and Irish Isles since December

1926 and the unique occurrence within a single winter of a second 1050hPa event over the British and Irish Isles. This event occurred more than a month later than any previous such occasion in the British and Irish Isles within the last two centuries and more. New post-WWII site records were established widely in northern, north-east and western Scotland and in Northern

Ireland and the north of the Republic of Ireland, while the previous British and Irish Isles March extreme pressure was exceeded by over 3hPa. Remarkably, between them, the January and March 2020 events established new long-term high pressure records in all four capital cities within the UK – in London and Cardiff on 20 January and Edinburgh and Belfast on 29 March.

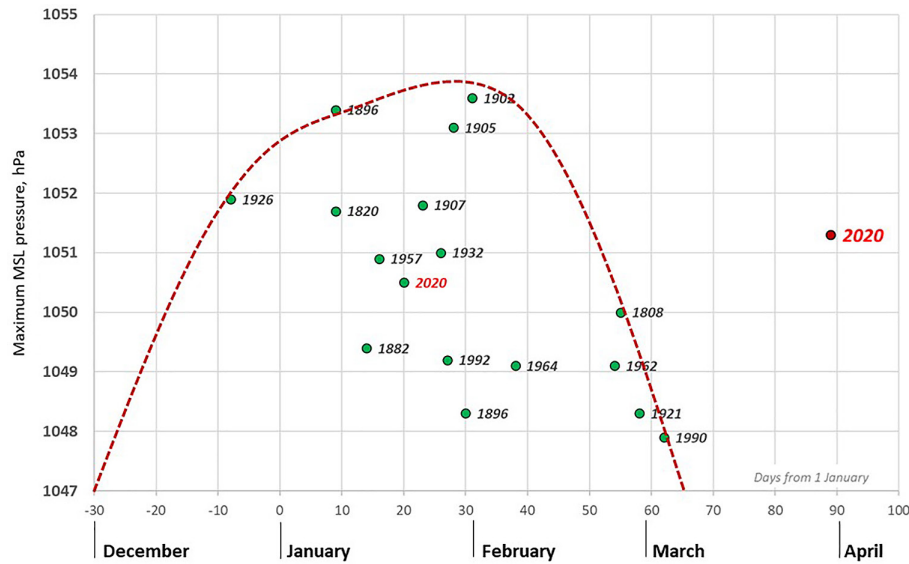


Figure 11. The highest MSL barometric pressures observed anywhere in the British and Irish Isles since about 1800, plotted against the date on which they occurred. The March 2020 event lies well outside the 'envelope' of all previous events within the last 200 years or more. The January 2020 event is also highlighted.

## References

- Burt S.** 1993. Another new North Atlantic low pressure record. *Weather* **48**: 98–103.
- Burt S.** 2006. Britain's highest barometric pressure on record is incorrect. *Weather* **61**: 210–211.
- Burt S.** 2007. The Highest of the Highs ... Extremes of barometric pressure in the British Isles, Part 2 – the most intense anti-cyclones. *Weather* **62**: 31–41.
- Burt S.** 2020. London's highest barometric pressure in over 300 years. *Weather* **75**: 109–116.
- McIlveen R.** 2010. *Fundamentals of Weather and Climate*, 2nd Edition. Oxford University Press: Oxford, UK, 632 pp.

Correspondence to: Stephen Burt

s.d.burt@reading.ac.uk

© 2020 Stephen Burt, all rights reserved

doi: 10.1002/wea.3840

This is an open access article under the terms of the Creative Commons Attribution License, which permits use, distribution and reproduction in any medium, provided the original work is properly cited.







